PETROLOGY AND GEOCHEMISTRY OF LEWISIAN PEGMATITES AND GRANITES, N.W. SCOTLAND

by

Graham John Cunningham B.Sc.(Lond.)

A thesis submitted for the degree of

Doctor of Philosophy in the

University of London

Royal School of Mines
Imperial College
London

June, 1981

ABSTRACT

Late Scourian pegmatite dykes and Laxfordian granite sheets and pegmatites intruded into the lithologically and structurally heterogeneous Lewisian gneisses of N.W. Scotland display wide variations in geochemistry and mineralogy reflecting their varied origins and evolutionary histories.

Laxfordian granites emplaced into the Laxford shear zone, Sutherland, have high Ba and Sr, relatively low K, Rb, Th and U and distinctive rare-earth element patterns which indicate their origin by partial melting of the depleted Scourie granulites. The Outer Hebrides granites of the same age may have originated by partial melting of undepleted amphibolite-facies grey gneisses.

The compositions of pegmatites associated with the granites are rationally explained by the partition of major and trace elements between crystals, liquids and/or fluids. Pegmatites which occur independently of the granites show comparable variations in their geochemistry, often evolving towards low-temperature, fluid dominated, garnet-muscovite pegmatites. The Late Scourian pegmatites are similar in their geochemistry to the mainland Laxfordian granites, and record high crystallisation temperatures (800°C) and oxygen fugacities (log $f_{O_2} = 10^{-12}$).

Metasomatic reactions occurring at higher (700°C) and lower (500°C) temperatures between acid pegmatites and basic host

rocks caused strong leaching of Ca from the basic rocks, with the introduction of K, resulting in the formation of reaction zones whose chemistry is similar to many semipelitic metasediments. Diffusion-controlled structures are important on a small scale, but infiltration of a pegmatite fluid provided efficient transport over larger (up to several cm) distances. Intrinsic diffusivities of elements were of less importance than the nature of mineral/fluid reactions and the influence of such factors as rock porosity and tortuosity to the relative transport of components.

LIST OF CONTENTS

Abstract 1
List of Contents 3
List of Figures 6
List of Tables 11
Acknowledgements 13

Chapter 1 INTRODUCTION

1.1 Aims of the thesis 14
1.2 The Lewisian Complex 15
1.2.1 The Lewisian assemblage 15
1.2.2 Structural development 19
1.3 Scope of the thesis 25

Chapter 2 GEOLOGICAL RELATIONSHIPS AND PETROGRAPHY

2.1 Relationships between the acid intrusive rocks and Lewisian structure 29
2.1.1 General distribution 29
2.1.2 The Laxford Front 29
2.1.3 South Harris 33
2.1.4 Discussion and extension to the rest of the Lewisian 37
2.2 Description of granites and pegmatites . . . 42
2.2.1 Laxfordian granites and related pegmatites 42
A. Laxford Front 42
B. Harris and Lewis 45
2.2.2 Other Laxfordian pegmatites: Northern and Southern types 49
2.2.3 Late Scourian pegmatites 56

Chapter 3 GEOCHEMISTRY OF THE GRANITES AND PEGMATITES

3.1 Introduction 59
3.2 Chemical variations 60
3.2.1 Laxfordian granites and related pegmatites 60

3.2.2 Northern-type and Southern-type pegmatites 75
3.3 Discussion 77
3.3.1 Major geochemical features of the granites 77
3.3.2 Late-stage processes in the granites, and pegmatite evolution 94
3.3.3 Independent Laxfordian pegmatites . . 109

Chapter 4 PHASE CHEMISTRY

4.1 Introduction 114
4.2 Laxfordian granites and related pegmatites. . 116
4.2.1 Feldspars 116
4.2.2 Ferromagnesian and oxide minerals . . 122
4.3 Laxfordian independent pegmatites 127
4.3.1 Feldspars 127
4.3.2 Ferromagnesian and oxide minerals: Northern-type assemblages 131
4.3.3 Ferromagnesian and oxide minerals: Southern-type assemblages. 136
4.4 Late Scourian pegmatites 151
4.4.1 Feldspars 151
4.4.2 Ferromagnesian and oxide minerals . . 164
4.5 Distribution of trace elements in pegmatite minerals 173
4.5.1 Ba, Sr and Rb 173
4.5.2 Rare-earth elements 178
4.6 Conclusions 186

Chapter 5 METASOMATISM

5.1 Introduction 190
5.1.1 Scope of the study: metasomatic reaction between basic host rocks and acid pegmatites 190
5.1.2 The development of metasomatic structures 191

5.2 Leenish, Isle of Barra: metasomatic reaction zones associated with small acid veins 198
5.2.1 Geological relationships 198
5.2.2 Petrography 202
5.2.3 Mineral composition and estimation of physical conditions 207
5.2.4 Chemical mass transfer 215
5.3 Garry-a-Siar, Benbecula: metasomatic zones associated with a large acid pegmatite 231
5.3.1 Geological relationships and petrography 231
5.3.2 Chemical mass transfer 243
5.3.3 Processes governing mass transfer . . . 253
5.4 Conclusions 264
5.4.1 Processes in metasomatism 264
5.4.2 Extent of chemical modification 267
5.4.3 Products of metasomatism 270

Chapter 6 DISCUSSION AND CONCLUSIONS

6.1 The problem of the granite and pegmatite source 274
6.1.1 Geochemical and mineralogical evidence 274
6.1.2 Structural evidence 276
6.1.3 The pegmatite environment 278
6.2 Conclusions 291

References 297

Appendix 1 Tables of rock analyses 313
Appendix 2 Methods of analysis 324

LIST OF MAPS AND FIGURES

MAPS

Map 1 Distribution of Lewisian rocks 16
Map 2 Parts of Sutherland 30
Map 3 Parts of Lewis and Harris 34
Map 4 The Southern Outer Isles:
a. General map 39
b. The Leenish peninsula, Isle of Barra . 40

FIGURES

2.1 The Laxford granite sheets at Rubha Ruadh, Sutherland 43
2.2 Pegmatite in a Laxford granite sheet 43
2.3 Breakdown of clinopyroxene to amphibole and sphene in a Laxford granite 43
2.4 Xenoliths in Laxfordian granite sheets, Beitarsaig, N.W. Harris 47
2.5 Ptygmatically-folded pegmatites, Colluscarve, N.W. Harris 47
2.6 Laxfordian pegmatite cut by Laxfordian leucogranite, Mangersta, S.W. Lewis . . . 50
2.7 Style of zoning in part of the Chaipeval pegmatite, S. Harris 54
2.8 Kyanite in a Late Scourian pegmatite, Scourie, Sutherland 54

3.1 Laxfordian granites: major element geochemistry 61
a. Major elements plotted against SiO_2. . 61
b. Bar graphs of SiO_2 concentrations . . 62
c. The granites plotted in the system Qz-Or-Ab-An 63

d. AFM diagram 64
e. Normative corundum or diopside plotted against SiO_2 64

3.2 Laxfordian granites: trace elements plotted against SiO_2 67
3.3 Variation of trace element concentrations between coexisting granite-pegmatite pairs . 69
3.4 REE patterns of the Laxfordian granites . . 72
3.5 Variation of $Eu:Eu^*$ and $Ce_N:Yb_N$ in the Laxfordian granites 74
3.6 Ca plotted against (a) Ba and (b) Sr for various Laxfordian acid rocks 76
3.7 USGS G-2 normalised trace element diagrams. (a) Laxfordian granites, (b) Lewisian gneisses 78
3.8 Trace element models for (a) Laxford and (b) Outer Hebrides granites 84
3.9 Variation of $Eu:Eu^*$, $Ce_N:Sm_N$, and REE and $Tb_N:Yb_N$ with SiO_2 in the Laxford granites 96
3.10 Geochemical variations across the Laxford granite sheets 97
3.11 Possible crystallisation paths of the granites in the system Qz-Or-Ab-An 100
3.12 Variation of $Eu:Eu^*$, $Ce_N:Sm_N$, REE and $Tb_N:Yb_N$ with SiO_2 in the Outer Hebrides granites 104
3.13 Cogenetic pegmatites from Loch Laxford and the Outer Hebrides plotted in the system Qz-Or-Ab-An 105
3.14 USGS G-2 normalised trace element diagram: the Northern-type and Southern-type pegmatites 110

4.1 Laxfordian granites: feldspar compositions . . 121
4.2 Laxford granites: amphibole compositions 125
4.3 Biotites from Northern-type and Southern-type pegmatites 134
4.4 Garnets from Southern-type pegmatites 142
4.5 Comparison of garnet compositions from Southern-type pegmatites with Green's (1977) data 143
4.6 Muscovites from Southern-type pegmatites . . . 149
4.7 Distribution of Fe and Mg between muscovite and garnet in two Southern-type pegmatites 149
4.8 Phase relations between muscovite, potash feldspar and sillimanite with varying pH . . 150
4.9 Estimated bulk feldspar compositions from Late Scourian pegmatites 156
4.10 Celsian- and anorthite-content of Late Scourian alkali feldspars plotted against estimated temperature 160
4.11 Ternary feldspar solvi determined by Seck (1971) 162
4.12 T-fO_2 conditions estimated for Late Scourian pegmatites 169
4.13 Exsolution textures and compositions of Fe-Ti oxide minerals from Late Scourian pegmatites 171
4.14 Distribution of Ba, Sr and Rb between pegmatite feldspars 177
4.15 REE patterns for pegmatite feldspars and garnets 180
4.16 Distribution of trace elements between alkali feldspars and plagioclases plotted against ionic radius 184

5.1	Effects of combined diffusion and infiltration metasomatism	196
5.2	Zoned aureoles at Leenish, Isle of Barra	200
5.3	Aureole widths plotted against vein widths at Leenish	201
5.4	Coarse perthites from an acid vein, Leenish	204
5.5	Microscopic features of a zoned aureole, Leenish	205
5.6	Estimates of (P,T) based upon mineral assemblages at Leenish	210
5.7	Section across a zoned aureole from Leenish	218
5.8	Estimated molar compositions of traverses across a zoned aureole	219
5.9	Variations of oxides across a zoned aureole normalised to the metadolerite composition	221
5.10	Al-fixed and Si-fixed oxide variation across a zoned aureole	226
5.11	Metasomatic reaction zones at Garry-a-Siar, Benbecula	233
5.12	Relationships between size of spherical diffusion structures and distance from pegmatite contact	234
5.13	Microscopic features of the Garry-a-Siar reaction zones	237
5.14	Transition from poikiloblastic to clear biotites	239
5.15	Variation of plagioclase composition across the reaction zone	242
5.16	Major element variation across the reaction zone	245
5.17	Variation of trace elements across the reaction zone	250
5.18	Development of the reaction zone geometry: a hypothetical model	256

5.19 Illustration of the growth of the spherical structures 257
5.20 Reaction zone compositions plotted in the systems CN-K-FM and AKFM 271

6.1 Jahns and Burnham's model of pegmatite evolution 280
a. The general model 281
b. Possible evolution of the Laxford granites and pegmatites 282
c. Possible evolution of the large pegmatite at Garry-a-Siar 282

LIST OF TABLES

1.1 Summary of major events of the Lewisian time-scale 20

4.1 Feldspars from Laxfordian granites and associated pegmatites 117

4.2 Ferromagnesian minerals from Laxfordian granites and associated pegmatites 123

4.3 Feldspars from Northern-type and Southern-type pegmatites 128

4.4 Biotites from Northern and Southern-type Laxfordian pegmatites 132

4.5 Garnets and oxide minerals in Southern-type pegmatites 137

4.6 Muscovites in Southern-type pegmatites 147

4.7 Feldspars in Late Scourian pegmatites 152

4.8 Estimates of temperature of feldspar equilibration in Late Scourian pegmatites . . . 158

4.9 Ferromagnesian and oxide minerals in Late Scourian pegmatites 165

4.10 Trace element concentrations in Lewisian pegmatite minerals 174

5.1 Mineral compositions from metadolerite, acid veins and aureoles at Leenish 208

5.2 Modal composition of reaction zone traverses and estimation of bulk composition . 217

5.3 Normative compositions of metadolerite, acid vein and aureole zones 223

5.4 (a) Mass-balance calculations, assuming one-stage growth of zoned aureoles 228

(b) Mass-balance calculations, assuming two-stage growth of zoned aureoles 229

5.5 Mineral compositions in Garry-a-Siar reaction zones and metabasic rock 240

5.6 Compositions of a series of samples taken across a reaction zone 246

5.7 Estimated matrix compositions in a reaction zone 248

ACKNOWLEDGEMENTS

I would like to thank my supervisors, Professor Janet Watson and Dr. Gloria Borley, for encouragement, criticism and many discussions.

The following provided instruction and advice in various aspects of the analytical work: Peter Watkins, Robin Parker, Paul Suddaby and Neil Wilkinson.

Many colleagues in the Mineralogy and Petrology section at Imperial college have provided valuable discussion during the work.

The thesis was typed by Mary Warner.

This work was carried out during the tenure of a N.E.R.C. research studentship, which is gratefully acknowledged.

CHAPTER 1

INTRODUCTION

1.1 AIMS OF THE THESIS

The aim of this work is to examine geochemical and phase-chemical evidence which may have some bearing upon the ultimate origin and conditions of formation of certain groups of acid intrusive rocks which form part of the Pre-cambrian Lewisian Complex of N.W. Scotland.

Most of the rocks under discussion were emplaced - as granite and pegmatite sheets and dykes - near the end of the Laxfordian cycle of deformation, metamorphism and magmatism, and in effect mark the end of what is normally considered to be the geological history of the Lewisian, at around 1750 m.y.b.p. In addition a small but perhaps important group of acid pegmatites which closely followed earlier, Scourian, granulite-facies metamorphic events at around 2600 m.y.b.p. is considered, both from the point of view of its relationship with the early history of the Lewisian and also as a basis for comparison with the much more abundant Late Laxfordian granitic rocks.

The value of rocks of magmatic origin, which form potential geological time-markers because they can be seen to cut rocks and structures formed earlier than their emplacement, and in turn may be affected by later

deformation, was perhaps recognised earliest in the Lewisian (Peach et al, 1907; Sutton and Watson, 1951). A suite of basic dykes - the Scourie metadolerite dyke suite - has long been used to separate earlier, Scourian, events from later, Laxfordian ones, and provides the main pivot around which discussions of the structural evolution of the Lewisian have proceeded. Locally, 2600 m.y. old pegmatites have provided the key to a more detailed geological history (Sutton and Watson, 1951; Dearnley and Dunning, 1968; Francis, 1969) which has been given geochronological support (Giletti et al, 1961; Francis et al, 1971).

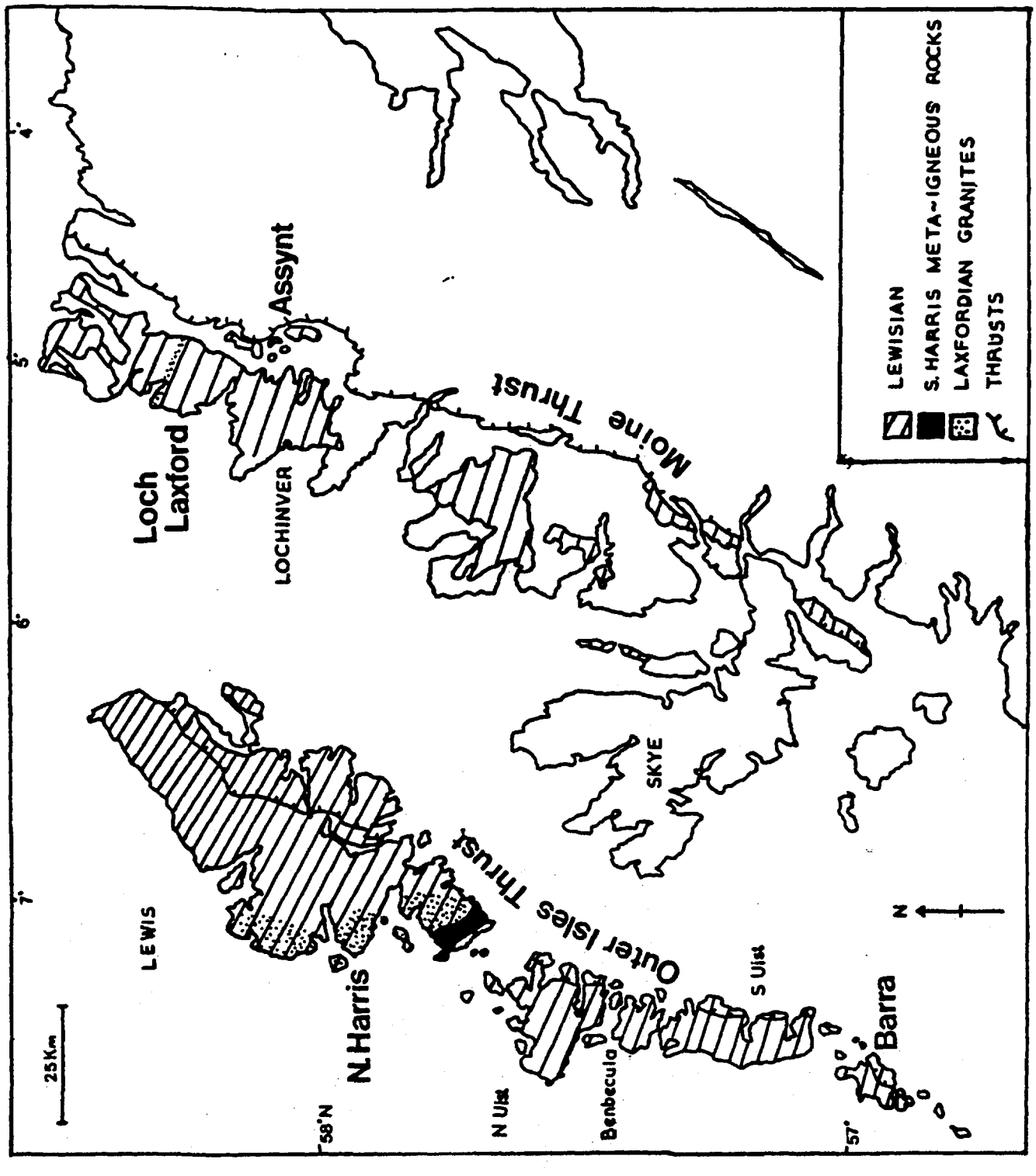
It is considered that the present study, combined with known geological relationships, may shed some light on aspects of Lewisian evolution between c. 2600 m.y.b.p. and c. 1700 m.y.b.p.

1.2 THE LEWISIAN COMPLEX

1.2.1 THE LEWISIAN ASSEMBLAGE

Basement rocks of Archaean age (Moorbath et al, 1969; 1975) outcrop to the west and east of the Caledonian Moine Thrust in N.W. Scotland, and form almost the whole of the Outer Hebrides archipelago, as well as certain parts of the Inner Hebrides.

Except for the inliers to the east of the Moine Thrust, which have been extensively reworked during the later Proterozoic and Phanerozoic, the Lewisian rocks



Map 1 Distribution of Lewisian rocks west of the Moine thrust.

have remained unaffected by significant deformation since the emplacement of late Laxfordian granites and pegmatites about 1750 m.y.b.p. (van Breemen et al., 1971) and form a stable cratonic basement to later Proterozoic (Torridonian) and Cambrian sedimentary rocks.

The great bulk of Lewisian rocks are orthogneisses which appear to have been in existence since at least 2800-2900 m.y.b.p. (Moorbath et al., 1969, 1975; Hamilton et al., 1980). In some areas the gneisses retain at least traces of anhydrous metamorphic mineral assemblages characteristic of the granulite facies. Granulite facies rocks predominate in the Scourie-Badcall-Lochinver region of the N.W. Scottish mainland, in the South Harris meta-igneous complex, and discontinuously down the eastern side of the Uists and Barra. Often, these granulite facies rocks have been retrogressed to amphibolite facies. Sutton and Watson (1951) demonstrated the progressive development of amphibolite facies metamorphism north of Scourie.

The granulite facies gneisses are predominantly intermediate in composition (probably tonalitic, on average) with lesser basic, ultrabasic and granitic components. In general, alkali feldspar is uncommon, and, as with granulite facies rocks found elsewhere (Heier, 1973) the elements K, Rb, U and Th appear to occur in unusually low concentrations, a geochemical characteristic which has been ascribed either to the removal of a granitic melt fraction (O'Hara, 1977; Pride and Muecke, 1980) or to metamorphic dehydration

(Hamilton et al, 1980).

Elsewhere, migmatitic gneisses rich in alkali feldspar foliae occur, for example in N.W. Harris and north of Loch Laxford in Sutherland (Sheraton et al, 1973). These gneisses are not depleted in K, Rb, U and Th, and Sheraton et al (1973) and Beach (1974) suggested that these rocks, shown by Moorbath et al (1969) and Moorbath (1975) to be of the same age as the granulites and therefore not a metamorphosed cover sequence, represent original amphibolite-facies gneisses formed at a level in the crust higher than that of the granulites. A similar relationship was proposed to relate the eastern (granulite facies) and western (amphibolite facies) gneisses of Barra (Francis, 1969; Coward et al, 1970).

Metasedimentary rocks occur over much of the Lewisian outcrop (Coward et al, 1969), but are significant in volume only in a few narrow belts, particularly those flanking the South Harris igneous complex. Near to Gairloch a group of metasedimentary rocks (the Loch Maree group) may be younger than most Lewisian rocks (Park, 1970, 1973), suggesting uplift to the surface of at least part of the Lewisian by around 2200 m.y.b.p. (Bickerman et al, 1975).

Other Lewisian rocks younger than the 2900-2700 m.y. age of the granulites are intrusive, and include:

a. A suite of early intrusive rocks found in eastern Barra and South Uist (Francis, 1969; Coward, 1969), which range from ultrabasic to tonalitic in composition.

b. The 2600 m.y.b.p. pegmatites at the N.W. Scottish mainland, Barra and S. Uist.

c. A suite of metabasic dykes (the Scourie dykes) emplaced over much of the Lewisian (Peach et al, 1907; Sutton and Watson, 1951; Dearnley and Dunning, 1968) and providing an age of around 2400 m.y. (Chapman and Moorbath, 1977).

d. Granite and pegmatite sheets and dykes emplaced at around 1750 m.y.

1.2.2 STRUCTURAL DEVELOPMENT

In the classic Scourie-Laxford area of Sutherland (Peach et al, 1907; Sutton and Watson, 1951) the structural history of the Lewisian gneisses has been considered in terms of a progressive reorientation of early NNE - SSW trending structures into a more E - W grain. The NNE - SSW structures represent the final outcome of the complex gneiss-forming event, at least a part of which was associated with granulite-facies metamorphism, which occurred between 2900-2700 m.y.b.p. (Moorbath et al, 1969; Hamilton et al, 1980). Their influence is seen on a regional scale in (a) the dominant NNE - SSW striking gneiss foliation of low dip around Scourie, (b) the similar orientation of the interface between granulite facies and amphibolite facies gneisses along the eastern side of the southern Outer Hebrides (Francis, 1969; Coward et al, 1970) and (c) the postulated

VOLCANIC & SEDIMENTARY ROCKS	INTRUSIVE ROCKS OTHER THAN GRANITES	PHASES OF DEFORMATION METAMORPHISM AND MIGMATISATION	GRANITE & PEGMATITE
	lamprophyric dykes	metamorphism and migmatisation	pegmatites
LAXFORDIAN		1850-1700 m.y.	granites and pegmatites
2200-1600 m.y.			
		repeated deformation and metamorphism of amphibolite or granulite facies	
	SCOURIE DYKE SWARM (tholeiites)		
		INVERIAN EPISODE	
		local deformation, metamorphism	
Loch Maree Group ?			pegmatites
			2600-2400 m.y.
	diorites etc. (Barra)		
SCOURIAN		BADCALLIAN EPISODE 2800 m.y.	
2800-2200 m.y.		gneiss-forming metamorphism granulite or amphibolite facies	granites
		interleaving of supracrustal, intrusive and gneissose layers	early tonalites ?
supracrustal units	basic/ultrabasic & anorthositic		
		formation of early gneiss complex ?	
PRE-SCOURIAN			

Table 1.1 Summary of major events of the Lewisian time-scale (after Watson, 1975).

plunge culmination situated in the Minch and apparently (Coward et al, 1970) affecting later structures (Laxfordian F_3 major folds).

The Laxfordian sequence of deformation events, defined by Sutton and Watson (1951) as those events affecting the Scourie metadolerite dyke swarm, include major E - W or WNW - ESE trending structures, in particular the major F_3 folds of the Outer Isles, similarly-trending major folds near Gairloch (e.g. the Tollie antiform) (Peach et al, 1907; Park, 1970), and numerous shear zones affecting the granulite facies gneisses between Loch Laxford and Lochinver. The largest Laxfordian shear zone is the Laxford shear zone, or Laxford Front, situated immediately south of the southern shore of Loch Laxford. Dearnley (1962) and Beach et al (1974) have compared the similarly-trending interface, between the South Harris Igneous Complex and its associated metasedimentary gneisses with the amphibolite-facies gneisses to the NNE, with the Laxford Front.

This rather simple structural synthesis has undergone a number of modifications regarding the relative age of some structures in the last decade, and these are discussed below. Nevertheless, for the purposes of the present study of rocks whose intrusion was strongly structurally-controlled, the imposition of two 'grains' upon the gneisses is of great importance, and generally accounts for the observed distribution of granites and pegmatites.

Despite the arguments of Bowes and Khoury (1965) and Bowes (1969), it is generally accepted that the Scourie dyke suite is a useful time-maker in Lewisian chronology, and the work of Dearnley (1962) and Dearnley and Dunning (1968) extended its applicability to the Outer Hebrides. Complications to Lewisian structural chronology have thus tended to bear upon the ages of deformation events relative to this dyke suite. Based on work in the Lochinver region, a number of workers recognised a pre-dyke amphibolite facies deformation event, with the formation of NW - SE trending shear belts, termed the Inverian episode by Evans and Lambert (1974). Park (1970) proposed the term "Badcallian" to describe granulite-facies events occurring earlier than the Scourian potash-pegmatites dated at around 2600 m.y.b.p., and Evans (1965) regarded the Inverian as covering events which took place between the intrusion of these pegmatites and the emplacement of the Scourie dyke suite. Watson (1975) pointed out that many occurrences of amphibolite-facies retrogression and deformation are undated relative to the Scourian pegmatites, or can be shown to be earlier, as at Barra (Francis, 1969) and Lower Badcall (Beach et al., 1974), and proposed the more broadly defined "late Scourian" for amphibolite facies events of pre-pegmatite and uncertain age. A further complicating factor is the uncertainty that exists as to the original Scourian (or Badcallian) metamorphic grade of many of the grey gneisses of the Outer Hebrides, and those north of Loch Laxford.

There is good evidence that the migmatitic, amphibolite facies gneisses of NW Harris and northern Sutherland were already in their presently-observed metamorphic state at the onset of Scourie dyke intrusion.

It is clear that retrogression and deformation was heterogeneous in the Lewisian at least from about 2700 m.y.b.p., and also that NW - SE trending structures existed before the development of the similarly-trending Laxfordian major structures. Thus Graham (1980) recognises NW - SE and NNE - SSW structural "grains" in South Harris, and (in the absence of Scourie dyke evidence) suggests that both are essentially Scourian in age. Control of Laxfordian structures by Scourian trends implies repeated movement on early shear zones, and it should therefore not be a matter for surprise if late Laxfordian intrusions are found in early fractures or shear zones. The possible significance of repeated movements on old shear zones is discussed in more detail in relation to South Harris and the Laxford Front in section 2.1.

Laxfordian deformation, which succeeded the intrusion of the Scourie dyke suite (at perhaps 2400-2200 m.y.b.p.; Moorbath and Park, 1972; Evans and Tarney, 1964, Chapman, 1979) after an unknown interval, was again markedly heterogeneous, the main granulite-facies terrains suffering little deformation other than the formation of shear zones. Deformation was extensive in the grey gneisses, although here too occur many regions of low Laxfordian strain (Coward et al, 1970) in which relatively undeformed (or at least discordant) Scourie

dykes may be found. Thus Laxfordian reworking was probably not sufficiently thorough to impose a totally new foliation upon most of the grey gneisses, and it is the preservation of the Scourian foliation in these rocks which allows their frequent contrast with the granulite facies gneisses to be identified - in particular the common abundance of alkali-feldspar rich foliae in some areas which suggests that granulite facies metamorphism associated with extensive loss of radiogenic elements (K, U, Th, Rb) was not ubiquitous during the Scourian, and which in turn indicates that the heterogeneous nature of Lewisian deformation and metamorphism extended back into the Badcallian.

Areas of low Laxfordian deformation were shown by Coward et al (1970) to occur largely in major Laxfordian F_3 antiforms, which are open structures, contrasting with the intervening tight synforms mapped in the Outer Hebrides which give the F_3 folds their characteristic cuspate appearance. Coward et al (1970) suggested that this fold style was the result of deformation of an interface between (underlying) granulite-facies rocks and an amphibolite facies cover - a lithological contrast of Scourian age.

The history of the Laxfordian cycle, and the nature of Laxfordian deformation, thus appears to have been influenced by earlier (Scourian, in the broad sense of pre-dyke events) structures and metamorphic heterogeneities. Possibly no new 'grain' was imposed; the basement-reactivation which can now be observed bears only an

indirect relationship with any Laxfordian "orogeny" which may have occurred.

1.3 SCOPE OF THE THESIS

To date, studies of the Lewisian acid intrusions which will be described here have been concerned with structural relationships and isotope geology - the latter concerned largely with dating the rocks, rather than petrogenesis. In addition, one mineralogical study (Von Knorring and Dearnley, 1960) has been made.

The aim of the present work is to investigate the Lewisian granites and pegmatites as igneous rocks, and sometimes as assemblages of minerals characteristic of igneous rocks. This approach is complicated by two main factors. Firstly, granitic rocks intruded as late-tectonic bodies (Myers, 1968) tend to develop tectonic fabrics and mineral textures, any igneous textures usually being much modified or obliterated. Secondly, in the case of many of the pegmatites, very little is understood of the (probably large) influence of a fluid phase upon the apparently-igneous crystallisation histories observed.

On the other hand, it may be possible to use acid rocks intruded into country rocks which were at elevated temperatures and confining pressures to make some statement about the physical conditions prevailing at the time of emplacement. This has been attempted in

the case of the Scourie dyke suite (Tarney, 1963; O'Hara, 1961). It seems logical, when dealing with igneous rocks in the plutonic environment (in the sense of Kennedy, 1948), to combine these quasi-metamorphic considerations with more conventional igneous interpretative methods.

Finally, there arises the question whether the interaction between plutonic acid rocks and their metamorphic host rocks is merely one of heat transfer and equilibration, or whether mass transfer played an important role. Evidence of metasomatic reaction which can be measured geometrically and chemically has been found locally, and is examined in detail in Chapter 5.

In any study of granitic rocks sensu stricto, such as the rocks described here, the question of their ultimate origin is bound to arise. This has always been a highly controversial matter, frequently reviewed (e.g. Read, 1957; Fyfe, 1969; Wyllie, 1978), and like all controversies it is continually subject to changes of fashion. While it can hardly be said that a concensus exists at present, it is probably true that advances in isotope geology and better understanding of the influence of geotectonics upon magmatism have at least reduced the range of views generally held. It may be fair to say that most geologists would accept a contribution to granite production from both the Earth's mantle (even if only in the form of heat) and crust (though not necessarily through melting). This, however,

leaves enormous scope for differences of opinion which in the view of the present writer are unlikely to be resolved in the near future. It is likely that future progress will be made, not by the application of isotope systematics alone, but by studies of specific groups of granitic rocks in relation to all the geological processes which might influence their mineralogy and geochemistry.

The rocks selected for this study were chosen because a combination of previous geological and geochronological work allows them to be placed in a fairly well-defined Lewisian setting. Excluded from the study are:

i) Early Scourian granite gneisses (Savage, 1979) and migmatite veins.

ii) 'Laxfordian' migmatite veins, many (? most) of which are in fact Scourian in age (see section 1.2), and which are intermingled in northern Sutherland and western Harris, with veins of undoubted Laxfordian age.

The rocks remaining can be subdivided as follows:

B. LAXFORDIAN

(i) Granite sheets intruded into the Laxford shear zone, Sutherland, and their associated pegmatites.

(ii) Granite sheets occurring in Western Harris and S.W. Lewis, and associated pegmatites.

(iii) Pegmatites which are not clearly related to granite intrusions. In Harris, these bodies can be subdivided into two groups: (a) NORTHERN-type pegmatites, occurring commonly in NW Harris, and (b) SOUTHERN-type pegmatites mainly occurring in the South Harris Igneous Complex and paragneisses.

A. SCOURIAN

(i) Late Scourian pegmatites occurring as scattered dykes in the granulite terrains of the NW Scottish mainland and (more rarely) in the Outer Hebrides.

In general, the Laxfordian rocks will be dealt with first, being more numerous and varied, comparison then being made with the earlier Scourian pegmatites.

CHAPTER 2

GEOLOGICAL RELATIONSHIPS AND PETROGRAPHY

2.1 RELATIONSHIPS BETWEEN THE ACID INTRUSIVE ROCKS AND LEWISIAN STRUCTURE

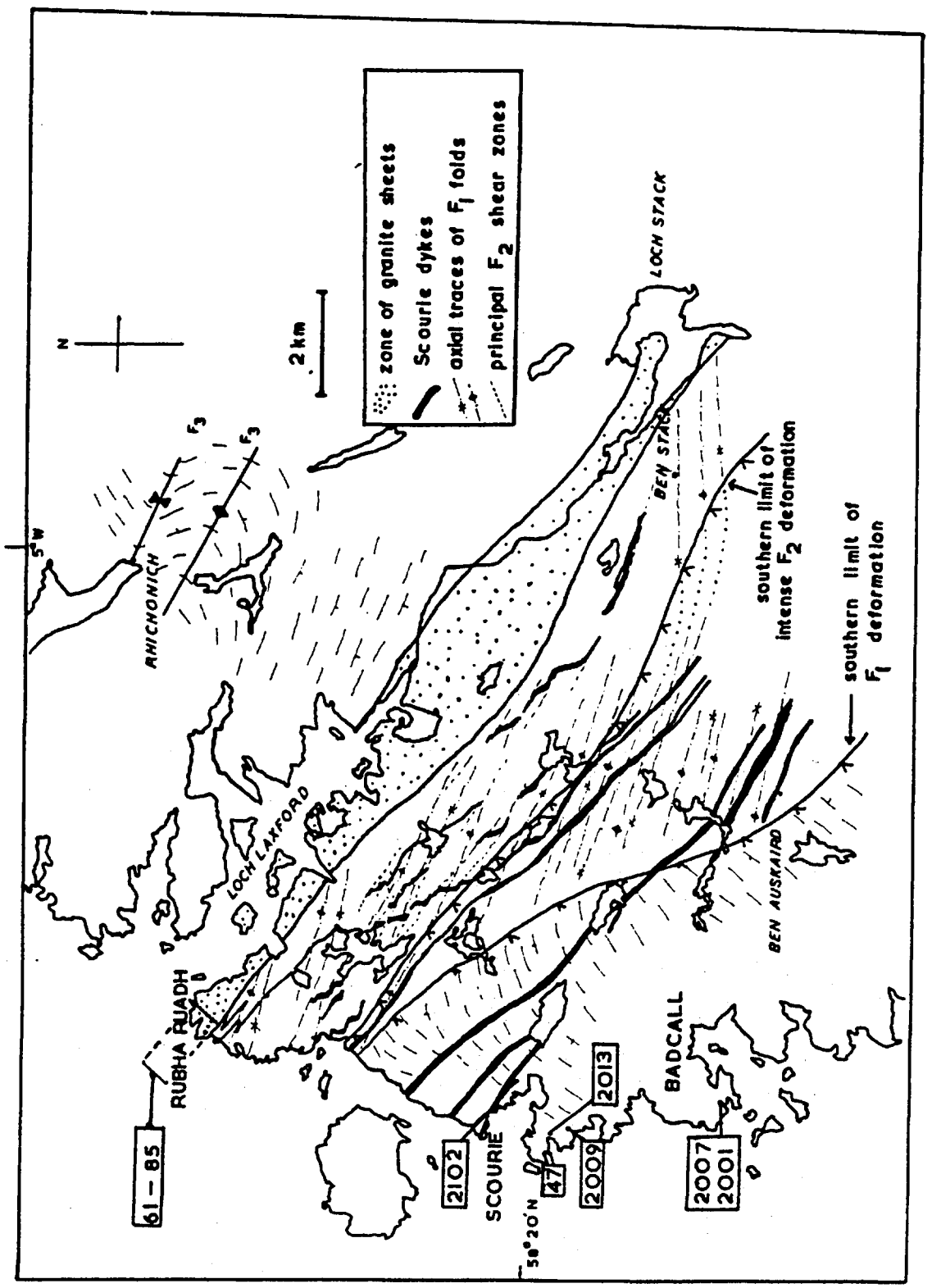
2.1.1 GENERAL DISTRIBUTION

The locations of the rocks considered here are shown in Maps 1-4. In the following three sections, the possible significance of the distribution of these intrusions is discussed in relation to Lewisian structure. Two areas which have been the subject of detailed mapping by a number of workers - the Laxford Front and South Harris - are used as examples, and an attempt is then made (section 2.1.4) to extend conclusions drawn from these areas to other parts of the Lewisian outcrop.

2.1.2 THE LAXFORD FRONT

Beach *et al*. (1974) have shown that a sequence of deformation phases has affected the Lewisian rocks on both sides of the Laxford shear zone:

(i) F_1. Upright folds which predate, and are therefore cut by, the Scourie dyke suite. The folds trend almost parallel to the Laxford Front, becoming tighter near to the Front itself.



Map 2 The Badcall - Scourie - Laxford area, Sutherland. Simplified after Beach et. al., 1974.

To the south, F_1 deformation becomes increasingly heterogeneous, suggesting decreasing ductility in that direction. This deformation phase appears to have been responsible for producing the swing in foliation-strike from a Scourian (NNE-SSW) trend to a 'Laxfordian' alignment. The apparent heterogeneity of development of the F_1 phase as a function of distance from the Laxford Front suggests that the Laxford Shear Zone was already in existence, and did not therefore have its origins in Laxfordian times.

(ii) F_2. Almost coplanar with F_1 structures, but affecting Scourie dykes, and possibly responsible for the increasing tightness of F_1 folds towards the Laxford Front. The southern limit of F_2 structures is not so far south as that of F_1 folds, suggesting increasingly rigid response to stress in the Scourie granulites. F_2 shear zones are sinistral, N side up.

(iii) F_3. Only seen north of the Laxford Front, F_3 folds deform F_2 structures in that region, but are again nearly coplanar. Shear zones are sinistral, N side up.

The N side up sense of movement on the SW-dipping Laxford shear zone indicated by F_2 and F_3 structures seems difficult to reconcile with the juxtaposition of the two gneiss terrains, because it implies the uplift of amphibolite-facies gneisses from deeper levels to lie alongside retrogressed Scourie granulites. However, the evidently long history of the Laxford shear zone (Beach et al., 1974; Davies, 1976) may suggest that repeated movement, not always in the same sense, took place, allowing S side up, overthrusting movement at the earliest stage (during or prior to F_1).

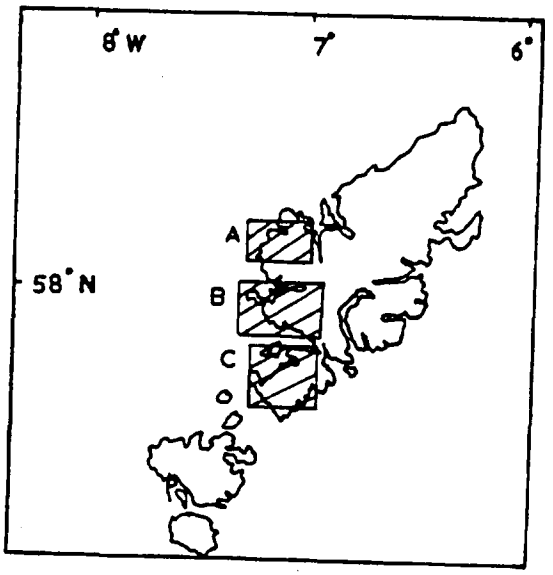
In relation to granite emplacement at the Laxford Front, normal or reverse movement is less important than the possibility of dilation sustained long enough for the emplacement of numerous granite sheets. If such dilation were the result of tectonic recovery after the F_3 deformation, then it should follow that phase closely. In fact, it is possible to argue that a set of acid veins was emplaced to north and south of the Laxford front after F_3 deformation. Since these veins are absent from the granite sheet zone itself, it is possible to argue that they are cut by the granite sheets, with which Beach et al. (1974) considered they were correlated.

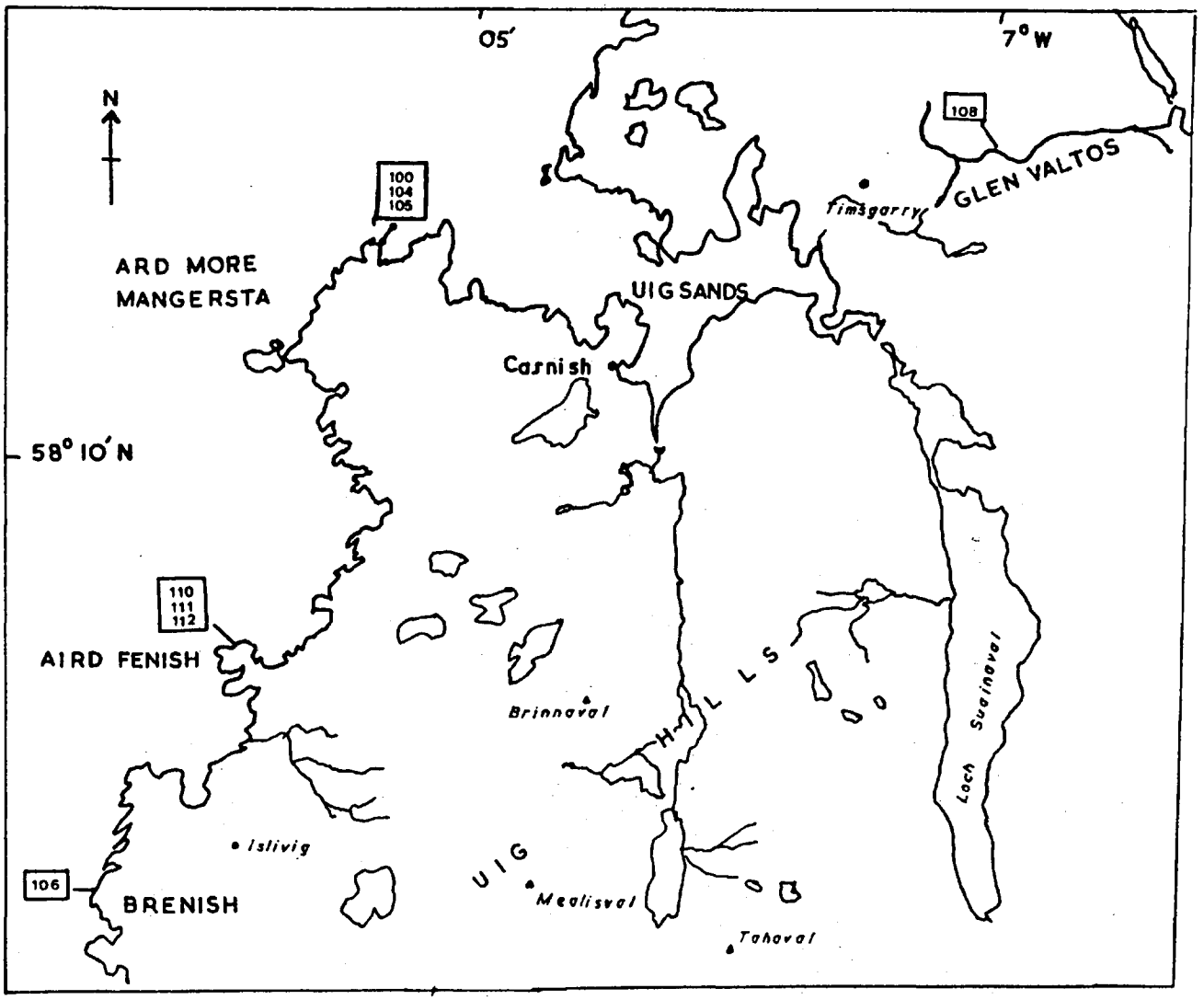
Thus it may be that two phases of reactivation of older fractures took place later than F_3, suggesting successive deformation phases of insufficient intensity to produce discernible structures in the gneisses, but strong enough to cause dilation of existing ones.

The N side up late stage of displacement on the shear zone implies stress conditions like those of normal faulting under which horizontal extension could be expected.

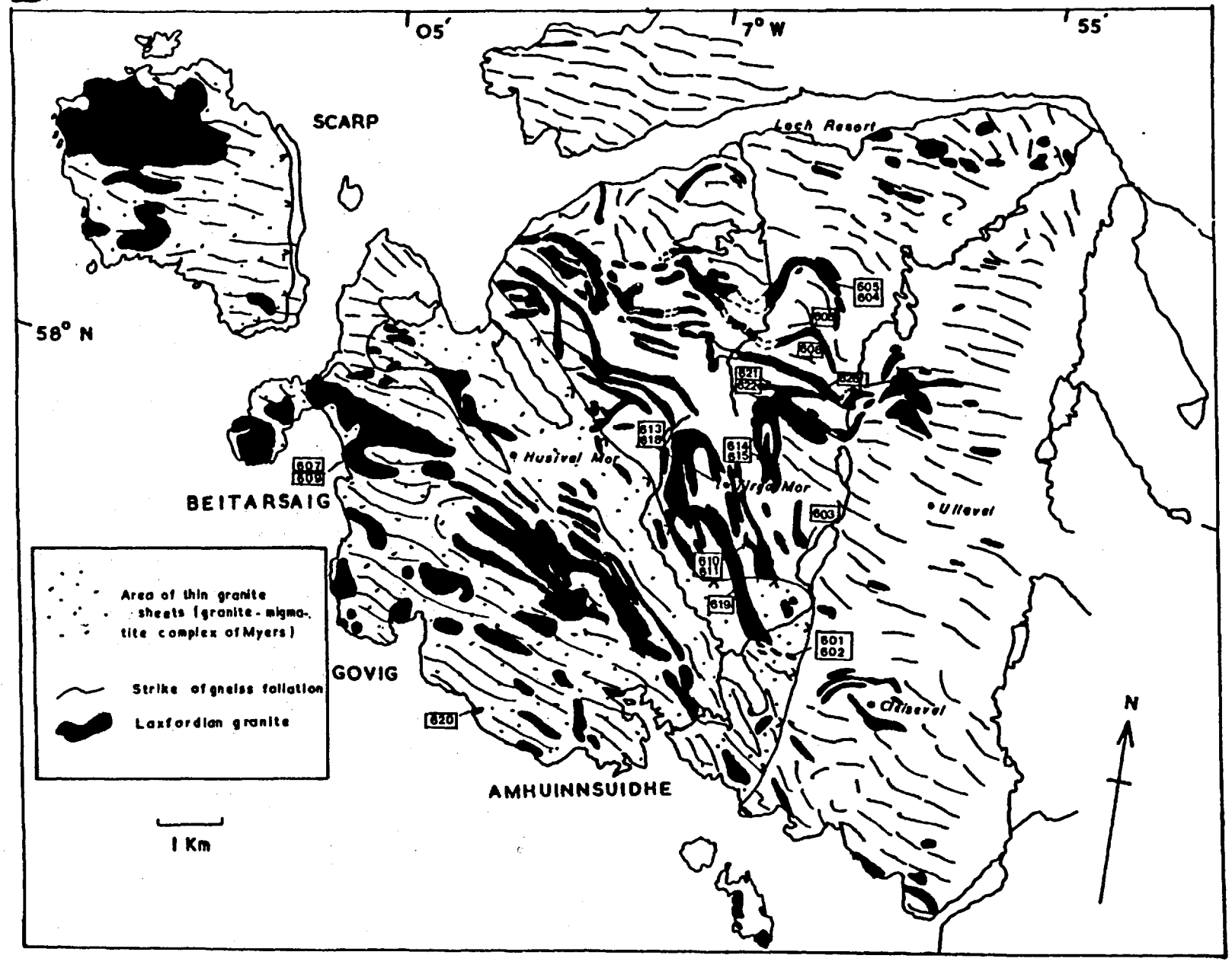
2.1.3 SOUTH HARRIS

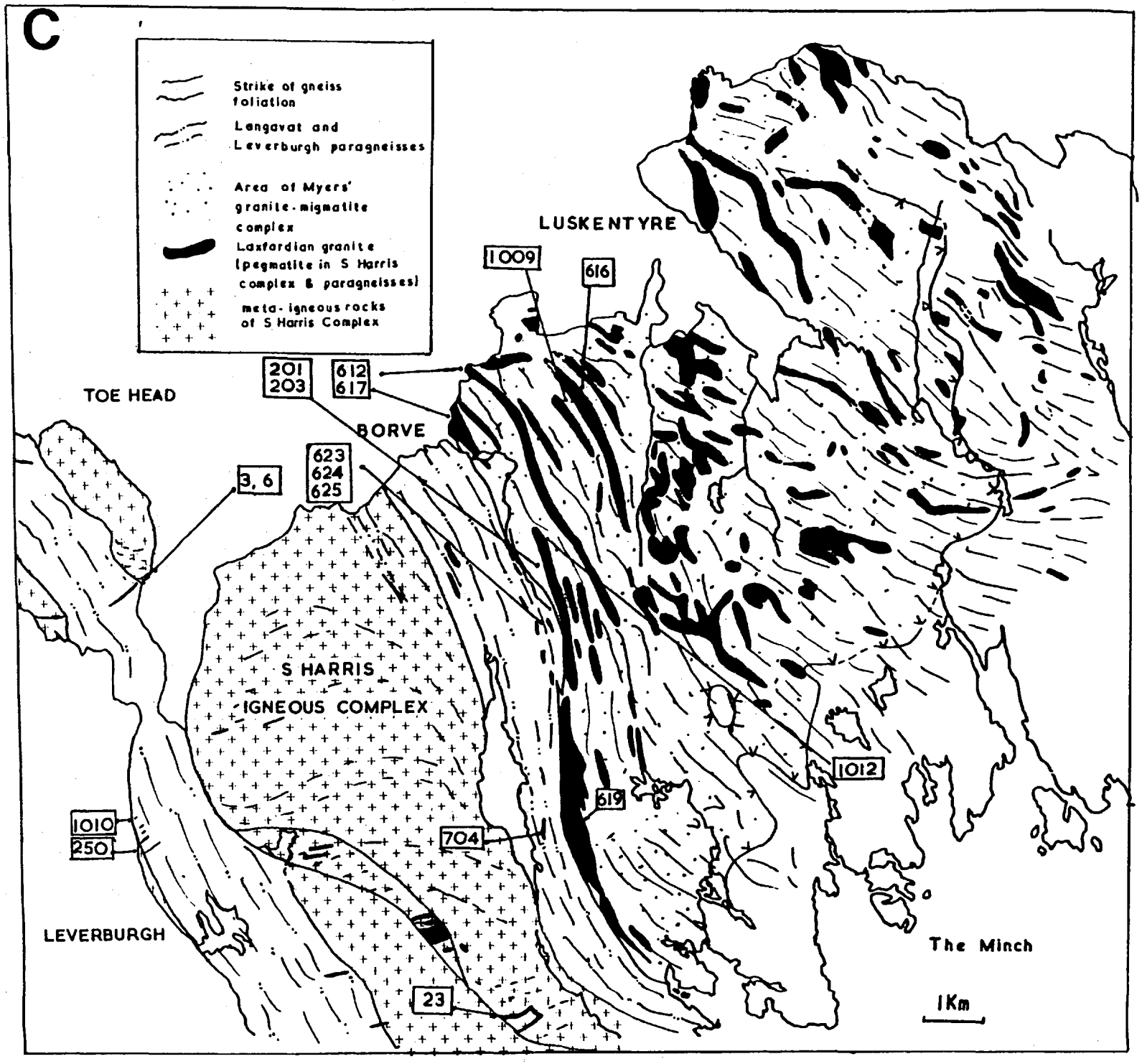
Along the northern side of Loch Langavat (Map 3), all granite and pegmatite intrusions in South Harris are roughly concordant with the NW-SE strike of the grey gneisses. Strike variations may be due to later folding on NE-SW axes (Myers, 1968) or to accommodation of the gneiss foliation around the relatively rigid tonalite which forms most of the South Harris Meta-igneous Complex (Graham, 1980). Towards the SW from Loch Langavat, pegmatites become grossly discordant, striking SW-NE. The interpretation of the structural development given by Graham (1980, see also Chapter 1) would suggest that the fractures occupied by these pegmatites originated at an early stage as shear zones, although their behaviour at the time of pegmatite emplacement must have been essentially brittle. The pegmatites may therefore indicate by their change in orientation an earlier stage of increasingly ductile behaviour of the gneisses to the NE. Dearnley (1962) ascribed this to the effects of the formation of the 'granite'migmatite' complex, and mapped zones of increasing development of retrogressive amphibolite-facies metamorphism in the Igneous Complex towards the NE.





Map 3 Parts of S.W. Lewis (A) and Western Harris (B,C). B,C simplified after Myers, 1971, except for S. Harris Igneous Complex and paragneisses, simplified after Dearnley, 1962 and Graham, 1980.


05'
7° W
55'
SCARP
Loch Resort
58° N
605
604
606
608
621
622
613
618
614
615
Huaival Mor
Tarbert Mor
BEITARSAIG
607
609
603
Ullaval
610
611
619
801
802
GOVIG
620
Clibeval
N
AMHUINNSUIDHE
Area of thin granite sheets (granite-migmatite complex of Myers)
Strike of gneiss foliation
Laxfordian granite
1 Km


C
Strike of gneiss foliation
Lengavat and Leverburgh paragneisses
Area of Myers' granite-migmatite complex
Laxfordian granite (pegmatite in S Harris complex & paragneisses)
meta-igneous rocks of S Harris Complex
LUSKENTYRE
1009
616
201
203
612
617
TOE HEAD
BORVE
623
624
625
3, 6
S HARRIS
IGNEOUS COMPLEX
1012
619
1010
250
704
LEVERBURGH
The Minch
23
1Km

In Section 2.2.2, however, it will be argued that the Harris granites were emplaced into rocks which were already in the lower amphibolite facies, and so the structural and metamorphic gradation mapped by Dearnley (1962) must represent an earlier stage. The point of interest is that the location and orientation of the Laxfordian acid intrusions in South Harris is heterogeneous, not because of spatial variations in stress at the time of their intrusion, but as a reflection of an earlier pattern of heterogeneity which left its mark on both structure and metamorphism.

2.1.4 DISCUSSION AND EXTENSION TO THE REST OF THE LEWISIAN

Consideration of South Harris and the Laxford Front suggests:

(a) terrains of contrasting metamorphic state were juxtaposed early in Lewisian history.

(b) Later deformation and metamorphism were strongly influenced by these early contrasts, and (perhaps because later metamorphic events occurred at successively lower temperatures) granulite terrains appear to have behaved in a progressively more brittle way.

(c) Late reactivation of shear zones is likely to have been a brittle event. Pegmatites and granites may intrude less ductile zones preferentially, and their

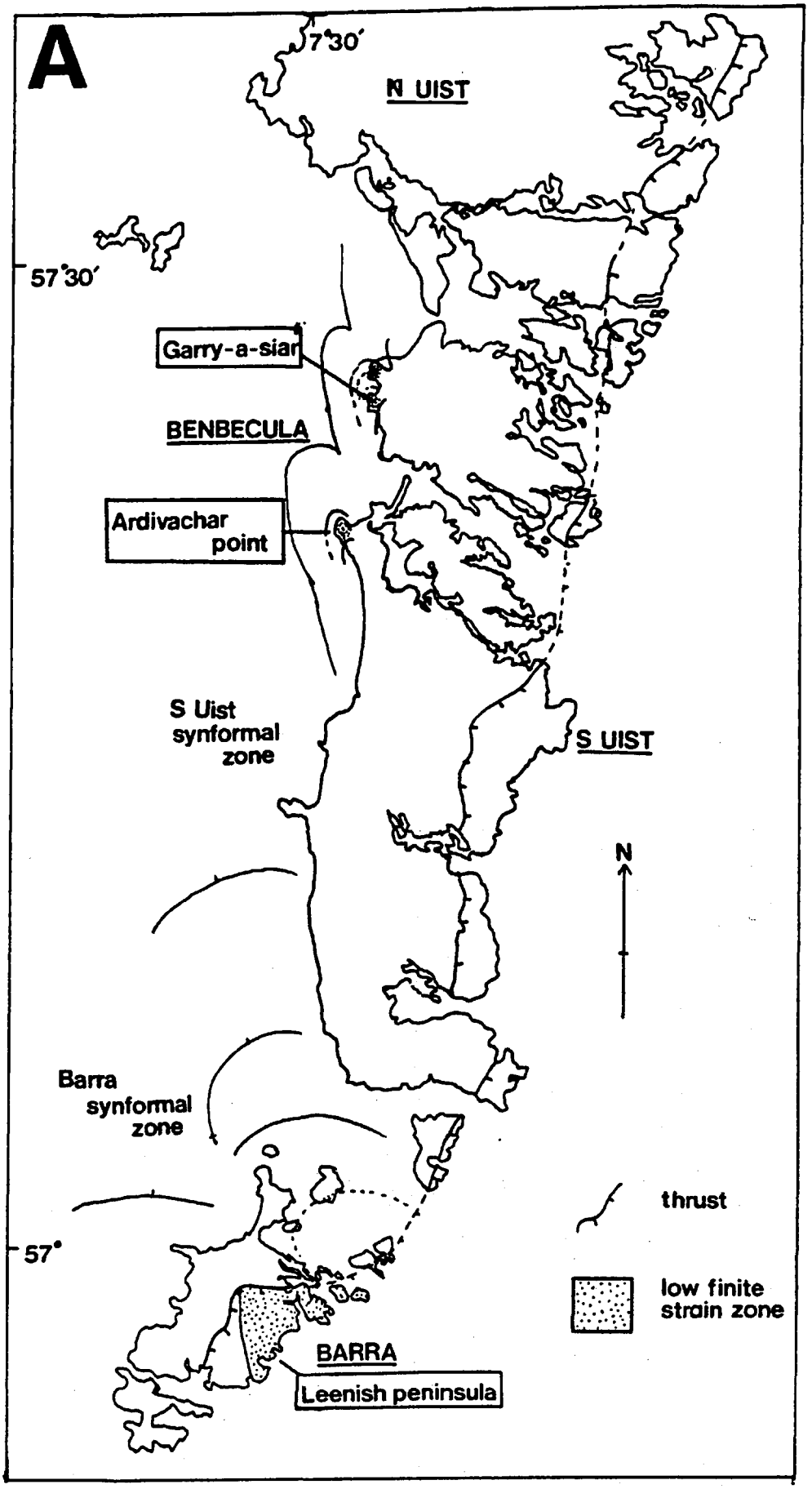
orientation (and, indeed, their presence) provides no evidence about the orientation of syn-intrusive principal stresses, other than to indicate dilation.

(d) Granite sheets are associated only with boundaries where the largest lithological contrasts are seen, and where deep-seated or major shear zones have been inferred (Graham, 1980; Beach et al., 1974).

Coward (1969) and Dearnley and Dunning (1968) have described areas of low Laxfordian strain in the Outer Hebrides, marked by the presence of Scourie dykes with discordant margins. In South Uist, at Ardivachar Point (Dearnley and Dunning, 1968), and on the western coast of Benbecula (Coward, 1969), such low-strain areas are also zones into which Laxfordian pegmatites have been emplaced.

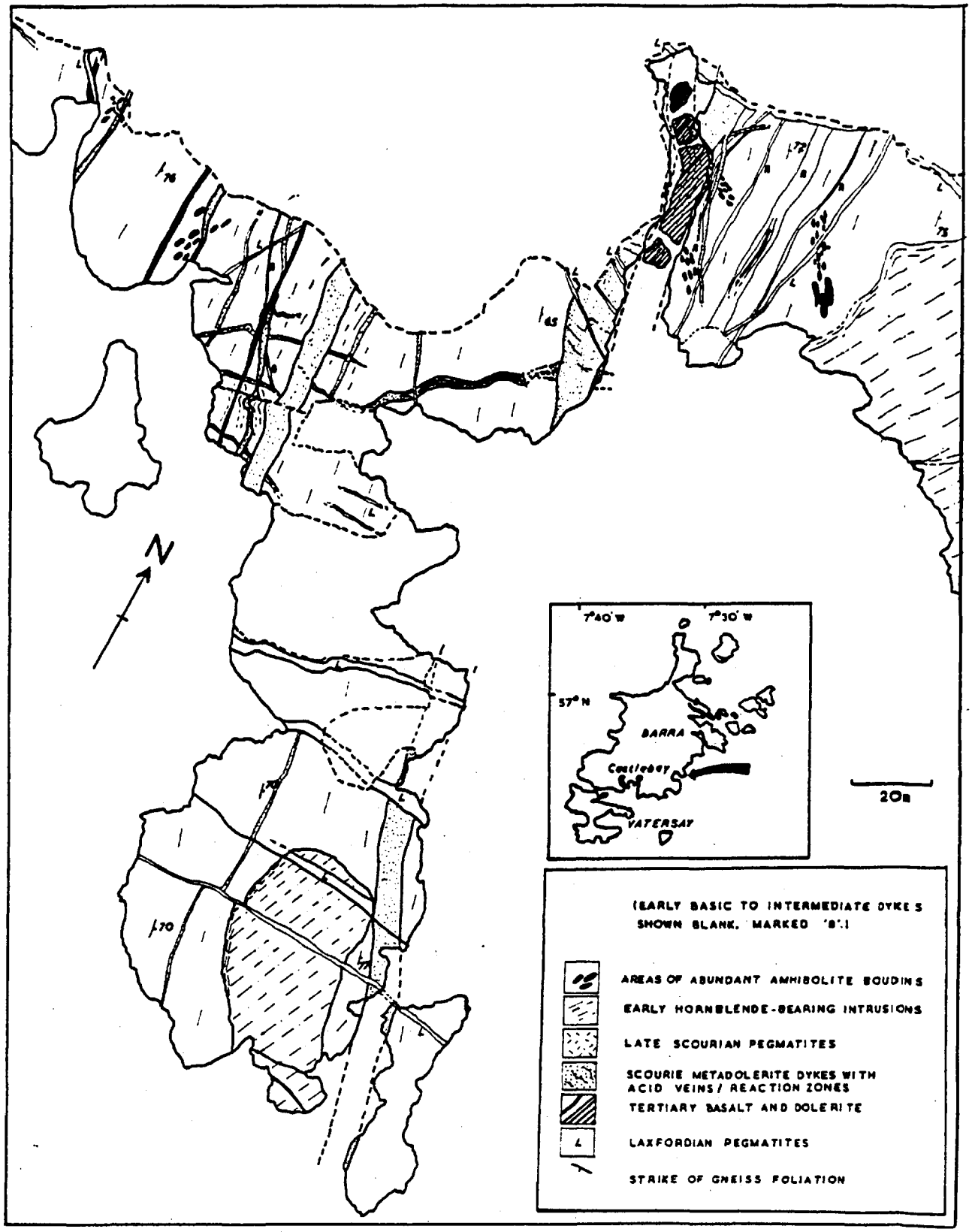
These areas are usually in the antiformal zones of large, cuspate F_3 folds (Coward et al., 1969), although Coward (1969) pointed out that they formed zones resistant to deformation from a much earlier stage. This last point tends to be supported by the presence of a deformed pegmatite of pre-Scourie dyke age at Ardivachar Point.

In Barra, pegmatites of Late Scourian and Laxfordian age are found in the eastern, retrogressed granulite facies gneisses (Francis, 1969; Francis et al., 1973) where relationships between pegmatites, Scourie dykes and earlier basic to intermediate intrusive rocks are clearly displayed at Leenish (Map 4b).



Map 4 The Southern Outer Isles. (A) Distribution of localities, (B) Geology of part of the Leenish peninsula.

B


7°40'W
7°30'W
57°N
BARRA
Castlebay
VATERSAY
20m
(EARLY BASIC TO INTERMEDIATE DYKES SHOWN BLANK, MARKED 'B')
AREAS OF ABUNDANT AMPHIBOLITE BOUDINS
EARLY HORNBLENDE-BEARING INTRUSIONS
LATE SCOURIAN PEGMATITES
SCOURIE METADOLERITE DYKES WITH ACID VEINS / REACTION ZONES
TERTIARY BASALT AND DOLERITE
LAXFORDIAN PEGMATITES
STRIKE OF GNEISS FOLIATION

Finally, in the granulite-facies terrains of the N.W. Scottish mainland, most Late Scourian pegmatites are found on the least-retrogressed area around Scourie, while Laxfordian pegmatites occur sparsely in the granulites, and only in their more-retrogressed marginal parts, a distribution which may reflect the increasing rigidity of the granulites discussed earlier.

It is likely that throughout the Lewisian a pattern of repeated deformation and metamorphism has been influenced by early spatial heterogeneities in the gneisses, and that even in areas where regular metamorphic changes can be mapped, as for example in the Scourie-Laxford area (Sutton and Watson, 1951), the variation may be the composite outcome of several events (Beach et al., 1974).

At Loch Laxford and in South Harris, the strongest lithological (and metamorphic) boundaries trend NW-SE, and may owe this trend to the influence of major crustal shear zones (this seems certain at Loch Laxford). These areas act as loci, however approximate, for granite sheet intrusion, and so the sites of granite emplacement are strongly influenced by these early structures.

In contrast, many Laxfordian pegmatites occur in local low strain zones, owing their location to relatively small-scale heterogeneities in the gneisses. The same contrast of scales may apply to the Late Scourian pegmatites. In this sense, the presence of discordant pegmatites in the Lewisian gneisses may provide a minimum estimate of the time at which different areas were no longer ductilely deformed to any great extent.

2.2 DESCRIPTION OF GRANITES AND PEGMATITES

2.2.1 LAXFORDIAN GRANITES AND RELATED PEGMATITES

A. LAXFORD FRONT

The Laxford granite sheets (The term 'Laxford' granites will be used for the rocks described in this section only, i.e. the granites of Laxfordian age occurring on the Scottish mainland: the more general term 'Laxfordian' granites or pegmatites refers to all the granites, both on the mainland and in Harris and Lewis.) are found immediately to the NNE of the prominent overhang by which the Laxford Front is marked at Rubha Ruadh, Sutherland (Map 2), and can be traced discontinuously along strike as far WSW as the Laxford River. The sheets partly underlie Loch Laxford, forming a string of islands along the SSW shore of the loch. At Rubha Ruadh an almost-complete dip section of about 100 metres across the granites is exposed (Figure 2.1).

The sheets dip steeply SSW, varying in thickness from 1-2m to perhaps 10m, and are interleaved concordantly with basic to intermediate gneisses which form less than 30% of the section. The gneisses show signs of folding and (especially) boudinage which are absent in the granites, and although the latter are quite often concordantly foliated, they clearly have had a much shorter geological history than the gneiss screens, into



Fig 2.1 The Laxford granite sheets at Rubha Ruadh, Sutherland



Fig 2.2 Pegmatite in a Laxford granite sheet

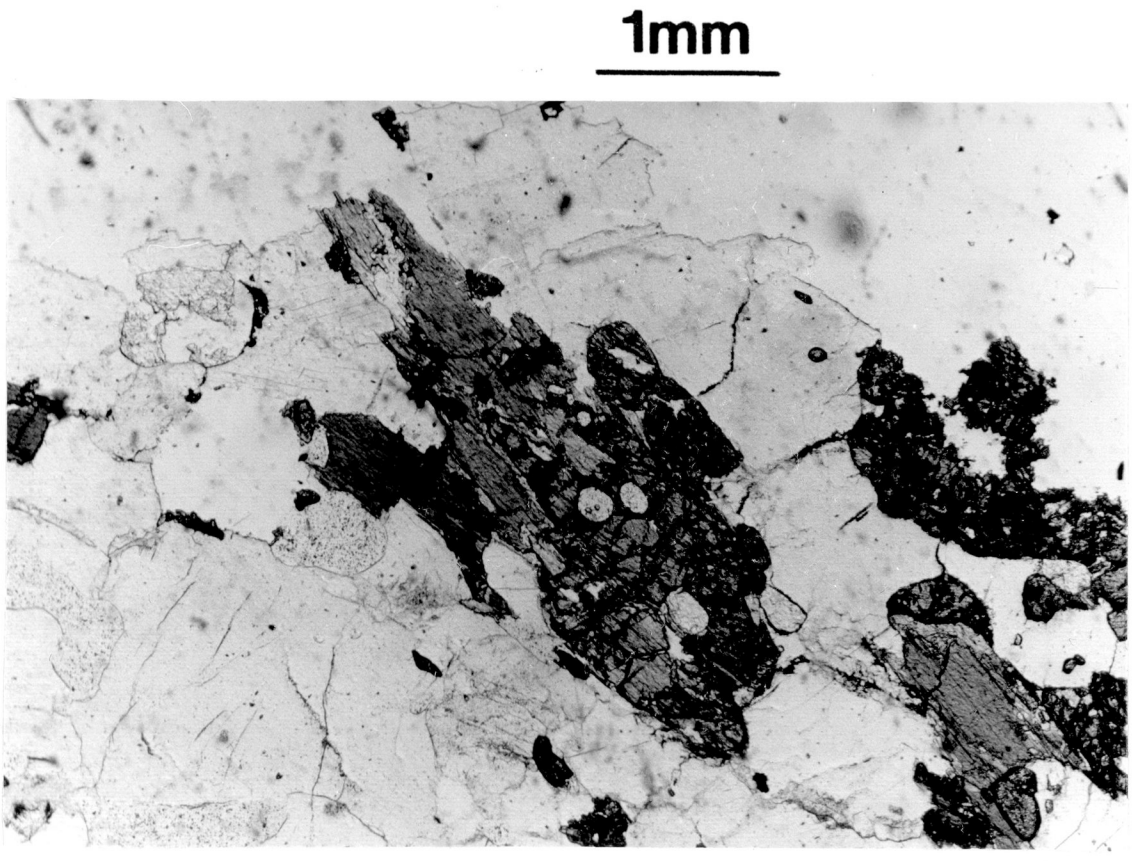


Fig 2.3 Breakdown of clinopyroxene to amphibole and sphene in a Laxford granite

which they are therefore intrusive. The granites are not cut by any later intrusions or veins, except for quite rare and small (usually less than 20cm thick) apparently-cogenetic concordant pegmatites (Fig. 2.2). The pegmatites occur only in the more melanocratic granites, which form about 90% of the total observed thickness of granite sheets and tend to occur mainly in the SSW.

The less-foliated melagranites often contain euhedral green hornblende. In one section clinopyroxene has been seen (Fig. 2.3) reacting to hornblende and sphene. The other major constituents are plagioclase, alkali feldspar, quartz and a green biotite. Zircon, magnetite, sphene and allanite occur as accessories, and epidote may be common. In most foliated samples, hornblende and biotite are replaced by chlorite.

Traces of igneous texture are not easy to identify. Euhedral hornblende and subhedral plagioclase may represent phenocryst phases, but in general recrystallisation has obscured any original igneous relationships. Plagioclase usually has an albite-richer rim, presumably formed during cooling. Alkali feldspar is only rarely perthitic, and then, usually in response to deformation, patchily.

The pegmatites are often noded (Fig. 2.2) and clearly deflect the granite foliation. Relative to the granites they are leucocratic, often apparently richer in plagioclase relative to alkali feldspar. They are unfoliated.

B. HARRIS AND LEWIS

The Outer Hebrides granites are much less localised than those found at the Laxford Front, extending as a broad but elongated belt of granite sheets which in South Harris often strikes parallel to the country rocks, but which as a whole, as it extends into N.W. Harris and S.W. Lewis, is oblique both to the strike of the individual granite sheets and country rocks. Overall, the individual granite sheets may have a crude en echelon relationship with the region or belt into which they are emplaced, and although the analogy with tension gash formation will not be stressed here, for descriptive purposes the relationship could be said to be sinistral.

In Lewis, as Myers (1970) pointed out, exposure is poor over large areas, and the relationships between the Uig Hills, where quite massive granite sheets occur, and the west coast, where granites and pegmatites form complex, cross-cutting sequences of relatively small veins, are unknown. A comparable east-to-west variation in the size of the sheets occurs in west Harris (Myers, 1968, 1971), although here the granites are much more strongly constrained in their orientation to a fairly constant, planar dip, in contrast to the often-winding veins of the Lewis coast. Variations in structural control may account for all these contrasts.

As at Loch Laxford, a minor proportion (again, perhaps 10%) of the granite sheets are leucogranites, although their distribution does not appear to be systematic. Most of the granites are foliated, or show a strong mineral (biotite) preferred orientation. In some, the foliation is emphasised by a close-spaced fracture cleavage. In all cases, foliation is concordant. Xenoliths are uncommon, although locally (at Beitarsaig, N.W. Harris) they may be abundant. Here the more acid and intermediate xenoliths may be almost completely assimilated (Fig. 2.4). Streaky coarse patches occur in the granites around xenoliths and sometimes near the hanging wall of the more massive sheets, which may be up to 30m thick. More sharply-defined pegmatites are common in places, and these tend to be ptygmatically folded (Fig. 2.5), the axial planes and long limbs of folds being invariably concordant with the margins of the granite sheets enclosing the pegmatites. This arrangement suggests that pegmatites initially slightly oblique to the sheet margins have been subjected to ductile flattening after their emplacement.

The invariable mineralogy of the Outer Hebrides granites is biotite-plagioclase-alkali feldspar-quartz-allanite/epidote-magnetite, with chlorite forming on foliation planes in the more-deformed granites. Allanite is usually mantled by epidote, and the resulting elongated composite crystal is often overgrown by biotite,



Fig 2.4 Xenoliths in Laxfordian granite sheets, Beitarsaig, N.W. Harris



Fig 2.5 Ptygmatically-folded pegmatites, Colluscarve, N.W. Harris

the whole aggregate tending to show a preferred orientation. Even more than is the case with the Loch Laxford granites, these rocks lack identifiable igneous textures, and may be texturally indistinguishable from the enclosing grey gneisses, the latter even commonly containing the same allanite/epidote/biotite composite grains.

Myers (1971) described cataclastic textures which are more strongly developed in the granites than in the grey gneisses enclosing them.

The associated pegmatites tend to be almost alkali feldspar-quartz rocks, in contrast to the plagioclase-rich pegmatites at Loch Laxford.

The nature of the structure and mineralogy of the Harris granites suggests they have equilibrated with the grey gneisses in the lower amphibolite facies, probably simultaneously deforming, at first in a pseudoplastic state (Pitcher, 1978), then perhaps more brittly, allowing the formation of sharply-bounded pegmatites which, along with the granite foliation, were then further deformed. The brittle style of deformation apparently undergone by the Loch Laxford pegmatites relative to the granites may indicate the importance of biotite and chlorite recrystallisation in these late deformation processes. Both groups of granites and pegmatites provide a similar story, of emplacement at fairly modest ambient temperatures into rocks which have had higher-grade early histories.

2.2.2 OTHER LAXFORDIAN PEGMATITES: NORTHERN AND SOUTHERN TYPE

Many pegmatites of Laxfordian age, occurring throughout the Outer Hebrides in particular, are either far removed from any granite intrusion or show no clear evidence of having been evolved from nearby granite sheets. Generally, these bodies occupy less-ductile zones in the amphibolite-facies grey gneisses or the granulites (Section 2.1.4).

In the Harris granite-injection complex, Myers (1968) attempted to set up a complex sequence of pegmatite and granite intrusive veins. Myers distinguished early ("Scourian") pegmatites which formed concordant alkali-feldspar-rich folia in migmatitic grey gneisses as the earliest group, and suggested that the bulk of the remaining pegmatites formed a complex sequence post-dating the emplacement of the Laxfordian granites, and were thus themselves of Laxfordian age. There appears, however, to be no clear evidence that any Laxfordian granites are cut by pegmatites, except in S.W. Lewis, where steep leucogranite veins are cut by coarse pegmatites (Fig. 2.6), but themselves cut earlier pegmatites. In N.W. Harris, despite the concentration of both granite sheets and large pegmatites, no cross-cutting relationships have been observed, except those between closely-related granites and pegmatites described in Section 2.2.2. It

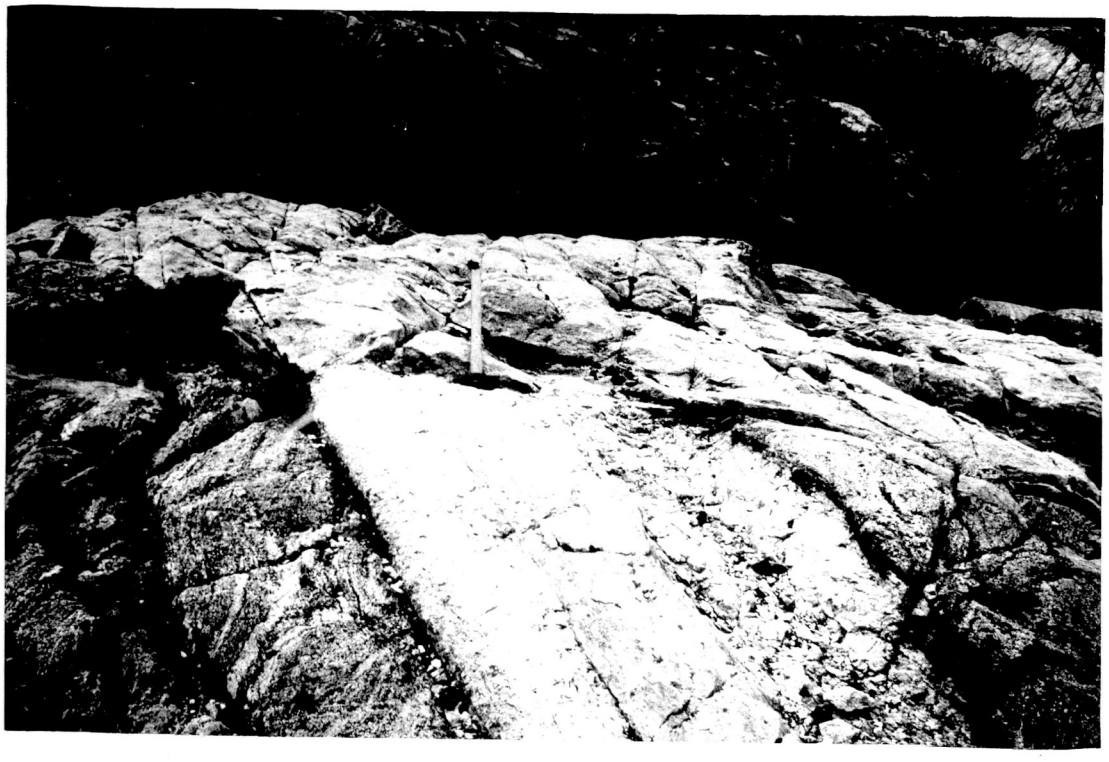


Fig 2.6 Laxfordian pegmatite cut by Laxfordian leucogranite, Mangersta, S.W. Lewis

is suggested that sequences of the type sometimes observed in S.W. Lewis cannot be used generally as a basis for age-classification for Laxfordian acid intrusions, but are valid perhaps only locally, and only when applied to the specific veins observed to cut one another. Consistent with this is the view that Laxfordian acid rocks were generated as a late result of the main Laxfordian cycle of deformation and metamorphism and that variations, either seen locally or when separate areas are compared, are a function of details of their origin and evolution, and are not a key to their relative ages.

In a loose way, it is possible to classify the independent (i.e. unrelated to granites) Laxfordian pegmatites by their mineralogy into two groups. Myers (1968) noted a strong tendency for the 'usual' mineral assemblage (quartz-alkali feldspar-plagioclase-biotite-magnetite-allanite) found in most Laxfordian pegmatites in the granite-injection complex to be replaced by quartz-muscovite-plagioclase-garnet in South Harris, and pegmatites with the latter assemblage dominate the metasedimentary Leverburgh and Langavat belts. Near to Borve, at the NE margin of the Langavat belt, the change is very striking, and coincides exactly with the contact between the metasediments and the granite-injected grey gneisses. Because of this marked contrast, the two pegmatite assemblages will be referred to as 'Northern-type' and

'Southern-type', although Northern-type assemblages are found far to the South, for example in Benbecula and Barra.

Examination of some larger pegmatites shows that the use of these mineral assemblages to discriminate between Northern-type and Southern-type pegmatites is not definitive, since both assemblages may be present. In this case the Southern-type assemblage usually succeeds the Northern-type assemblage, and it is clear that the mineral assemblage is a function of the stage of evolution reached by an individual pegmatite. Only larger bodies contain evidence of these succeeding stages, as might be expected. Nevertheless, the pegmatites as presently exposed do show a spatial variation which corresponds to the Northern-type and Southern-type categories, and these terms will be used to refer to the Laxfordian pegmatites, recognising that they represent only ideal mineral assemblages, and where necessary qualifying the categorisation of individual pegmatites.

Below, several of the larger Laxfordian pegmatites are described in more detail to show the relationship between the two assemblages:

a. Chaipeval, South Harris [NF 983925].

A steeply NW-dipping pegmatite, 3-4m wide, crosses the Toe Head peninsula from SW-NE (Von Knorring and Dearnley, 1960). Northern-type mineralogy is uncommon, and the characteristic minerals of this type are

sometimes found (partly) altered - alkali feldspar is apparently replaced by albite-rich plagioclase, which may completely pseudomorph large crystals, while biotite may be overgrown epitaxially by muscovite. Occasionally, garnet contains magnetite inclusions. The Southern-type assemblage is found in a range of textural associations (Fig. 2.7), and small-scale (1-2cm) zoning is common, with complex interactions between crystal size and concentration, and the presence or absence of muscovite. Such zones may be cut by later veins of similar mineralogy. Curiously, the mineral assemblage becomes quartz-alkali feldspar-muscovite-plagioclase without garnet as the pegmatite passes from the Leverburgh pelitic metasediments north-eastwards into part of the South Harris meta-igneous complex. The change is very sharp, and may be the result of later faulting at this contact, in which case the relationships may suggest an increasingly Northern-type mineralogy with depth.

b. Sletteval, South Harris [NG 060855].

A tuning-fork shaped body, up to 20m wide, consisting mainly of giant alkali feldspar, quartz, plagioclase and biotite crystals. Some of the alkali feldspar crystals are up to 1m long, and are conspicuously growth-zoned, graphic crystals. The zoning is marked by alternate tapering-out and thickening of discontinuous quartz graphic rods and sheets, and also by zones of tiny plagioclase and magnetite inclusions.

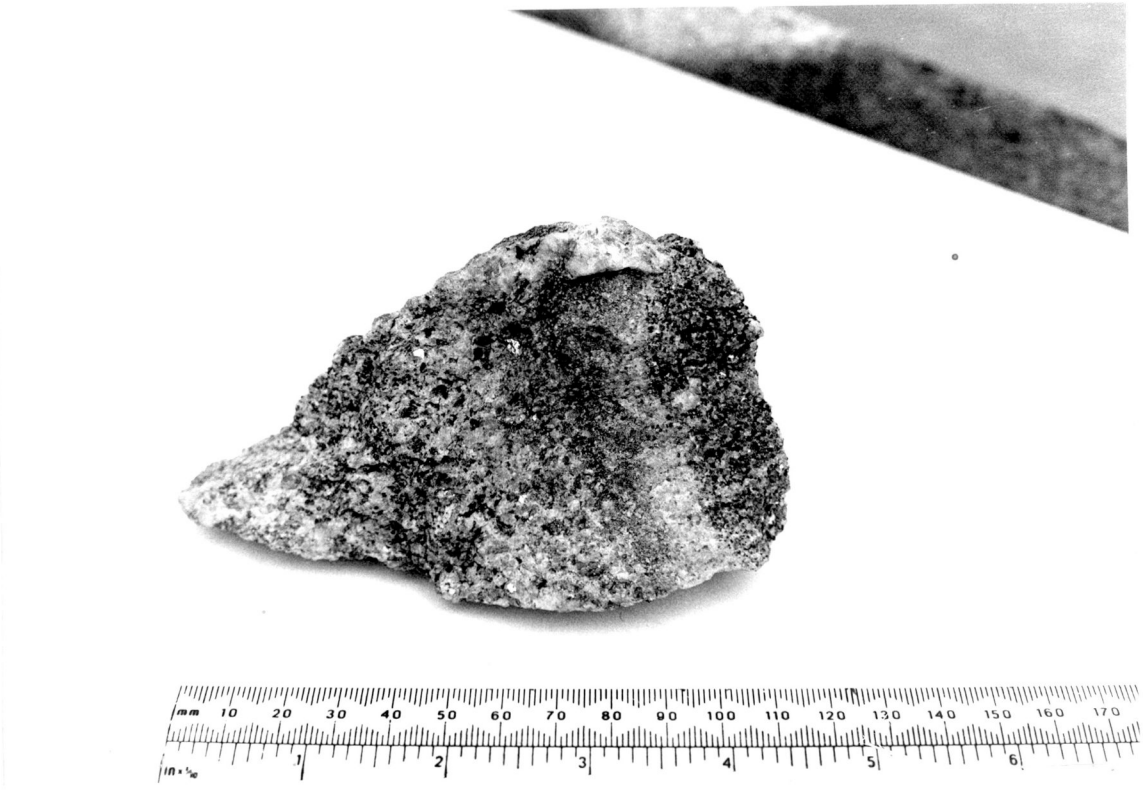


Fig 2.7 Style of zoning in part of the Chaipeval pegmatite, S. Harris

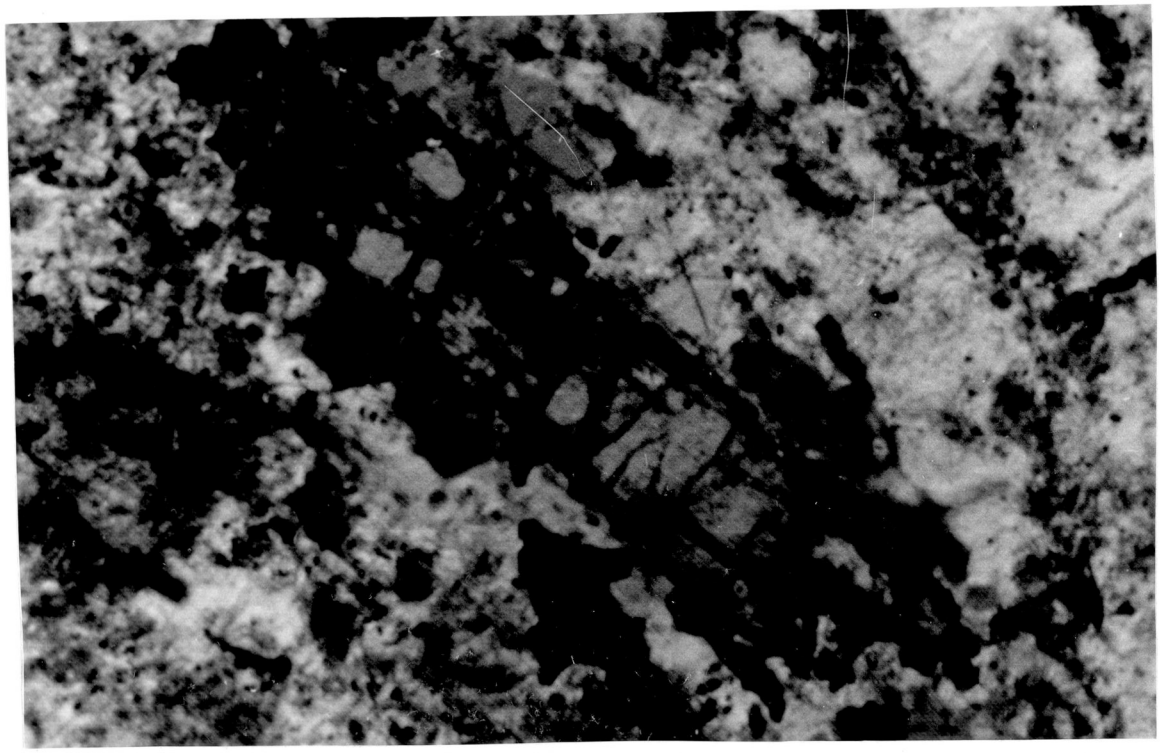


Fig 2.8 Kyanite in a Late Scourian pegmatite, Scourie, Sutherland

Discontinuously, down the centre of the pegmatite, is a zone of Southern-type mineralogy, which may be from 2cm to 0.5m wide. This zone appears to be the last part of the pegmatite to have crystallised.

c. Garry-a-Siar, Benbecula [NF 756534].

(See also Chapter 5).

In the largest pegmatite amongst several which occur along part of the west coast of Benbecula, the dominant mineralogy is again of Northern-type, with very large (2-3m) giant feldspar crystals and biotite books, and some tendency to zoning, with plagioclase dominant at the margins. Emplaced at both margins are patches of aplitic material - fine-grained quartz and feldspar, sometimes with garnet - and muscovite-bearing pegmatitic patches. Again, these areas of Southern-type mineralogy appear to represent the last phase of the pegmatite.

d. Lower Badcall, Sutherland [NC 147 417].

This pegmatite cuts a Scourie metadolerite dyke (Sutton and Watson, 1951), and contains quartz, plagioclase, alkali feldspar, muscovite and garnet. In places, the muscovite-garnet assemblage appears to be breaking down, with biotite as a product mineral. This appears to be the only instance in which a Southern-type assemblage is replaced by Northern-type minerals.

2.2.3 LATE SCOURIAN PEGMATITES

In the Scourie-Badcall area of Sutherland, several late Scourian pegmatites form vertical dykes 2-7m wide. All are giant-textured quartz-alkali feldspar rocks, with varying amounts of plagioclase which occurs either as (?) exsolved rims around alkali feldspars, or as distinct giant crystals. Biotite and large (up to 5cm) magnetite crystals are common, while hornblende crystals reacting marginally to quartz and biotite were found in one pegmatite. In several of these Scourian pegmatites, quartz is bluish and alkali feldspar is brick-red. Most bodies show some evidence of late brittle deformation. Pegmatite strikes vary from E-W to NNE-SSW, the latter being very close to the foliation strike of the Scourian granulites in this area.

A pegmatite at Scouriemore, dated by Giletti et al. (1961) at 2560 m.y.b.p., shows evidence of zoning; an outer coarse zone is succeeded by a giant-feldspar zone and finally by a quartz-rich core. Similar zoning is seen in a pegmatite of similar age at Leenish, Barra (Francis et al., 1971). The giant plagioclases and alkali feldspars at Scouriemore contain 20-30% by volume of quartz in the form of blebs and stringers in a graphic intergrowth.

Xenolithic material is rare in these pegmatites but can be recognised in a pre-Scourie dyke pegmatite at Lower Badcall, where amphibolite balls, which are arguably of tectonic origin and are widespread in the granulite

facies gneisses, are found. Kyanite crystals, which seem likely to be xenocrystic in the sense that they may be derived from pelitic gneiss material, are found in one sample (2009), and are extensively retrogressed, the products including a green biotite (Fig. 2.8). Kyanite is rarely found in Scourian granulites in the Scourie-Badcall area (Beach, 1976), and some rocks are apparently metasedimentary, so the presence of a kyanite-granulite not at present exposed would present no great problem.

The degree of deformation suffered by the Late Scourian pegmatites is extremely variable. At Lower Badcall (Sutton and Watson, 1951) and at Ardivacher Point, S. Uist (Dearnley and Dunning, 1968) [NF 737 456], pegmatites are intensely deformed, the latter in particular being best described as a pegmatitic augen-gneiss. Since the orientation of the pegmatite suggests they may occupy Scourian shear zones, this variable deformation may be the result of continuing heterogeneous reactivation of these shear zones. Although they show little evidence of internal deformation, the Scouriemore and Leenish pegmatites have irregular shapes, sudden kinks in their traces suggesting late offsetting. At Leenish, a 'kink plane' coincides with the gneiss foliation, suggesting some shear parallel to this dominant fabric during or after the formation of the pegmatite. This kink zone contains large irregular concentrations of opaque oxides and zircon, and fairly

abundant monazite. Possibly kinking occurred during crystallisation, the kink forming a natural focus for a 'pocket' of accessory minerals.

Contrasts between the typical mineralogy of the Late Scourian pegmatites and that of the "Northern-type" Laxfordian bodies include the presence of hornblende and coarsely perthitic alkali feldspar in the former, and the apparent absence of allanite, which is common in Laxfordian pegmatites. Monazite has been found in two Late Scourian pegmatites, in association either with zircon and opaque oxides (Barra) or with apatite (Scouriebeag).

CHAPTER 3

GEOCHEMISTRY OF THE GRANITES AND PEGMATITES

3.1 INTRODUCTION

The geochemistry of a range of granites and pegmatites is presented in Appendix 1, and sample locations are indicated on Maps 1-4. The compositions of these rocks are described in Section 3.2, and used in Section 3.3 to assess some of the processes which have influenced the Laxfordian acid intrusive rocks at various stages of their evolution.

Granites and associated pegmatites from Loch Laxford and the Outer Hebrides, and representatives of the Northern-type and Southern-type pegmatites from Harris have been analysed for a range of major and trace elements. Clearly, many giant-textured or massively-zoned pegmatites cannot be analysed in this way, because of the impossibility of obtaining representative samples. Indirect approaches to this problem are made in Chapter 4, by making use of variations in phase chemistry where they can be matched with likely differences in rock chemistry. One object of the present chapter is to provide a framework for such indirect methods. Among the rocks which are for this reason not examined in this chapter are the Late Scourian pegmatites of Sutherland, Barra and South Uist.

The point was made in Chapter 2 that the absence of cross-cutting relationships between the Outer Hebrides granites and the Northern-type pegmatites in Harris makes the relative age-relations of these groups of rocks doubtful. It is suggested that the geochemical nature of the Harris granites and pegmatites is unlikely to resolve this problem, and the approach will be to regard all Laxfordian acid rocks as having been the last expression of the Laxfordian cycle, formed broadly contemporaneously. The evident range of rock types produced during this stage suggests that geochemistry may provide significant evidence about the reasons for their diversity.

3.2 CHEMICAL VARIATIONS

3.2.1 LAXFORDIAN GRANITES AND RELATED PEGMATITES

The Laxfordian granites are oversaturated, peraluminous granites in the sense of Shand (1927), with silica contents typical of the range from granodiorites to granites *sensu stricto*, the latter being overwhelmingly dominant (Fig. 3.1). The relatively narrow range of silica-contents and the dominance of true granites suggests comparisons with the S-type granites of Chappell and White (1974), perhaps surprisingly in view of the paucity of exposed metasedimentary gneisses in the Lewisian (Coward *et al.*, 1969). A further distinctive feature of the silica

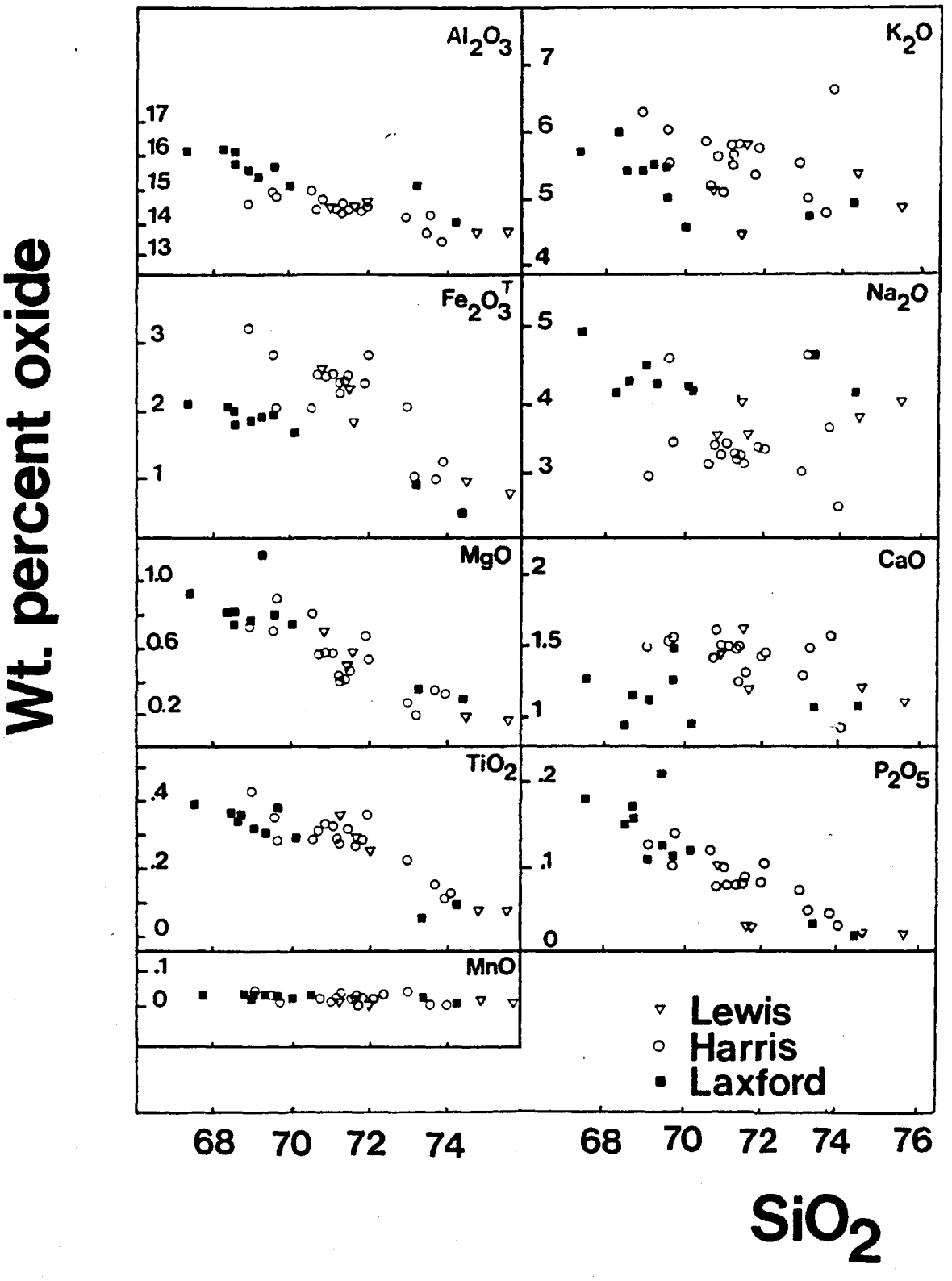


Fig 3.1a Major elements plotted against SiO_2 for the Laxfordian granites.

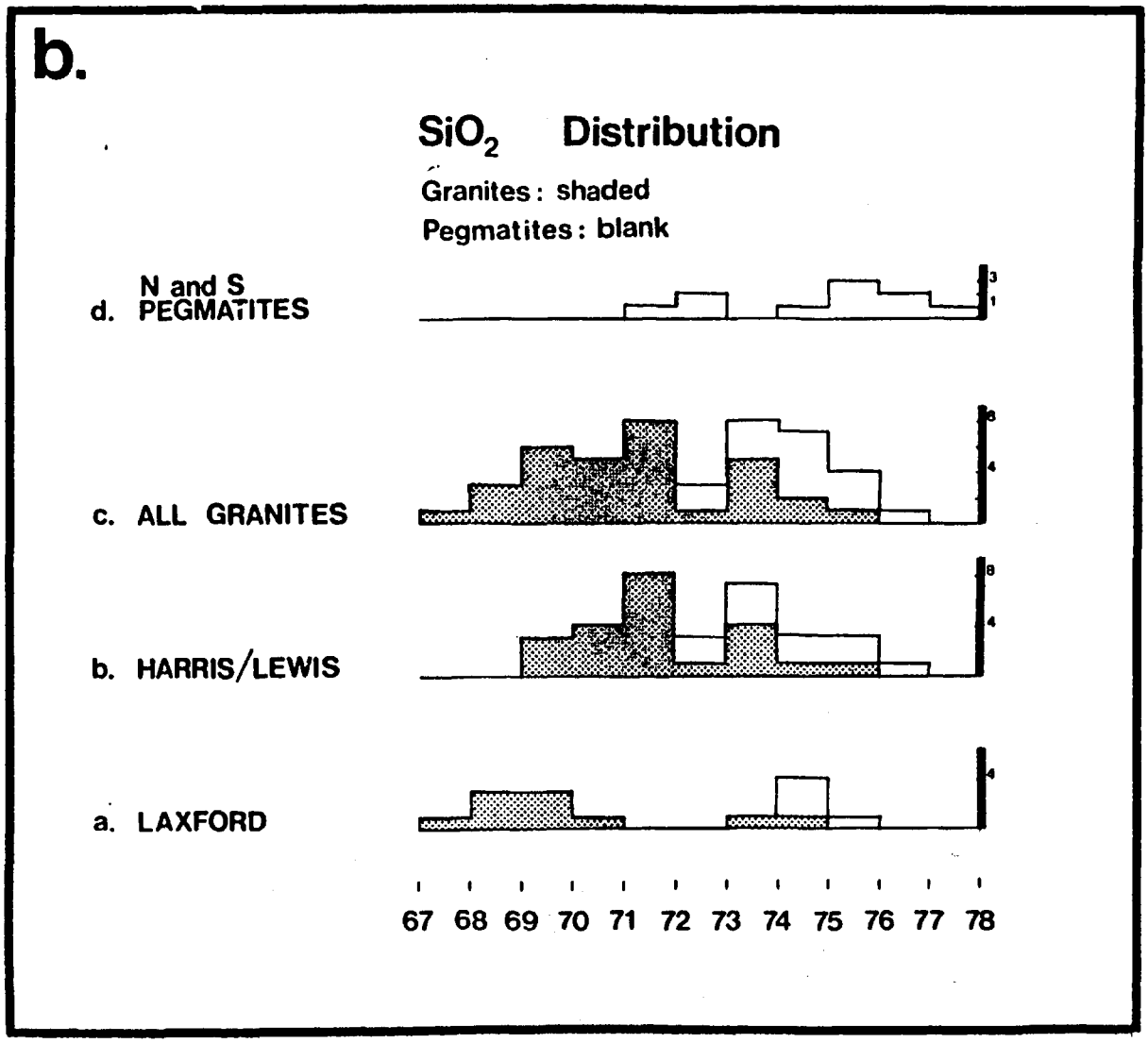


Fig 3.1b distribution of SiO_2 concentrations in the Laxfordian granites and other Laxfordian acid rocks.

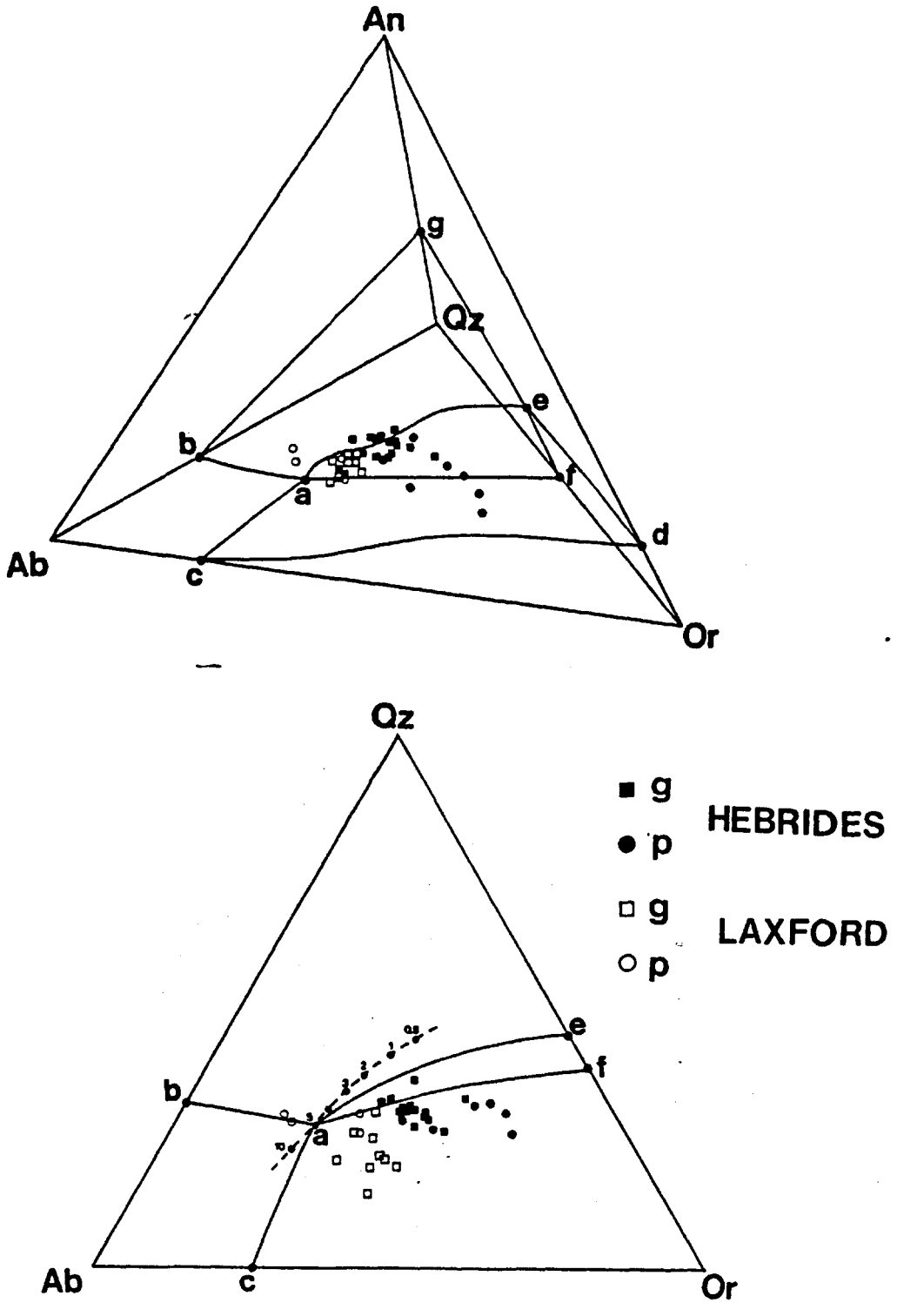


Fig 3.1c Granites and pegmatites plotted in the system Qz-Or-Ab-An
Phase boundaries shown are for P_{H_2O} = 5Kbar (Winkler, 1976).
Dashed curve in Qz-Ab-Or projection shows position of
"minimum melting" point a at a range of water-saturated
pressures from 500bar to 10Kbar(Luth, 1976).

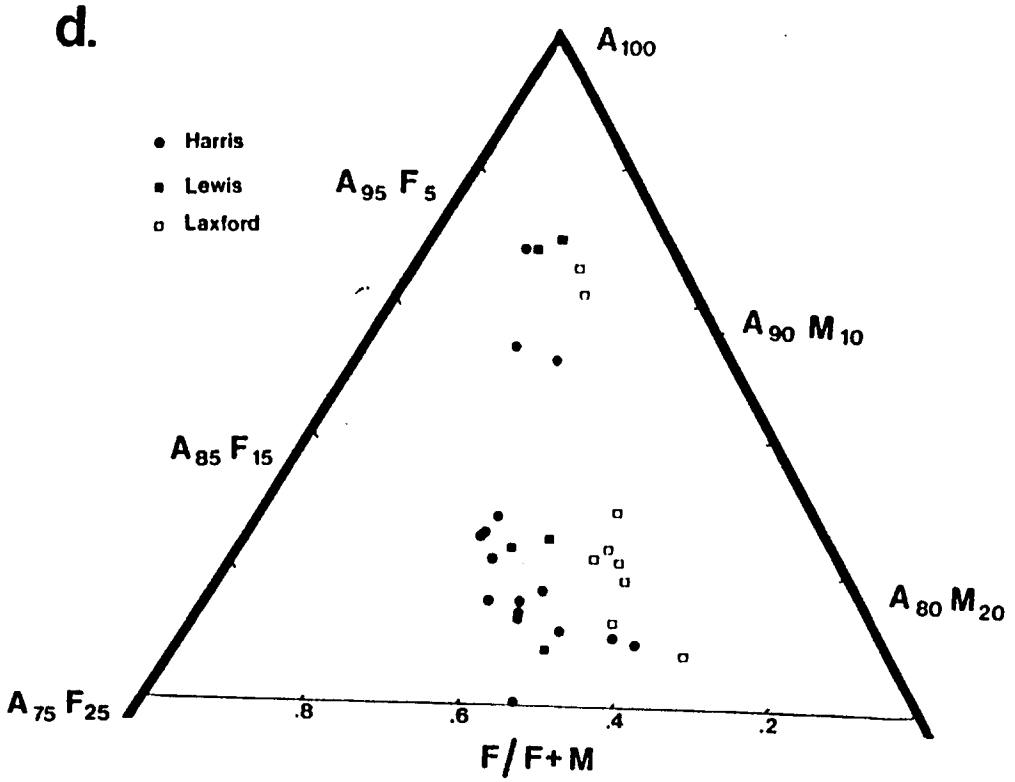


Figure 3.1e – diopside/corundum

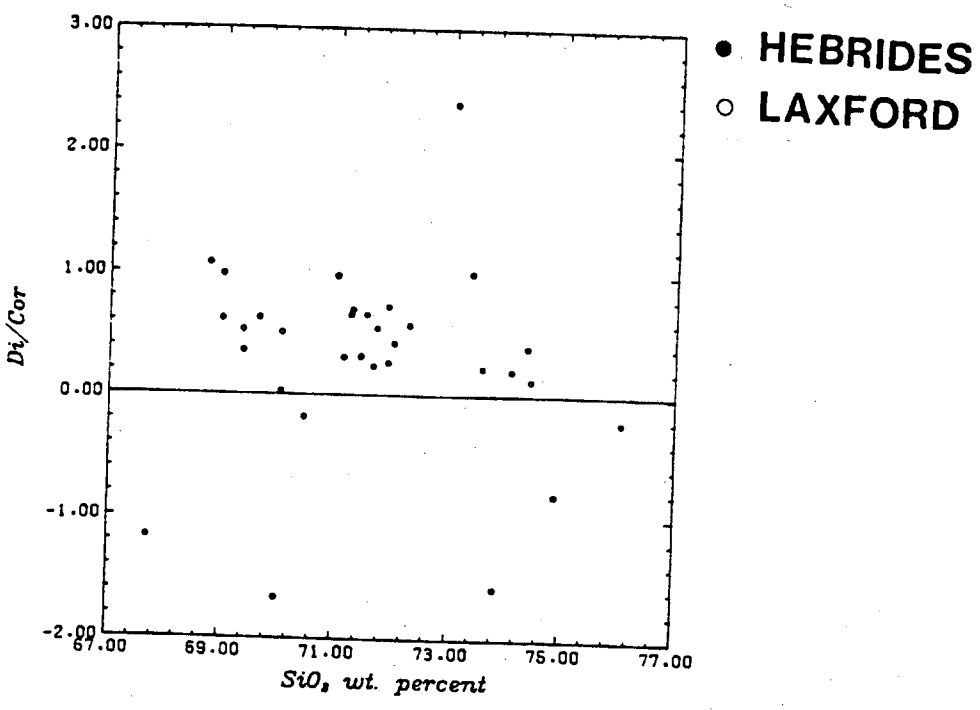


Fig 3.1d AFM diagram

Fig 3.1e Diopside/corundum diagram.

concentrations is their bimodality, both at Loch Laxford and in the Outer Hebrides, with few granites falling in the range 73±1% SiO_2 (Figure 3.1b). This bimodality corresponds to a natural division into melagranites and leucogranites, the latter forming no more than about 10% of the total volume of granites. Figure 3.1b shows that there is a strong overlap in silica-contents between the leucogranites and pegmatites.

Several clear distinctions between the Laxford and Hebrides granites are apparent in Figure 3.1c. The Laxford granites have relatively lower CaO and higher $Na_2O:K_2O$, resulting in rather low normative orthoclase combined with a distinctively albite-rich normative plagioclase composition (Figure 3.1c). F:(F + M) is lower in the Laxford granites (Figure 3.1d). Normative corundum is present inmost Laxfordian granites, showing slightly higher values in the Laxford granites (Figure 3.1e).

Pegmatites associated with both groups of granites display similar major element geochemistry to that of the respective leucogranites (Figure 3.3), except that the difference in alkali concentrations between Loch Laxford and the Outer Hebrides is much more extremely developed. Thus the Laxford granites are associated with pegmatites which have soda:potash ratios rather higher than those of the granites, while the Outer Hebrides pegmatites are much more potassic than the granites with which they are associated.

Furthermore, it is possible to argue that the granites analysed from S.W. Lewis show higher soda:potash

ratios than do the Harris rocks, for a given silica-content. Since a weak trend towards higher soda:potash with increasing silica can be discerned in the Outer Hebrides granites as a whole, it is possible that the granites sampled in S.W. Lewis are generally more evolved than those from Harris, and the relatively weak structural control of granite intrusion in Lewis could indicate that these intrusions are perhaps exposed at a higher structural level.

In summary, the major element concentrations in Laxfordian granites and related pegmatites allow some distinctions to be drawn between rocks sampled in different areas; the clearest contrasts are those between the Loch Laxford and Outer Hebrides granites, although some variation may exist between Harris and Lewis.

The concentrations of a range of trace elements in the granites and pegmatites are shown in Figure 3.2, while chondrite-normalised rare-earth element diagrams are given in Figure 3.4.

In general, the Outer Hebrides granites and pegmatites are richer in Rb, but very much poorer in Sr and Ba than the Laxford granites. While Rb is not unusually low in the Laxford granites when compared with other granites sensu stricto, the levels of Sr (1100-2000ppm) and Ba (3000-5000ppm) are strikingly higher than those expected in typical granites. Krauskopf (1967) for example quotes 600ppm and 285ppm as average values for Ba and Sr respectively in granites, so that the observed concentrations

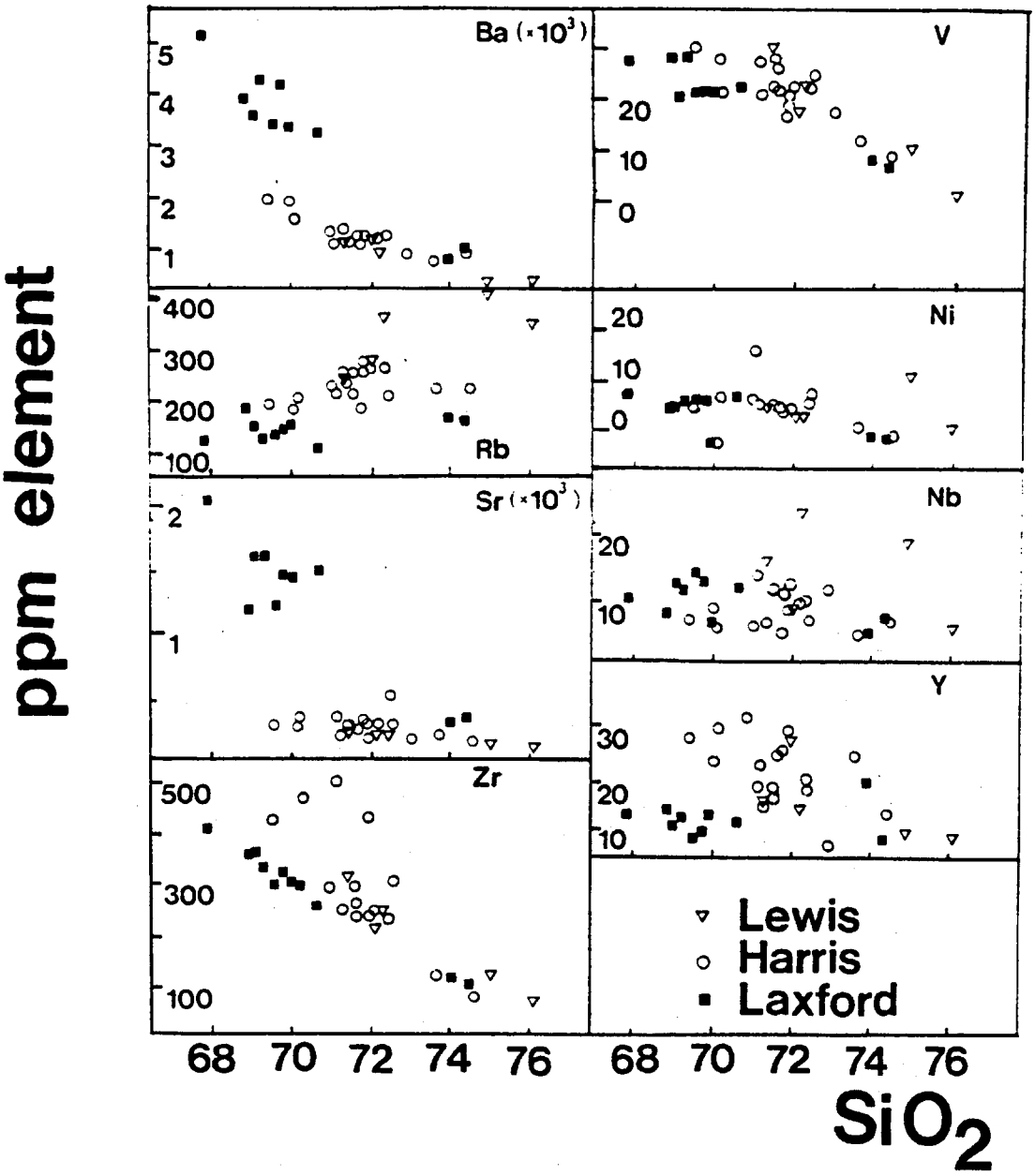
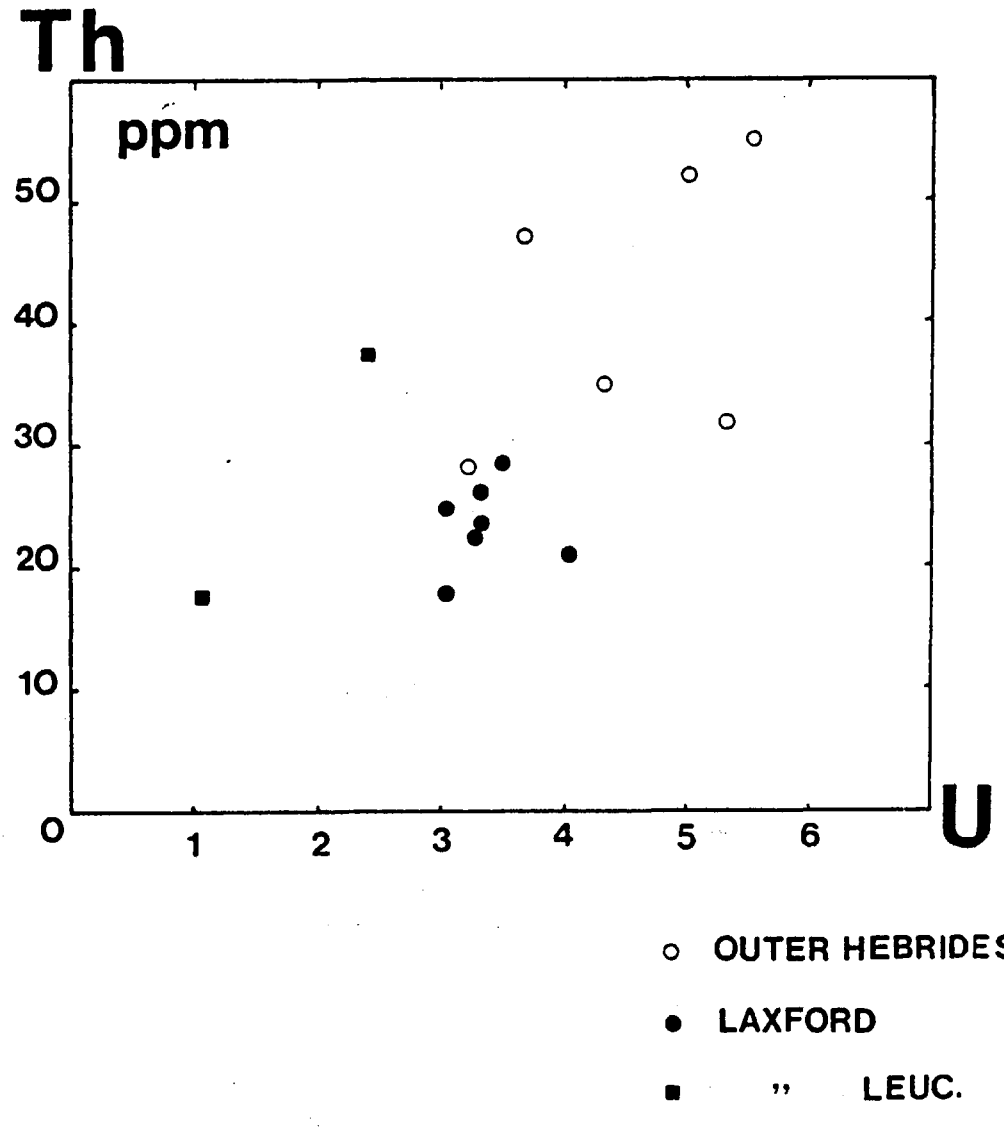


Figure 3.2a Laxfordian granites: trace elements plotted against SiO_2 .



b. Comparison of U and Th in Laxfordian granites from Loch Laxford (including two leucogranites) and the Outer Hebrides.

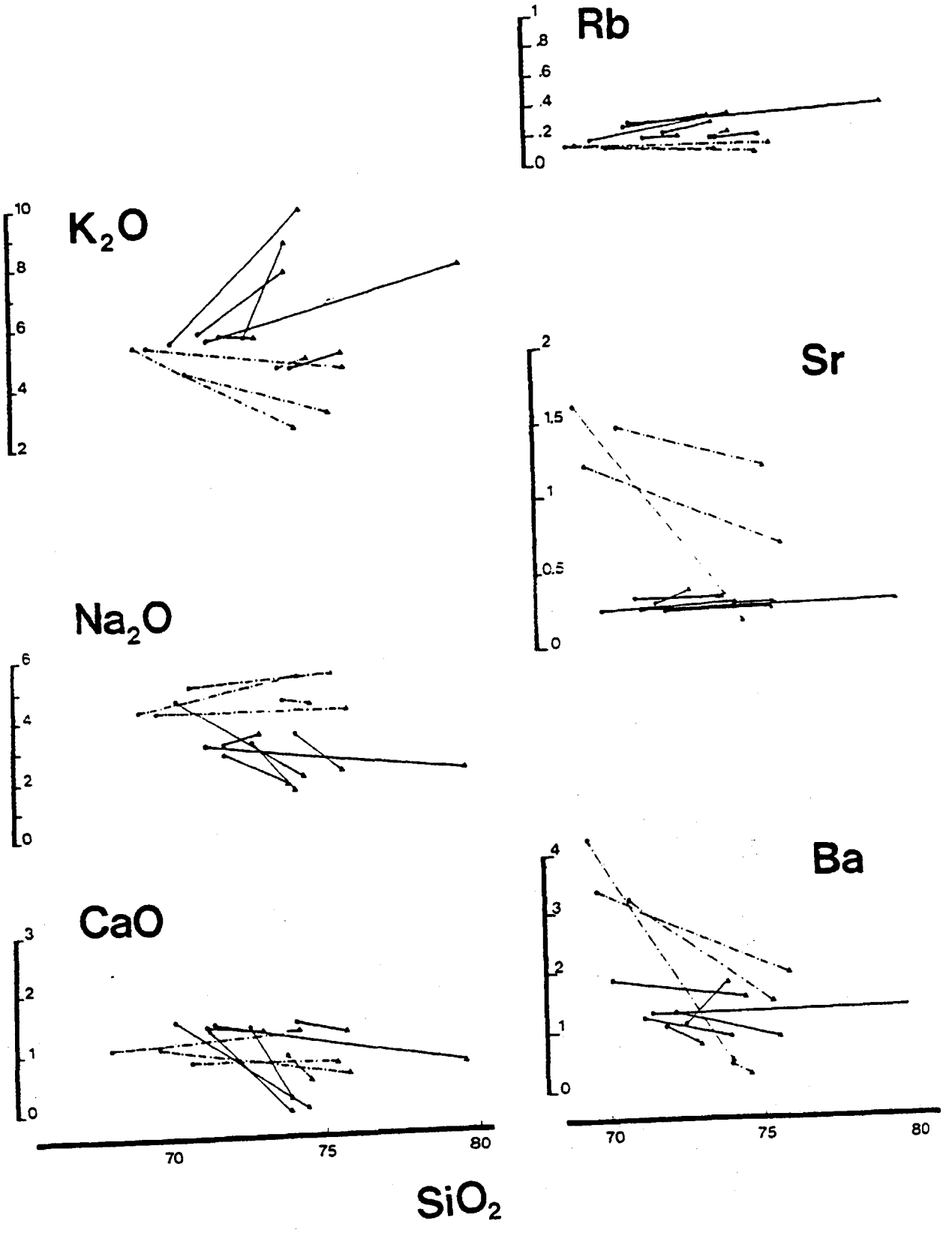


Fig 3.3 Variation of trace element concentrations between coexisting granite-pegmatite pairs . Triangles - pegmatites, circles - granites Solid tielines - Outer Hebrides granites, dot-dash tielines - Laxford granites.

of these elements in the Outer Hebrides granites are normal. Similarly, lavas of rhyolitic composition from recent island-arc suites (Carmichael et al., 1974) do not differ significantly from Krauskopf's (1967) average granite values. Attempts to find rocks with Ba and Sr concentrations similar to those of the Laxford granites lead to peralkaline rocks (e.g. Shonkinites of the Shonkin Sag (Nash and Wilkinson, 1970)) whose compositions are otherwise far removed from the corundum normative Laxford granites, which far from being ultrapotassic have potash concentrations which are probably at the lower end of the granite compositional spectrum.

High Ba and Sr values are more typical of the Laxford melagranites than the leucogranites or pegmatites. The granite-pegmatite pairs shown in Figure 3.3 indicate a fall in Ba and Sr in the pegmatites (if a genetic relationship is assumed). A similar but smaller fall in Ba is apparent in the Outer Hebrides granite-pegmatite pairs, but no clear trend is shown by Sr. Possibly significantly, the most Rb-rich and Ba-poor pegmatites are those analysed from S.W. Lewis, and these rocks are also poor in Sr.

The concentrations of several other trace elements (Figure 3.2) provide further bases for comparison between the Laxford and Outer Hebrides granites. Thus the Laxford granites may be relatively poor in Y, V and Nb, although little difference can be seen in the concentrations of

these elements in the leucogranites. U, and to a lesser extent Th, may be present in relatively lower concentrations in the Laxford granites (Figure 3.2b).

All melagranites have light rare-earth enriched chondrite-normalised patterns (Figure 3.4), in common with most granites. Between La and Tb, the Laxford granites apparently have higher concentrations of each rare-earth element than the Outer Hebrides granites, despite the fact that over this atomic number range their chondrite-normalised patterns are less steep. Between Tb and Yb, the Laxford granites have the steeper patterns, the overall effect being to produce a weakly convex-up rare-earth pattern for the Laxford granites, and a convex-down pattern for the Outer Hebrides granites. The Outer Hebrides granites have a distinct negative Eu anomaly, while a weak anomaly is developed only in the least rare-earth rich Laxford granites. Figure 3.5 shows a clear increase in the size of the negative Eu anomaly in the Laxford granites, both as a function of silica and of $Ce_n:Yb_n$.

Two analysed leucogranites show much less-fractionated rare-earth patterns than do the melagranites, presumably because they have low modal abundances of light rare-earth rich accessory minerals such as allanite.

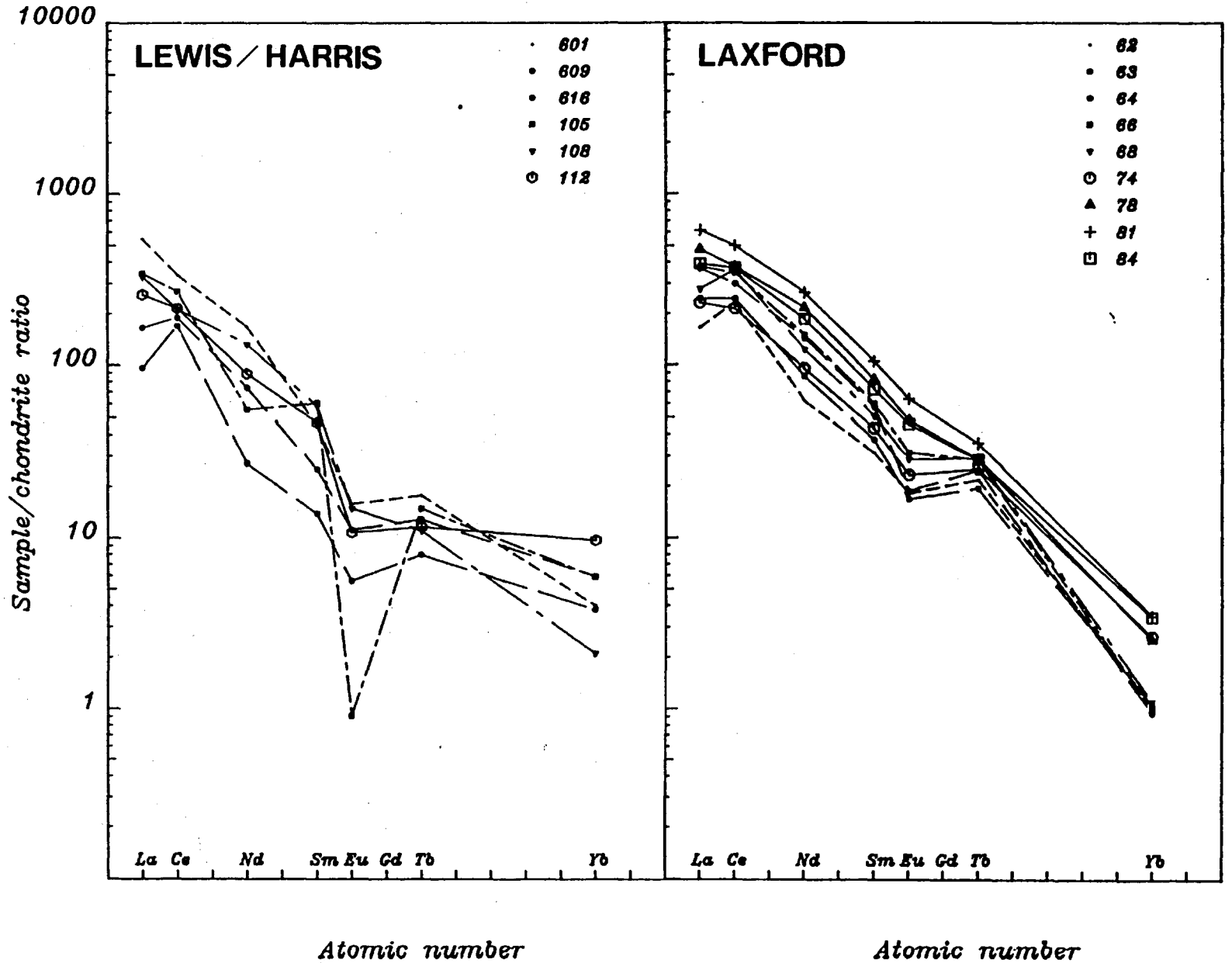
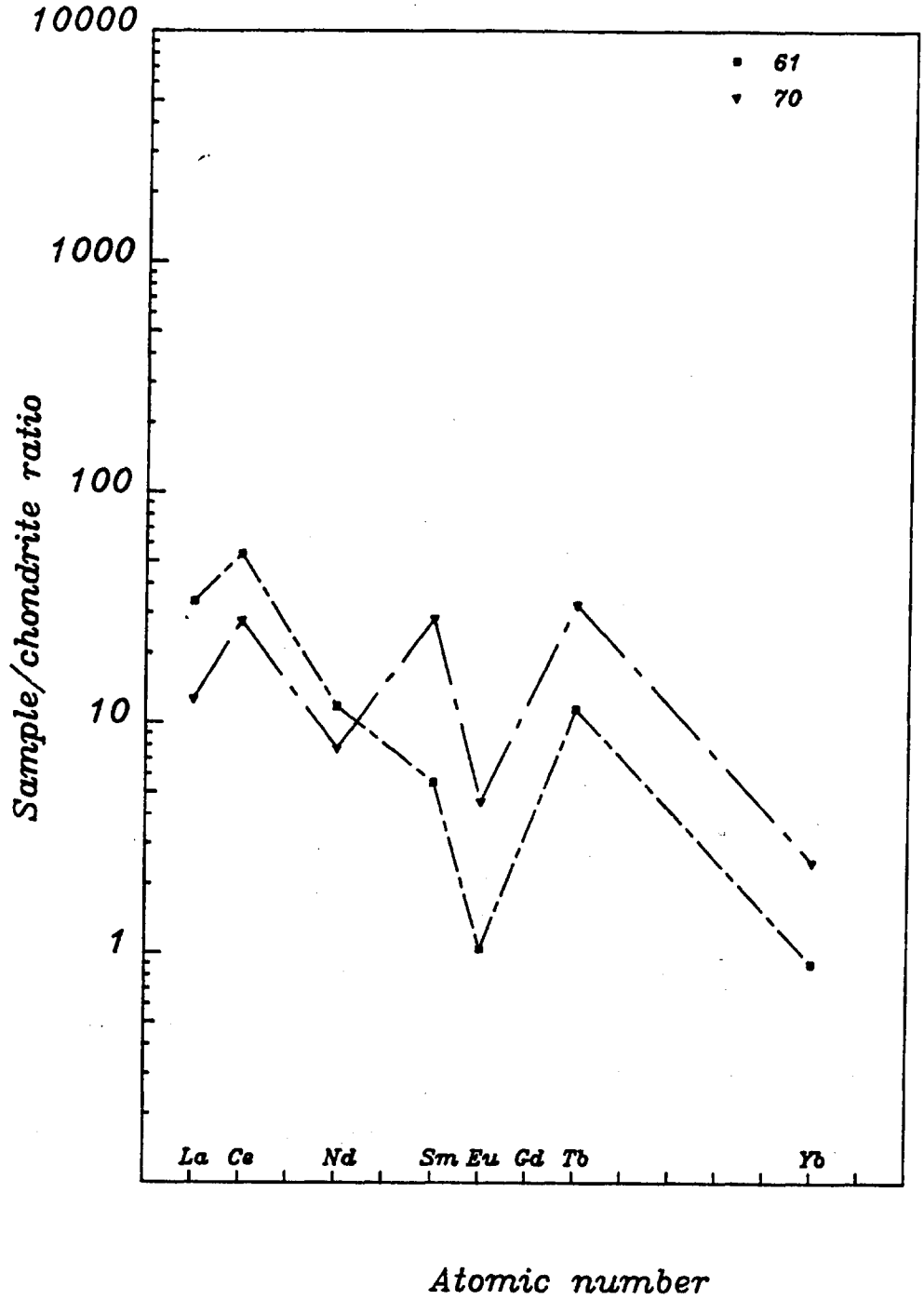


Fig 3.4a REE patterns of the Laxfordian granites



b. Chondrite-normalised rare-earth patterns for two leucogranites from Loch Laxford.

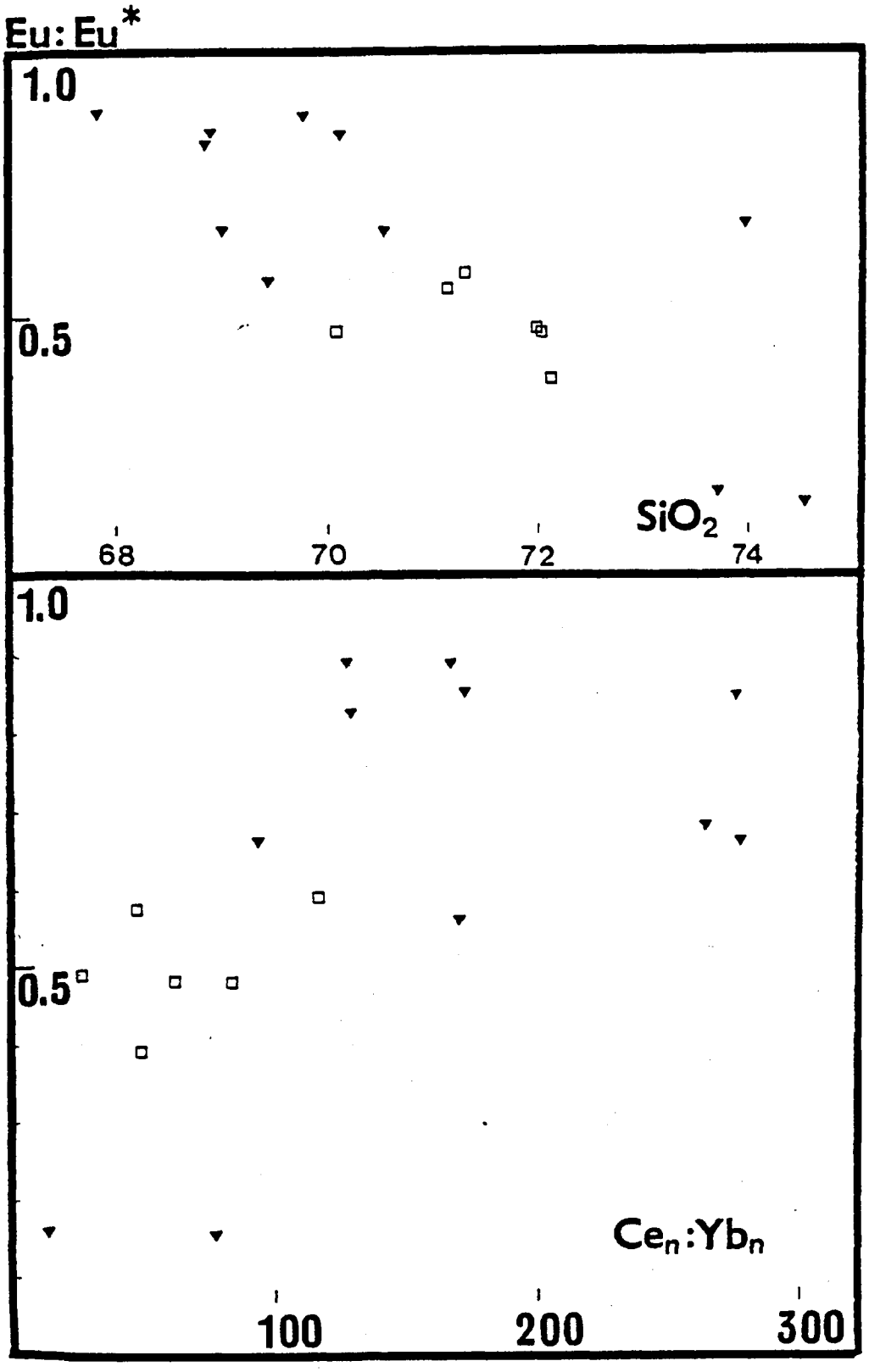


Fig 3.5 Variation of $Eu:Eu^*$ and $Ce_N:Yb_N$ in the Laxfordian granites

Squares - Outer Hebrides granites, Triangles - Laxford granites.

3.2.2 NORTHERN-TYPE AND SOUTHERN-TYPE PEGMATITES

In addition to pegmatites collected in North and South Harris, some intrusions from S.W. Lewis are described in this section. All these pegmatites appear to have originated independently of the Laxfordian granites.

The Southern-type pegmatites of South Harris are poor in Ca and K, and extremely poor in Ba and Sr, while Rb is fairly high. The combination of low K and high Rb is presumably a reflection of the unusual mineralogy of these rocks, in which muscovite and an albite-rich plagioclase predominate. By contrast, the Northern-type pegmatites contain quite large concentrations of Ca and somewhat higher levels of Ba and Sr. K and Rb are low.

These geochemical characteristics are seen in Figure 3.6a where the pegmatites are compared with the rocks described in the previous section. The pegmatites from S.W. Lewis compare most closely with the Southern-type pegmatites, being relatively poor in Ba and Sr and rich in Rb, characteristics which seem to be common also to the granites from Lewis.

In Figure 3.6b, Ca is plotted against Ba for all the rocks described in this and the previous section, and this diagram gives a good impression of the geochemical discontinuities present in the Laxfordian acid rocks.

Pegmatites generated from Laxfordian granites in general contain less Ca and higher concentrations of Ba, while the Northern and Southern-type pegmatites show very low Ba concentrations and contrasting Ca, features which

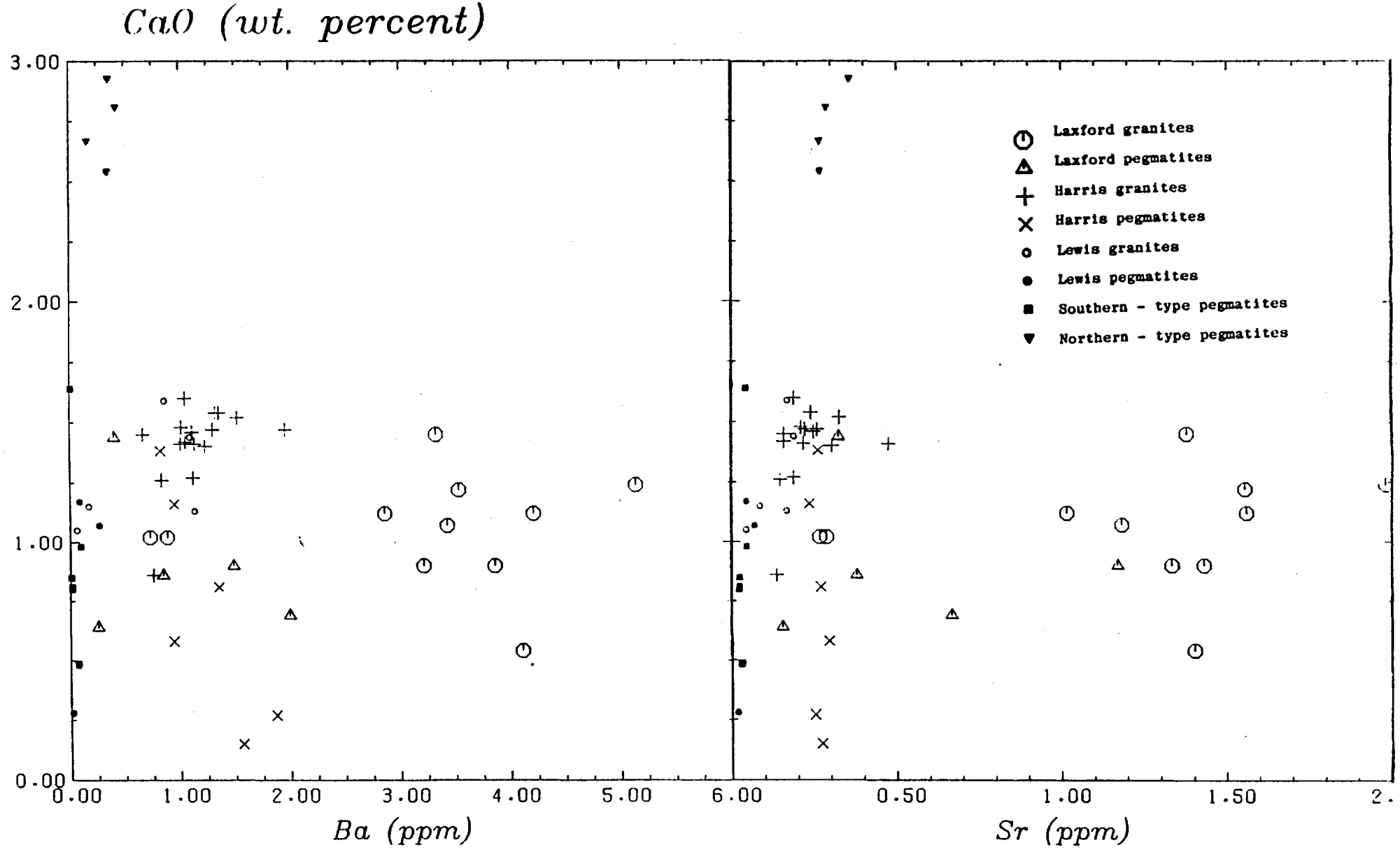


Fig 3.6 Ca plotted against (a) Ba and (b) Sr for various Laxfordian acid rocks . . . . . .

make a common origin for all pegmatites unlikely. Figure 3.6 shows, if the Laxford granites and pegmatites are compared with the Southern-type pegmatites, that low Sr is not simply a function of low Ca or of a normative albite-rich plagioclase.

3.3 DISCUSSION

3.3.1 MAJOR GEOCHEMICAL FEATURES OF THE GRANITES

Despite significant compositional variations within each of the groups of granites from Loch Laxford and the Outer Hebrides respectively, most members of each group show a number of characteristics which suggest distinct origins for the granites found in the two regions. The Laxford granites have relatively high Mg:Fe and Na:K, very high Ba and Sr, high total rare-earth concentrations with chondrite-normalised patterns distinct from those of the Outer Hebrides and a small or negligible Eu anomaly, low Rb, Ca, Ti and Y, low U and Th.

Figure 3.7 shows a range of trace-element concentrations in the Laxford and Outer Hebrides granites, normalised to a standard granite (USGS G-2); also shown are similar patterns for Lewisian granulite-facies and amphibolite-facies grey gneisses. The use of USGS G-2 tends to exaggerate the differences already described in the rare-earth patterns and concentrations of Rb, Sr and Ba. The most obvious contrasts between the patterns for the two groups of granites are seen in Rb, Sr and Ba - the G-2 normalised

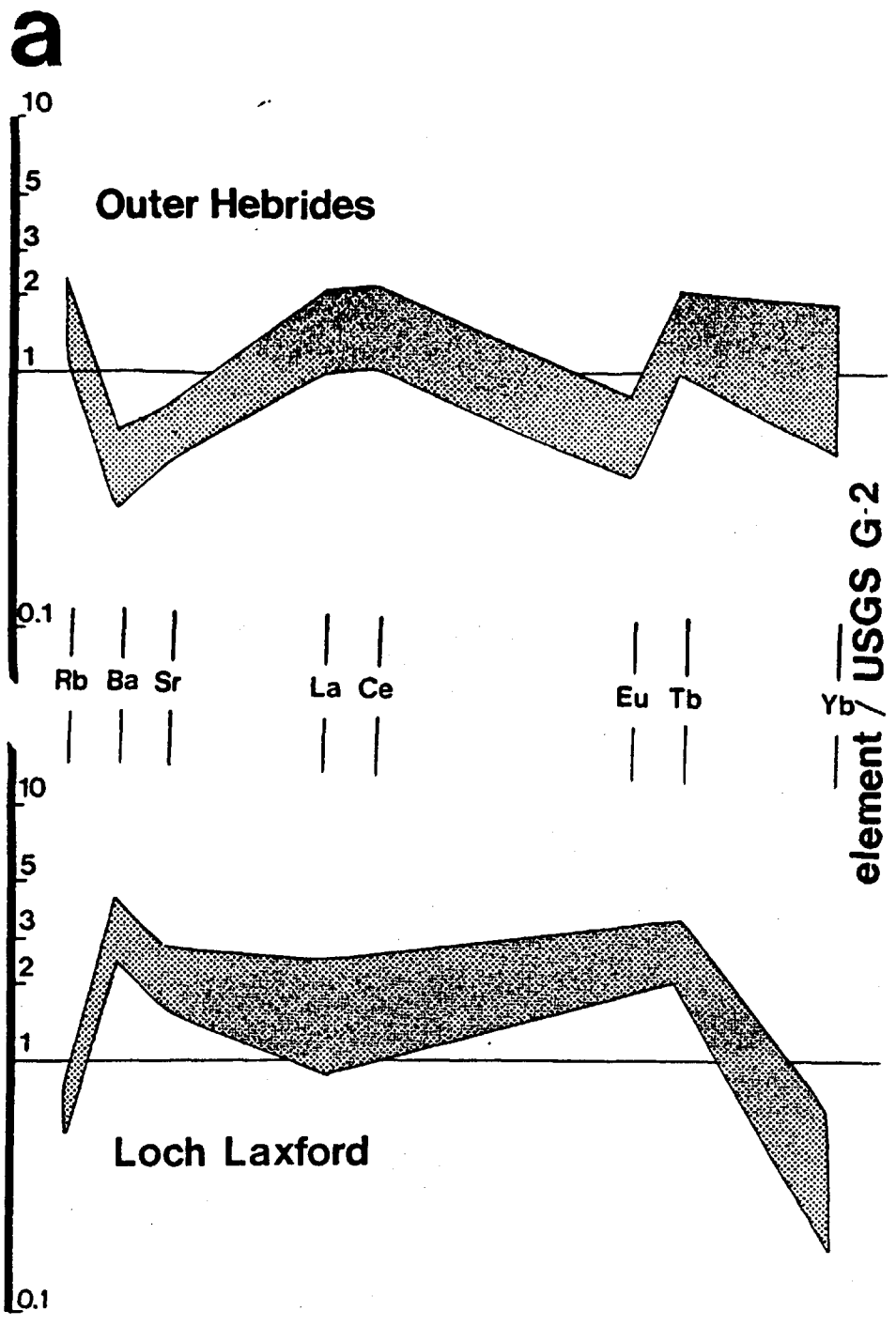
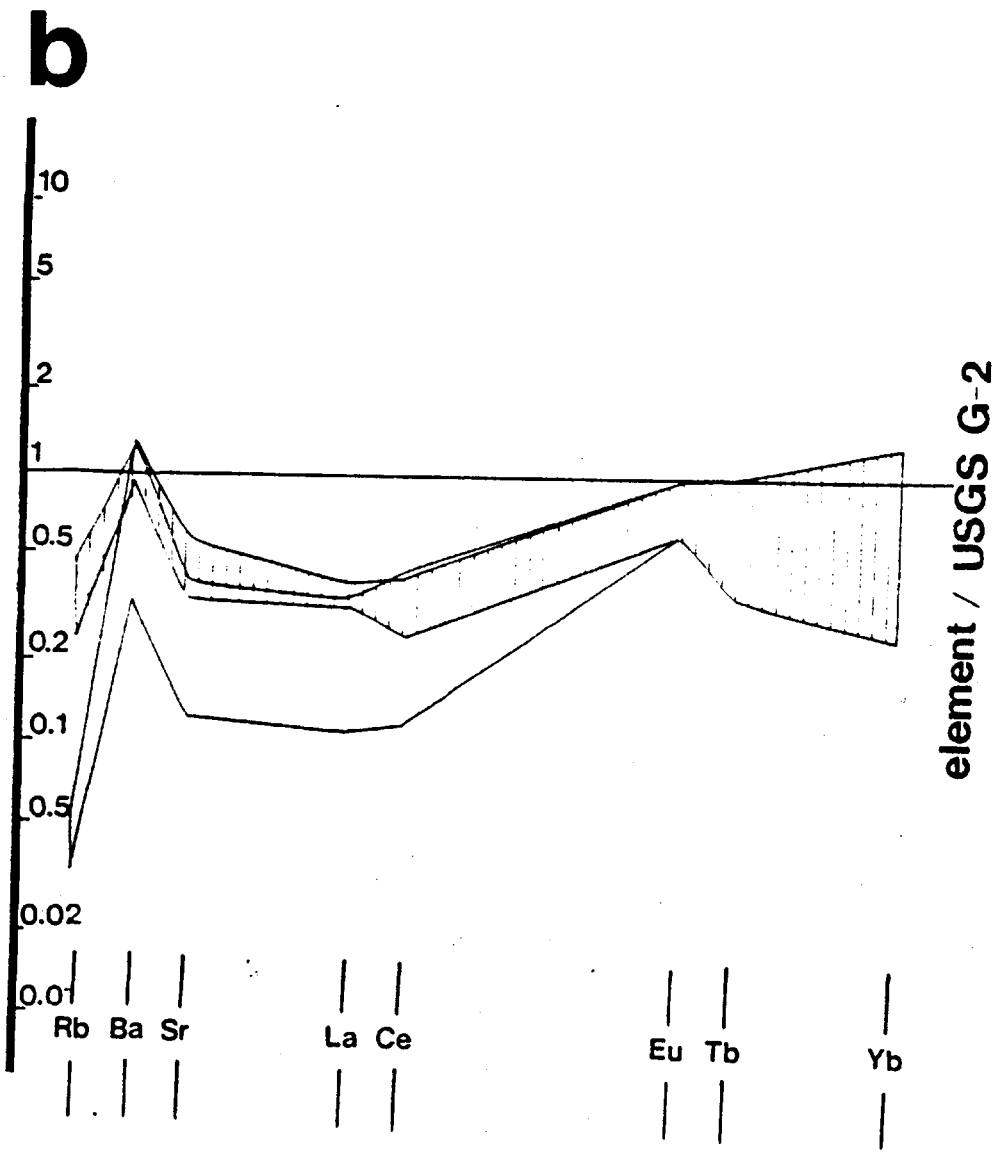


Fig 3.7 USGS G-2 normalised trace element patterns for (a) Laxfordian granites and (b) Lewisian gneisses (amphibolite facies gneisses shaded, granulite facies gneisses left blank.)


b
10
5
2
1
0.5
0.2
0.1
0.5
0.02
0.01
Rb
Ba
Sr
La
Ce
Eu
Tb
Yb
element / USGS G-2

patterns over this range are almost mirror-images. The Lewisian gneisses have patterns similar to those of the Laxford granites, differing from the granites in having lower concentrations of the elements shown, particularly in the case of Rb in the granulite-facies gneisses, and in having lower concentrations of rare-earth elements as well as less-fractionated patterns. The Laxford granites are only slightly more-fractionated in rare-earths than the gneisses except at the heavy rare-earth end of their patterns.

These features can be discussed in relation to two broad hypotheses about the origins of the Laxfordian granites

(a) The granites originated from some source other than the Lewisian basement (i.e. they represent a Proterozoic addition of mantle-derived material to the crust). If this is so, similarities between the patterns for the Laxford granites and grey gneisses in Figure 3.7 would indicate similarities in the fractionation histories of these two groups of rocks distinct from processes which have affected the Outer Hebrides granites.

(b) The granites were derived from the gneisses by partial melting within the crust at some level below that exposed at present. In this case, the Outer Hebrides granites either had a different source from that of the Laxford granites, or they underwent extensive fractionation of some form after melting, while the Laxford granites retained a relatively unchanged distribution of the trace elements of

figure 3.7.

The role of feldspar minerals is clearly of great importance in any proposed evolutionary model involving Ba, Sr, Rb and Eu. Thus it could be argued that plagioclase fractionation (either by fractional crystallisation and separation of plagioclase or by the separation of a magma from a plagioclase-rich residue) must have played a significant part in the development of the Outer Hebrides granites, since they are markedly depleted in Sr and Eu relative to K, Rb, and Ba, while high concentrations of Ba and Sr indicate that no feldspar can have played such a part in the evolution of the Laxford granites, since both would be strongly partitioned into crystallising alkali feldspar and plagioclase respectively.

Tarney et al. (1979), discussing the relatively high concentrations of Ba and Sr in Lewisian granulites when compared with recent volcanic rocks of a similar range of compositions, proposed that deep-crustal fractionation of Hornblende under conditions of high P_{H_2O} gave rise to predominantly-tonalitic rocks with a distinctive chemical signature involving high Ba and Sr. Subsequent granulite-facies metamorphism would tend to strengthen their Ba and Sr-rich character as the fugitive elements K, Rb, Th and U were depleted (Moorbath et al., 1969; Heier, 1973). This depletion is thought by many workers (Tarney et al., 1979; Tarney and Windley, 1977; Hamilton et al., 1980) to be the

result of partitioning of these elements into a metamorphic fluid phase removed during granulite facies dehydration. Other authors (O'Hara, 1977; Pride and Muecke, 1980) suggest the generation of the granulites was associated with the removal of a melt phase. The presence of a distinctive geochemistry is generally agreed, however, even though not all workers would extend such a geochemical model to the lower crust as a whole (Taylor and McLennan, 1979). Examination of the patterns in Figure 3.7 suggests that the amphibolite-facies gneisses are not depleted to the same extent in Rb, and the hydrous mineral assemblages and frequently-migmatitic nature of these rocks would be consistent with the view that they have not undergone the same degree of depletion.

In relation to the present discussion the possibly-unique chemical nature of the granulite facies gneisses offers an opportunity to test models of crustal origin for the Laxfordian granites - the Laxford granites in particular, with high Ba and Sr and low K, Rb, Th and U relative to the Outer Hebrides granites, may have inherited these geochemical features from the granulites.

As stated earlier, high levels of Sr and Ba in the Laxford granites indicate that plagioclase and alkali feldspar cannot have remained as substantial components of a melting residuum, nor can significant volumes of either mineral have separated from an ascending magma. In the case of plagioclase, this argument is not totally exclusive, since the ratio Sr:Ba is lower in the granites than in the Lewisian gneisses, allowing a minor modifying

role to plagioclase. Rb, which should partition into liquids very efficiently during melting (relative to Ba and Sr), seems unexpectedly low in the Laxford granites, with Rb:Sr ratios almost as low as those of the Lewisian granulites. This feature suggests the availability of only small amounts of Rb during the melting process itself.

In Figure 3.8a, the effects of varying degrees of partial melting upon the trace element concentrations of liquids similar in composition to the Laxford granites, and derived from the Lewisian granulites, are shown. For no more than 5% melting, the patterns are reasonably similar to those of the Laxford granites; the generation of melt fractions greater than 5% would rapidly dilute the Rb in the liquid, since Rb partitions very efficiently into melt relative to solids. If Rb concentrations similar to those of the amphibolite-facies grey gneisses are assumed for the parent rock, the same degree of melting would result in Rb concentrations an order of magnitude greater than those actually observed in the Laxford granites. High Sr and Ba in the granites seems intuitively to be in agreement with a rather small melting fraction (not greater than about 5%), and it therefore seems that rocks with concentrations of Rb, Sr and Ba similar to those of the Lewisian gneisses could have provided a crustal source for the Laxford granites if the granites represent compositions not far removed from the primary liquids generated.

A. C_o (granulite facies gneiss): dashed line.

C_l (liquid generated by batch melting of C_o): solid line.
1% melting (upper values) and 5% melting (lower values) with a plagioclase-free a
amphibole-free residuum (60clinopyroxene,40garnet).

B. C_o (felsic amphibolite facies gneiss): dashed line.

C_l : solid line.
20% melting (upper values) with 40% plagioclase in residuum, and 30% melting with
plagioclase in residuum (lower values). Up to 20% residual amphibole.

C_o and C_l are related by

$$C_l/C_o = 1/((D_o - PF) + F)$$ (Shaw, 1970; Hanson, 1978)

where

$$D_o = \Sigma_i^n X^i K_d{}^i$$

$$P = \Sigma_i^n p^i K_d{}^i$$ for any trace element

X^i : weight fraction of phase i in the solid.

$K_d{}^i$: mineral/melt distribution coefficient of a tract element for phase i.

D_o : bulk distribution coefficient of a given trace element at the onset of melting.

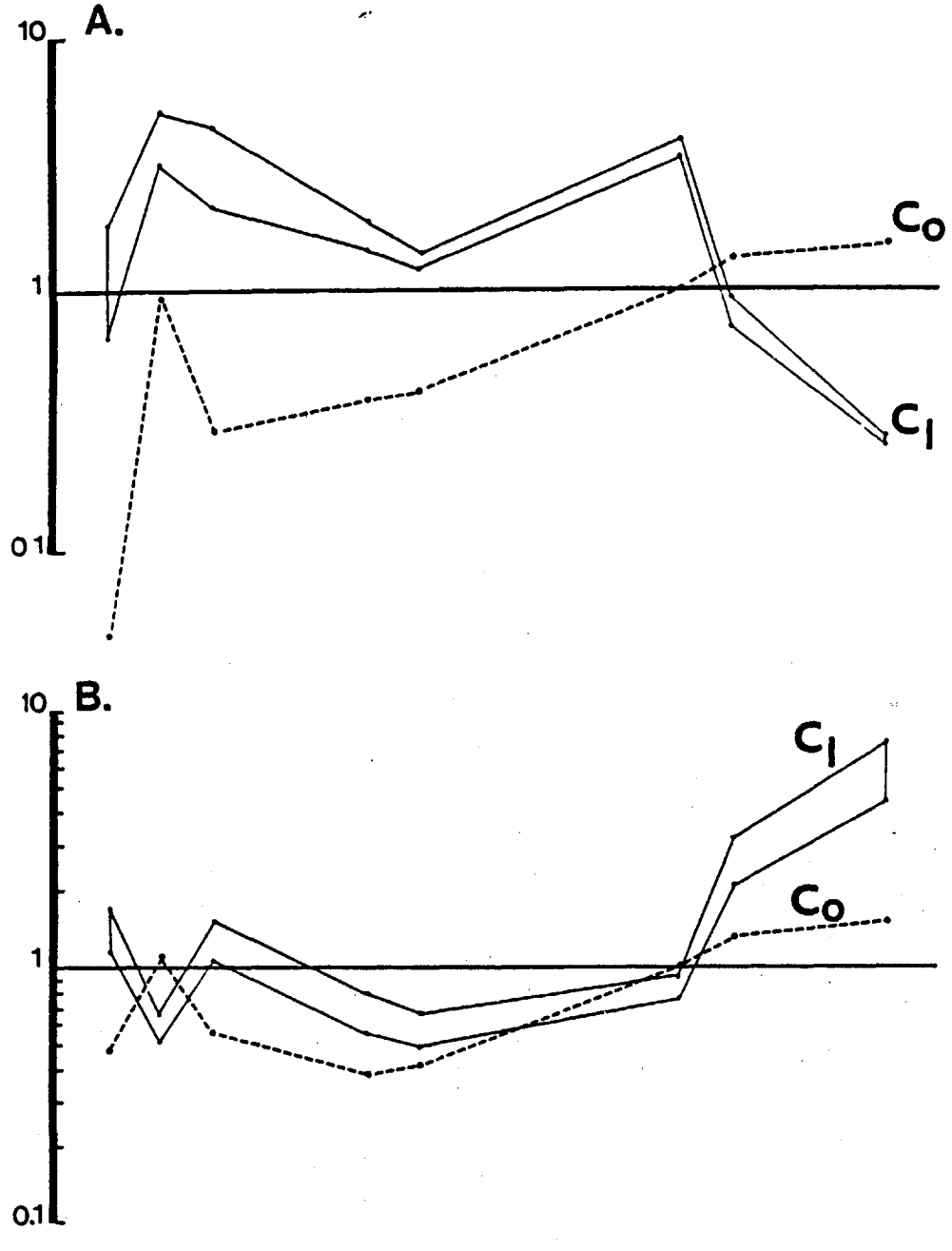
p^i : fractional contribution of phase i to the liquid.

C_o : weight concentration of atrace element in the parent.

C_l : weight concentration of a trace element in a derived melt.

F : weight fraction of melt relative to original parent.

Fig 3.8 Trace element models for (A) Laxford and (B) Outer Hebrides granites. Batch partial melting model (above) assumed. Model concentrations (relative to USGS G-2) over page.


A.
10
1
0.1
C_o
C_I
B.
10
1
0.1
C_I
C_o

ASSUMPTIONS

A. Approximate modal compositions of gneisses and granites:

	Laxford granites	Harris/Lewis granites	GG*	PxG*
Qz	25	26	13.5	12
Or	20	31	16.3	5
Plag	40	35	53.3	45
Hornblende	5	-	17	38
Biotite	10	8	-	-

*GG - grey gneiss (amphibolite facies): PxG - pyroxene granulite

B. Trace element concentrations (ppm)

Rb	150	200	88	8
Sr	1500	300	500	451
Ba	4000	1000	850	521
Ce	150	160	58	45
Eu	4	1	1	1
Tb	9	4.5	2.4	2.4
Yb	0.65	2.44	1.5	1.5

C. Distribution coefficients (mineral/liquid):

	Hb	Bi	Kf	Pf	Garnet
Rb	.014	3.26	.659	.041	.0085
Sr	.22	.12	3.87	4.4	.015
Ba	.044	6.36	6.12	.31	.017
Ce	1.6	.30	.045	.28	.3
Eu	5.0	.16	1.0	2.2	1.5
Tb	10.0	.28	.006	.08	10.5
Yb	8.0	.4	.007	.05	40

The model used in Figure 3.8 assumes that no plagioclase is present in the residuum left by removal of a liquid. This is consistent with the absence of a marked negative Eu anomaly in the granites although, as has already been argued on the basis of Sr:Ba ratios, a small amount of plagioclase in the residuum is permissible. The Lewisian granulites include predominantly basic to intermediate rocks, the latter of which predominate and have positive Eu anomalies (Pride and Muecke, 1980). The granulites may on average have a positive anomaly, therefore, further permitting the presence of plagioclase as a residual phase. Amongst other possible minerals in the residuum is pyroxene, which has low partition coefficients relative to liquids for all the trace elements shown, but might have a strong influence on the low concentrations of Ni and Cr in the granites. Large amounts of pyroxene in the residuum would have the general effect of increasing the concentrations of Rb, Sr and Ba, and also the rare-earths, in the liquid. In addition, a clinopyroxene-rich residuum could account for the low lime content of the Laxford granites without having any significant effect on alumina, as would be the case with plagioclase. Hornblende, which would have a similar effect on lime and alumina, has high partition coefficients relative to liquids for the middle rare earth elements - say, those between Nd and Tb (Hanson, 1977), and is not considered to be an important residual phase because of the convex-up, and hence middle rare-earth rich, chondrite-normalised patterns seen (Figure 3.4). On the other hand, the complete or almost-complete melting or reaction-out of hornblende originally present in the parent rock

could have contributed to the middle rare-earth rich patterns, at the same time giving rise to residual clinopyroxene as a product of the melting reactions.

The rare clinopyroxene present in the Laxford granites and seen in a reaction relationship with hornblende could represent residual material formed in melting reactions and retained in the viscous granite magma.

The degree of fractionation or light rare-earth enrichment of the Laxford granites is not adequately reflected by $Ce_n:Yb_n$, which is a measure only of average slope in the chondrite-normalised patterns, and is largely the result of extreme depletion of Yb (Y, often used as a heavy rare-earth, and plotted in Figure 3.8, shows the same tendency to low relative concentrations). Between Ce and Tb, the Laxford granites are actually less-fractionated, as well as being of higher absolute abundance in rare-earth elements, than G-2 and the Outer Hebrides granites, and are only slightly more fractionated than the Lewisian granulites. Thus this fractionated rare-earth pattern may well be an inherited feature from the granulites. Garnet is often cited as a residual phase for igneous rocks showing strongly-fractionated patterns, but this need not be the case for crustal melting of already-fractionated rocks such as the bulk of the Lewisian granulites. It can be suggested that residual garnet was the cause of the observed low Yb and Y concentrations in the Laxford granites, but published partition coefficients for garnet (Arth and Hanson, 1975) do not suggest strong depletion of Yb relative to Tb.

The phases which have been suggested as possible residual minerals - pyroxene, perhaps plagioclase and some garnet - might also have been fractionating phases from a more-basic parental liquid. However, just as the trace element evidence indicates that only 5% or less of an anatectic source can have melted to give the Laxford granite magma, so fractional crystallisation of some 95% of a basic liquid would be required to produce the final granite compositions. No evidence of the fate of the necessary large volumes of cumulates can be found.

It is concluded that the Laxford granite sheets were derived by about 5% partial melting of depleted Lewisian granulites, with fairly efficient separation of the melt fraction from an anhydrous, probably clinopyroxene-rich, residuum. The parent material was tonalitic to basic in composition, and any hydrous minerals which may have been present before melting were completely reacted-out. Hornblende or biotite could have been present in small but sufficient amounts to provide the water needed for melting. On the disappearance of such minerals, a ($P_{H_2O} < P_{Total}$) liquid could have existed over a large range of temperatures in equilibrium with residual crystals without its composition being modified, unless the dry liquidus of the residual crystal assemblage was reached (Wyllie, 1978). The Outer Hebrides granites, despite being more voluminous, are relatively much more homogeneous than the Laxford granites. Although they have lower overall rare-earth

concentrations, they have more-fractionated chondrite-normalised patterns, at least between Ce and Tb, and they compare fairly closely with the granite used for normalisation in Figure 3.8, USGS G-2.

Just as the Outer Hebrides granites show distributions of Ba, Sr and Rb which are mirror-images of those of the Laxford granites in Figure 3.8, so they tend to suggest conclusions about their origins which are the reverse of those drawn about the Laxford granites.

Combined with the marked negative Eu anomaly, the lower concentrations of Sr in the Hebrides granites indicate that plagioclase played an important role as a residual phase during melting or fractional crystallisation. Similarly, the higher Rb:Ba ratios of the Hebrides granites suggest derivation from a parent which was not greatly depleted in Rb. This agrees also with the higher K:Na ratios found in these granites. It is possible, therefore, to test the hypothesis that these granites were the result of partial melting of a parent similar to the amphibolite-facies grey gneisses.

Figure 3.8b shows the effects of 20-30% melting of amphibolite-facies gneisses, leaving a residuum containing 40-50% plagioclase. The concave-upwards chondrite-normalised rare-earth patterns (Figure 3.4) for these granites suggest amphibole may have been an important residual mineral. The main factor determining the large degree of melting is the need to dilute Rb in the magma. Since the gneisses of

Harris and S.W. Lewis are often migmatitic, with substantial proportions of alkali feldspar-rich foliae (Myers, 1971), a high melting fraction seems more reasonable than would be the case for the alkali feldspar poor granulite-facies gneisses. The suggested modal composition of the residuum is close to that of many tonalitic grey gneisses.

The Sr-isotope evidence of Van Breemen et al. (1971) is consistent with the derivation of the gneisses from an isotopically-heterogeneous source, the initial $^{87}Sr:^{86}Sr$ ratios being variable but generally high enough (0.704-0.714, assuming a common age of 1750m.y.) to suggest a crustal source at least 800m.y. old at the time of granite intrusion; the amphibolite-facies grey gneisses may represent such a heterogeneous source (Moorbath et al., 1975).

So far, it has been shown that the geochemistry of the Laxfordian granites is consistent with an origin by partial melting of Scourian crustal rocks, the main controls on the geochemistry being the nature (granulite- or amphibolite-facies, chemical composition) of the source rocks, and the degree of melting. The positions of the granites in relation to the system Qz-Or-Ab-An (Figure 3.1c) may also suggest, in a qualitative way, that the Laxford granites originated at higher pressures than the Outer Hebrides granites. This would be supported by the obvious difficulties involved in melting nearly-anhydrous granulite-facies gneisses - a process which can perhaps

only reasonably be envisaged as occurring under extreme deep-crustal conditions. In this context, the availability of the Laxford shear zone to facilitate upward intrusion of the Laxford granites may well have been crucial.

Of the models for granite production in Figures 3.8a and 3.8b, the latter gives the poorer fit with the observed geochemistry of the granites. Part of the problem may lie in the assumption made (in the absence of any detailed geochemical study) that the amphibolite-facies grey gneisses have rare-earth concentrations similar to those of the granulite-facies gneisses. A more-fractionated source would give a better fit, and since it has already been argued that the amphibolite-facies gneisses include rocks of fairly acid composition, it is possible that the average degree of rare-earth fractionation in the Hebrides granite source was greater than that of the granulites, whose more acid members are generally tonalitic.

A further weakness of the model for the Outer Hebrides granites is the absence, so far as can be ascertained, of distinctive geochemical characteristics in the proposed source, such as those present in the granulites (low K, Rb, Th, U and high Sr and Ba) which place strong constraints on the discussion of the origins of the Laxford granites. Thus extensive plagioclase fractionation of a more basic magma of mantle origin is a realistic possibility for the Hebrides granites, and indeed the large volumes of granite produced must raise

questions about the capacity of the crust to provide a source for these rocks.

The isotope evidence of Van Breemen et al. (1971) to some extent provides arbitration between mantle and crustal sources for the Hebrides granites. Initial $^{87}Sr:^{86}Sr$ is high, and although the Hebrides granites do not contain inherited zircons of Scourian age, this lack of direct evidence of derivation from a crustal source need not be taken as positive evidence of mantle origin (Pidgeon and Aftalion, 1978). On balance, it seems reasonable to conclude, as did Van Breemen et al. (1971), that the Outer Hebrides granites consist entirely or predominantly of crustally-derived material of Scourian age, such as the amphibolite-facies grey gneisses.

A final complicating factor is the presence in some Hebrides granites of xenolithic material which is clearly of Lewisian amphibolite-facies gneiss origin, and which often displays extensive degrees of assimilation (Chapter 2). The gneiss foliation of these xenoliths is undisrupted, and sharp edges and corners on xenolith blocks suggest relatively local derivation - the xenoliths are not necessarily representative of the source of the granites. However, the fact that assimilation is seen suggests the possibility that this process may account for some of the crustal character of the granites. The nature of one type of interaction between acid intrusive rocks and country rocks is examined in Chapter 5, and

its bearing on the possible contamination of the Laxfordian granites is considered in Chapter 6.

To summarise, the Laxfordian granites of N.W. Scotland are divisible into two groups, of which those occurring at Loch Laxford have been generated by a small amount of partial melting in source rocks similar to the Scourian granulite-facies gneisses, resulting in analogous geochemical characteristics - low K, Rb, Th and U relative to the Outer Hebrides granites, and very high Ba and Sr. Plagioclase fractionation, resulting either from the separation of a magma from a plagioclase-rich source, or from plagioclase precipitation, played an important part in the evolution of the Hebrides granites, which have marked negative Eu anomalies and high Rb:Sr and Rb:Ba. A source similar to the amphibolite-facies grey gneisses is consistent with the geochemistry of these granites.

3.3.2 LATE-STAGE PROCESSES IN THE GRANITES, AND PEGMATITE EVOLUTION

The discussion of section 3.3.1 made the simplifying assumption that the Laxfordian granites form compositionally-homogeneous groups of rocks which are geochemically representative of the liquids formed during partial melting or by crystal fractionation. A concensus view probably exists amongst geologists (Chappell and White, 1974; Wyllie, 1978; Luth, 1976) that granite magmas may never in their histories have consisted entirely of liquid, and often contain restitic crystals from their sources. Wyllie (1978) suggested that magmas less silicic than

granodiorites could only be generated in the crust as liquid-poor crystal mushes. Such intermediate magmas are not the subject of this study, but the possibility that some restitic material may have been retained by the ascending granite magmas is supported by the presence of rare clinopyroxene in the Laxford granites. The apparent reaction of this pyroxene to produce hornblende indicates that, at least at relatively late stages, restitic crystals are unlikely to survive, but may contribute significantly to the total amount of ferromagnesian material present in the magma.

The crystallisation of hornblende in the Laxford granites, followed by biotite, may therefore represent the ultimate stages of re-equilibration of restitic material with the granitic liquids. Amphibole could have been present in the magmas through a significant part of their upward transport, but rare-earth evidence (Section 3.3.1) shows that it could not have separated from the liquids, since this would tend to deplete the magma in the middle range of rare-earth elements.

Examination of variations in the rare-earth patterns of the Laxford granites (Figure 3.9) shows a progressive fall in total rare-earth concentrations with increasing silica, with an apparently disproportionate depletion in the middle rare earths. It is suggested that this regular internal variation is the result of the gradual separation of increasingly leucocratic material from more-crystalline, and particularly more amphibole-rich,

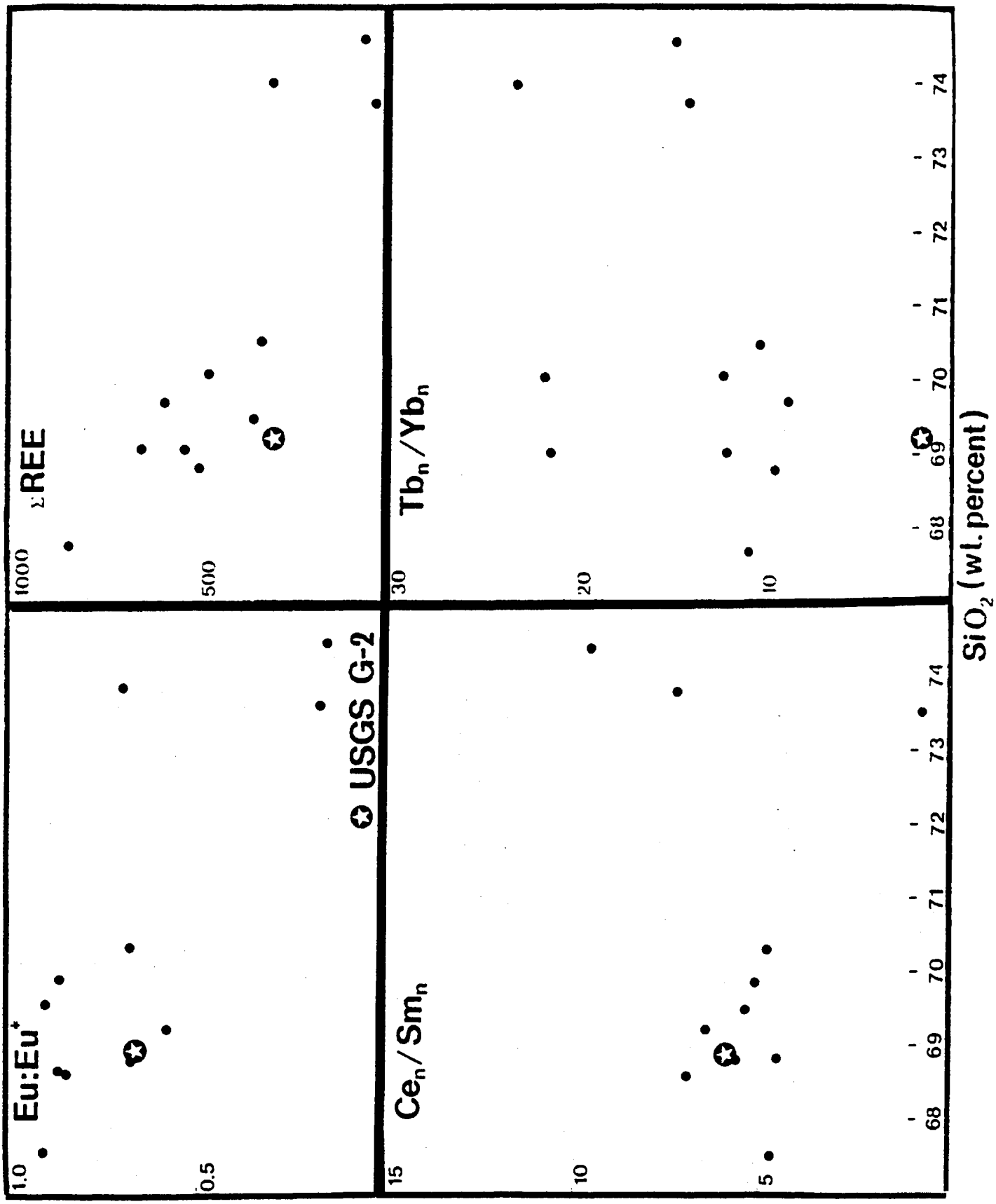


Fig 3.9 Variation of $Eu:Eu^*$, $Ce_N:Sm_N$, and REE and $Tb_N:Yb_N$ with SiO_2 in the Laxford granites . . . . . .

material. The depletion in middle rare-earths leads to an increase in Ce_n:Sm_n with increasing silica (Figure 3.9), and this tendency is paralleled by a developing negative Eu anomaly (Figure 3.9), suggesting that crystalline plagioclase was present in the amphibole-rich material. The Laxford melagranites probably represent this material, and in this sense may be thought of as having a cumulus relationship with the leucogranites.

Spatially, there is some evidence that this trend is roughly reflected by the successive compositions of the granites across the dip-section sampled, leucogranites succeeding melagranites to the NNE: this is shown in Figure 3.10. Simple comparison with chemically-layered igneous bodies would suggest that the reverse spatial variation should be seen, since the leucogranites occur at the bottom of the dip-section (see Figure 2.1). However, there is no reason to suppose that the Laxford granites form a single differentiated intrusion, and irregularities in the simple pattern of Figure 3.10 demonstrate the polyintrusive nature of the sheeted granites.

It is suggested that the exposed granites are representative of various stages in the late evolution of a number of granite sheets, the observed differences being the result of variations in the depth relative to the present erosion surface at which each sheet either began to crystallise large amounts of material, or (perhaps as a result of strain-rate variations) began the process of leucogranite separation. This model envisages each sheet

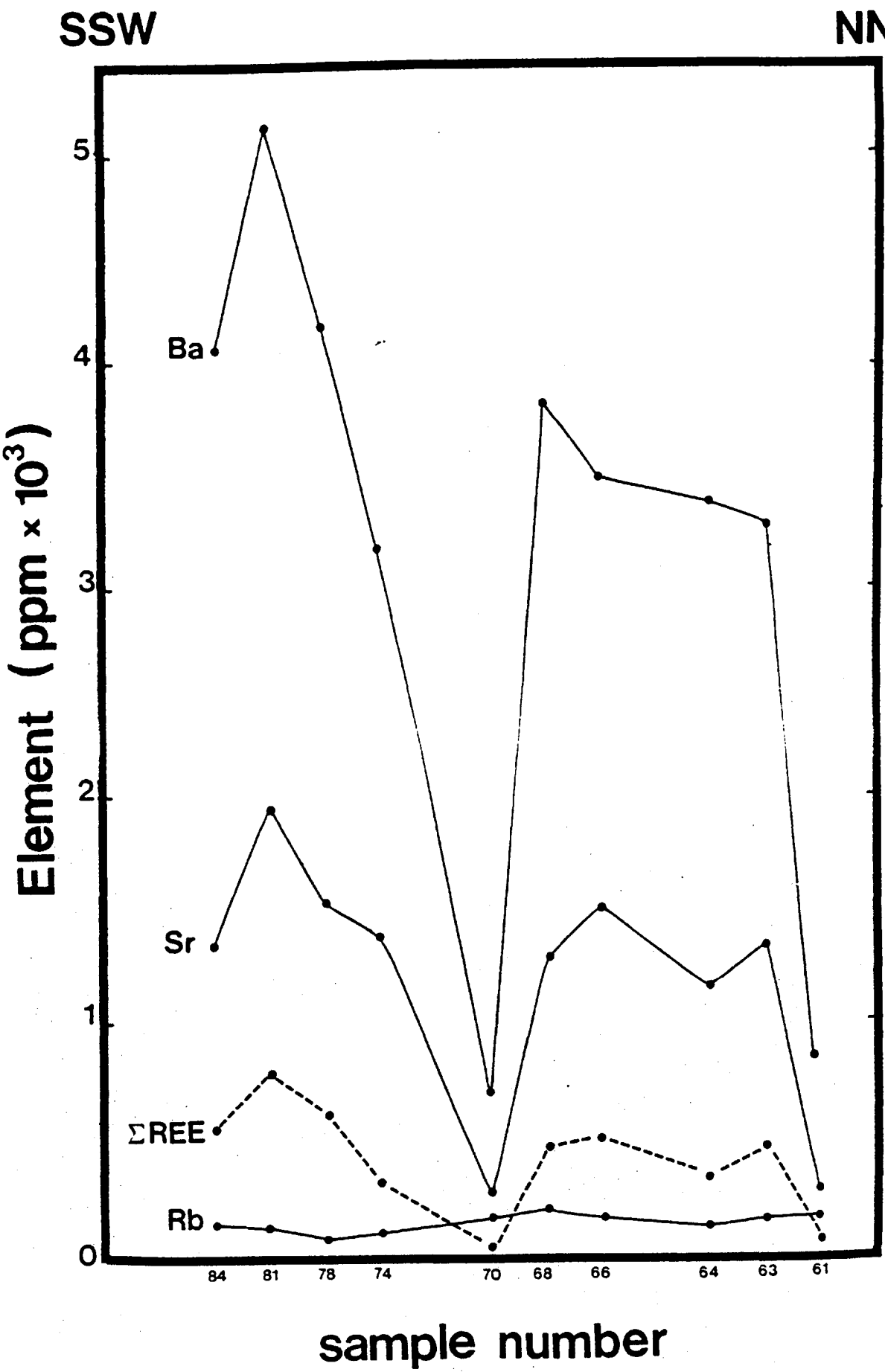


Fig 3.10 Geochemical variations across the Laxford granite sheets

as being compositionally zoned in a near-vertical sense, as a result of the intrusion process itself. Since the whole composition range of the granites appears to be exposed in one or another of the sheets, it seems likely that this process would have taken place fairly rapidly over only a small vertical distance. The apparent regularity of the chemical variation across the granite sheets could be the result of successive intrusion taking place almost always on the same side of the Laxford shear zone, a gradual heating-up of the zone perhaps delaying crystallisation slightly in sheets intruded successively to the SSW.

Whatever the validity of the interpretation given, it seems clear that the separate granite sheets had a common origin, as discussed in section 3.3.1.

Very high concentrations of Ba and Sr in the supposedly-cumulus melagranites suggest not only that plagioclase and amphibole were present as solid phases, but that alkali feldspar, which has a high partition coefficient for Ba relative to liquid, had also begun to crystallise in large amounts. The crystallisation of both feldspars simultaneously takes place, in the system An-Ab-Or-Qz, on the cotectic surface aedc in Figure 3.11, where alkali feldspar and plagioclase coexist with liquid. The plotted positions of the Laxford granites lie slightly above this surface at 5Kbar (Winkler, 1976) and are likely to do so over quite a large range of pressures. Figure 3.11 indicates that quartz did not begin to crystallise until the cotectic line a-e was reached, so that the liquid

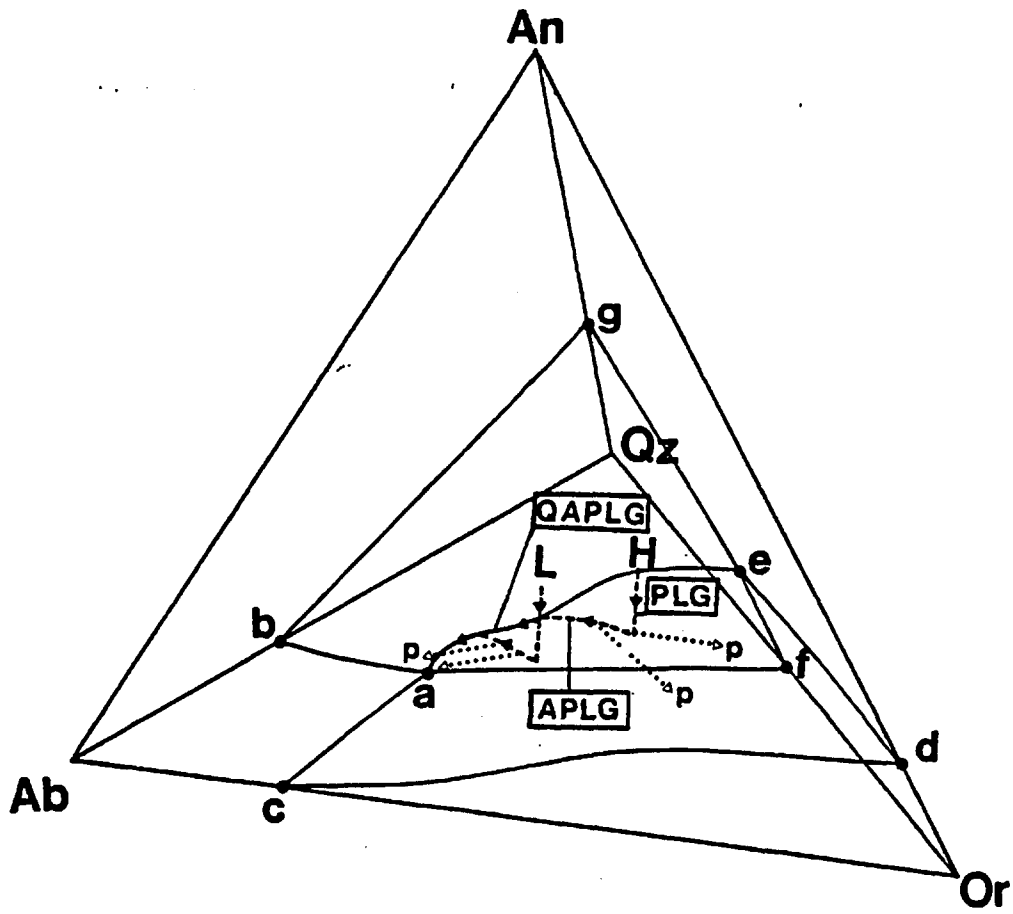


Fig 3.11 Possible crystallisation paths of the granites in the system Qz-Or-Ab-An.

Solid arrows show paths for Laxford(L) and Outer Hebrides (H) liquids, with phases present at each stage - quartz(Q), alkali feldspar(A), plagioclase(P), liquid(L) and gas(G) - shown for Outer Hebrides granites only.

Separation of pegmatites shown diagrammatically for both groups by open arrows.

coexisting with crystallising feldspars would be increasingly quartz-normative. The leucogranites lie close to the cotectic line, and also to the eutectic point a, and may thus represent near-eutectic liquid compositions in the granite system. Note that the melagranites must represent not liquid but cumulus compositions. The relative proximity of all the plotted compositions to the eutectic point a is taken to indicate the relatively compressed composition range over which these crustally-derived magmas may vary, and need not suggest a particularly simple history.

The contrasting behaviour of Ba (which is rapidly depleted through the Laxford granite sequence) and Rb (which is not) reflects the tendency of Rb to partition into liquids relative to all solid phases except biotite, which may be present in the melagranites in sufficient amounts only to prevent significant concentration of Rb in successively more acid granites.

A steady decrease in Zr with increasing silica indicates the crystallisation of zircon from a relatively early stage, a likely process in peraluminous rocks. Zircon has a high partition coefficient for Yb (250) relative to Tb(20), according to Hanson (1977), and so it is capable, in a way in which garnet and amphibole probably are not, of removing the heaviest rare earth elements rapidly. Thus the variation in Tb_n:Yb_n with increasing silica (Figure 3.9) may be the result of zircon crystallisation. If this is so, not only is the

need (Section 3.3.1) to invoke residual garnet reduced, but it becomes even more likely that the Laxford granite magmas originated with chondrite-normalised rare-earth patterns little more fractionated than those of the granulites. The fact that the variation in Tb_n:Yb_n occurs at a late stage means that garnet cannot have been responsible.

In addition to zircon, the low overall concentrations of rare-earth elements in the leucogranites may be the result of crystallisation of allanite and epidote in the melagranites. Clearly, total rare-earth concentrations in granitic rocks are highly-sensitive to the onset of accessory-mineral crystallisation, after which the rare earths are rapidly removed from liquids.

Pegmatites forming sheets within the melagranite sheets are generally more acid than, and poorer in Ba, Sr and rare-earth elements than the granites (see, for example, Figure 3.10), showing contrasts comparable to those of the leucogranites. Unlike the leucogranites, however, the pegmatites are interpreted here as having been derived from the granites in which they are found. If this is so, the granites must have been in an almost-solid state at the time of their formation and intrusion, though remaining ductile enough to accommodate subsequent deformation of the pegmatites (Chapter 2).

Not only is Ba less-abundant in coexisting pegmatites than in the granites, but it also occurs in lower concentrations in the pegmatite alkali feldspars than in

the alkali feldspars from the granites. This is despite the modal decrease in alkali feldspar seen in the pegmatites, which gives rise to their relatively albite-rich normative compositions. Phase compositions in the Laxford granites and pegmatites are further discussed in Chapter 4.

The Outer Hebrides granites do not show the relatively large variations of the Laxford granites (Figure 3.12), although the presence of identifiable leucogranites, poor in rare-earth elements, and cogenetic pegmatites with comparable evidence of late-intrusive deformation suggests a similar late history.

Leucogranites and pegmatites are more K and Rb-rich than melagranites in the Outer Hebrides. This, together with the lower concentrations of Sr and Na, and fairly steady Ba, suggests that while plagioclase crystallisation had reached a fairly advanced stage in the melagranites at the time of pegmatite formation, alkali feldspar had barely begun to crystallise. This is not inconsistent with the plotted position of the Hebrides granites above the surface aedc in Figure 3.11, but it indicates that pegmatite formation may have happened very quickly after the cotectic was reached.

The Hebrides pegmatites are almost entirely quartz-alkali feldspar rocks, plotting (Figure 3.13) near the quartz-orthoclase sideline in the system An-Ab-Or-Qz, not only in a region remote from any likely eutectic

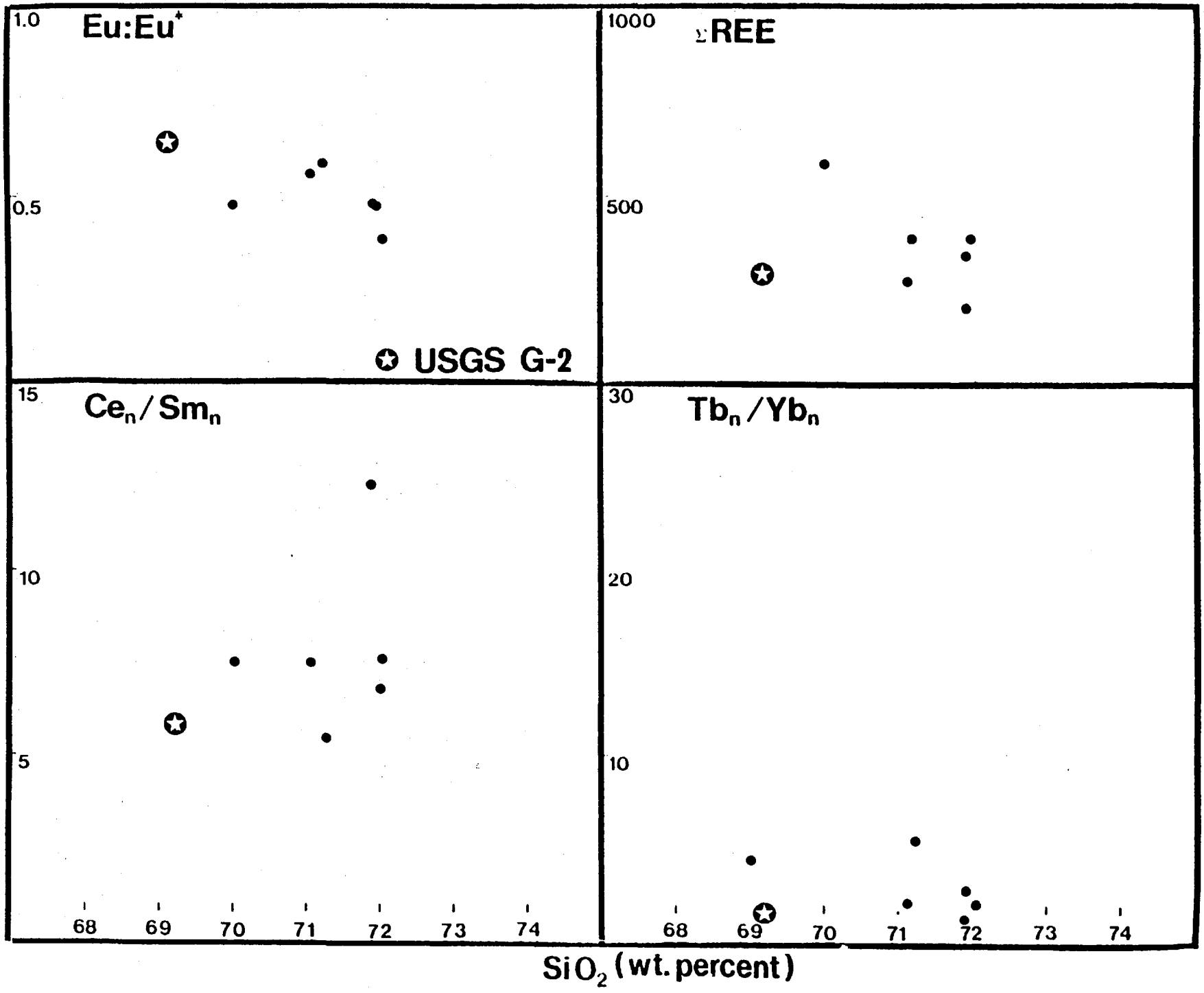


Fig 3.12 Variation of $Eu:Eu^*$, $Ce_N:Sm_N$, REE and $Tb_N:Yb_N$ with SiO_2 in the Outer Hebrides granites . . . . . .

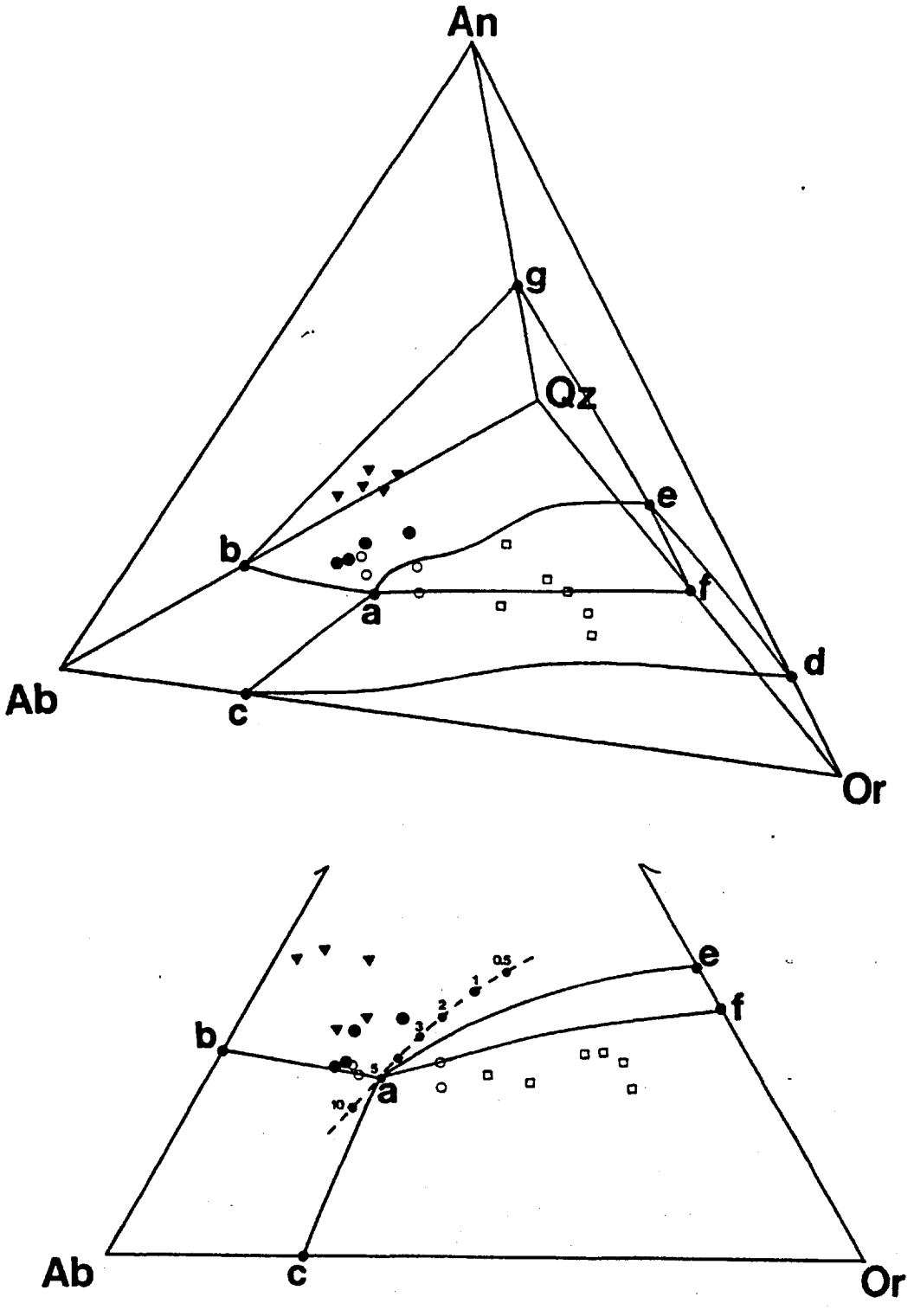


Fig 3.13 Pegmatites occurring with Laxford (open circles) and Outer Hebrides (squares) granites compared with Northern-type (triangles) and Southern-type(closed circles) pegmatites, plotted in the system Qz - Or - Ab - An.

point, but well below the volume in which liquids are likely to be stable. This is in marked contrast to the Laxford pegmatites, which could easily represent eutectic liquid compositions. This relationship suggests that the Hebrides pegmatites were not formed simply as a result of (even water-saturated) liquid-crystal equilibria. Possibly, at the time of their formation, a granitic liquid either was not present or was greatly subordinate to a hydrous vapour phase, as suggested by Jahns and Burnham (1969) for many pegmatites. The possible composition of such a vapour phase is crucial to its role in pegmatite generation.

Luth's 'tentative conclusions' on the vapour phase (Luth, 1976), for which almost no experimental data exist, suggest that:

(a) for a vapour phase coexisting with liquid and crystals, the vapour phase is enriched in normative quartz relative to the liquid,

(b) where the crystals comprise quartz and alkali feldspar, the vapour is more sodic than the liquid, while in the case of vapour+liquid+quartz+albite it is more potassic.

The geochemical evidence presented here suggests that plagioclase dominated the crystal assemblage at this stage in the Outer Hebrides granites, so that extreme fractionation of potash (and presumably of Rb) into the vapour phase may have been possible. A third general conclusion reached

by Luth (1976) was that with increasing pressure between about 5Kbar and 10Kbar, the normative vapour composition approaches that of the liquid, while the amount of silicate material dissolved in the vapour increases (perhaps to 8% at 10Kbar).

Thus a crystal residuum dominated by plagioclase, combined with rather low ambient pressure (say, closer to the 5Kbar value used in Figures 3.11 and 3.13), might give rise to the observed pegmatite compositions. With falling temperature, the vapour would become more quartz-rich (Luth, 1976), perhaps giving rise to the late quartz cores observed in many of the pegmatites.

Further support for the necessary low pressures comes from the coexistence of epidote with a plagioclase more calcic than albite (Fettes et al., 1976) in the granites.

By comparison, it has already been suggested that alkali feldspar formed a significant proportion of the crystal assemblage in the Laxford granites on pegmatite formation, so the possibility of an albite-rich vapour phase exists. The Laxford pegmatites, however, lie close to reasonable eutectic compositions, and this could be the result of a dominant role played by a liquid phase, or of the closer approach of vapour and liquid compositions because of the different solid assemblage or because of higher ambient pressures. Although epidote coexists with plagioclase more calcic than albite in the Laxford granites, the plagioclases are commonly zoned, with albite

rims, and it is not clear if the epidote is in equilibrium with the plagioclase interiors.

The rather small volumes of pegmatitic material produced in association with the Laxford granites may indicate contrasting amounts of hydrous vapour in the granites from the two regions, another factor which would facilitate departure of the Hebrides pegmatite compositions from the eutectic.

In conclusion, it seems likely that in both groups of granites the melagranites represent the stage at which most ferromagnesian and feldspar phases had at least begun to crystallise, while the greatly subordinate leucogranites possibly represent a closer approach to liquid compositions and more efficient separation from residual crystals. The pegmatites, which on structural grounds can be said to have formed when the granites were almost solid but still undergoing syn-intrusive ductile deformation, were probably substantially influenced in their geochemistry by the presence of a hydrous vapour phase, particularly in the case of the Hebrides pegmatites. It is suggested that detailed examination of the geochemistry of these related rocks reveals evidence, discussed in this and the previous section, that a range of processes from melting to late crystallisation and vapour phase formation have operated in the Laxfordian granites. Luth (1976) commented as follows:

". . . . granitic rocks are products of multi-stage processes and . . . attempts to treat such rocks (other

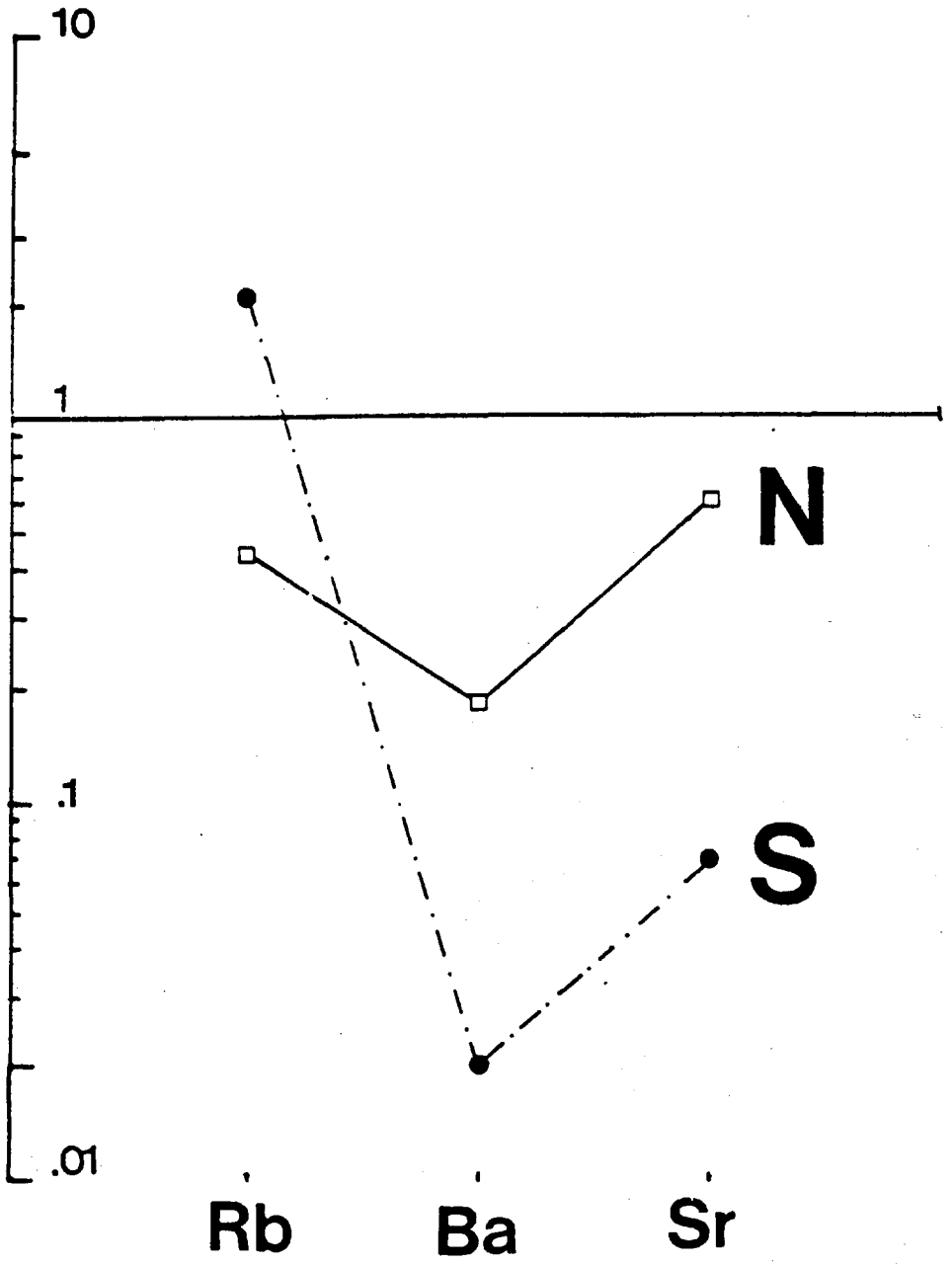
than in exceptional cases) as products of single-stage magmatic or metamorphic processes, are subject to severe limitations."

3.3.3 INDEPENDENT LAXFORDIAN PEGMATITES

It is clear from diagrams such as Figure 3.6 and 3.14 that whatever the origins of the Northern and Southern-type pegmatites, their geochemistries depart significantly from those of the Laxfordian granites and their related pegmatites.

The analysed pegmatites were selected on the basis of their apparent mineralogical homogeneity, as representatives of a somewhat artificial classification. It has already been stated (Chapter 2) that some Laxfordian pegmatites display features common to both Northern and Southern-type pegmatites, and the tentative conclusion was reached that the two 'ideal' types may be linked by time-related evolutionary processes. The existence of 'mixed' pegmatites means that compositions intermediate between the relatively-homogeneous groups of Figure 3.6 must exist, although the evident structural complexity of such intermediate bodies would not be well represented by their average composition.

In Figure 3.14, concentrations of Rb, Sr and Ba in the Northern-type and Southern-type pegmatites are shown, normalised to USGS G-2. In comparison with the rocks shown in Figure 3.7, these pegmatites have very high Rb and low Sr and Ba, with relative distributions most like



3.14 USGS G-2 normalised trace element diagram: the Northern-type and Southern-type pegmatites

those of the Outer Hebrides granites. The relative depletion in Sr and Ba (apparent from this diagram and Figure 3.6) in the Southern-type pegmatites relative to the Northern-type pegmatites is consistent with the crystallisation in the latter of alkali feldspar and plagioclase.

By analogy with the Outer Hebrides granites, it is suggested that the Northern- and Southern-type pegmatites were derived from the amphibolite-facies gneisses. Variations in geochemistry between the two groups are the result of element partioning during the separation of a magma or fluid from crystals precipitated to form Northern-type pegmatites. In the same way as has been argued for the Laxford granite sheets, many pegmatites may be chemically heterogeneous in the direction of intrusion, while others are clearly zoned inwards or into marginal pockets.

It has been suggested that many Laxfordian pegmatites have evolved from a Northern to a Southern character, and throughout their individual histories have shown significant geochemical contrasts with the pegmatites which were evolved from Laxfordian granites, demonstrating their independent origin. The distribution of these pegmatite types may provide some clues as to this origin.

Although the generalisation can be made that most pegmatites of Southern type are found within the metasedimentary gneisses or the meta-igneous complex of South Harris (Myers, 1968), similar rocks are found in

S.W. Lewis, at Lower Badcall and in Benbecula. It is only in South Harris, however, that bodies of Southern type not only predominate but usually show no Northern-type characteristics. The preservation of Northern-type minerals in South Harris appears to be a function of the size of the pegmatites, the smaller bodies generally lacking alkali feldspar, biotite or magnetite. Since the mineralogy of the South Harris pegmatites includes aluminous phases such as garnet and muscovite, it could be suggested that these pegmatites have either been derived from, or reacted with, the host pelitic gneisses. However, the evident continuity of the Northern and Southern-type pegmatites, and the presence of Northern-type bodies in areas poor in obviously-metasedimentary rocks, suggests that the direct melting of pelitic gneisses to generate Southern-type pegmatites is unlikely. If all Southern-type pegmatites originated as Northern-types, the spatial relationship with the metasediments may indicate that reaction between pegmatites and country rocks has occurred, not necessarily in the static sense described in Chapter 5, but perhaps as a result of the transport of pegmatitic material through the country rocks.

A less obvious association between Southern-type pegmatites and their host rocks could be seen in the fact that they intrude granulite-facies gneisses in South Harris and at Lower Badcall, and, assuming the pegmatites to have been vapour-rich, a significant fluid pressure gradient could have existed between the pegmatites

and country rocks, possibly facilitating reaction. The apparent relationship between pegmatite size and the degree of preservation of Northern-type pegmatites in South Harris would be consistent with some reaction between the pegmatites and metasediments.

It seems likely, then, that the independent pegmatites analysed from several regions of the Lewisian have a similar origin and show a tendency, which may be more or less completely developed, depending on the chemistry and metamorphic state of the host gneisses, to evolve from Northern-type to Southern-type mineralogy and geochemistry.

Although the geochemical relationship which has tentatively been established between the pegmatites and host gneisses does not in itself indicate the local production of the pegmatites, it may provide circumstantial support for the possibility, suggested in Chapter 2, that pre-existing Lewisian structural and metamorphic heterogeneity was closely involved with the spatial location of the Laxfordian pegmatites. Thus it is possible to suspect, in contrast to the probable deep-crustal origin of the granites, that the pegmatites are of relatively local origin.

CHAPTER 4

PHASE CHEMISTRY

4.1 INTRODUCTION

Variations in the geochemistry of the Laxfordian granites and pegmatites are reflected in differences in mineral assemblages (for example, the Northern-type and Southern-type pegmatite assemblages), and the aim of the present chapter is to use the phase compositions of the constituent minerals in these assemblages to draw further inferences about the development of, and relationships between, the groups of rocks so far defined.

Many pegmatites can only be investigated in this way, because of their very large crystal size, and phase chemical data can be used indirectly to indicate relationships between these and other, analysed, pegmatites. The Late Scourian pegmatites all depend on this type of treatment.

Some mineral assemblages present in acid igneous rocks can be used to provide an estimate of the physical conditions under which the minerals equilibrated: in two-feldspar assemblages, the distribution of albite between alkali feldspar and plagioclase is a function of temperature (Stormer, 1975; Powell and Powell, 1977a); the composition of biotite coexisting with alkali feldspar, quartz and magnetite is sensitive to temperature and oxygen fugacity

(Buddington and Lindsley, 1964; Powell and Powell, 1977b). Within the mineral assemblages found in the Lewisian granites and pegmatites, however, there is no means available to make estimates of pressure.

The use of phase equilibria to estimate physical conditions is not only subject to possible error in the available thermodynamic models, but is made even more uncertain by the likelihood that many mineral assemblages in the rocks studied here do not reflect unique events so much as sequences of events in which the rocks have crystallised then equilibrated (and possibly continuously re-equilibrated) with the metamorphic rocks into which they were emplaced. The comments of Luth (1976), quoted at the end of section 3.3.2 are apt in this connection. In many Lewisian granites and pegmatites, evidence of more than one thermal event can be seen in perthitic exsolution (sometimes in several successive generations) in alkali feldspars, while oxide phases may display synneusis oxidation-exsolution textures characteristic of solid-state re-equilibration with cooling. As is the case with poly-metamorphic rocks, additional textural evidence about the history of a rock is likely to be present at the expense of the quantitative application of thermodynamic models.

All the rocks studied here are treated as acid igneous rocks which may show evidence of post-intrusive, metamorphic events, and not as repositories of rare minerals. The main stress will be upon the major constituents of the mineral assemblages, accessories only being dealt with where they provide useful supplementary information.

4.2 LAXFORDIAN GRANITES AND RELATED PEGMATITES

4.2.1 FELDSPARS (Table 4.1)

Many of the geochemical features of the Laxford and Hebrides granites are reflected in the composition of their feldspars: in general, plagioclase compositions are close to those estimated by normative albite and anorthite, those in the Laxford granites ranging from An_3-An_{17}, while the plagioclases from the Hebrides granites cluster around An_{20-22}. Some variation is present in the Laxford granites: plagioclases from the melagranites are slightly more An-rich.

Alkali feldspars in all the granites are near to or greater than Or_{90}. Albite is therefore partitioned strongly into plagioclase in pairs of feldspars from individual rocks, and temperature estimates based on the models of Stormer (1975) and Powell and Powell (1977) are inevitably low. Since the granites show abundant evidence of recrystallisation which continued to a late stage in their emplacement history, it cannot be surprising that the feldspars continued to re-equilibrate down to temperatures well below those which could be considered to reflect igneous conditions. The albite-rich rims present on most plagioclases in the Laxford granites may represent the last exchange of Na between the feldspars, indicating that a more albite-rich alkali feldspar was originally present. The absence of zoning in alkali

FELDSPARS, LAXFORD GRANITES AND PEGMATITES

	1	2	3	4	5	6	7	8
SIO2	67.91	64.57	67.05	63.57	64.23	64.42	64.19	64.64
A2O3	20.09	18.26	20.43	19.10	21.26	18.05	20.91	18.47
CAO	.81	.04	1.54	.05	3.55	0	2.52	0
NA2O	10.79	.78	9.72	.61	9.71	.57	9.81	.52
K2O	.05	16.55	.38	15.38	.11	16.02	.12	15.93
BAO	0	.28	0	1.17	0	.93	0	.56
SUM	99.65	100.48	99.12	99.88	99.41	99.50	99.46	99.70
SI	2.974 2.974	2.988 2.988	2.955 2.955	2.960 2.960	2.944 2.944	2.992 2.992	2.914 2.914	2.983 2.983
AL	1.037 1.037	.996 .996	1.061 1.061	1.048 1.048	1.149 1.149	.996 .996	1.086 1.086	1.014 1.014
CA	.038	.002	.073	.002	.169	0	.119	0
NA	.916	.070	.830	.055	.935	.052	.939	.052
K	.003	.977	.021	.913	.006	.956	.697	.965
BA	0 .957	.005 1.054	0 .925	.021 .992	0 1.010	.017 1.025	0 .954	.012 1.014
O	8.000	8.000	8.000	8.000	8.000	8.000	8.000	8.000
AN	3.97	.19	7.86	.25	15.70	0	12.34	0
AB	95.74	6.64	89.83	5.55	82.49	5.05	86.96	5.52
OR	.29	92.69	2.31	92.05	.42	93.29	.70	93.33
CN	0	.49	0	2.15	0	1.66	0	1.15

1 PLAG 64
2 KSP 64
3 PLAG 81
4 KSP 81
5 PLAG 65
6 KSP 65
7 PLAG 75
8 KSP 75

	9	10	11	12	13	14	15	16
SIO2	65.07	63.36	63.84	63.87	65.35	64.30	63.43	63.39
A2O3	22.34	18.82	22.56	18.70	20.25	18.14	22.44	18.54
CAO	2.75	.06	3.64	.16	1.13	.02	3.73	0
NA2O	9.67	.79	9.64	.81	10.92	.55	9.43	.48
K2O	.35	15.32	.17	15.44	.09	16.28	.35	15.10
BAO	0	1.54	0	1.20	0	.15	0	1.57
SUM	100.18	99.89	99.85	100.18	99.27	99.44	99.33	99.40
SI	2.857 2.857	2.961 2.961	2.823 2.823	2.969 2.969	2.951 2.951	2.996 2.996	2.821 2.821	2.973 2.973
AL	1.156 1.156	1.036 1.036	1.175 1.175	1.024 1.024	1.053 1.053	.996 .996	1.176 1.176	1.025 1.025
CA	.129	.003	.172	.008	.053	.001	.190	0
NA	.823	.072	.826	.073	.933	.050	.813	.073
K	.020	.913	.010	.916	.001	.968	.014	.903
BA	0 .972	.028 1.016	0 1.008	.022 1.018	0 .989	.003 1.021	0 1.007	.023 1.005
O	8.000	8.000	8.000	8.000	8.000	8.000	8.000	8.000
AN	13.31	.30	17.10	.78	5.40	.10	17.99	0
AB	84.68	7.05	81.95	7.17	92.68	4.87	80.71	7.24
OR	2.02	89.88	.95	89.90	.11	94.77	1.41	89.89
CN	0	2.78	0	2.15	0	.27	0	2.87

9 PLAG 73
10 KSP 73
11 PLAG 68
12 KSP 68
13 PLAG 61
14 KSP 61
15 PLAG 95A
16 KSP 95A

Table 4.1 Feldspars from Laxfordian granites and associated pegmatites.

FELDSPARS, LAXFORD GRANITES AND PEGMATITES

	17		18		19		20		21		22		23		24	
SIO2	65.67		68.68		63.57		64.31		64.71		68.46		64.44		64.11	
A2O3	20.92		19.32		18.57		22.25		17.85		19.91		18.34		21.84	
CAO	2.42		.32		.48		3.38		0		.32		.03		3.26	
NA2O	9.52		10.58		.81		9.65		.53		11.66		.02		9.81	
K2O	.14		.15		15.82		.12		15.55		.05		15.75		.15	
BAO	0		0		1.27		0		.37		0		.05		0	
SUM	98.67		99.05		100.52		99.71		99.17		100.40		99.23		99.17	
SI	2.915	2.915	3.015	3.015	2.959	2.959	2.842	2.842	3.015	3.015	2.980	2.980	2.997	2.997	2.850	2.850
AL	1.094	1.094	1.000	1.000	1.019	1.019	1.159	1.159	.990	.990	1.021	1.021	1.005	1.005	1.144	1.144
CA	.115		.015		.024		.160		0		.015		.001		.155	
NA	.819		.901		.073		.827		.067		.984		.006		.136	
K	.008		.008		.939		.007		.924		.003		.934		.009	
BA	0	.942	0	.924	.023	1.059	0	.994	.007	.993	0	1.002	.001	.993	0	1.009
O	8.000		8.000		8.000		8.000		8.000		8.000		8.000		8.000	
AN		12.21		1.63		2.26		16.11		0		1.44		.15		15.38
AB		86.95		97.46		6.90		83.21		6.28		99.23		5.83		83.77
OR		.84		.91		88.65		.68		93.04		.28		94.13		.84
CN		0		0		2.19		0		.68		0		.03		0

17 PLAG 74, CORE
18 PLAG 74, RIM
19 KSP 74
20 PLAG 67
21 KSP 67
22 PLAG 71
23 KSP 71
24 PLAG 64

	25		26		27		28		29		30		31		32	
SIO2	63.44		66.25		63.71		66.82		64.33		65.52		64.37		63.40	
A2O3	18.35		20.95		19.25		20.37		18.59		20.95		18.26		22.79	
CAO	0		2.35		.07		1.43		0		2.36		.12		3.48	
NA2O	.50		9.97		.45		10.77		.95		9.51		1.15		9.61	
K2O	15.80		.24		15.32		.15		14.23		.32		15.23		.32	
BAO	1.03		0		1.05		0		.51		0		.52		0	
SUM	99.12		99.76		99.85		99.54		100.44		98.66		100.15		99.60	
SI	2.980	2.980	2.914	2.914	2.961	2.961	2.942	2.942	2.978	2.978	2.911	2.911	2.990	2.990	2.812	2.812
AL	1.016	1.016	1.086	1.086	1.054	1.054	1.057	1.057	1.013	1.013	1.097	1.097	.998	.998	1.191	1.191
CA	0		.111		.003		.067		0		.112		.006		.155	
NA	.046		.850		.041		.919		.075		.819		.103		.527	
K	.947		.013		.908		.008		.953		.018		.917		.018	
BA	.019	1.011	0	.974	.019	.971	0	.995	.003	1.044	0	.950	.009	1.034	0	1.010
O	8.000		8.000		8.000		8.000		8.000		8.000		8.000		8.000	
AN		0		11.37		.36		6.78		0		11.83		.57		16.38
AB		4.50		87.25		4.17		92.38		7.31		86.26		9.47		81.83
OR		93.62		1.38		93.50		.85		91.81		1.91		89.55		1.79
CN		1.87		0		1.97		0		.88		0		.41		0

25 KSP 66
26 PLAG 78
27 KSP 78
28 PLAG 79
29 KSP 79
30 PLAG 79
31 KSP 79
32 PLAG 94

(Table 4.1)

FELDSPARS, LAXFORD GRANITES AND PEGMATITES

	33	
SIO2	63.42	
A2O3	18.50	
CAO	.32	
NA2O	.75	
K2O	15.22	
BAO	1.38	
SUM	99.59	
SI	2.969	2.969
AL	1.021	1.021
CA	.016	
NA	.068	
K	.909	
BA	.025	1.018
O	8.000	
AN		1.58
AB		6.69
OR		89.25
CN		2.49

33 KSP 84

FELDSPARS, OUTER HEBRIDES GRANITES

	1		2		3		4		5		6		7		8	
SIO2	63.97		63.40		63.85		63.25		64.41		63.41		64.25		63.50	
A2O3	18.02		22.81		18.10		22.96		18.01		22.75		18.20		22.56	
CAO	0		3.51		0		4.55		0		4.30		.12		4.24	
NA2O	.44		9.58		.50		8.53		.43		8.82		1.31		8.96	
K2O	16.02		.30		16.12		.32		16.24		.10		15.71		.25	
BAO	0		0		0		0		0		0		0		0	
SUM	98.45		99.60		98.57		99.61		99.11		99.39		99.59		99.51	
SI	12.009	12.009	11.248	11.248	11.985	11.985	11.217	11.217	12.021	12.021	11.255	11.255	11.980	11.980	11.271	11.271
AL	3.986	3.986	4.769	4.769	4.004	4.004	4.798	4.798	3.951	3.951	4.760	4.760	3.980	3.980	4.719	4.719
CA	0		.667		0		.865		0		.818		.024		.005	
NA	.160		3.295		.182		2.933		.156		3.035		.363		3.034	
K	3.836		.068		3.859		.072		3.871		.023		3.719		.057	
BA	0	3.996	0	4.030	0	4.041	0	3.870	0	4.026	0	3.876	0	4.106	0	3.947
O	32.000		32.000		32.000		32.000		32.000		32.000		32.000		32.000	
AN		0		16.55		0		22.34		0		21.10		.58		20.43
AB		4.01		81.76		4.50		75.79		3.96		78.32		8.85		78.13
OR		95.99		1.68		95.50		1.87		96.14		.58		90.57		1.43
CN		0		0		0		0		0		0		0		0

1 AF 616
2 PF 616
3 AF 607
4 PF 607

5 AF 618
6 PF 618
7 AF 618
8 PF 618

	9		10		11		12	
SIO2	64.36		63.61		64.50		63.42	
A2O3	18.05		22.80		18.11		22.88	
CAO	.05		4.11		0		3.61	
NA2O	.50		9.32		.55		9.47	
K2O	14.31		.20		16.40		.20	
BAO	0		0		0		0	
SUM	99.27		100.04		99.56		99.58	
SI	12.003	12.003	11.240	11.240	11.999	11.999	11.245	11.245
AL	3.967	3.967	4.747	4.747	3.970	3.970	4.781	4.781
CA	.010		.778		0		.686	
NA	.181		3.193		.198		3.256	
K	3.880		.045		3.891		.045	
BA	0	4.071	0	4.016	0	4.090	0	3.937
O	32.000		32.000		32.000		32.000	
AN		.25		19.37		0		17.20
AB		4.44		79.50		4.85		81.65
OR		95.31		1.12		95.15		1.13
CN		0		0		0		0

9 AF 617
10 PF 617

11 AF 1212
12 PF 1212

(Table 4.1)

feldspar is a reflection of the rapidity of alkali diffusion relative to the coupled substitution necessary in plagioclase re-equilibration (Foland, 1974).

Celsian is an important minor component in alkali feldspars from the Laxford granites, ranging up to 1.57 wt.% in one granite (85) in which the alkali feldspar is $Or_{90}Ab_{7}Cn_{3}$. Again, the Laxford leucogranites show a lower alkali feldspar celsian-content.

Smith (1974), reviewing the chemistry of feldspars, suggested that Ba-content is a function of temperature in alkali feldspars, with volcanic sanidines often having relatively high levels. The clear correlation between alkali feldspar celsian-content and rock Ba content (Figure 4.1) suggests that Ba is strongly partitioned into alkali feldspar in the Laxford granites and pegmatites, and its concentration in the feldspars is therefore a reflection of the high rock concentrations. The large quantities of Ba present in these rocks may be a reflection of relatively high temperatures achieved during the generation of the magma from which the feldspars eventually crystallised, but it seems much more likely, and it has already been argued, that it is essentially a feature inherited from the granulite source rocks which gave rise to the granites.

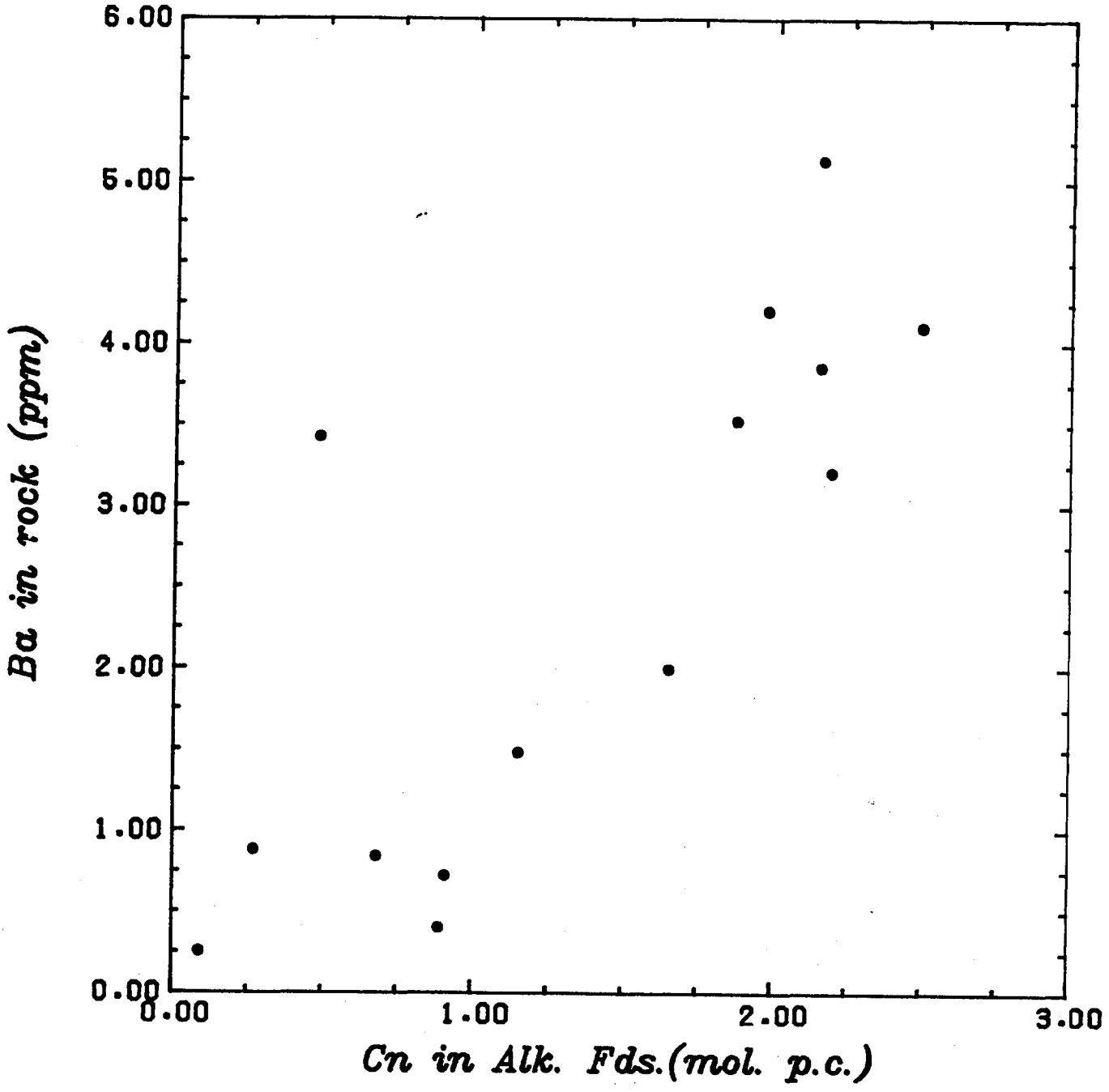


Fig 4.1 Celsian content of alkali feldspars plotted against Ba content of Laxford granites.

4.2.2 FERROMAGNESIAN MINERALS (Table 4.2)

Amphibole is present only in some of the Laxford granites, in the form of a potassian ferroedenitic hornblende (Leake, 1978). A-sites are completely filled, and although the alkali content of these amphiboles is around 4 wt.% they are calcic, not alkali amphiboles, with about 1.8 Ca cations in the B-site. The filling of the A-sites, and the relatively high potash content (comparable to, but never greater than, that of soda), possibly reflect the relatively high activities of K_2O and Na_2O in the liquids with which the amphiboles equilibrated. Amphiboles similar to those of the Laxford granites have been described from a wide range of saturated granitic and syenitic rocks (Borley and Frost, 1963; Larsen, 1976; Mitchell and Platt, 1978); while they are not in themselves indicators of high alumina activity, they provide circumstantial support for the peraluminous history of the granites (Figure 4.2).

The amphiboles in the Laxford granites are pleochroic from light to medium green, unlike, for example, those described by Mitchell and Platt (1978), which are brown amphiboles. The latter, apart from being very Fe-rich (Fe/(Fe + Mg) = 0.95), contain around 3 wt% TiO_2, while the Laxford granite amphiboles are very poor in TiO_2. Possibly Ti has a major influence upon amphibole colour.

Green biotites from the Laxford granites are also very poor in TiO_2, while the only brown biotites (sample 61)

	1		2		3		4		5	
SIO2	36.67		38.53		35.51		46.22		38.38	
TIO2	1.21		1.09		2.75		.85		1.06	
A203	15.25		13.88		15.24		32.51		13.39	
FEO	18.51		18.57		24.14		5.70		17.58	
MNO	.56		.41		.32		0		.26	
MGO	13.70		12.54		7.43		1.16		13.61	
CAO	0		0		0		0		0	
NA20	.15		.30		.42		.19		.27	
K20	9.65		10.18		9.97		11.34		10.10	
BAO	0		0		0		0		0	
SUM	94.49		94.41		93.03		94.12		93.59	
SI	5.642		5.929		5.733		6.414		5.932	
AL	2.358	8.000	2.071	8.000	2.267	8.000	1.586	8.000	2.068	8.000
AL	.407		.446		.632		3.239		.370	
FE	2.382		2.390		3.259		.661		2.272	
MN	.073		.053		.044		0		.034	
MG	3.142	6.004	2.876	5.766	1.788	5.723	.240	4.141	3.135	5.811
CA	0		0		0		0		0	
NA	.045		.090		.131		.051		.081	
K	1.894		1.998		2.053		2.007		1.991	
BA	0	1.939	0	2.088	0	2.184	0	2.058	0	2.072
O	22.000		22.000		22.000		22.000		22.000	
F/M	.781		.849		1.847		2.757		.736	
F/FM	.439		.459		.649		.734		.424	

	6		7		1		2		3	
SIO2	36.77		36.28		42.59		42.35		42.67	
TIO2	1.96		.73		.35		.34		.32	
A203	15.26		15.41		9.12		8.90		9.24	
FEO	19.23		18.74		22.08		21.55		21.90	
MNO	.58		.52		.54		.39		.46	
MGO	11.28		13.52		8.30		8.09		8.15	
CAO	0		0		10.09		10.88		10.55	
NA20	.36		.42		2.32		1.96		2.36	
K20	9.69		9.55		1.68		1.61		1.91	
BAO	0		0		-0		-0		-0	
SUM	93.17		94.44		96.72		95.73		97.24	
SI	5.760		5.598		6.676		6.698		6.661	
AL	2.240	8.000	2.402	8.000	1.324	8.000	1.302	8.000	1.339	8.000
AL	.577		.400		.360		.356		.361	
FE	2.519		2.418		2.894		2.850		2.859	
MN	.077		.068		.072		.052		.061	
MG	2.634	5.807	3.110	5.996	1.939	5.266	1.907	5.166	1.896	5.177
CA	0		0		1.695	1.695	1.844	1.844	1.764	1.764
NA	.109		.126		.705		.601		.714	
K	1.936	2.045	1.880	2.005	.336	1.041	.325	.926	.380	1.095
O	22.000		22.000		23.000		23.000		23.000	
	.986		.800		1.530		1.522		1.540	
	.496		.444		.605		.603		.606	

1 BIOTITE 66
2 BIOTITE 74
3 BIOTITE 61
4 MUSCOVITE 61
5 BIOTITE 78
6 BIOTITE 64
7 BIOTITE 85A

1 HORNBLENDE 81
2 HORNBLENDE 84
3 HORNBLENDE 85A

Table 4.2 Ferromagnesian minerals from Laxfordian granites and associated pegmatites.

BIOTITES, OUTER HEBRIDES GRANITES

SUPER RECAL 1			2		3		4	
SIO2	76.23		36.51		36.32		36.56	
TIO2	2.14		2.27		2.31		2.06	
A2O3	15.50		15.32		15.55		15.61	
FEO	23.71		24.11		24.20		24.10	
MNO	.52		.50		.46		.50	
MGO	7.70		7.63		7.23		7.42	
CAO	0		0		0		0	
NA2O	.51		.32		.55		.50	
K2O	9.73		9.61		9.58		10.21	
SUM	96.04		96.27		96.20		96.96	
SI	5.632		5.659		5.641		5.646	
AL	2.368	8.000	2.341	8.000	2.359	8.000	2.354	8.000
AL	.471		.458		.486		.487	
FE	3.082		3.125		3.143		3.113	
MN	.068		.066		.061		.065	
MG	1.784		1.763		1.674		1.708	
TI	.250	5.655	.265	5.676	.270	5.633	.239	5.612
CA	0		0		0		0	
NA	0	2.083	0	1.996	0	2.063	0	2.161
K	1.929	2.083	1.900	1.996	1.898	2.063	2.011	2.161
O	22.000		22.000		22.000		22.000	
ANN		63.85		64.42		65.68		65.04
PHLO		36.15		35.58		34.32		34.96
F/M		1.766		1.810		1.914		1.861
F/FM		.638		.644		.657		.650

1 BIOTITE, 616
2 BIOTITE, 618
3 BIOTITE, 617
4 BIOTITE, 1013

(Table 4.2)

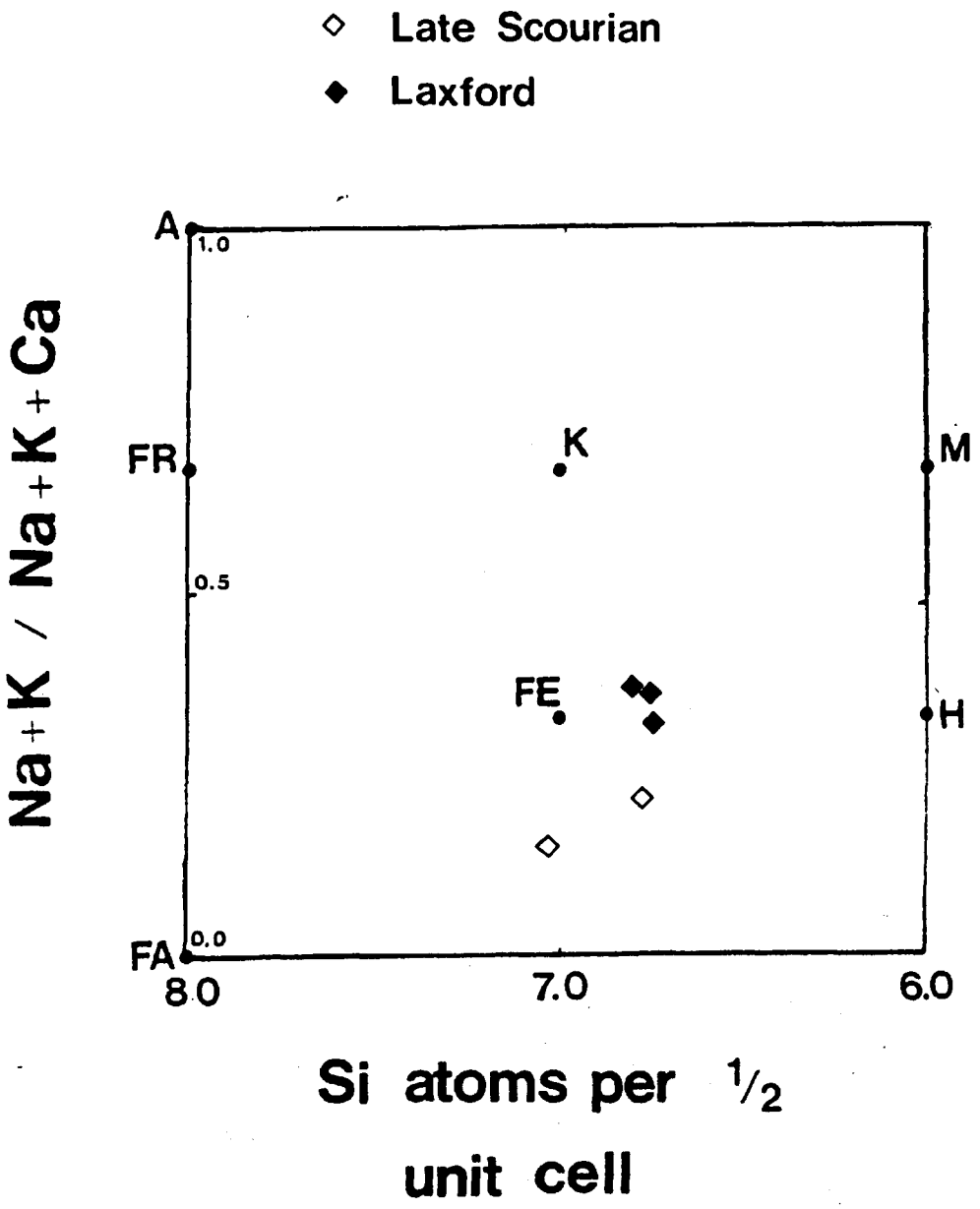


Fig 4.2 Amphibole compositions from Late Scourian pegmatites and Laxford granites.

FE - Ferroedenite, H - Hastingsite, M - Mboziite, K - Katophorite, FR - Ferrorichterite, A - Arfvedsonite, FA - Ferroactinolite

contain 2.75wt% TiO_2. While the green biotites range from $Annite_{42-49}$, that from sample 61 is significantly richer in Fe ($Annite_{64}$). The latter is also often overgrown by a late muscovite. Biotites from the Hebrides granites are invariably brown, with high TiO_2 and FeO, most resembling those from sample 61.

Since all oxide minerals are end-member magnetite, the only other mineral in the granites to contain Ti is sphene, which occurs in the Laxford melagranites apparently as a result of the breakdown of rare clinopyroxene to produce hornblende. The presence of sphene rather than ilmenite may indicate high oxygen fugacity (Haggerty, 1976), while the assemblage sphene + magnetite indicates both high f_{O_2} and a_{SiO_2} (Carmichael and Nicholls, 1967).

The contrast seen between the Fe-contents of the brown and green biotites may reflect falling temperature and f_{O_2}, assuming the biotites coexist with quartz, alkali feldspar and magnetite (Wones and Eugster, 1965). Haggerty (1976) has shown that many oversaturated acid to intermediate intrusive rocks are apparently buffered at conditions of f_{O_2} slightly above but parallel to the quartz-magnetite-fayalite curve, often showing evidence of continuous buffering with cooling. The absence of ilmenite in the Laxfordian granites is certainly consistent with a similar picture for their evolution, and the higher Fe-content of the brown biotites suggests that these micas equilibrated at lower T - f_{O_2} conditions than those of the Laxford melagranites. The feldspar minerals do not retain any evidence of higher temperatures in the

Laxford melagranites, but it seems possible that the ferromagnesian minerals may give some indication of earlier, higher T - f_{O_2} conditions.

The apparent retention of mineralogical information from an extensive part of the cooling history of the Laxford granites suggests that the process of late-intrusive recrystallisation was relatively incomplete in these rocks, in contrast with the Hebrides granites. This contrast may be related to a lower degree of water-saturation in the Laxford granites, a factor suggested in Chapter 3.

4.3 LAXFORDIAN INDEPENDENT PEGMATITES

4.3.1 FELDSPARS (Table 4.3)

As with the Laxfordian granites and pegmatites, plagioclase compositions in the Northern and Southern-type pegmatites reflect rock lime content. The most calcic plagioclases are those in the Northern-type pegmatites from North Harris, while the Southern-type bodies from South Harris typically contain an albite-rich (An_{10} or thereabouts) plagioclase, consistent with their very low total lime content.

Temperature-estimates (Stormer, 1975; Powell and Powell, 1977) again suggest re-equilibration of feldspars down to quite low temperatures, which may reflect the thermal conditions obtaining in the country rocks at the

SUPER RECAL FELDSPARS, LAXFORDIAN PEGMATITES

	1	2	3	4	5	6	7	8
SIO2	64.34	62.31	64.44	62.94	65.35	62.02	64.42	62.55
A203	18.59	23.92	18.81	24.09	19.41	23.78	18.72	24.12
CAO	0	5.44	0	5.39	0	5.62	0	5.36
NA2O	.54	8.10	.48	7.09	.44	8.22	.71	7.96
K2O	15.96	.10	15.69	.10	14.21	.17	15.75	.11
BAO	.42	0	0	0	0	0	.40	0
SUM	99.85	99.87	99.42	100.00	100.41	99.81	100.40	100.12

SI	2.985	2.985	2.759	2.759	2.986	2.986	2.762	2.762	3.004	3.004	2.754	2.754	2.986	2.986	2.760	2.760
AL	1.016	1.016	1.248	1.248	1.027	1.027	1.254	1.254	.997	.997	1.244	1.244	1.016	1.016	1.254	1.254
CA	0		.258		0		.255		0		.267		0		.259	
NA	.049		.695		.043		.675		.033		.708		.063		.331	
K	.944		.006		.927		.006		.959		.010		.926		.006	
BA	.009	1.001	0	.959	0	.971	0	.935	0	.999	0	.995	.007	.996	0	.942
O	8.000		8.000		8.000		8.000		8.000		8.000		8.000		8.000	
AN		0		26.91		0		27.27		0		27.15		0		27.01
AB		4.85		72.50		4.44		72.13		3.95		71.87		6.37		72.33
OR		94.38		.59		95.56		.60		96.04		.98		92.91		.66
CN		.76		0		0		0		0		0		.72		0

1 AF 200
2 PF 200
3 AF 608
4 PF 608
5 AF 603
6 PF 603
7 AF 1003
8 PF 1003

	9	10	11	12	13	14	15	16
SIO2	65.26	62.76	65.42	62.10	65.31	62.31	65.39	62.10
A203	18.49	23.86	18.62	23.76	19.73	24.01	18.95	23.68
CAO	0	5.29	0	5.65	0	5.44	0	5.52
NA2O	.36	8.61	.70	8.12	.72	8.00	.53	8.10
K2O	16.07	.17	16.12	.10	14.92	.10	16.42	.14
BAO	0	0	0	0	0	0	0	0
SUM	100.18	100.69	100.86	99.73	100.78	99.86	100.39	99.64

SI	3.004	3.004	2.761	2.761	2.995	2.995	2.757	2.757	2.991	2.991	2.758	2.758	2.995	2.995	2.759	2.759
AL	1.003	1.003	1.237	1.237	1.005	1.005	1.243	1.243	1.011	1.011	1.252	1.252	1.001	1.001	1.240	1.240
CA	0		.249		0		.269		0		.258		0		.263	
NA	.032		.734		.062		.699		.064		.687		.096		.599	
K	.943		.010		.941		.006		.934		.006		.959		.009	
BA	0	.975	0	.993	0	1.004	0	.973	0	1.000	0	.950	0	1.015	0	.973
O	8.000		8.000		8.000		8.000		8.000		8.000		8.000		8.000	
AN		0		25.10		0		27.61		0		27.15		0		27.49
AB		3.29		73.94		6.19		71.81		6.39		72.25		5.51		71.70
OR		96.71		.96		93.81		.58		93.61		.59		94.49		.82
CN		0		0		0		0		0		0		0		0

9 AF 1006
10 PF 1006
11 AF 1007
12 PF 1007
13 AF 1005
14 PF 1005
15 AF 1003
16 PF 1003

Table 4.3 Feldspars from Northern-type and Southern-type pegmatites.

FELDSPARS, LAXFORDIAN PEGMATITES

	17	18	19	20	21	22	23	24
SIO2	64.97	65.80	65.96	66.90	64.70	66.48	65.04	66.21
A203	18.31	21.85	17.94	20.72	17.95	20.57	18.68	20.70
CAO	0	2.53	0	1.85	0	2.74	0	2.26
NA20	.69	10.56	.61	9.92	.52	9.92	.42	10.29
K20	16.23	.18	15.94	.15	16.52	0	16.32	.02
BAO	0	0	0	0	0	0	0	0
SUM	100.20	100.92	100.45	99.54	99.69	99.71	100.46	99.48
SI	2.998 2.998	2.872 2.872	3.026 3.026	2.939 2.939	3.006 3.006	2.924 2.924	2.992 2.992	2.919 2.919
AL	.996 .996	1.124 1.124	.970 .970	1.072 1.072	.983 .983	1.066 1.066	1.012 1.012	1.076 1.076
CA	0	.118	0	.087	0	.129	0	.107
NA	.062	.894	.054	.845	.047	.846	.037	.880
K	.955	.010	.933	.008	.979	0	.957	.001
BA	0 1.017	0 1.022	0 .987	0 .940	0 1.026	0 .975	0 .995	0 .988
O	8.000	8.000	8.000	8.000	8.000	8.000	8.000	8.000
AN	0	11.58	0	9.26	0	13.24	0	10.81
AB	6.07	87.44	5.50	89.85	4.57	86.76	3.76	89.07
OR	93.93	.98	94.50	.89	95.43	0	96.24	.11
CN	0	0	0	0	0	0	0	0

17 AF 704 APLITE
18 PF 704 APLITE
19 AF GC6
20 PF GC6
21 AF 201 LANGAVAT
22 PF 201
23 AF 104 MANGERSTA, LEWIS
24 PF 104

	25	26	27	28	29	30	31	32
SIO2	65.36	66.33	65.25	66.00	65.32	65.89	65.44	63.31
A203	17.94	20.87	18.13	21.13	18.56	21.02	18.32	22.95
CAO	0	2.21	0	2.41	0	2.16	.01	4.52
NA20	1.15	10.03	.72	9.43	.77	9.66	.40	8.43
K20	15.08	0	16.23	.15	15.87	.05	16.23	.22
BAO	0	0	0	0	0	0	0	0
SUM	99.53	99.44	100.33	99.12	100.52	98.78	100.40	99.43
SI	3.019 3.019	2.921 2.921	3.007 3.007	2.914 2.914	2.998 2.998	2.918 2.918	3.008 3.008	2.808 2.808
AL	.977 .977	1.083 1.083	.984 .984	1.099 1.099	1.004 1.004	1.097 1.097	.992 .992	1.200 1.200
CA	0	.104	0	.114	0	.102	.000	.215
NA	.103	.856	.064	.807	.069	.829	.036	.725
K	.889	0	.954	.008	.929	.003	.952	.012
BA	0 .992	0 .961	0 1.018	0 .930	0 .997	0 .935	0 .988	0 .952
O	8.000	8.000	8.000	8.000	8.000	8.000	8.000	8.000
AN	0	10.85	0	12.26	0	10.96	.05	22.56
AB	10.39	89.15	6.32	86.83	6.87	88.73	3.61	76.13
OR	89.61	0	93.68	.91	93.13	.30	96.34	1.31
CN	0	0	0	0	0	0	0	0

25 AF GC23, SLETTEVAL
26 PF GC23
27 AF GSP3 GARRY-A-SIAR
28 PF GSP3
29 AF GSP2 GARRY-A-SIAR
30 PF GSP2
31 AF LP13 LEENISH, BARRA
32 PF LP13

(Table 4.3)

FELDSPARS, LAXFORDIAN PEGMATITES

	33	34	35	36	37	38	39	40
SIO2	64.66	66.32	65.28	66.26	65.20	66.20	65.30	66.44
A203	17.82	21.60	17.99	21.03	18.36	20.89	18.15	21.89
CAO	0	1.84	0	2.03	.05	2.24	.04	1.84
NA20	.73	9.90	1.03	10.30	.52	9.63	.77	9.82
K20	16.61	.75	15.37	.16	16.33	.22	16.29	.32
BAO	0	0	0	0	0	0	0	0
SUM	99.82	100.41	99.67	99.78	100.46	99.18	100.55	100.31
SI	3.005 3.005	2.901 2.901	3.016 3.016	2.913 2.913	3.000 3.000	2.923 2.923	3.004 3.004	2.900 2.900
AL	.976 .976	1.113 1.113	.979 .979	1.089 1.089	.996 .996	1.087 1.087	.984 .984	1.126 1.126
CA	0	.086	0	.096	.002	.106	.002	.086
NA	.066	.840	.092	.878	.046	.824	.069	.831
K	.985	.042	.906	.009	.959	.012	.956	.018
BA	0 1.050	0 .968	0 .998	0 .983	0 1.007	0 .943	0 1.027	0 .935
O	8.000	8.000	8.000	8.000	8.000	8.000	8.000	8.000
AN	0	8.91	0	9.73	.24	11.24	.19	9.20
AB	6.26	86.76	9.24	89.35	4.61	87.45	6.69	88.89
OR	93.74	4.32	90.76	.91	95.15	1.31	93.12	1.91
CN	0	0	0	0	0	0	0	0

33 AF 203 LANGAVAT
34 PF 203
35 AF 2001 LOWER BADCALL
36 PF 2001

37 AF AP2 ARDIVACHAR POINT, S. UIST
38 PF AP2
39 AF GSP1 GARRY-A-SIAR
40 PF GSP1

	41	42	43	44
SIO2	65.32	62.82	65.03	62.66
A203	18.41	23.24	18.66	23.20
CAO	.05	4.71	0	4.46
NA20	.52	8.77	.64	8.81
K20	16.41	.13	16.02	.04
BAO	0	0	0	0
SUM	100.71	99.67	100.35	99.17
SI	2.999 2.999	2.786 2.786	2.992 2.992	2.790 2.790
AL	.996 .996	1.215 1.215	1.012 1.012	1.217 1.217
CA	.002	.224	0	.213
NA	.046	.754	.057	.760
K	.961	.007	.940	.002
BA	0 1.010	0 .985	0 .997	0 .976
O	8.000	8.000	8.000	8.000
AN	.24	22.72	0	21.81
AB	4.58	76.54	5.73	77.96
OR	95.17	.75	94.27	.23
CN	0	0	0	0

41 AF LP12 LEENISH, BARRA
42 PF LP12

43 AF LP11 LEENISH, BARRA
44 PF LP11

(Table 4.3)

time of pegmatite formation. Unlike the granites, however, many pegmatites retain textures which are not consistent with recrystallisation after their original crystallisation. Inclusion-zoned giant alkali feldspars in the Sletteval pegmatite have clearly re-equilibrated on the scale of the small plagioclase inclusions they contain, but seem unlikely to have undergone exchange on a much larger scale. It becomes necessary to conclude that many coarse-grained pegmatites initially formed with feldspars whose compositions reflect temperatures of crystallisation well below 600°C. This strongly suggests the important influence of a hydrous vapour phase in pegmatite crystallisation. This is even more apparent in the Southern-type bodies of South Harris, where apparently-primary mineral assemblages are far removed from the quartz-plagioclase-alkali feldspar-biotite-magnetite of the granites.

4.3.2 FERROMAGNESIAN AND OXIDE MINERALS: NORTHERN-TYPE ASSEMBLAGES (Table 4.4)

Biotites display a range in Fe-content (Figure 4.3), the most iron-rich being found in garnet-bearing bodies. Most biotite compositions plot above the hematite-magnetite oxygen buffer if temperature estimates from coexisting feldspar compositions are used, and the conclusion must again be that biotites have not re-equilibrated to the

Table 4.4 Biotites from Northern and Southern-type pegmatites

BIOTITES, NORTHERN-TYPE PEGMATITES

	1		2		3		4		5		6	
SIO2	36.97		36.91		37.24		37.54		36.25		37.09	
TIO2	3.29		3.69		2.02		2.62		2.56		2.86	
A2O3	15.71		15.43		16.58		16.37		16.64		15.60	
FEO	19.99		19.66		20.12		20.35		19.98		19.99	
MNO	.31		.18		.20		.16		.26		.32	
MGO	9.76		9.50		9.94		8.98		9.45		9.18	
CAO	0		0		0		0		0		0	
NA2O	.20		.22		.28		.10		.29		.32	
K2O	9.78		9.92		9.62		9.33		9.84		9.58	
SUM	96.01		95.51		96.00		95.45		95.27		94.94	
SI	5.624		5.641		5.648		5.713		5.563		5.700	
AL	2.376	8.000	2.359	8.000	2.352	8.000	2.287	8.000	2.437	8.000	2.300	8.000
AL	.440		.420		.611		.649		.573		.525	
FE	2.543		2.513		2.552		2.590		2.564		2.569	
MN	.040		.023		.026		.021		.034		.042	
MG	2.213		2.164		2.247		2.037		2.162		2.103	
TI	.376	5.612	.424	5.544	.230	5.666	.300	5.597	.295	5.628	.331	5.569
CA	0		0		0		0		0		0	
NA	0	1.956	0	1.999	0	1.943	0	1.841	0	2.012	0	1.973
K	1.897	1.956	1.934	1.999	1.861	1.943	1.811	1.841	1.926	2.012	1.878	1.973
O	22.000		22.000		22.000		22.000		22.000		22.000	
	ANN	53.86		53.96		53.43		56.17		54.58		55.39
	PHLO	46.14		46.04		46.57		43.83		45.42		44.61
	F/M	1.167		1.172		1.147		1.282		1.202		1.242
	F/FM	.539		.540		.534		.562		.546		.554

1 BIOTITE 200
2 BIOTITE 608
3 BIOTITE 603
4 BIOTITE 1009
5 BIOTITE 1005
6 BIOTITE 1008

BIOTITES, SOUTHERN-TYPE LAXFORDIAN PEGMATITES

	1	2	3	4	5	6	7	8
SIO2	36.29	37.84	36.25	35.08	36.52	36.43	37.80	36.43
TIO2	2.39	1.95	3.55	2.55	1.82	1.99	1.80	3.01
A203	16.39	17.24	16.46	18.23	16.28	16.71	16.60	16.52
FEO	21.90	21.59	21.52	22.45	21.83	21.54	20.53	20.93
MNO	.51	.55	1.08	.22	.25	.35	.20	.80
MGO	7.68	6.25	7.05	8.40	7.92	8.05	8.20	8.35
CAO	0	0	0	0	0	0	0	0
NA20	0	.28	0	0	.25	.27	.30	.22
K20	10.20	9.89	9.67	8.89	9.80	9.91	9.53	9.82
SUM	95.36	95.59	95.58	95.82	94.67	95.25	94.96	96.08

SI	5.628		5.801		5.595		5.382		5.685		5.632		5.791		5.577	
AL	2.372	8.000	2.199	8.000	2.405	8.000	2.618	8.000	2.315	8.000	2.368	8.000	2.209	8.000	2.423	8.000
AL	.623		.915		.589		.679		.671		.677		.788		.557	
FE	2.840		2.768		2.778		2.881		2.842		2.785		2.630		2.680	
MN	.067		.071		.141		.029		.033		.046		.026		.104	
MG	1.775		1.428		1.622		1.921		1.838		1.855		1.873		1.905	
TI	.279	5.585	.225	5.407	.412	5.542	.294	5.803	.213	5.596	.231	5.594	.207	5.525	.347	5.593
CA	0		0		0		0		0		0		0		0	
NA	0	2.018	0	2.017	0	1.904	0	1.740	0	2.021	0	2.035	0	1.951	I	1.983
K	2.018	2.018	1.934	2.017	1.904	1.904	1.740	1.740	1.946	2.021	1.954	2.035	1.862	1.951	1.918	1.983
O	22.000		22.000		22.000		22.000		22.000		22.000		22.000		22.000	
	ANN	62.09		66.53		64.28		60.23		61.01		60.41		58.65		59.36
	PHLO	37.91		33.47		35.72		39.77		38.99		39.59		41.35		40.64
	F/M	1.630		1.988		1.800		1.514		1.564		1.526		1.419		1.461
	F/FM	.621		.665		.643		.602		.610		.604		.587		.594

1 ROINEVAL, S.HARRIS
2 CHAIPEVAL, S.HARRIS
3 GSP3, BENBECULA
4 2001, BARCALL, SUTHERLAND

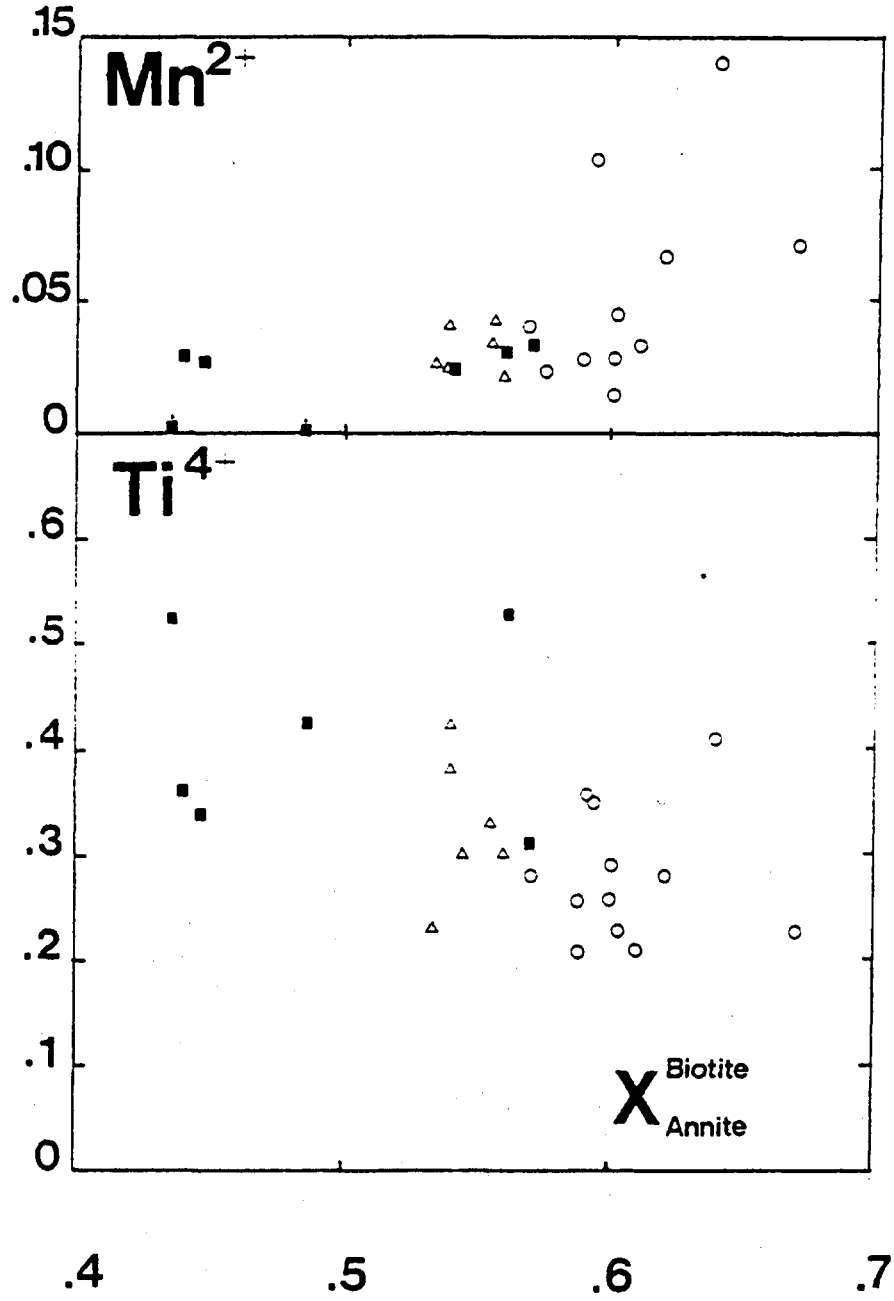
5 201, LOCH LANGAVAT
6 203, LOCH LANGAVAT
7 AP2, S. UIST
8 GSP2 BENBECULA

	9	10	11	12
SIO2	36.66	37.24	37.36	37.92
TIO2	2.20	2.45	3.12	2.25
A203	16.71	16.54	16.32	16.75
FEO	20.82	20.32	20.83	21.01
MNO	.21	.31	.20	.10
MGO	8.23	8.76	8.10	7.83
CAO	0	0	0	0
NA20	0	.28	.48	.12
K20	9.65	9.50	9.63	9.43
SUM	94.48	95.40	96.04	95.41

SI	5.672		5.687		5.686		5.781	
AL	2.328	8.000	2.313	8.000	2.314	8.000	2.219	8.000
AL	.719		.664		.613		.790	
FE	2.694		2.595		2.651		2.679	
MN	.028		.040		.026		.013	
MG	1.898		1.994		1.838		1.779	
TI	.256	5.594	.281	5.574	.357	5.485	.258	5.519
CA	0		0		0		0	
NA	0	1.904	0	1.933	0	2.011	0	1.869
K	1.904	1.904	1.850	1.933	1.870	2.011	1.834	1.869
O	22.000		22.000		22.000		22.000	
	ANN	58.91		56.93		59.30		60.20
	PHLO	41.09		43.07		40.70		39.80
	F/M	1.434		1.322		1.457		1.513
	F/FM	.588		.569		.593		.602

9 GSP1 BENBECULA
10 LP15, LEEMISH, HARRA
11 LP12 HARRA
12 LP1, HARRA

(Table 4.4)



4.3 Biotites from Northern-type and Southern-type pegmatites

Fig 4.3 Biotites from Northern-type (triangles) and Southern-type (circles) pegmatites, compared with biotites from Late Scourian pegmatites (squares).

same low temperatures recorded by feldspars. The range of biotite compositions may be a reflection of variations in the initial T-f_{O_2} conditions of crystallisation of the pegmatites, and are consistent with progressively-lower crystallisation temperatures corresponding to the transition from Northern-type to Southern-type mineralogy. Of the minor elements in biotites, Ti is fairly low and Mn high.

End member magnetite is the common opaque oxide mineral in Northern-type pegmatites, but ilmenite-pyrophanite solid solutions are found in two bodies which contain both Northern and Southern assemblages - in the largest pegmatite at Garry-a-Siar, Benbecula, and in the Sletteval pegmatite. In both cases the Fe-Ti-Mn oxide rims magnetite, apparently overgrowing the more common oxide at a rather late stage. Haggerty (1976), commenting on the occurrence of Fe-Ti-Mn oxides in acid intrusive rocks, concluded that low modal oxide contents in the rock and the expected strong partitioning of Mn into the orthorhombic phase resulted in the high Mn-content of these oxides, despite the low Mn-content of the rock. However, Mn is quite high in biotites from both pegmatites in which pyrophanite occurs, and of course both bodies later crystallised Mn-rich garnet. Thus while Mn may be of low abundance in these rocks, the sequence from Northern-type to Southern-type involves a degree of relative fractionation amongst the ferromagnesian components, Fe and Mn increasing at the expense of Mg,

pointing towards the eventual stability of Mn-rich phases.

4.3.3 FERROMAGNESIAN AND OXIDE MINERALS: SOUTHERN-TYPE ASSEMBLAGES

Garnet.

Almandine-spessartine garnets are the common ferromagnesian minerals in Laxfordian pegmatites intruding the South Harris megasedimentary gneisses, and in pegmatites elsewhere containing Southern-type assemblages. Texturally, garnet occurrences vary considerably (Chapter 2), but it is clear from the large Chaipeval pegmatite that garnet developed as part of an initial mineral assemblage also containing quartz, muscovite and albite-rich plagioclase.

Despite the rapid variations in grain-size, mode and sometimes in mineralogy of successive zones in the Chaipeval body, garnet compositions show little variation and only very weak individual development of chemical zoning, with Mn-poorer rims being developed in many crystals. Similar zoning in pelitic metasediments is common, and may be attributable to depletion in Mn from the effective volume supplying material to the growing garnet (Hollister, 1969). In the Chaipeval pegmatite, garnets were growing from a liquid or fluid phase, in which diffusion of species towards a growing garnet might be very much more rapid than would be the case for garnet growth in a solid matrix. Thus zoning might indicate depletion of a relatively

GARNETS, LAXFORDIAN PEGMATITES, N.W. SCOTLAND

	1	2	3	4	5	6
SIO2	36.75	36.99	37.09	36.57	36.49	36.60
A203	21.04	20.20	20.50	20.89	20.52	20.67
FEO	22.18	22.66	24.73	27.05	19.53	20.14
MNO	16.97	17.59	16.27	11.08	23.22	19.37
MGO	1.24	1.16	.42	1.63	0	1.05
CAO	2.34	.84	.92	2.03	.95	1.39
SUM	100.52	99.44	99.93	99.25	100.71	99.22
SI	5.960 5.960	6.073 6.073	6.076 6.076	5.983 5.983	5.987 5.987	6.014 6.014
AL	4.021 4.021	3.908 3.908	3.957 3.957	4.028 4.028	3.967 3.967	4.002 4.002
FE	3.008	3.111	3.388	3.701	2.680	2.768
MN	2.331	2.446	2.258	1.535	3.227	2.696
MG	.300	.284	.103	.398	0	.257
CA	.407 6.046	.148 5.989	.161 5.910	.356 5.990	.167 6.073	.245 5.966
O	24.000	24.000	24.000	24.000	24.000	24.000
ALM	49.76	51.95	57.33	61.79	44.12	46.39
SPE	38.56	40.84	38.20	25.63	53.13	45.19
PYR	4.96	4.74	1.74	6.64	0	4.31
GRO	6.73	2.47	2.73	5.94	2.75	4.10
F/M	17.813	19.577	55.050	13.174	0	21.245
F/FM	.947	.951	.982	.929	0	.955

	7	8	9	10	11
SIO2	36.21	36.16	36.91	37.05	37.23
A203	20.42	19.98	20.63	20.69	20.99
FEO	17.70	22.28	22.45	30.65	30.94
MNO	22.80	19.68	16.20	8.69	8.74
MGO	.76	.96	1.54	1.01	1.16
CAO	1.49	.58	2.19	2.11	.93
SUM	99.38	99.64	99.92	100.20	99.99
SI	5.978 5.978	5.985 5.985	6.008 6.008	6.031 6.031	6.055 6.055
AL	3.973 3.973	3.897 3.897	3.957 3.957	3.969 3.969	4.022 4.022
FE	2.444	3.084	3.056	4.172	4.208
MN	3.188	2.759	2.234	1.198	1.204
MG	.187	.237	.374	.245	.281
CA	.264 6.083	.103 6.183	.382 6.045	.368 5.983	.162 5.855
O	24.000	24.000	24.000	24.000	24.000
ALM	40.18	49.88	50.55	69.73	71.87
SPE	52.42	44.62	36.95	20.02	20.56
PYR	3.07	3.83	6.18	4.10	4.80
GRO	4.33	1.66	6.32	6.15	2.77
F/M	30.115	24.671	14.157	21.916	19.247
F/FM	.968	.961	.934	.956	.951

1 201 RIM
2 201 CORE
3 2001 RIM ZONED GARNET
4 2001 CORE
5 2001 SMALL EUHEDRAL GARNETS
6 GSP3 GARRY-A-SIAR
7 104, HANGERSTA, LEWIS
8 GC23 SLETTEVAL CORE
9 GC23 RIM
10 704 APLITE, LANGAVAT, CORE
11 704 RIM

Table 4.5 Garnets and oxide minerals in Southern-type pegmatites.

GARNETS, GC6 (CHAIPEVAL) ZONED SECTION A F

	1		2		3		4		5	
SIO2	36.99		36.50		36.96		36.79		36.63	
A203	21.26		21.13		21.26		20.81		21.00	
FEO	20.70		20.07		20.45		20.67		20.80	
MNO	19.68		20.12		19.63		19.83		19.74	
MGO	.65		.56		.78		.69		.60	
CAO	.80		.76		.80		.90		.76	
SUM	100.16		99.14		99.88		99.69		99.53	
SI	6.021	6.021	6.007	6.007	6.024	6.024	6.029	6.027	6.013	6.013
AL	4.078	4.078	4.098	4.098	4.083	4.083	4.019	4.019	4.062	4.062
FE	2.829		2.762		2.787		2.833		2.855	
MN	2.713		2.805		2.710		2.753		2.744	
MG	.158		.137		.189		.169		.147	
CA	.140	5.839	.134	5.838	.140	5.826	.158	5.912	.134	5.880
O	24.000		24.000		24.000		24.000		24.000	
ALM	48.44		47.31		47.84		47.92		48.56	
SPE	46.47		48.04		46.51		46.56		46.67	
PYR	2.70		2.35		3.25		2.85		2.50	
GRO	2.39		2.30		2.40		2.67		2.27	
F/M	35.142		40.525		29.012		33.139		38.147	
F/FM	.972		.976		.967		.971		.974	

	6		7		8		9		10	
SIO2	37.09		36.70		37.31		37.02		37.53	
A203	21.23		21.40		21.50		21.63		21.61	
FEO	21.19		20.14		20.74		20.27		20.06	
MNO	19.13		20.06		20.15		20.00		20.53	
MGO	.54		.68		.62		.36		.52	
CAO	.85		.71		.76		.88		.74	
SUM	100.03		99.69		101.08		100.16		100.99	
SI	6.041	6.041	5.998	5.998	6.018	6.018	6.017	6.017	6.045	6.045
AL	4.074	4.074	4.121	4.121	4.087	4.087	4.143	4.143	4.102	4.102
FE	2.886		2.753		2.798		2.755		2.702	
MN	2.639		2.777		2.753		2.753		2.801	
MG	.131		.166		.149		.087		.125	
CA	.148	5.805	.124	5.820	.131	5.831	.153	5.749	.128	5.756
O	24.000		24.000		24.000		24.000		24.000	
ALM	49.72		47.30		47.98		47.92		46.95	
SPE	45.46		47.72		47.21		47.89		48.66	
PYR	2.26		2.85		2.56		1.52		2.17	
GRO	2.56		2.14		2.25		2.67		2.22	
F/M	42.148		33.382		37.237		63.162		44.080	
F/FM	.977		.971		.974		.984		.978	

1 A - CORE
2 A - RIM
3 B - CORE
4 B - RIM
5 C - CORE
6 C - RIM
7 D - CORE
8 D - RIM
9 F - CORE
10 F - RIM

(Table 4.5)

OXIDES, GSP3 AND SLETTEVAL PYROPHANITE-ILMENITES AND MAGNETITES

	1	2	3
SIO2	.28	.33	.33
TIO2	50.85	0	52.37
A203	0	0	0
FEO	25.06	92.75	13.03
MNO	24.31	0	34.56
MGO	0	0	0
CAO	0	0	0
SUM	100.50	93.08	100.29
RECALCULATED ANALYSIS -			MAGNETITE-ULVOSPINEL BASIS
F203	-31.40	68.05	-34.74
FEO	53.35	31.44	44.32
TOTL	97.39	99.82	96.85
USP	144.33	1.27	149.14
RECALCULATED ANALYSIS -			ILMENITE-HEMATITE BASIS
F203	4.02	102.51	.61
FEO	21.44	.39	12.48
TOTL	100.90	103.24	100.35
ROMB	96.22	.85	99.43

MOL PROPS	RO2	RO	R203
1	96.22	0	3.78
2	.64	50.00	49.36
3	99.43	0	.57

1 Ilmenite - pyrophanite, sample GSP3, Garry-a-siar, Benbecula.

2 Magnetite rimmed by 1, GSP3.

3 Ilmenite - pyrophanite, sample GC23, Sletteval, S. Harris.

(Table 4.5)

larger volume. The repeated return of garnet compositions to a fairly constant Fe:Mn ratio through all zones in the pegmatite suggests that the liquid or fluid from which the garnets developed represented a very large reservoir relative to the volume of garnet crystallised. With the development of successive zones, any local depletion caused by garnet crystallisation was quickly replenished.

In the garnet-bearing zone in the Sletteval pegmatite, the large garnets include a Mn-rich core within an outer, Mn-poorer zone. The transition is sharp, and the two zones are interpreted as representing the successive growth of two unzoned (neither zone varying internally) garnet compositions. Assuming an approach to equilibrium between the garnets and the reservoir from which they grew, a significant change in the reservoir composition is indicated, possibly corresponding to the arrival of successive pulses of pegmatite magma or fluid.

At Lower Badcall, the corroded garnets in a Laxfordian pegmatite (Chapter 2) are quite strongly zoned, with Mn-rich rims and core compositions which are the most Fe-rich found in any Laxfordian pegmatite. Since the retrogressive growth of biotite at the expense of garnet and muscovite is likely to have caused the chemical zoning, a reaction similar to:

Mn-poor Garnet + Muscovite = Mn-richer Garnet + biotite

is likely. Small unzoned euhedral garnets occurring in the same pegmatite are Mn-rich, suggesting that only the more Fe-rich garnets became unstable in this pegmatite. Again,

the apparent presence of more than one initial garnet composition may provide evidence about sequential development of some of the Southern-type pegmatites.

A single garnet-bearing aplite from the Langavat belt contains garnet crystals which are optically zoned, an inclusion filled core being deeper-pink than the clear outer parts. Despite the colour-zoning, chemical variation is limited to a decrease in the small concentration of Ca present, relative to all other components in the garnets.

The textural and chemical evidence suggests widely-varying conditions of formation for the garnets found in Southern-type assemblages, and is consistent with changing liquid or fluid compositions during the development of several bodies. The observed variations are therefore interpreted as being essentially geochemical in nature, rather than responses to varying physical conditions.

Some generalisations can be made. Firstly (Figure 4.4) all the analysed garnets are Mn-rich, with never less than 20 mol.% spessartine, and are very poor in Mg and Ca (grossular + pyrope is always less than 15 mol.%). Most are much more Mn-rich than common garnets from many natural silicic igneous rocks (Figure 4.5 and Green, 1977).

Secondly, chemical zoning in these pegmatite garnets is usually normal (Mn-depleted rims), while reverse zoning may be typical of calc-alkaline igneous rocks (Green, 1977). If, as has already been suggested, normal zoning is the result of transient Mn-depletion because of strong partitioning of Mn into garnet, the extent of such zoning

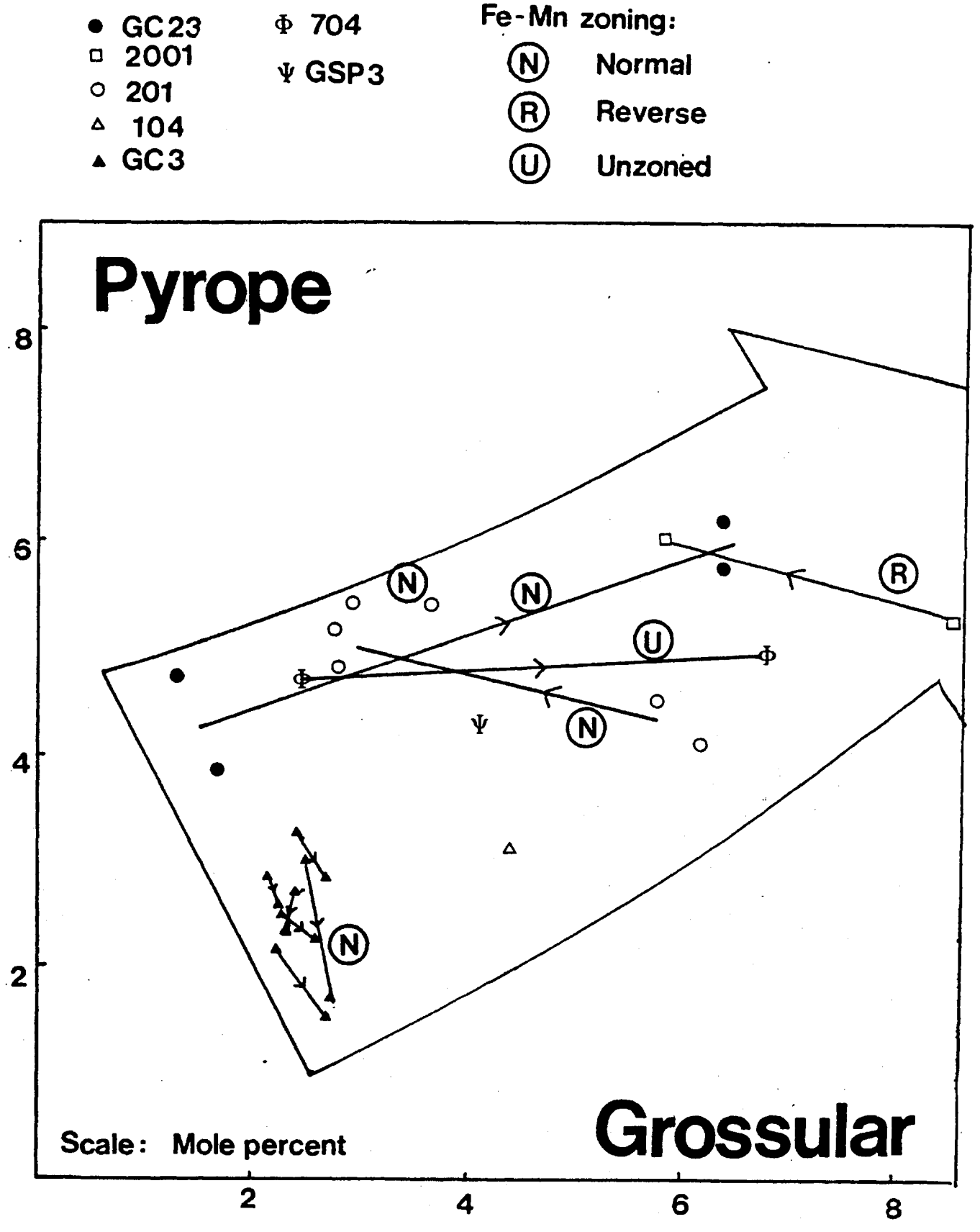


Fig 4.4 Pyrope and grossular content of garnets from Southern-type Laxfordian pegmatites. Large arrow indicates general tendency for both minor components to increase together, although the reverse may be true of individual zoned garnets.

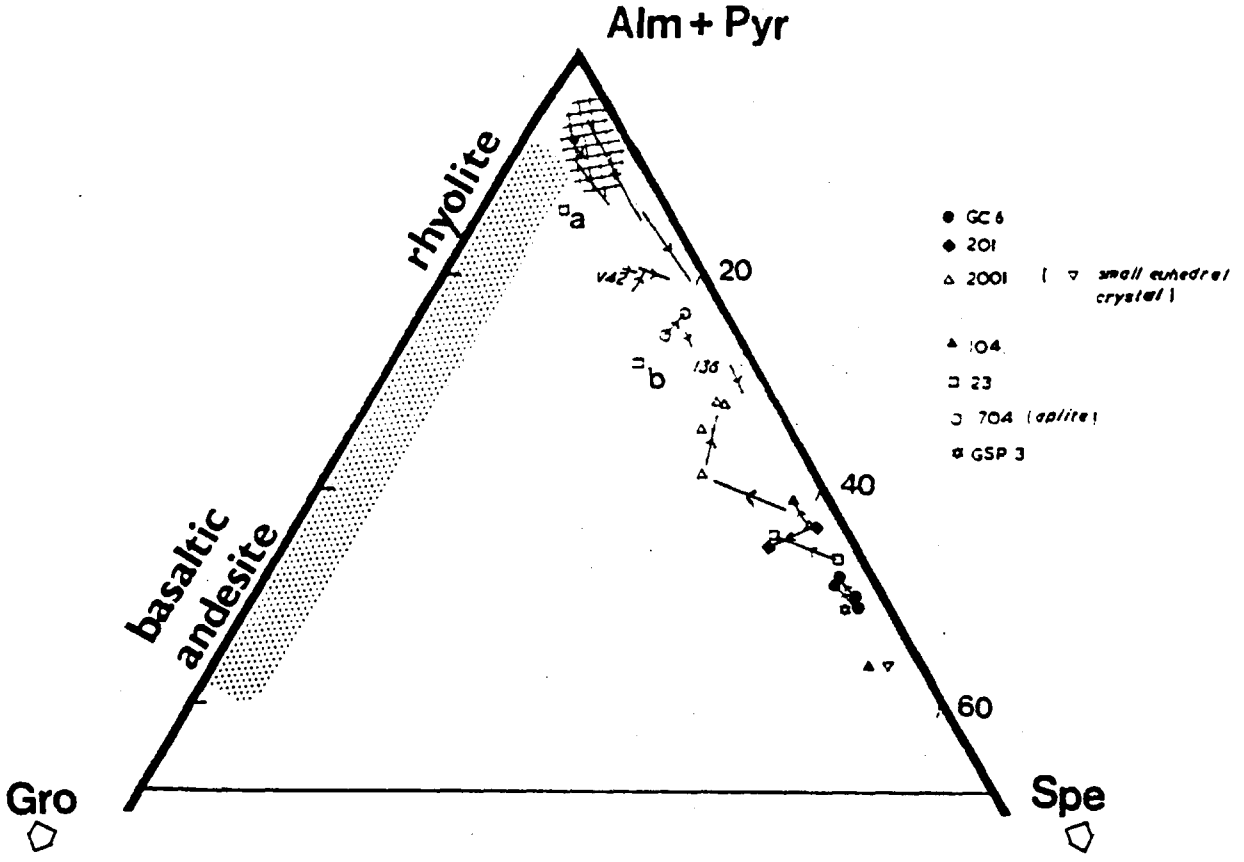


Fig 4.5 Comparison of garnet compositions from Southern-type pegmatites with Green's (1977) data

Cross-hatched area - common garnet compositions in silicic igneous rocks. Dotted - compositions of synthetic garnets from melting experiments on a wide range of igneous rocks. a - synthetic garnets from melting experiments on pelite with 0.2% added MnO. b - as a, but with 1% added MnO.

should to some extent be a function of reservoir Mn-content. Figure 4.5 may indicate that Mn-depleted rims are absent or less-marked in the garnets of highest overall Mn-content, supporting the expected behaviour of Mn-richer reservoirs. It is suggested that in the Chaipeval pegmatite at least, a relatively large, Mn-rich reservoir was able to eliminate Mn-depleted zones during phases of non-precipitation of garnet. Redistribution of Mn in a liquid/fluid reservoir is a mechanism not generally available in metamorphic rocks.

The observed breakdown of Mn-poorer garnets in the Lower Badcall pegmatite raises the question of the importance of pressure, temperature and composition on the development of garnet in these rocks. Garnet is found commonly in corundum-normative silicic igneous rocks (Green and Ringwood, 1968a, 1972; Fitton, 1972), and also in diopside-normative granites (Warren, 1970). It may also originate in contaminated rocks (Vennum and Meyer, 1979).

In most cases, the garnets are interpreted as having equilibrated with a magma at depths of at least 25 km (Green, 1977). Green (1977) investigated the problem experimentally and crystallised garnets from a range of igneous liquid compositions from basaltic endesite to granite, and from the liquid products of melting experiments on pelitic compositions. Figure 4.5 shows the compositions of garnets crystallised in these experiments. Progressively more-basic liquid compositions precipitate garnets of increasing Ca-content at increasing minimum

pressures. The range of garnet compositions does not coincide with the range found in natural rocks, and Mn-rich garnets similar to those in the Laxfordian pegmatites are produced only from melts derived from pelitic compositions with substantial (1.Owt%) added MnO, at pressures of 4-6K bar, much the lowest pressures at which garnets were crystallised experimentally. The strong spatial relationship between the Southern-type pegmatites and the pelitic gneisses of South Harris has already been noted. Although the gneisses are unlikely to contain as much as 1.Owt.% MnO, Figure 4.5 suggests that most synthetically-grown garnets are poorer in spessartine than their natural equivalents, and the experimental results cannot be invoked to reject the possibility of participation of the pelites in pegmatite formation by melting.

Green (1977) also found a decrease in CaO content of garnets with falling pressure, and increasing partitioning of Fe relative to Mg into garnet with falling temperature. Almandine-spessartine garnets are thus consistent with crystallisation at low pressures and temperatures.

Variations in Mg and Ca (Figure 4.4) within and between garnets from Laxfordian pegmatites show a distinct correlation between the two elements, although most variation is in Ca. Concentrations of both are so low that variations may be entirely the result of geochemical differences between reservoirs, and the occasional Ca-zoning found in garnets is consistent with

Ca depletion in a low-Ca reservoir. The presence of albite-rich plagioclases in garnet-bearing pegmatites suggests low reservoir Ca as a condition for garnet crystallisation at the low pressures obtaining.

Muscovite (Table 4.6)

Figure 4.6 compares muscovite compositions from Laxfordian pegmatites with those of muscovites from granitic (Neiva, 1974) and metamorphic (Guidotti, 1978) rocks. Guidotti (1978) has suggested that muscovites from synmetamorphic granites have compositions characteristic of regional metamorphic grades. The Laxfordian pegmatite muscovites are fairly phengitic (Figure 4.6), indicating rather low ambient temperatures.

Distribution of Mg and Fe between muscovite and garnet may be described by the reaction:

$$3K_2(FeAl_3)Si_7AlO_{20}(OH)_4 + Mg_3Al_2Si_3O_{12} = 3K_2(MgAl_3)Si_7AlO_{20}(OH)_4 + Fe_3Al_2Si_3O_{12}$$

Fe-Phengite — Pyrope — Mg-Phengite — Almandine

The equivalent exchange reaction for the mineral pair garnet and biotite is a sensitive function of temperature, and has been calibrated as a geothermometer by Thompson (1976) and Ferry and Spear (1974). High values of $(Mg:Fe)_{bio}/(Mg:Fe)_{gar}$ correspond to lower temperatures.

Table 4.6 Muscovites in two Southern-type pegmatites.

	1	2	3	4	5	6
SIO2	46.55	45.50	46.28	45.68	46.86	46.17
TIO2	0	0	0	0	0	0
A2O3	31.88	31.85	31.89	31.53	31.39	31.71
FEO	3.67	3.61	3.54	4.08	4.36	3.85
MNO	0	0	0	0	0	0
MGO	.65	.54	.44	.53	.53	.54
NA2O	0	.34	.41	0	0	.15
K2O	11.04	10.58	10.85	10.93	11.15	10.91
SUM	93.79	92.42	93.41	92.75	94.29	93.33
SI	6.379	6.327	6.368	6.349	6.412	6.367
AL	1.621 8.000	1.673 8.000	1.632 8.000	1.651 8.000	1.588 8.000	1.633 8.000
AL	3.526	3.545	3.539	3.513	3.474	3.519
FE	.421	.420	.407	.474	.499	.444
MN	0	0	0	0	0	0
MG	.133	.112	.090	.110	.108	.111
TI	0 4.079	0 4.077	0 4.036	0 4.097	0 4.081	0 4.074
NA	0	.092	.109	0	0	.040
K	1.930 1.930	1.876 1.968	1.904 2.014	1.938 1.938	1.946 1.946	1.919 1.959
O	22.000	22.000	22.000	22.000	22.000	22.000
PAR	0	4.66	5.43	0	0	2.05
MUSC	100.00	95.34	94.57	100.00	100.00	97.95
F/M	3.168	3.751	4.514	4.319	4.616	4.017
F/FM	.760	.790	.819	.812	.822	.801

1 GC6 ZONE A
2 GC6 ZONE B
3 GC6 ZONE C
4 GC6 ZONE D
5 GC6 ZONE E
6 AVERAGE

	1	2	3	4	5	6	7	8
SIO2	45.17	45.22	45.79	45.22	45.04	45.15	45.69	45.33
TIO2	.27	0	.26	.32	0	0	.20	.15
A2O3	33.17	32.69	34.10	32.81	32.77	32.55	33.06	33.02
FEO	2.31	2.44	2.27	2.55	2.59	2.67	2.72	2.51
MNO	0	0	0	0	0	0	0	0
MGO	.29	.21	.25	.28	.25	.38	.30	.28
NA2O	.26	.33	0	.36	.34	0	.31	.23
K2O	10.35	10.03	10.78	10.22	10.21	10.51	10.16	10.32
SUM	91.82	90.92	93.45	91.76	91.20	91.26	92.44	91.84
SI	6.265	6.324	6.241	6.282	6.295	6.312	6.296	6.288
AL	1.735 8.000	1.676 8.000	1.759 8.000	1.718 8.000	1.705 8.000	1.688 8.000	1.704 8.000	1.712 8.000
AL	3.686	3.711	3.717	3.654	3.692	3.675	3.665	3.686
FE	.268	.285	.259	.296	.303	.312	.313	.291
MN	0	0	0	0	0	0	0	0
MG	.060	.044	.051	.058	.052	.079	.062	.058
TI	.028 4.042	0 4.040	.027 4.054	.033 4.041	0 4.047	0 4.066	.021 4.061	.016 4.050
NA	.070	.089	0	.097	.092	0	.083	.061
K	1.831 1.901	1.789 1.879	1.874 1.874	1.811 1.908	1.820 1.912	1.874 1.874	1.786 1.869	1.827 1.888
O	22.000	22.000	22.000	22.000	22.000	22.000	22.000	22.000
PAR	3.68	4.76	0	5.08	4.82	0	4.43	3.26
MUSC	96.32	95.24	100.00	94.92	95.18	100.00	95.57	96.74
F/M	4.469	6.519	5.095	5.110	5.813	3.942	5.087	5.024
F/FM	.817	.867	.836	.836	.853	.798	.836	.834

1 L BADCALL 1
2 L BADCALL 2
3 L BADCALL 3
4 L BADCALL 4
5 L BADCALL 5
6 L BADCALL 6
7 L BADCALL 7
8 AVERAGE

Although no similar calibration has been attempted for the garnet-phengite exchange reactions (and the low concentrations of Fe and Mg in phengite would certainly result in very large potential errors), the distribution of Fe and Mg between the two phases may vary in the same sense. Thus the stronger partitioning of Mg into muscovite in the Chaipeval pegmatite when compared with the Lower Badcall pegmatite (Figure 4.7) may indicate higher temperatures of garnet-muscovite equilibration in the latter, lending some support to the interpretation of the Fe-richer garnets from Lower Badcall as part of a higher-temperature assemblage than that including the small Mn-rich garnets.

The rims of muscovites from Lower Badcall are poor in phengite component, reflecting the new development of biotite at the expense of garnet and muscovite.

Muscovite generally occurs in alkali feldspar-free mineral assemblages, although both are sometimes found to coexist. In the absence of an aluminium silicate polymorph, the two potash-bearing phases are related by the ionic reaction:

$$\underset{\text{Muscovite}}{K_2Al_6Si_6O_{20}(OH)_2} + \underset{\text{Quartz}}{12SiO_2} + \underset{\text{Fluid}}{4K^+} = \underset{\text{K-feldspar}}{6KAlSi_3O_8} + \underset{\text{Fluid}}{4H^+}$$

(Velde, 1965; Eugster, 1970).

Figure 4.8 (Eugster, 1970) shows the phase boundary for this reaction as a function of temperature and a_{K^+}

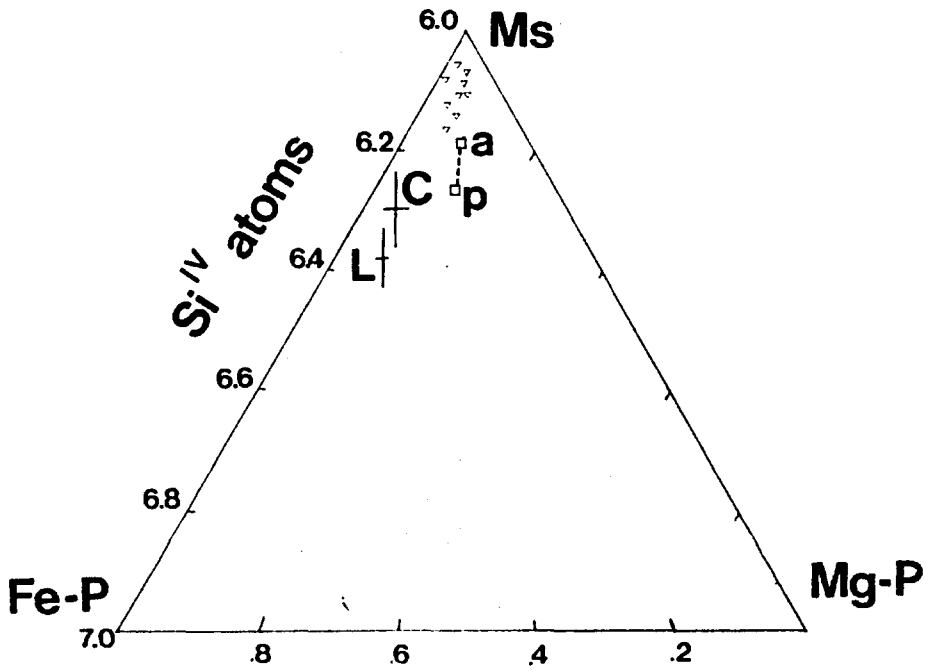


Fig 4.6 Muscovites from Southern-type pegmatites.

C Chaipeval pegmatite (GC6)

L Lower Badcall pegmatite (2001).

Open triangles: muscovites from garnet-muscovite bearing granitoids, Central North Portugal (Neiva, 1974)
Squares: muscovites from U. Sillimanite zone, South Central Maine (Guidotti, 1978). Pelite(p) and adamellite (a).

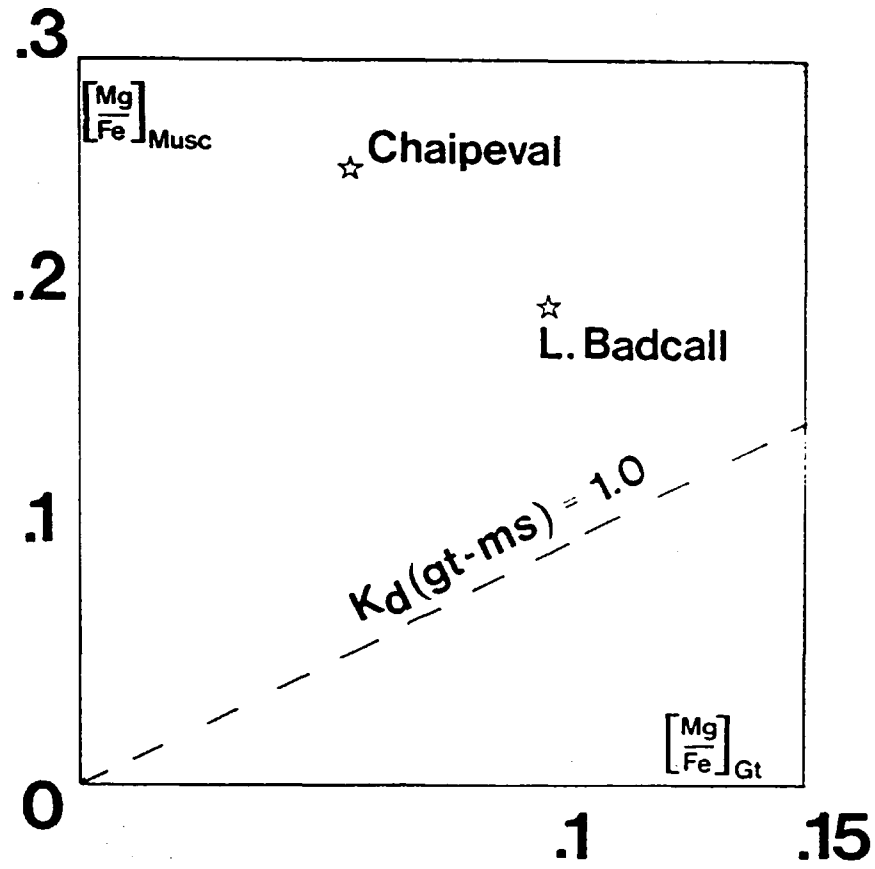


Fig 4.7 Distribution of Fe and Mg between muscovite and garnet in two Southern-type pegmatites

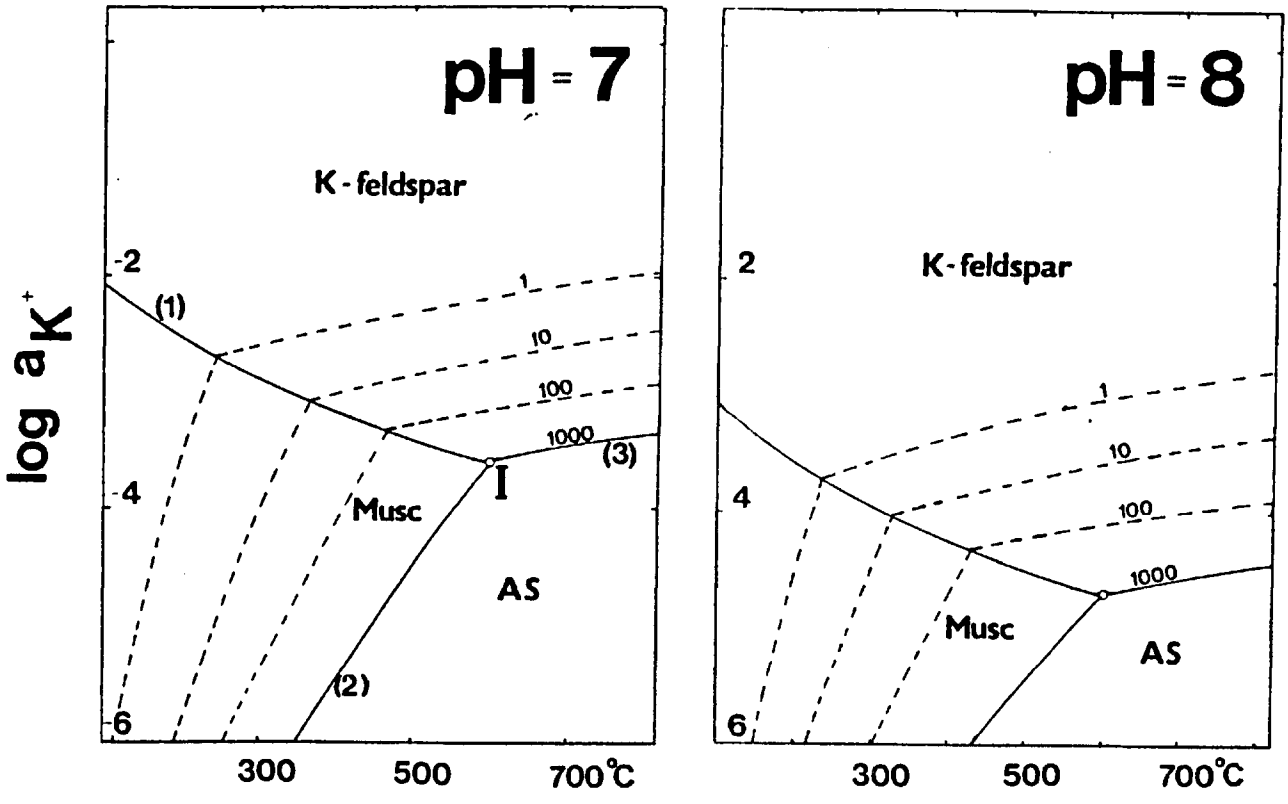


Fig 4.8 Phase relations between muscovite, K-feldspar and aluminium silicate polymorph with varying pH (from Eugster, 1970).

The solid curves are for f_{H_2O}= 1000 bars, and define the reactions:

(1) Musc + 6Qz + $2K^+$ = 3Kf + $2H^+$

(2) 2Musc + $2H^+$ = 3AS + 3Qz + $2K^+$ + $3H_2O$

(3) 2Kf + $2H^+$ = AS + 5Qz + $2K^+$ + H_2O

Intersecting at point I.

The positions of the curves at 100, 10 and 1 bar are shown by the dashed lines.

at two different values of pH. Muscovite is stable at low temperature and low a_{K^+}(fluid), its stability field expanding into higher a_{K^+}(fluid) with falling pH.

Since the activity of hydrogen ions may increase as a result of the dissociation of species such as H_2O, HCl and HF in the fluid, such dissociation would tend to increase the stability field of muscovite at the expense of alkali feldspar. Since ionic species are probably completely associated at temperatures above about 500°C (Eugster, 1977), it follows that the stabilisation of muscovite relative to potash feldspar is likely to occur with falling temperature in the pegmatite fluid, and that at least part of the formation of the Laxfordian pegmatites took place at temperatures at or below 500°C.

4.4 LATE SCOURIAN PEGMATITES

4.4.1 FELDSPARS (Table 4.7)

The alkali feldspars display a number of features which distinguish them from those present in the Laxfordian granites and pegmatites. They are coarsely perthitic, the perthite lamellae lying parallel to at least one of the microcline twin planes, suggesting perthite exsolution to have occurred at the same time as structural monoclinic/triclinic inversion. The regularity and coarseness of the perthites indicates an origin by cooling from an initially-homogeneous feldspar.

FELDSPARS, SCOURIAN PEGMATITES, SUTHERLAND

	1	2	3	4	5	6	7	8
SIO2	64.66	61.57	61.55	65.23	62.56	62.31	65.54	63.14
A203	18.57	24.87	24.67	18.26	24.31	24.40	18.14	23.67
CAO	.22	5.82	5.49	0	5.69	5.77	0	4.17
NA20	1.43	7.61	7.98	1.00	7.44	7.23	.67	7.91
K20	14.82	.37	.31	15.06	0	.10	15.82	.53
BAO	.73	0	0	.90	0	0	.44	0
SUM	100.43	100.24	100.00	100.45	100.00	99.81	100.61	99.42
SI	2.981 2.981	2.722 2.722	2.727 2.727	3.005 3.005	2.759 2.759	2.754 2.754	3.012 3.012	2.797 2.797
AL	1.009 1.009	1.296 1.296	1.288 1.288	.991 .991	1.263 1.263	1.271 1.271	.982 .982	1.235 1.235
CA	.011	.276	.261	0	.269	.273	0	.198
NA	.128	.652	.686	.089	.636	.620	.060	.679
K	.871	.021	.018	.885	0	.006	.927	.030
BA	.013 1.023	0 .949	0 .964	.016 .990	0 .905	0 .898	.008 .995	0 .907
O	8.000	8.000	8.000	8.000	8.000	8.000	8.000	8.000
AN	1.06	29.05	27.04	0	29.71	30.41	0	21.82
AB	12.49	68.75	71.14	9.02	70.29	68.96	6.00	74.88
OR	85.16	2.20	1.82	89.34	0	.63	93.20	3.30
CN	1.29	0	0	1.64	0	0	.80	0

1 2009 PERTHITE HOST
2 2009 PERTHITE LAMELLAE
3 2009 PLAGIOCLASE
4 2103 PERTHITE HOST
5 2103 PERTHITE LAMELLAE
6 2103 PLAGIOCLASE
7 2102 PERTHITE HOST
8 2102 PERTHITE LAMELLAE

	9	10	11	12	13	14	15	16
SIO2	62.67	65.47	67.92	69.68	63.57	65.53	64.65	62.62
A203	24.01	18.50	19.87	19.38	22.84	18.63	18.53	22.92
CAO	5.53	.16	.44	.18	4.39	.07	.11	4.17
NA20	7.53	2.10	10.47	10.85	8.65	.52	1.67	9.30
K20	.33	13.75	.30	.10	.28	16.31	13.94	0
BAO	0	.19	0	0	0	.07	1.02	0
SUM	100.07	100.17	99.00	100.19	99.73	101.13	99.92	99.01
SI	2.766 2.766	2.998 2.998	2.989 2.989	3.023 3.023	2.813 2.813	2.995 2.995	2.988 2.988	2.795 2.795
AL	1.249 1.249	.998 .998	1.030 1.030	.991 .991	1.191 1.191	1.003 1.003	1.009 1.009	1.205 1.205
CA	.262	.008	.021	.008	.208	.003	.005	.199
NA	.644	.186	.893	.913	.742	.046	.150	.805
K	.019	.803	.017	.006	.016	.951	.822	0
BA	0 .925	.003 1.001	0 .931	0 .927	0 .966	.001 1.002	.018 .995	0 1.004
O	8.000	8.000	8.000	8.000	8.000	8.000	8.000	8.000
AN	28.29	.78	2.23	.90	21.54	.34	.55	19.86
AB	69.70	18.63	95.96	98.50	76.82	4.60	15.03	80.14
OR	2.01	80.25	1.81	.60	1.64	94.93	82.56	0
CN	0	.34	0	0	0	.13	1.86	0

9 2102 PLAGIOCLASE
10 47 PERTHITE HOST
11 47 PERTHITE LAMELLAE
12 47 PERTHITE BLEB
13 47 ANTIPERTHITE HOST
14 47 ANTIPERTHITE LAMELLAE
15 2007 PERTHITE HOST
16 2007 PERTHITE LAMELLAE

Table 4.7 Feldspars in Late Scourian pegmatites.

	17	18	19	20	21	22	23	24
SIO2	61.91	64.24	67.81	62.61	65.45	67.84	64.25	66.21
A203	23.69	18.24	19.96	23.89	18.18	19.92	21.68	18.91
CAO	5.69	0	.11	5.42	0	.86	3.86	.24
NA20	7.66	.56	11.57	8.19	2.36	10.52	9.25	4.61
K20	.22	16.05	.45	0	14.57	.22	.13	9.72
BAO	0	.17	0	0	.22	0	0	.13
SUM	99.17	99.26	99.90	100.11	100.78	99.36	99.17	99.82
SI	2.761 2.761	2.995 2.995	2.972 2.972	2.764 2.764	2.997 2.997	2.979 2.979	2.855 2.855	2.995 2.995
AL	1.245 1.245	1.002 1.002	1.031 1.031	1.243 1.243	.981 .981	1.031 1.031	1.135 1.135	1.008 1.008
CA	.272	0	.005	.256	0	.040	.184	.012
NA	.662	.051	.983	.701	.210	.896	.797	.404
K	.013	.954	.025	0	.851	.012	.007	.561
BA	0 .947	.003 1.008	0 1.013	0 .957	.004 1.064	0 .949	0 .988	.002 .979
O	8.000	8.000	8.000	8.000	8.000	8.000	8.000	8.000
AN	28.72	0	.51	26.78	0	4.27	18.60	1.19
AB	69.96	5.02	97.01	73.22	19.68	94.43	80.65	41.30
OR	1.32	94.67	2.48	0	79.95	1.30	.75	57.28
CN	0	.31	0	0	.37	0	0	.24

17 2007 PLAGIOCLASE
18 AP1 PERTHITE HOST
19 AP1 PERTHITE LAMELLAE
20 AP1 PLAGIOCLASE
21 LP4 ALKALI FELDSPAR HOST
22 LP4 PERTHITE LAMELLAE
23 LP4 PLAGIOCLASE
24 47 BULK AF(30P.C. LAMELLAE)

	25	26	27	28	29	30	31
SIO2	63.77	63.61	64.82	64.38	65.93	65.13	65.74
A203	22.42	20.71	19.80	20.20	18.88	18.67	18.39
CAO	3.96	2.12	1.25	1.82	.21	.03	.10
NA20	7.84	3.53	2.84	3.06	3.71	3.31	3.34
K20	1.88	9.91	11.23	10.24	11.05	12.15	12.85
BAO	.01	.48	.31	.61	.11	.13	.19
SUM	99.88	100.36	100.25	100.31	99.89	99.42	100.61
SI	2.831 2.831	2.891 2.891	2.946 2.946	2.924 2.924	2.994 2.994	2.989 2.989	2.995 2.995
AL	1.173 1.173	1.109 1.109	1.060 1.060	1.081 1.081	1.010 1.010	1.010 1.010	.987 .987
CA	.188	.103	.061	.089	.010	.001	.005
NA	.675	.311	.250	.269	.327	.295	.295
K	.106	.574	.651	.593	.640	.711	.747
BA	.000 .970	.009 .997	.006 .968	.011 .962	.002 .979	.002 1.010	.003 1.050
O	8.000	8.000	8.000	8.000	8.000	8.000	8.000
AN	19.42	10.35	6.29	9.21	1.04	.15	.46
AB	69.58	31.19	25.86	28.01	33.37	29.17	28.10
OR	10.98	57.60	67.28	61.66	65.39	70.45	71.11
CN	.02	.86	.57	1.13	.20	.23	.32

25 47 BULK AF(10 P.C. LAMELLAE)
26 2009 BULK AF (34 P.C. LAMELLAE)
27 2102 BULK AF (30 P.C. LAMELLAE)
28 2013 BULK AF (32 P.C. LAMELLAE)
29 2007 BULK AF (25 P.C. LAMELLAE)
30 AP1 BULK AF (25 P.C. LAMELLAE)
31 LP4 BULK AF (25 P.C. LAMELLAE)

(Table 4.7)

Later generations of perthite lamellae can sometimes be seen, and must represent a later event or sequence of events in the cooling history of the pegmatites. As well as being very fine, later perthites are patchily developed, and are probably the result of minor deformation of the feldspars.

Plagioclase is only very rarely antiperthitic, and then irregularly so. Both feldspars contain fine inclusions which are usually orientated parallel to cleavage planes. In alkali feldspars these inclusions appear to be rutile rods, a feature thought to be characteristic of alkali feldspars formed under granulite-facies conditions (Watson, 1949).

Chemically, the Late Scourian pegmatite feldspars share two distinctive features:

(a) Alkali feldspars contain varying amounts of celsian ($BaAl_2Si_2O_8$).

(b) Perthite plagioclase lamellae are not albite, but oligoclase between An_{22} and An_{30}, similar in composition to matrix plagioclase.

The concentration of celsian in alkali feldspar appears to be characteristic for each individual pegmatite body, as do the detailed compositions of feldspars in general, indicating bulk geochemical differences between members of the group. Celsian in alkali feldspar and anorthite in plagioclase appear to be roughly correlated, the large

body at Scouriemore (Giletti et al., 1961) and the examples from Barra andSouth Uist containing the most albite-rich plagioclases and celsian-poor alkali feldspars.

Although the high celsian content of the alkali feldspars may not, as Smith (1974) suggested, in itself be an indication of high crystallisation temperatures (see also discussion of high celsian in alkali feldspars from the Laxford granite sheets, section 4.2.1), these feldspars evidently possessed initial contents of albite and anorthite higher than any found in the Laxfordian rocks, assuming the coarse perthites exsolved from an initially-homogeneous feldspar. Estimated initial compositions are shown in Figure 4.9.

If pairs of feldspars equilibrated, first as separate homogeneous alkali feldspars and plagioclases, then as coexisting perthite lamellae, then temperatures prevailing at two stages in the evolution of the pegmatites can be estimated.

Pressures of equilibration are unknown, and may, in contrast with the Laxfordian rocks, have been more characteristic of deep-crustal conditions. A probable underestimate of 5Kbar will be used here, which results in an average underestimate of temperature of about 10°C for each Kbar above 5Kbar, which is probably acceptable given the inherent uncertainties of the models used (Stormer, 1975; Powell and Powell, 1977a).

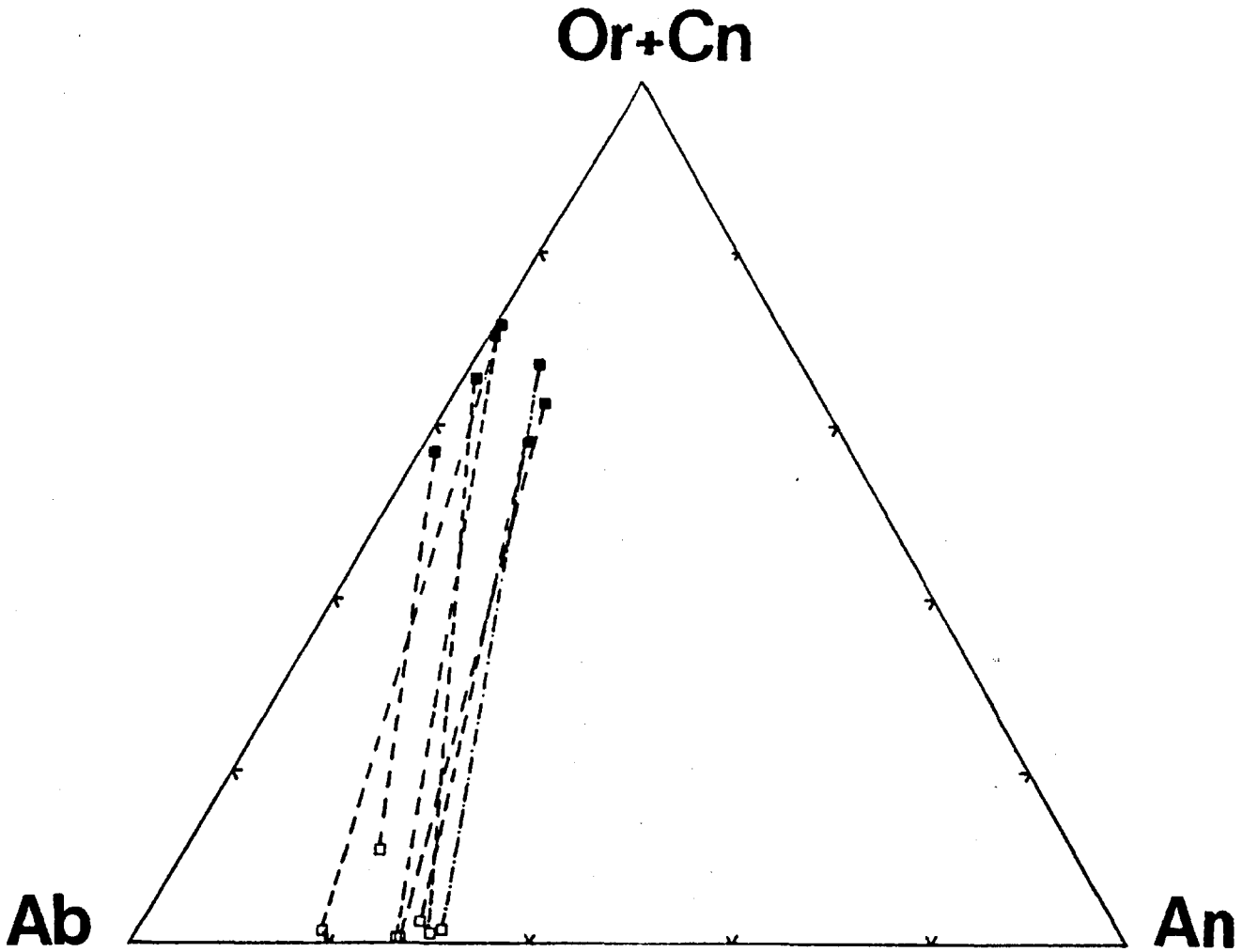


Fig 4.9 Estimated bulk feldspar compositions from Late Scourian pegmatites

Much larger uncertainties are associated with the presence of significant concentrations of Ca and Ba in the alkali feldspars. Powell and Powell's (1977a) model takes account of the presence of small amounts of Ca in alkali feldspar, otherwise being identical to Stormer's (1974) geothermometer. To some extent, the variable feldspar compositions in the Late Scourian pegmatites may provide a test of the adequacy of the two models. The effect of celsian is unknown. Despite the divalent charge of the Ba cation, celsian clearly partitions preferentially into alkali feldspar, the large ionic radius of Ba presumably being more important than valency (Smith, 1974). Gay and Roy (1969) suggested that high temperature solid solution of $KAlSi_3O_8$ and $BaAl_2Si_2O8$ is succeeded at lower temperatures by a complex system of solvi analogous to those of the plagioclases. The procedure adopted here, in the absence of any reasonable model for the mixing of the two components, will be to estimate two temperatures, one of which ignores the effect of celsian while the other assumes celsian and orthoclase to be identical, involving the addition of the mole fractions of the two components. Neither assumption is satisfactory, but the estimated temperature differences turn out to be quite small (Table 4.8).

The estimated temperatures for equilibration of the bulk feldspar compositions are given in Table 4.8a, and may represent conditions close to those of crystallisation of the pegmatites. The very large range in the estimates

A. Bulk feldspars

Sample	T_1	T_2	T_3
47	867	843	846
2009	738	574	588
2102	691	606	614
2013	719	580	596
2007	770	753	756
AP1	702	699	701
LP4	792	790	803

T_1 - Stormer (1974)

T_2 - Powell and Powell (1977)

T_3 - " " , with $X_{Or}^{AF} = X_{KAlSi_3O_8}^{AF} + X_{BaAl_2Si_2O_8}^{AF}$

B. Perthites

Sample	T_1	T_2	T_3	T_4
47(perthite)	517	506	510	580
47(antiperthite)	334	330	372	420
2009	533	512	524	582
2102	408	402	409	454
2013	475	461	475	520
2007	529	506	523	583
AP1	352	351	353	401
LP4	329	327	327	377

T_4 - Whitney and Stormer (1977), microcline-plagioclase

Table 4.8 Estimated temperatures for equilibration of Late Scourian pegmatite two-feldspar assemblages.

(580°C to 846°C) could be caused by initial differences in pegmatite crystallisation temperatures, exchange of albite component between the feldspars after crystallisation but before perthite exsolution, or by inadequacies in the feldspar geothermometers.

The first possibility seems unlikely if the pegmatites were generated at about the same time under similar crustal conditions, while the second would require the smallest degree of exchange to occur in the pegmatite from Scouriemore which contains the most albitic plagioclase; diffusion would be less-dependent on the transport of Al in anorthite-poor feldspars, and should continue to lower temperatures. The apparent origin of at least some plagioclase by exsolution of a single homogeneous feldspar was suggested in Chapter 2, however, so large-scale exsolution cannot be ruled out.

Figure 4.10 shows there is a significant relationship between estimated temperatures and bulk alkali feldspar anorthite and celsian contents. Powell and Powell's (1977) model ignores the effect of ternary feldspar solution: the effect of Ca in alkali feldspar is merely to reduce the activity of $KAlSi_3O_8$ in the calculation, tending to lower temperature estimates. Seck's (1971) ternary feldspar data suggest a strong correlation between Ca content and temperature in alkali feldspars, and a corresponding correlation between K content and temperature in plagioclase, as the compositions of coexisting feldspars move away from the Or-Ab and Ab-An

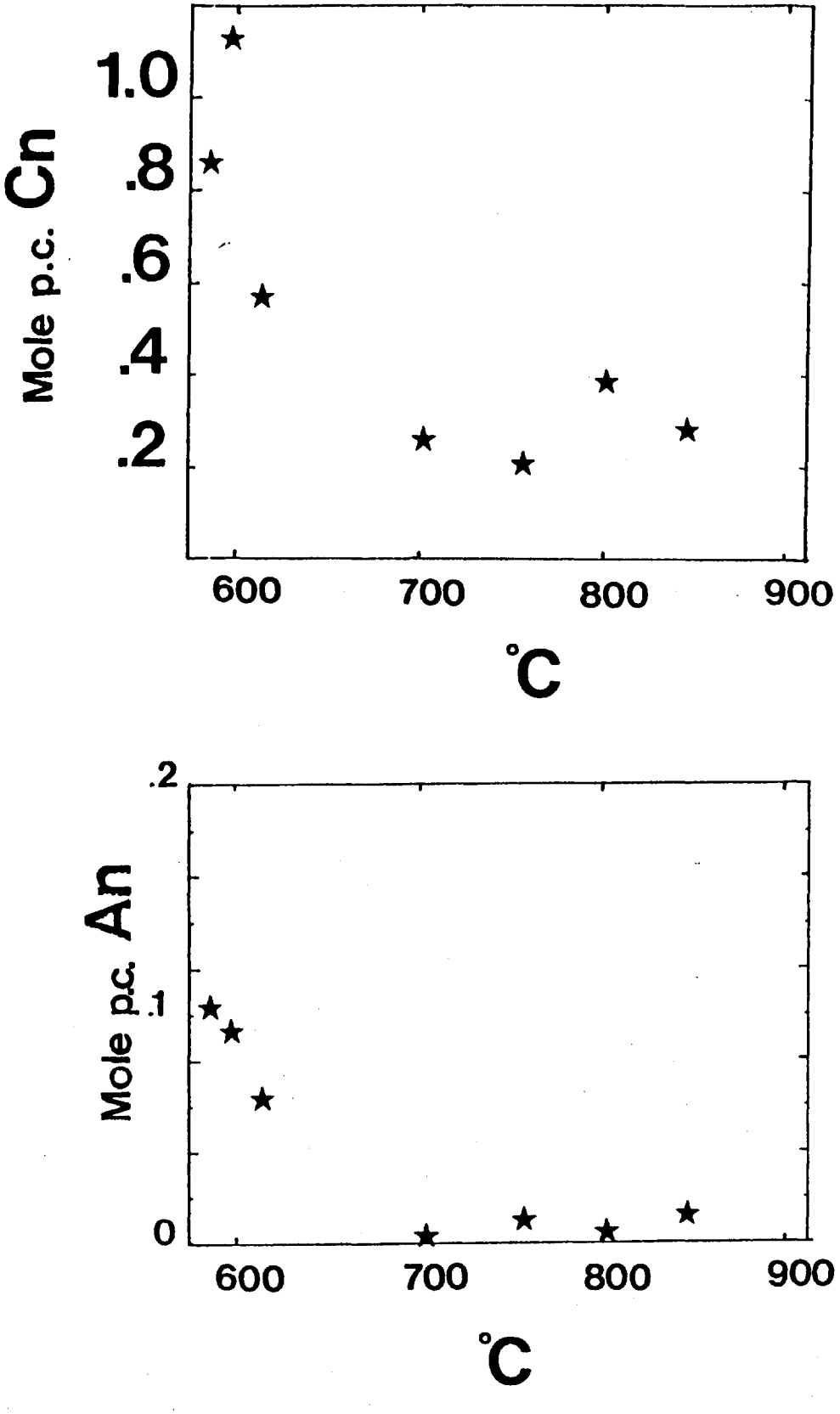
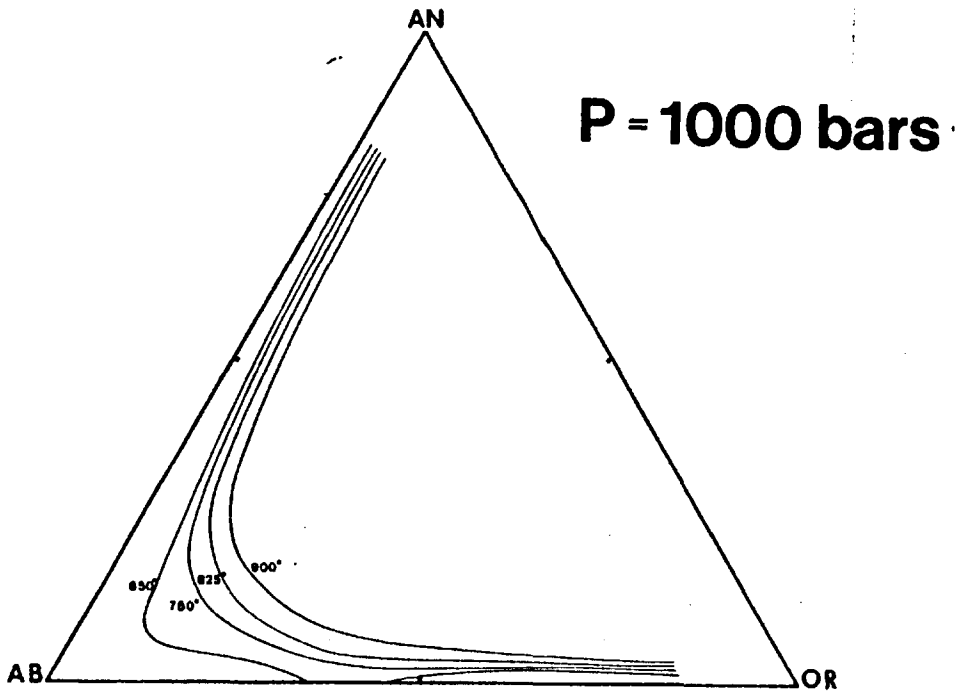


Fig 4.10 Celsian- and anorthite-content of Late Scourian alkali feldspars plotted against estimated temperature

sidelines in ternary feldspar diagrams (Figure 4.11). It is suggested that the temperatures given in Table 4.8a systematically fall below the real equilibration temperatures as Ca increases in alkali feldspar. The effect of Ba is relatively small, and the apparent correlation between temperature underestimation and Ba may reflect geochemical variations between pegmatites.

It is possible to suggest that Ba has a secondary effect on the composition of the alkali feldspars. Assuming the Ba content of alkali feldspars to reflect geochemical differences, with Ba always partitioning strongly into alkali feldspar relative to plagioclase, it follows that alkali feldspars from high-Ba pegmatites must have a lower atomic Si:Al ratio than those from Ba-poor pegmatites. Analyses of the alkali feldspars certainly show divergence from the usual 1:3 ratio (Table 4.7), the result of the coupled substitution $BaAl \gtrless KSi$. As Gay and Roy (1969) point out, there is no reason why Ba and Ca should not exchange readily and the departure of the alkali feldspars from normal Si:Al stoichiometry may facilitate the partitioning of Ca into alkali feldspar. Thus the high levels of Ba may cause significant departures from the distribution of Ca between the feldspars predicted by Seck (1971).

In Table 4.8b, estimated equilibration temperatures are given for perthite lamellae. In addition to some of the uncertainties already discussed, the structural state of the alkali feldspar component has to be considered,



4.11 Ternary feldspar solvi determined by Seck (1971)

since inversion to microcline was associated with perthite exsolution. Stormer (1977) presented a geothermometer for microcline-plagioclase equilibration, and this was used to calculate the temperatures shown in Table 4.8b. Estimates result which are about 50°C higher than those obtained using the model of Powell and Powell (1977a). It could be argued that since the perthite lamellae have the monoclinic symmetry of the microcline twins, they exsolved from a monoclinic feldspar, perhaps having the intermediate structure of orthoclase, and estimated temperatures should fall between those based on the completely-ordered and completely-disordered models. Thus while the estimates of Table 4.8a may be based on the equilibration of disordered feldspars (Martin, 1974, suggests alkali feldspars are completely disordered above about 700°C at 5Kbar), those in Table 4.8b may be subject to significant errors because of uncertainties about structural state.

Against this structural uncertainty, the effect of anorthite in alkali feldspar is much reduced. Most temperatures cluster around 520-580°C, and probably represent minimum estimates of the temperatures of perthite exsolution, while a few as low as 400°C were obtained from irregularly-developed perthites and antiperthites, and may reflect strain-induced perthite formation at a much later stage. This is supported by the contradictory estimates obtained from the perthites

and antiperthites in a single pegmatite at Scouriemore.

The consistency of temperature estimates from perthites in several samples suggests that these temperatures may also reflect thermal equilibration between the pegmatites and the surrounding gneisses (this is further supported by the textural evidence for slow cooling and coarsening of the alkali feldspars), providing a reasonable estimate (580°C) for the temperature of the Scourie gneisses at about 2560 m.y.b.p.

To summarise, feldspar thermometry suggests that the initial crystallisation of the pegmatites at temperatures of 700°C or more was followed by re-equilibration of the feldspars by perthite exsolution as the pegmatites cooled to the ambient temperature (580°C) of the gneisses. Ordering of alkali feldspars to microcline and perthite exsolution occurred at some temperature between these two estimates. Later deformation caused further irregular perthite exsolution in some pegmatites.

4.4.2 FERROMAGNESIAN AND OXIDE MINERALS Table 4.9

If equilibrium was achieved between alkali feldspar, biotite, magnetite and quartz in the pegmatites, the T-f_{O_2} histories of these rocks may be traced, at least in a qualitative way (Wones and Eugster, 1965).

Figure 4.12 shows the relative oxygen fugacities of several pegmatites. Positions of individual pegmatites

Table 4.9 Ferromagnesian and oxide minerals in Late Scourian pegmatites.

BIOTITES, LATE SCOURIAN PEGMATITES

	1		2		3		4		5		6		7	
SIO2	37.29		35.18		37.82		37.94		36.22		37.08		35.77	
TIO2	3.76		4.57		3.01		3.15		2.61		4.80		.20	
A203	16.41		15.64		14.10		14.30		17.02		16.90		15.81	
FEO	17.70		21.42		17.83		17.74		20.37		16.19		20.45	
MNO	0		.23		.21		.22		.24		0		.18	
MGO	12.56		9.52		12.54		12.70		8.78		11.89		9.91	
CAO	0		0		0		0		0		0		0	
NA20	0		0		0		.07		0		0		.27	
K20	10.56		9.59		9.68		9.53		9.95		9.32		9.74	
SUM	98.28		96.15		95.19		95.65		95.19		96.18		92.33	
SI	5.487		5.401		5.736		5.717		5.567		5.494		5.690	
AL	2.513	8.000	2.599	8.000	2.264	8.000	2.283	8.000	2.433	8.000	2.506	8.000	2.310	8.000
AL	.332		.230		.256		.256		.650		.445		.654	
TI	.416		.528		.343		.357		.302		.535		.024	
FE	2.178		2.750		2.261		2.235		2.618		2.006		2.721	
MN	0		.030		.027		.028		.031		0		.024	
MG	2.755	5.681	2.178	5.716	2.835	5.722	2.852	5.729	2.011	5.612	2.626	5.612	2.350	5.772
CA	0		0		0		0		0		0		0	
NA	0	1.982	0	1.878	0	1.873	0	1.852	0	1.951	0	1.761	0	2.059
K	1.982	1.982	1.878	1.878	1.873	1.873	1.832	1.852	1.951	1.951	1.761	1.761	1.976	2.059
0	22.000		22.000		22.000		22.000		22.000		22.000		22.000	
ANN		44.16		56.07		44.67		44.25		56.85		43.31		53.88
PHLO		55.84		43.93		55.33		55.75		43.15		56.69		46.12
F/M		.791		1.276		.807		.794		1.317		.764		1.168
F/FM		.442		.561		.447		.442		.568		.433		.539

1 BIOTITE, LP4 LEENISH
2 BIOTITE, 2009 SCOURIEMORE
3 BIOTITE, 47 SCOURIEMORE
4 BIOTITE, 2102 SCOURIEMORE
5 BIOTITE, AP1 ARDIVACHAR PT, S. UIST
6 BIOTITE, 2103 SCOURIEMORE
7 BIOTITE, NEXT TO KYANITE, 2009

AMPHIBOLES, LATE SCOURIAN PEGMATITES

	1		2	
SIO2	47.69		45.70	
TIO2	.50		.59	
A203	7.22		11.08	
FEO	12.31		14.29	
MNO	.33		.45	
MGO	13.50		12.22	
CAO	11.83		12.20	
NA20	.93		1.37	
K20	.88		1.03	
SUM	95.19		98.93	
SI	7.135		6.674	
AL	.865	8.000	1.326	8.000
AL	.408		.581	
TI	.056		.065	
FE	1.540		1.745	
MN	.042		.056	
MG	3.010	5.057	2.660	5.107
CA	1.896		1.909	
NA	.104	2.000	.091	2.000
NA	.166		.297	
K	.168	.334	.192	.489
0	23.000		23.000	
FEMN		34.45		40.37
MG		65.55		59.63
F/M		.526		.677
F/FM		.344		.404

1 AMPHIBOLE, 47 SCOURIEMORE

2 AMPHIBOLE, 2013 SCOURIEMORE

OXIDES, 2102, SCOURIEMORE

	1	2	3	4
SIO2	.17	8.51	.07	1.04
TIO2	12.42	64.90	48.92	43.74
A203	.08	1.44	.08	.62
FEO	79.06	17.21	49.33	46.19
MNO	0	.20	.54	1.94
MGO	0	.57	.32	.31
CAO	0	6.58	.94	1.28
SUM	91.73	99.41	99.30	95.12
RECALCULATED ANALYSIS - MAGNETITE-ULVOSPINEL BASIS				
F203	41.63	-82.31	-27.99	-23.12
FEO	41.55	91.36	74.47	67.02
TOTL	95.86	91.25	96.53	92.83
USP	37.68	211.04	139.64	132.60
RECALCULATED ANALYSIS - ILMENITE-HEMATITE BASIS				
F203	75.07	-47.39	7.07	10.36
FEO	11.43	59.90	42.96	36.86
TOTL	99.17	94.71	100.00	96.15
ROMB	25.13	142.18	93.15	88.83

MOL PROPS	RO2	RO	R203
1	18.84	50.00	31.16
2	0	0	0
3	93.15	0	6.85
4	88.83	0	11.17

OXIDES, 2013 SCOURIEMORE

	1	2	3	4	5
SIO2	.30	1.98	.59	1.38	1.41
TIO2	12.16	52.31	53.94	54.64	53.61
A203	.20	.81	.34	.57	.46
FEO	77.27	27.82	29.76	31.30	35.91
MNO	.09	10.40	8.35	5.57	2.90
MGO	.26	1.25	.28	.54	.37
CAO	0	2.20	2.34	3.67	1.11
SUM	90.28	96.77	95.60	97.67	95.77
RECALCULATED ANALYSIS - MAGNETITE-ULVOSPINEL BASIS					
F203	40.77	-41.43	-42.14	-43.93	-43.79
FEO	40.54	65.14	67.72	70.88	75.36
TOTL	94.32	92.66	91.42	93.32	91.43
USP	37.90	157.77	161.51	161.74	163.64
RECALCULATED ANALYSIS - ILMENITE-HEMATITE BASIS					
F203	73.69	-7.30	-8.59	-9.52	-10.31
FEO	10.88	34.40	37.50	39.88	45.20
TOTL	97.58	96.05	94.75	96.73	94.75
ROMB	25.30	105.82	107.96	108.29	109.48

MOL PROPS	RO2	RO	R203
1	18.95	50.00	31.05
2	0	0	0
3	0	0	0
4	0	0	0
5	0	0	0

OXIDES, LP4 BARRA

	1	2	3
SIO2	.18	.28	.30
TIO2	16.36	0	49.95
A203	.17	.26	0
FEO	78.32	93.47	48.24
MNO	.28	0	1.47
MGO	0	0	0
CAO	0	0	0
SUM	95.31	94.01	99.96
RECALCULATED ANALYSIS - MAGNETITE-ULVOSPINEL BASIS			
F203	35.99	68.54	-30.21
FEO	45.90	31.73	75.45
TOTL	98.88	100.80	96.97
USP	47.76	1.07	142.97
RECALCULATED ANALYSIS - ILMENITE-HEMATITE BASIS			
F203	70.55	103.18	4.94
FEO	14.76	.52	43.79
TOTL	102.30	104.23	100.45
ROMB	31.88	.71	95.31

MOL PROPS	RO2	RO	R203
1	23.88	50.00	26.12
2	.53	50.00	49.47
3	95.31	0	4.69

(Key over page)

(Table 4.9)

2102

1 Host Fe-Ti oxide grain

2 Coarse exsolution lamellae

3 Fine ilmenite lamellae (2nd order exsolution) in 1.

4 " " " (" " ") in 2.

2013

1 Host Fe-Ti oxide grain

2-5 zoned exsolution lamellae, rim(2) to centre (5)

LP4

1 Host Fe-Ti oxide grain

2 Exsolved magnetite lamella

3 Ilmenite rim around magnetite lamella

depend on the Mg/(Mg+Fe) ratio of biotite and the temperature of crystallisation estimated in section 4.4.1. Oxygen fugacities are very much more sensitive than temperature to biotite composition. However, the pegmatites appear to plot systematically closer to the QFM buffer as a function of temperature, a fact which may be related to the suggested underestimation of temperature in many pegmatites containing Ca-rich alkali feldspars. If this is so, the pegmatites may well have crystallised at T-f_{O_2} conditions near the QFM buffer, as suggested by Haggerty (1976) for a wide range of acid intrusive rocks. It is suggested that the pegmatites crystallised at 700-850°C, with oxygen fugacities between $10^{-12.5}$ and 10^{-15} bar.

Amphiboles in the Late Scourian pegmatites are edenitic hornblendes, with low Ti concentrations similar to those of the Laxford granite amphiboles, but contrasting with the younger amphiboles by having unfilled A-sites (low Na,K) and much lower Fe/(Fe-Mg). The two groups of amphiboles are compared in Figure 4.2.

The rather high Ti contents of the Late Scourian biotites (apart from the green, Ti-poor biotite which is associated with the breakdown of rare kyanite inclusions) contrast strongly with the compositions of the biotites from the Laxford granites. Since sphene, which in the Laxford granites is a product of pyroxene breakdown, is not found as a discrete phase in the Late Scourian

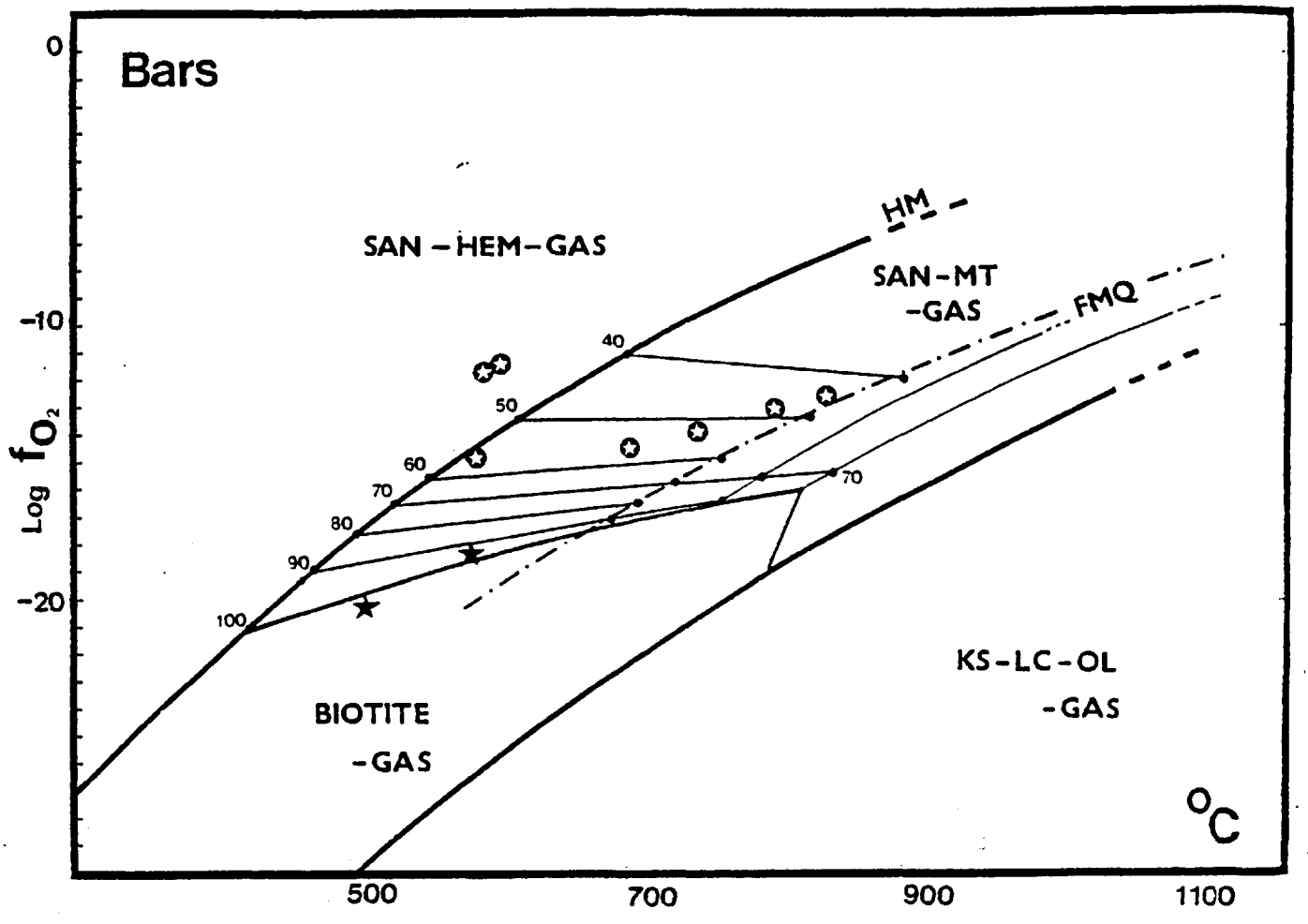


Fig 4.12 (From Wones and Eugster, 1965)

Estimated T - f_{O_2} conditions for equilibration of Late Scourian pegmatite mineral assemblages. Open stars - biotite coexisting with alkali feldspar, magnetite and quartz, using temperature estimates from alkali feldspar - plagioclase equilibration. Numbered contours are mol. p.c. annite in biotite.

Closed stars - estimates based on compositions of exsolved oxide minerals in two Late Scourian pegmatites.

pegmatites, the contrast between the two groups of rocks may be a function of oxygen fugacity (lower in the late Scourian pegmatites which lack the assemblage magnetite-sphene) rather than of magma composition.

In addition to the euhedral magnetite crystals common to all the Late Scourian pegmatites, irregular grains have been found in a few samples in which an Fe-Ti oxide host contains exsolved lamellae of contrasting composition. Intergrowth/exsolution and compositional features are shown in Figure 4.13 and summarised below:

a. Sample 2102, Scouriebeag, Sutherland.

An Fe-rich host, probably initially (magnetite-ulvospinel)ss, contains coarse Ti-rich lamellae in which TiO_2 is well above the normal maximum for (ilmenite-hematite)ss, and in which a significant amount of CaO is present.

Both host and coarse lamellae contain finer parallel lamellae, all of which are near to end-member ilmenite. Fine lamellae in the early coarse lamellae again contain significant CaO.

The textures are interpreted as two exsolution phases: (i) exsolution of (ilm-hem)ss from an initial homogeneous (mt-usp)ss, followed by (ii) oxidation-exsolution of ilmenite from both phases. The high CaO content of the coarse lamellae and their daughter lamellae indicate the presence of finely-disseminated sphene, the second phase of exsolution having occurred



Fig 4.13 Exsolution texture in an Fe-Ti oxide mineral from a Late Scourian pegmatite

as a result of sphenitisation of the Ti-rich coarse lamellae, a process considered by Haggerty (1976) to be associated with low-temperature oxidation.

b. Large pegmatite, Barra.

A variety of intergrowth textures suggest the formation of an initial intergrowth of (mt-usp)ss and (ilm-hem)ss. Many grains have later exsolved further lamellae, usually (ilm-hem)ss near to ilmenite. One grain, in which (mt-usp)ss is near to pure magnetite and is rimmed by ilmenite which it is thought was exsolved from the magnetite, has been used (Figure 4.12) to estimate the T-f_{O_2} conditions of exsolution (Buddington and Lindsley, 1964).

c. Sample 2013, Scouriemore, Sutherland.

The host oxide is (mt-usp)ss, and lamellae are (ilmenite-pyrophanite)ss with significant CaO, which again probably indicates the presence of fine sphene. The lamellae are strongly zoned, with pyrophanite-rich edges.

It is clear that at least a substantial part of the exsolution in these oxides has occurred at low temperatures and oxy gen fugacities, which may approximately be given by the calculated conditions for the Barra pegmatite (Figure 4.12), and which may roughly correspond with the country rock conditions estimated from alkali feldspar perthite lamellae.

Many oxide analyses cannot successfully be recast in terms of (mt-usp)ss and (ilm-hem)ss end-members, and it is unlikely that these represent homogeneous mineral phases, but include substantial amounts of rutile (in Ti-rich compositions) and sphene (in Ca-rich compositions). Sphenitisation involves some Ca-metasomatism of the oxide grains (Haggerty, 1976).

4.5 DISTRIBUTION OF TRACE ELEMENTS IN PEGMATITE MINERALS

4.5.1 Ba, Sr and Rb

In Chapter 3, it was shown that concentrations of these three elements in the Laxfordian granites and pegmatites provide an important part of the evidence allowing the origins and evolutions of several groups of rocks to be distinguished. The presence of significant amounts of Ba in alkali feldspars from the Late Scourian pegmatites suggests that some aspects of the evolution of these rocks are shared with the Laxford granite sheets, and the main object of this section is to use the indirect trace element evidence obtained from minerals to extend the comparison to Rb and Sr.

Concentrations of trace elements in pegmatite minerals are given in Table 4.10. Alkali feldspars from Late Scourian pegmatites and Laxford granite pegmatites are much poorer in Rb and richer in Ba and Sr than those from most Laxfordian pegmatites. Similarly lower relative concentrations of Rb and high Ba and Sr are found in Late

A. Rb, Sr, Ba

Sample	Alkali feldspars			Plagioclase feldspars		
Late Scourian						
47	421	152	737	12.5	256	72
2009	263	700	5964	10.5	188	99
2013	25.6	522	1429	10.2	506	148
2102	608	173	1041	17.2	434	117
2007	6.0	502	158	8.0	128	81
LP4	388	344	1488	23.1	408	66
AP1	228	256	193	12.4	400	107
Laxfordian						
2001	1232	90.7	24	60.1	23.4	10.1
GSP3	1122	19.5	8.9	112	96.2	16.1
GSP2	982	31	7.2	55.1	71	7.7
GSP1	1248	26	11.0	132	44.3	36.5
AP2	1140	34.1	25.5	6.3	65.4	16.3
GC6	2486	26.1	145	83.3	7.0	8.1
GC23	1568	33.4	101	112	56.3	23.6
LP13	1048	44.1	26.1	62.4	29	14.7
LP19	1341	12.3	77.4	71	41.2	11.8
LP21	882	19.8	60.3	27.2	43.8	29.9
107	715	54	197	19.7	84.3	1.5
Pegmatites from Laxford Granite sheets						
67	336.1	487.5	1641			
65	238.4	916.1	4248			
Phyllosilicates						
GC6(Ms)	4219	24.3	16.9			
2001(Ms)	6754	48.7	37.2			
2013(Bi)	1184	14.1	340			
47(Bi)	2677	18	126			
LP13(Bi)	1010	7.8	190			
GSP3(Bi)	1451	11.8	101			

Table 4.10 Trace element concentrations in Lewisian pegmatite minerals.

B. REE

garnets

Element	1	2	3	4
La	12.7	4.33	4.68	13.5
Ce	654	792	242	178
Nd	36.2	10.1	26.1	55.9
Sm	30.4	21.5	13.7	25.4
Eu	-	-	-	-
Tb	64.4	26.9	52.0	53.1
Ho	130	91.1	63.4	87.8
Tm	55.1	79.6	16.3	64.4
Yb	651	966	257	126
Lu	73.0	127	25.3	10.3

1 GC6 (1)

2 GC23 (1)

3 GC23 (2)

4 GC6 (2)

feldspars

Element	1	2	3	4	5	6	7	8
La	8.85	14.2	5.59	11.3	0.80	3.90	0.44	2.91
Ce	8.41	19.4	6.83	22.5	0.33	7.72	0.41	2.52
Nd	0.39	6.76	0.29	7.02	0.20	2.37	0.04	0.63
Sm	0.31	0.79	0.33	0.90	0.10	0.54	0.15	0.33
Eu	1.22	0.92	1.15	0.72	0.13	0.59	0.41	0.39
Tb	0.02	0.03	0.03	0.05	0.01	0.03	0.06	0.16
Yb	0.09	0.18	0.05	0.22	0.89	0.04	0.08	0.27

1 AF47 (Scouriemore)

2 PF47

3 AF 2013 (Scouriemore)

4 PF 2013

5 AF GC6 (Chaipeval, S. Harris)

6 PFGC6

7 AF GC23 (Sletteval, S. Harris)

8 PF GC23

Scourian plagioclases. If the feldspar minerals are assumed to dominate the trace element geochemistry of the Late Scourian pegmatites, the contrast with most Laxfordian feldspar compositions both for alkali feldspar and plagioclase indicates that the Late Scourian pegmatites as a group are poor in Rb and rich in Ba and Sr. The same geochemical features found in the Laxford granites were used in Chapter 3 to suggest an origin by partial melting of granulite-facies gneisses: a similar argument applied to the Late Scourian pegmatites would suggest they are fairly localised melts derived from the granulites into which they are emplaced.

Details in which the separate bodies seem to differ from each other in a systematic way (e.g. varying major element concentrations in feldspars, widely varying $BaAl_2Si_2O_8$ in alkali feldspars, and quite large differences in Ba, Sr and Rb in both feldspars shown in Table 4.10) may reflect variations in the local geochemistry of the gneisses, despite which the general features common to all the pegmatites remain clear.

Figure 4.14 shows the fairly regular distribution of Ba, Sr and Rb between alkali feldspars and plagioclases from Late Scourian and Laxfordian pegmatites. Ratios such as Rb:Sr and Ba:Rb for the pegmatites differ by 2-3 orders of magnitude between the two groups.

The same trace element ratios show a much smaller difference when the amphibolite facies and granulite facies gneisses are compared (Chapter 3); this suggests that although the distribution of Ba, Sr and Rb in the Late Scourian and Laxfordian acid rocks may be related

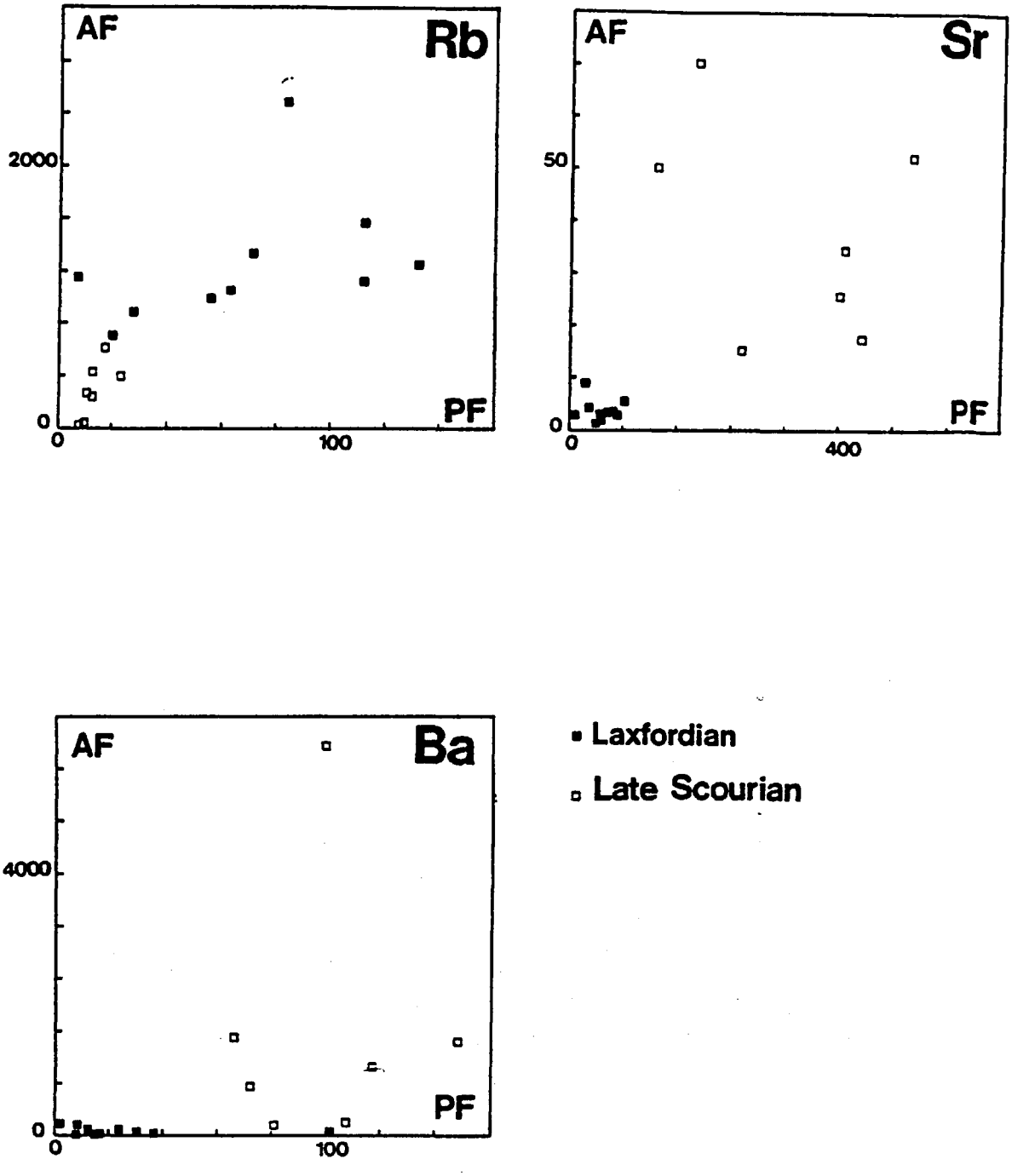


Fig 4.14 Distribution of Rb, Sr and Ba between pegmatite feldspars.

to the contrasting geochemistry of the gneisses, differences in the behaviour of the three elements have been exaggerated in the granites and pegmatites.

Rb occurs in high concentrations in all analysed biotites and muscovites, and this must have the effect in the Late Scourian pegmatites of modifying ratios such as Rb:Sr and Ba:Rb, although relatively low modal concentrations of biotite (probably never greater than about 5%) limit this effect, and since a similar relatively small modal proportion of biotite is present in Northern-type Laxfordian pegmatites the qualitative geochemical contrast between the Late Scourian and most Laxfordian pegmatites cannot be affected.

Muscovites from Southern-type Laxfordian pegmatite assemblages contain very large concentrations of Rb, a feature correlating with the high Rb content of alkali feldspars in these rocks. Rb is likely to partition strongly into liquid or fluid phases relative to solids at early stages in granite crystallisation (Hanson, 1978), and the high concentrations present in these minerals in Southern-type bodies provides further evidence of fractionation between Northern and Southern-type assemblages, and precipitation of Southern-type assemblages from an Rb-rich fluid or magma.

4.5.2 RARE EARTH ELEMENTS

Rare earth concentrations in feldspars are invariably low compared with those of the accessory minerals - monazite,

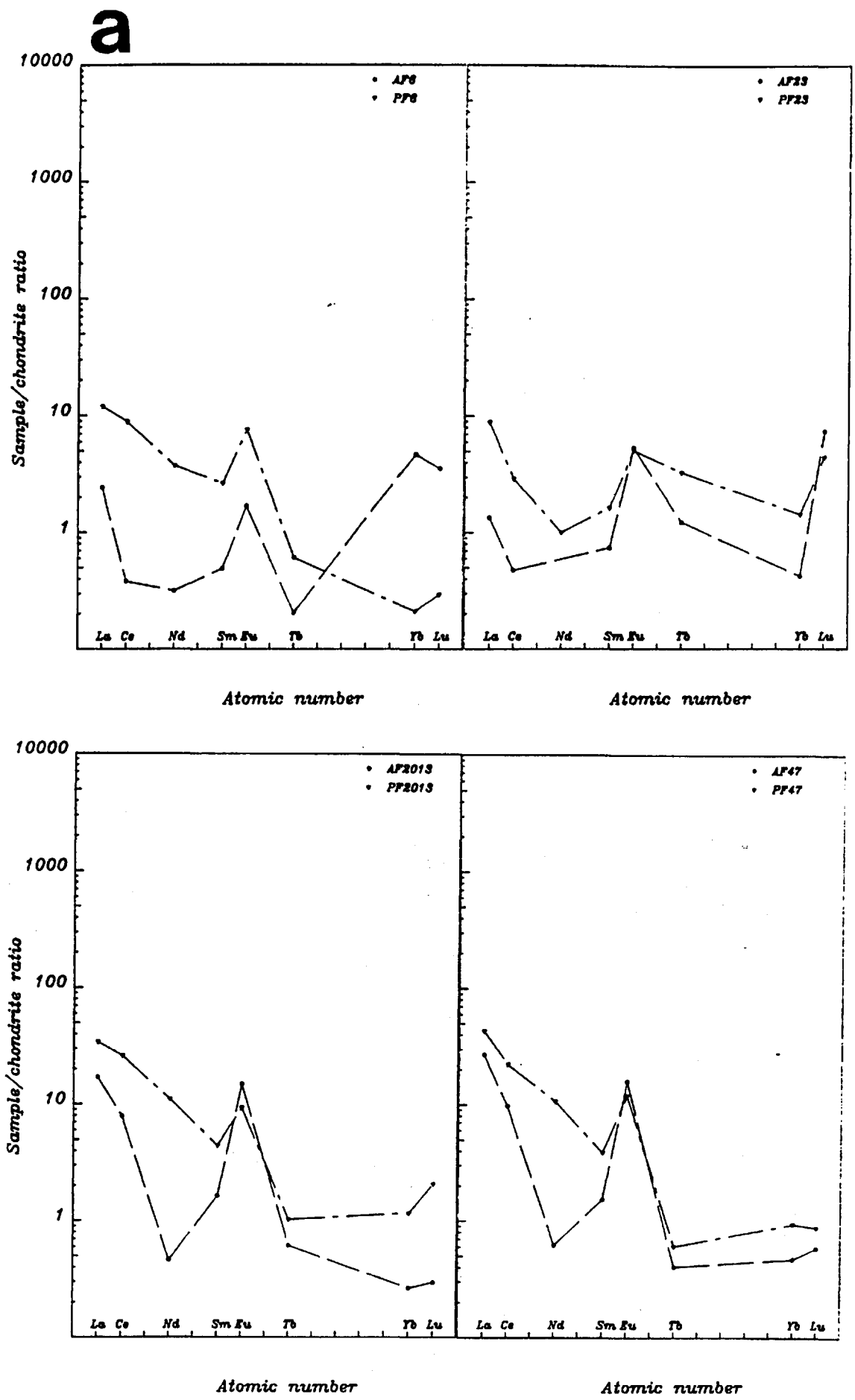
zircon, apatite, allanite - characteristic of acid rocks. Nevertheless, the chondrite-normalised patterns given in Figure 4.15 suggest that concentrations of most rare-earth elements are higher in Late Scourian pegmatite feldspars by about an order of magnitude than in Laxfordian pegmatites.

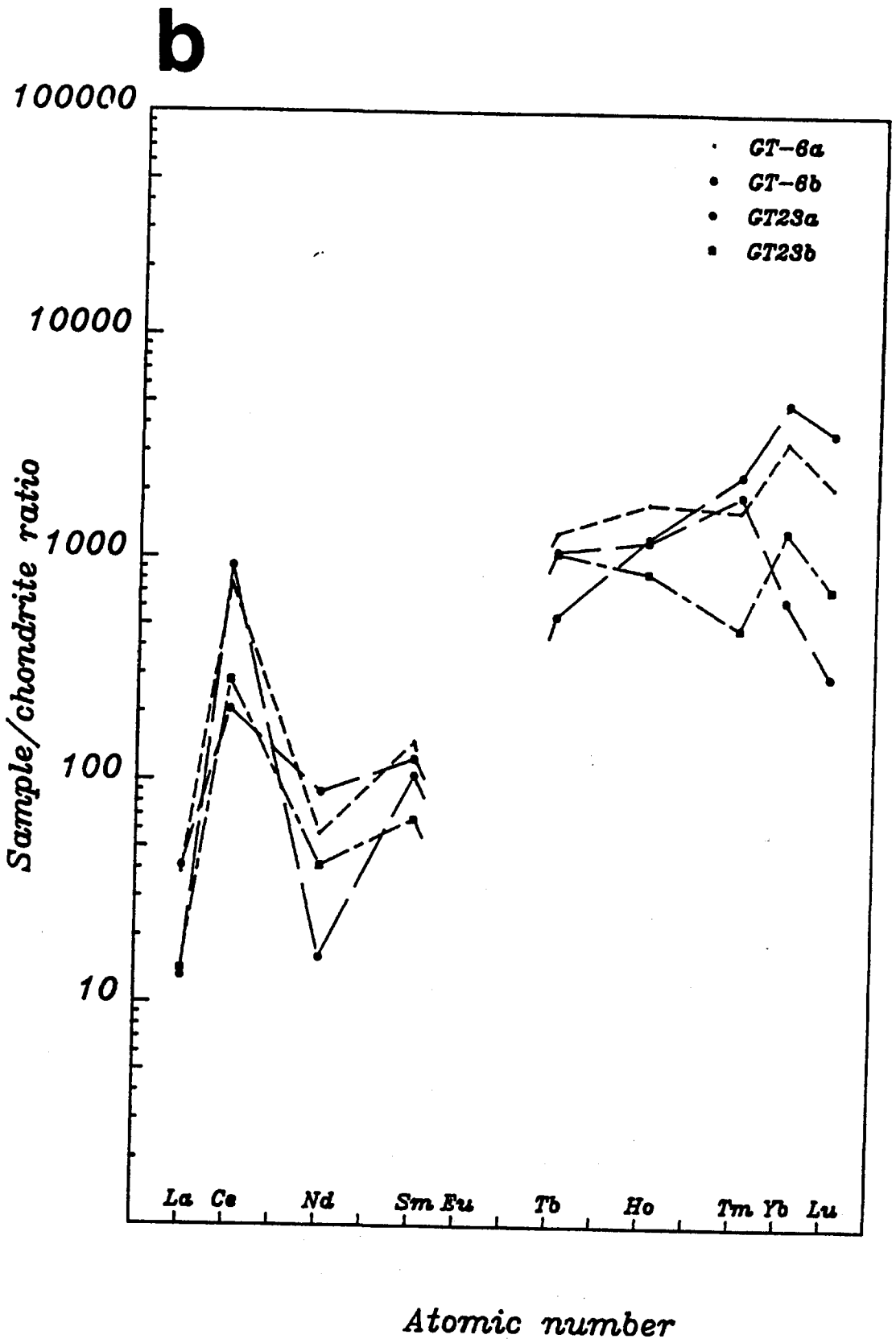
All feldspar patterns show a pronounced positive Eu anomaly - most Eu is probably contained in the feldspars, since all of the accessory minerals contain little or no measurable Eu (Hanson, 1978). While the plagioclases, into which most rare-earth elements are partitioned relative to alkali feldspars, have fractionated, light rare-earth enriched patterns, alkali feldspars display a steep drop from La to Ce, the pattern between Ce and Yb then being flat or possibly slightly heavy rare-earth enriched. The positive Eu anomaly is thus larger (if measured by the ratio $Eu:Eu^{*}$) in the alkali feldspars than in the plagioclases, and Eu may be present in higher absolute concentrations in the alkali feldspars.

The difference between the patterns for the two feldspars and the behaviour of Eu may be considered in relation to the distribution of all the measured trace elements between alkali feldspars and plagioclases. It has already been suggested, following Gay and Roy (1969) that the major influence on Ba distribution is the ionic radius of the trace element. In Figure 4.16 the concentration ratios between the feldspars are plotted against ionic radius for a range of trace elements. Eu

Fig 4.15 REE patterns for pegmatite feldspars and garnets.
(a) Feldspars - Southern-type Laxfordian pegmatites (above), Late Scourian (below).

(b) Garnets from two Southern-type Laxfordian pegmatites


a
10000
1000
100
10
1
Sample/chondrite ratio
AF6
PF6
AF23
PF23
AF2013
PF2013
AF47
PF47
La Ce Nd Sm Eu Tb Yb Lu
Atomic number


b
100000
10000
1000
100
10
Sample/chondrite ratio
GT-6a
GT-6b
GT23a
GT23b
La
Ce
Nd
Sm
Eu
Tb
Ho
Tm
Yb
Lu
Atomic number

is assumed to be divalent, and this is supported by its strong partitioning into feldspars relative to other phases; Eu is likely to be almost entirely in the reduced (divalent) state at the low oxygen fugacities suggested in Section 4.4.2 to have prevailed in all the Lewisian acid rocks (Drake and Weill, 1975). Six-fold co-ordination values are used for all cations in Figure 4.16 (Whittaker and Muntus, 1969); although the co-ordination polyhedron for M-cations in alkali feldspars is irregular (Smith, 1974), Gait et al.(1970) found that the lowest electrostatic charge imbalances for low albite were obtained for this value.

Figure 4.16 shows that the strongest partitioning of rare earth elements into plagioclase relative to alkali feldspar is for elements with ionic radii nearest to those of Ca, with Ce showing the strongest partitioning into plagioclase; this may account for the large chondrite-normalised difference between La and Ce in alkali feldspars. Eu is weakly partitioned preferentially into alkali feldspar relative to plagioclase. Sr, whose ionic radius is slightly smaller than that of divalent Eu, may prefer either alkali feldspar or plagioclase. A similar pattern of trace element partitioning is seen between feldspars from the Narragansett Pier granite, Massachusetts (Buma et al., 1971).

A curved relationship between distribution coefficients and ionic radius is indicated by Figure 4.16, and similar patterns have been described for crystal/liquid trace element distribution (Jensen, 1973). In the latter case

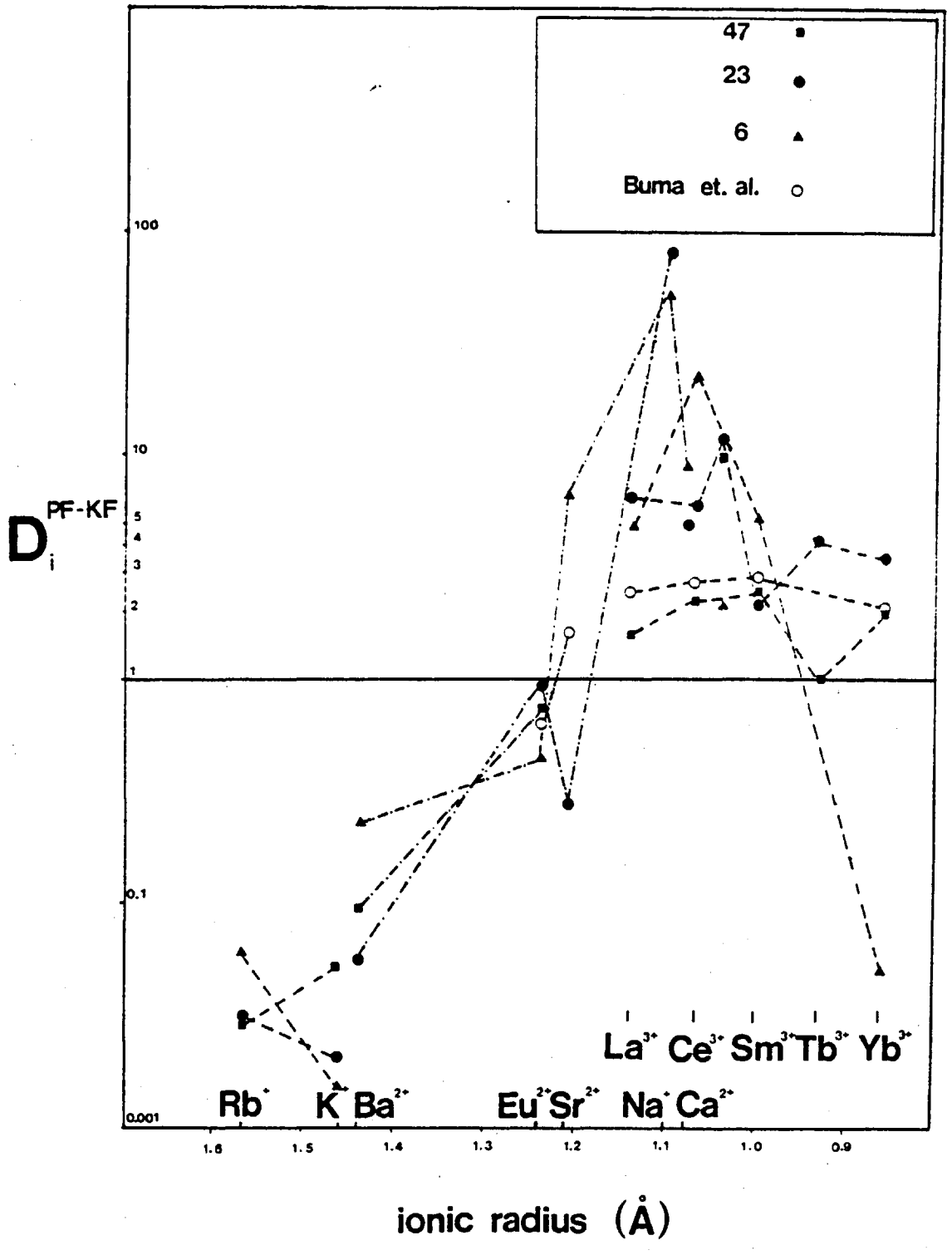


Fig 4.16 Distribution of trace elements between alkali feldspars and plagioclases plotted against ionic radius

the pattern is explained in terms of preferred effective ionic radii for distinct sites in phenocryst phases, with a major element cation lying close to, but not necessarily exactly on, the 'ideal' ionic radius. Trace elements whose ionic radii diverge from the 'ideal' are found progressively further out on the limbs of the curved pattern.

Clearly, a diagram such as Figure 4.16 provides information only about element distribution between feldspars, and cannot indicate the behaviour of liquid or fluid. The curved pattern which reaches a maximum at the ionic radius of Ca (and is close to Na) follows the explanation used for crystal/liquid distribution fairly well, suggesting some degree of equilibration between the feldspars. A minimum, corresponding to the ionic radius of K, would be expected in the pattern, and elements such as Rb and Ba whose ionic radii lie close to this minimum would be expected to partition preferentially into alkali feldspar. Strictly, cations of the same valency should be compared (Jensen, 1973), since each valency-group plots on its own curve although all curves appear to share the same maxima and minima. The heavy rare earths do not partition strongly into either of the feldspars, not (as is the case with Eu and Sr) because they lie in a position of intermediate ionic radius, but because their ionic radii are too small for them to be easily accommodated in the feldspar structure.

Chondrite-normalised rare-earth patterns for garnet samples from Laxfordian pegmatites are shown in Figure 4.15. Very high concentrations of the heavy rare earths are found, while Eu is almost absent. The anomalously high Ce values are due to the presence of very small monazite inclusions in some garnets.

The overall impression given by rare-earth behaviour during pegmatite crystallisation is of the strong influence of crystallising phases on the removal of elements from liquids and fluids. Thus the higher levels of rare-earth elements in Late Scourian pegmatite feldspars relative to Laxfordian samples may be entirely due to varying modal amounts of accessory minerals, while the heavy rare-earth enriched patterns of garnets need not imply a similar pattern for the fluids from which they crystallised.

4.6 CONCLUSIONS

The phase chemical evidence discussed in this chapter has been used to (a) support and extend the geochemical arguments about the origins and evolutionary paths of the Lewisian acid intrusive rocks, in particular bringing the Late Scourian pegmatites into the discussion, and (b) assess the conditions under which the various groups of rocks evolved.

The distribution of trace elements, and especially of Ba, Sr and Rb, in the Late Scourian pegmatites indicates

that these rocks, in common with the Loch Laxford granite sheets, originated by the partial melting of depleted granulite-facies gneisses, both retaining the relative distribution of trace elements found in the granulites and at the same time greatly enhancing certain trace element ratios (Sr:Rb and Ba:Rb). This increase in trace element contrasts over that observed in the gneisses may be largely due to the effects of partitioning between the liquid and crystalline residuum formed by partial melting of K and Rb-depleted granulites, as discussed in Chapter 3.

An important difference between the Laxford granites and the Late Scourian pegmatites, partly implied by their great age-difference (1750 m.y. and 2560 m.y. respectively), may have been the distance between their respective zones of generation and emplacement. Local melting of the granulites is much easier to envisage in the case of the older group of rocks, and is perhaps indicated by the chemical heterogeneity of the Late Scourian pegmatites as a group. Further evidence is provided by the preservation of high temperature feldspar compositions in these bodies.

Feldspars from all the Laxfordian rocks indicate low temperatures of equilibration, a feature consistent with the evidence in the granites of continuous re-equilibration and recrystallisation under ambient low-amphibolite facies conditions in the granites. Many Northern and Southern-type pegmatites, on the other hand, apparently crystallised

directly at temperatures as low as about 500°C, suggesting the important participation of a hydrous vapour phase in their formation.

The mineral assemblages present in a wide range of Lewisian acid rocks seem to have equilibrated near to or above the quartz-fayalite-magnetite oxygen buffer, and in the rare cases where T-f_{O_2} conditions can be assessed at more than one stage in the evolution of a single pegmatite, cooling appears to have taken place parallel to the QFM buffer. This cooling path may apply widely to the evolution of Northern-type into Southern-type Laxfordian pegmatites, since the latter contain the most iron-rich biotites (where present) and ultimately magnetite disappears as the Southern-type assemblages crystallise.

Of the Southern-type minerals, the presence of a phengite-rich muscovite at the expense of alkali feldspar indicates high P_{H_2O} (Velde, 1965; Helgeson, 1967) and high $a_{H^+}:a_{K^+}$ (Eugster, 1970, 1977), as well as falling temperature and oxygen fugacity. The Mn-rich phases, garnet and rare ilmenite-pyrophanite, are almost certainly stabilised at the prevailing conditions of crystallisation by their high Mn-content (Green, 1977; Haggerty, 1976), since their Mn-poor equivalents would require much higher pressures and oxygen fugacities respectively. The presence of ilmenohematite only in the Late Scourian pegmatites further underlines the interdependence of T and f_{O_2} in the acid rocks as a whole.

Attempts to estimate physical conditions of crystallisation in the present chapter have been made with

the aim of elucidating trends in the evolution of rocks, rather than (given many of the weaknesses inherent in the methods employed) in the expectation of providing highly accurate and precise values. It is suggested that in this and the last chapter, several such trends have been defined, involving (a) the evolution of leucogranites and pegmatites from the Laxfordian melagranites, (b) the evolution of Northern into Southern-type Laxfordian pegmatite assemblages and (c) the absence of the evolution of assemblages similar to those of the Southern-type pegmatites in the Late Scourian pegmatites, a factor attributable to the higher-temperature crystallisation of these rocks, or to a less water-saturated magma.

CHAPTER 5

METASOMATISM

5.1 INTRODUCTION

5.1.1 SCOPE OF THE STUDY - METASOMATIC REACTION BETWEEN BASIC HOST ROCKS AND ACID PEGMATITES

This chapter provides an examination in detail of the chemical, structural and textural features of the products of reaction between acid and basic rocks at elevated temperatures.

The two localities at which evidence of reaction of this type has been found are: (a) the Leenish peninsula, Barra [NL 704986] and (b) Garry-a-Siar, Benbecula [NF 756534]. The first of these occurrences may represent a unique or at least uniquely recognisable event in Lewisian chronology, but the second involves the emplacement of a fairly characteristic Laxfordian pegmatite.

Previous detailed studies of the development of metasomatic structures have been applied to spheroidal segregations in pelitic metasediments (Fisher, 1970, 1973; Eugster, 1970), to the formation of calc-silicate bands between metamorphosed pelites and limestones (Vidale, 1969; Brock, 1972; Vidale and Hewitt, 1973; Thompson, 1975) and to "black-wall" zones formed between ultramafic and pelitic or quartzofeldspathic rocks (Read, 1934; Curtis

and Brown, 1969). There has been no examination of compositional pairs of simple acid and basic type and their reaction products.

The present investigation was undertaken because a similar phenomenon has not been described, and also to provide an indication of the type and extent of chemical modification possible in Lewisian acid intrusive rocks as a result of metasomatism.

5.1.2 THE DEVELOPMENT OF METASOMATIC STRUCTURES

The processes involved in metasomatism are those of metamorphism: (a) reaction resulting in the growth or dissolution of mineral species and (b) the transport of chemical components along chemical potential gradients to and from the sites of reaction. Strictly, all metamorphic reactions are metasomatic, in that mass transfer is inevitable in the growth of new mineral phases, but in practice metasomatism is normally referred to only when a rock undergoes a bulk change in composition; that is, when the transport path of chemical components is regarded as significant. In this chapter, metasomatic processes will be described in which transport paths range from less than 1 mm to at least several centimetres.

As Thompson (1959) has pointed out, the description of metasomatism in natural rocks is necessarily incomplete, since only the final products can be observed. Nevertheless, extensive development of the theory of mass

transfer has taken place (Korzhinskii, 1970; Fisher, 1973; Weare et al., 1976; Frantz and Mao, 1976; Brady, 1975, 1977). The theory is developed here only insofar as it provides a basis for the interpretation of natural metasomatic structures, and the approach in this chapter will be to identify the likely processes which control the development of these structures, without any expectation that quantitative statements can be made about the rates at which they occur.

Korzhinskii (1970) distinguished two mechanisms of metasomatic transport - infiltration and diffusion metasomatism. In the former, transport is effected by the movement through the pore spaces in a rock of a fluid solvent, so the velocity of components dissolved in the fluid is equal or nearly equal to that of the fluid. In the case of diffusion, transport takes place in response to chemical potential gradients in a stationary fluid (it is assumed here that intragranular or solid state diffusion is not a significant process in comparison with intergranular diffusion or infiltration (Fisher, 1977)). In the present context infiltration clearly cannot be ignored, and it is probably generally true that both infiltration and diffusion processes combine in natural metasomatism. A "diffusion-only" end-member might be represented by the reaction of alternating pelite and limestome sedimentary bands to produce calc-silicate rocks, although even here mixing of the main fluid phases, H_2O and CO_2, would represent a limited form of infiltration.

Leaving aside, for the present, the need to consider metasomatism as a multicomponent process, the flux of a component, J (the mass flow across a unit area in a plane perpendicular to the direction of transport) is given by (Fletcher and Hofmann, 1974):

$$J = J_D + J_I \qquad \ldots 1$$

where the flux due to diffusion is

$$J_D = -D(\partial c/\partial z) \qquad \ldots 2$$

where z is in units of distance in the direction of transport, c is the concentration of the component in the fluid and D, the effective diffusivity of the component in the porous rock, is related to the intrinsic diffusivity of the component in the fluid medium alone by

$$D = \tau\beta D_i \qquad \ldots 3$$

where β is the volume fraction of pore fluid, and τ is a function of the difficulty of the diffusion path, or tortuosity.

The flux due to infiltration is given by

$$J_I = \beta\bar{v}c \qquad \ldots 4$$

where $\bar{v}$ is the average fluid velocity.

These equations refer only to transport in the fluid. Solid phases can be taken into account if it is assumed that the component partitions between the fluid and solid

phases at all points along the transport path, or in other words that local equilibrium is maintained (Thompson, 1959). The assumption of local equilibrium leads to two important conclusions:

a. Partitioning (reaction) is very rapid relative to transport, and therefore metasomatic processes are controlled by transport. Fisher (1977), ignoring infiltration, regarded all natural metamorphic processes as diffusion-controlled, reaction rates being relatively rapid.

b. Chemical potential gradients cannot exist between adjacent rocks of identical mineralogy, even if modal variations cause differences in bulk composition, since the two mineral assemblages, being identical, would be in equilibrium with identical fluids. Diffusive mass transfer would not occur. The corollary of this point is that metasomatism tends to result in the formation of sharply-bounded zones, or sequences of zones (Korzhinskii, 1970). At each interzonal boundary, at least one mineral phase disappears or is replaced, with the result that a chemical potential gradient can be maintained across a sequence of zones. Such zones may be developed with planar geometry between parallel rock layers, or as coronas or diffusion haloes around growing or dissolving porphyroblasts (Fisher, 1970).

Similarly, assumption of local equilibrium during infiltration metasomatism demands the presence of sharply-

bounded replacement fronts (Korzhinskii, 1970, p.21). Infiltration, however, is driven by fluid pressure gradients rather than by chemical potential gradients. Fletcher and Hofmann (1974) have derived simple models for combined infiltration and diffusion metasomatism, and some of their conclusions are summarised in Figure 5.1. In general, while diffusion may dominate the metasomatic process at first, tending to reduce chemical potential gradients, infiltration eventually becomes dominant at any point in a growing reaction zone, producing fluid concentration plateaux which terminate (in Figure 5.1b) in a normal diffusion profile, and on the whole tending to maintain chemical potential gradients. Fletcher and Hofmann (1974) conclude that diffusion metasomatism acting alone is effective over distances of the order of centimetres or less, while infiltration, requiring fluid pressure gradients as low as 1 bar km^{-1}, can be effective quite rapidly over much larger distances. Nevertheless, diffusion may be important as a rate-controlling influence at growing reaction zone boundaries.

Finally, consideration must be given to the multi-component nature of mass transfer. Equations such as (1) above are adequate for the description of self-diffusion, in which it is assumed that composition remains constant. Since diffusion is a function of composition, the transport of any single species is a function of the chemical potential gradients of all other components, while any coefficient of diffusivity must take into account

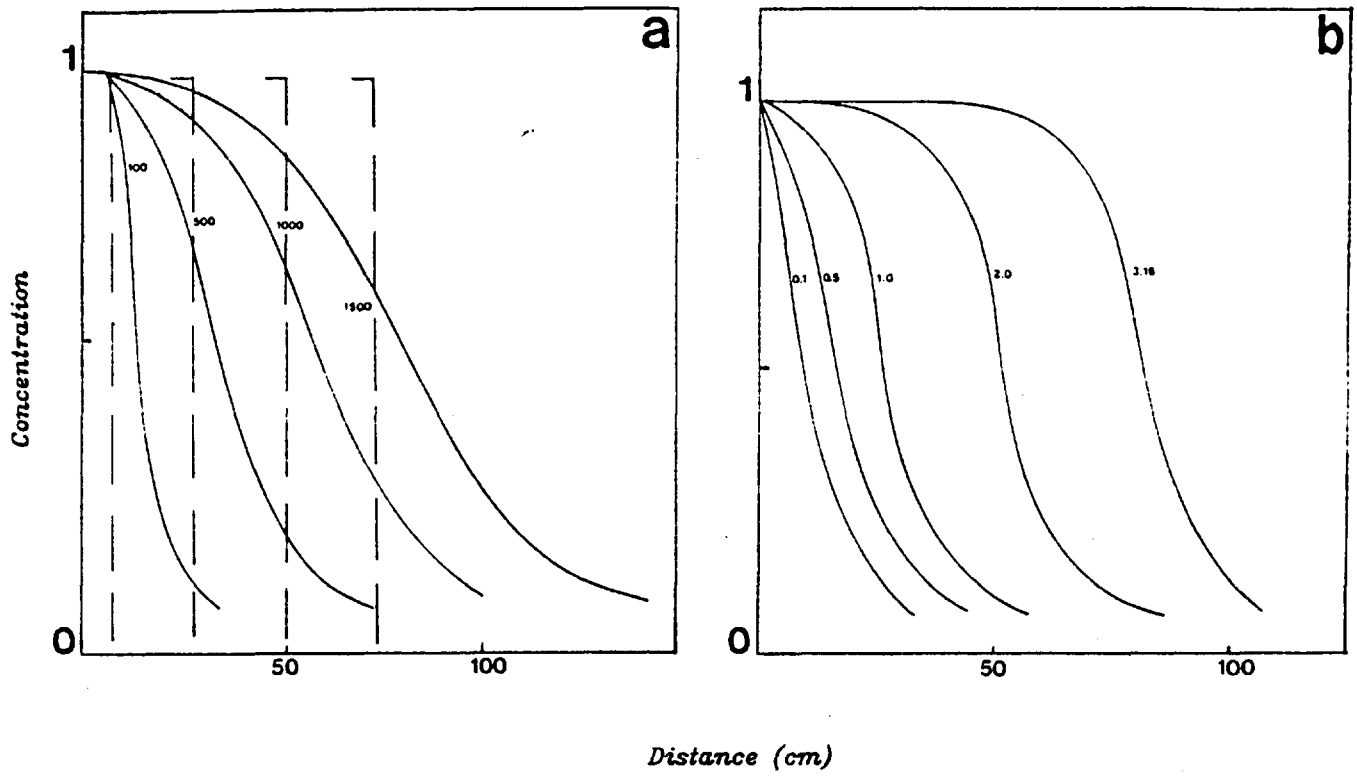


Fig 5.1 Effects of combined diffusion and infiltration metasomatism

a. Concentration profiles (relative to a standard concentration) as a function of distance for times of 100–1500 years, with an infiltration flux $\beta\bar{\nu} = 0.5 cm^3 cm^{-2} yr^{-1}$, and effective diffusivity $D = 10^{-8}\ cm^2\ sec^{-1}$. Pure infiltration profiles for the same values of $\beta\bar{\nu}$ and t are shown by the dashed lines.

b. Concentration profiles as a function of distance for t = 500yr, and for a range of infiltration fluxes from 0.1 (almost pure diffusion) to 3.16 $cm^3 cm^{-2} yr^{-1}$.

interactions between all the components. A flux equation analogous to Fick's first law describes multicomponent diffusion:

$$J_i^D = -\sum_{j=1}^{n} L_{ij}^D \nabla\mu_j \qquad \ldots 5$$

(Fisher, 1977)

where J_i^D is the diffusive flux of component i, $\nabla\mu_j$ is the chemical potential gradient of component j, and the elements (L_{ij}^D) of the diffusion matrix are of two types - those similar to intrinsic diffusion coefficients, which lie on the leading diagonal of the matrix and are of the type L_{ii}, L_{jj}, L_{kk}, etc., and the off-diagonal coefficients which involve interaction between components (for example, electrostatic coupling). Comprehensive sets of these coefficients suitable for quantitative application of equations such as (5) are not available, although some estimates of relative magnitudes have been made (Fisher and Joesten, quoted in Fisher, 1977; Lerman et al., 1975; Hurd and Theyer, 1975). Detailed sets of equations for the description of multicomponent diffusive mass transfer have been developed by Frantz and Mao (1976) and Weare et al. (1976), and the latter authors successfully modelled the growth of kaolinite and gibbsite crusts during the dissolution of alkali feldspar in water. These models will not be considered further here, since they concentrate upon pure diffusion metasomatism.

Equations (1) - (4) above may be taken to indicate the range of controlling factors whose relative influences might be assessed by examination of natural metasomatic rocks. As they stand, these equations assume the metasomatic process to be isothermal, both spatially and temporally. Variations in the thermal state of natural rocks during the formation of metasomatic reaction zones are unlikely to be discernible in the final products, but it should be stressed that any such variations may have an important effect on these products.

5.2 LEENISH, ISLE OF BARRA: METASOMATIC REACTION ZONES ASSOCIATED WITH SMALL ACID VEINS IN METADOLERITE

5.2.1 GEOLOGICAL RELATIONSHIPS

The acid veins and metasomatic structures described here occur within the largest Scourie metadolerite at Leenish (Map 4). The dyke itself is straight and trends NNW-SSE, and is cut by numerous narrow (less than 1 mm up to 5 cm) acid veins which trend very roughly at right angles to the dyke. Both the dyke and the veins are vertical. None of the veins can be traced into the country rock gneisses, nor in general into the amphibole-rich margins of the dyke. In the interior of the dyke, however, where the metadolerite assemblage is pyroxene + plagioclase ± garnet, the veins are parallel-sided, except in the case

of a few which 'wedge out', suggesting intrusion into dilating fissures. Where veins cross-cut each other, both dextral and sinistral transverse movement of the later vein margins is evident. Sigmoidal quartz growth from the margins of the larger veins shows the continuation of transverse movement during vein crystallisation.

All veins are flanked by dark-coloured, amphibole-rich parallel aureoles, in which the growth of amphibole has produced a texture coarser than that of the pyroxene-plagioclase metadolerite host. Several of the larger veins display zoned aureoles, in which an inner garnet zone next to the vein containing large (2 mm) pink garnets and biotite is succeeded by the hornblende zone already described. These characteristic minerals will be used as index names for the two zones. The contact between the two zones is very sharp and exactly parallel with the vein margin. In contrast, the outer margin of the hornblende zone is rather diffuse. All these features can be seen in Figure 5.2. Garnet is absent in the inner part of the garnet zone. Here biotite, which is abundant in the garnet zone, becomes dominant.

Measurement of vein widths and aureole widths allows the diagram shown in Figure 5.3 to be drawn. The simple straight-line relationship can be expressed roughly as

total width of structure (vein + symmetrical aureole) = 3 X vein width.

Garnet zones are present only in some of the larger aureoles, and do not form an addition to the net aureole



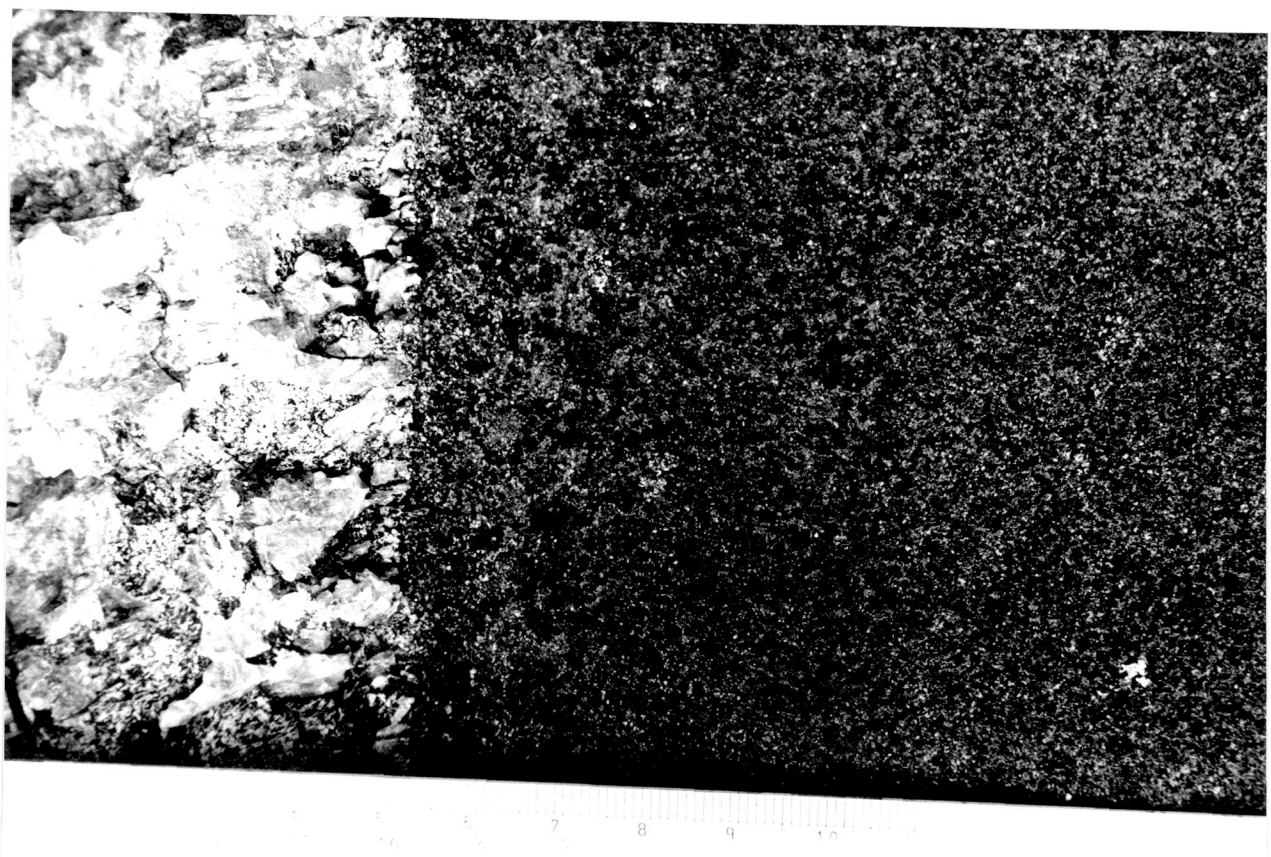


Fig 5.2 Zoned aureoles at Leenish, Isle of Barra

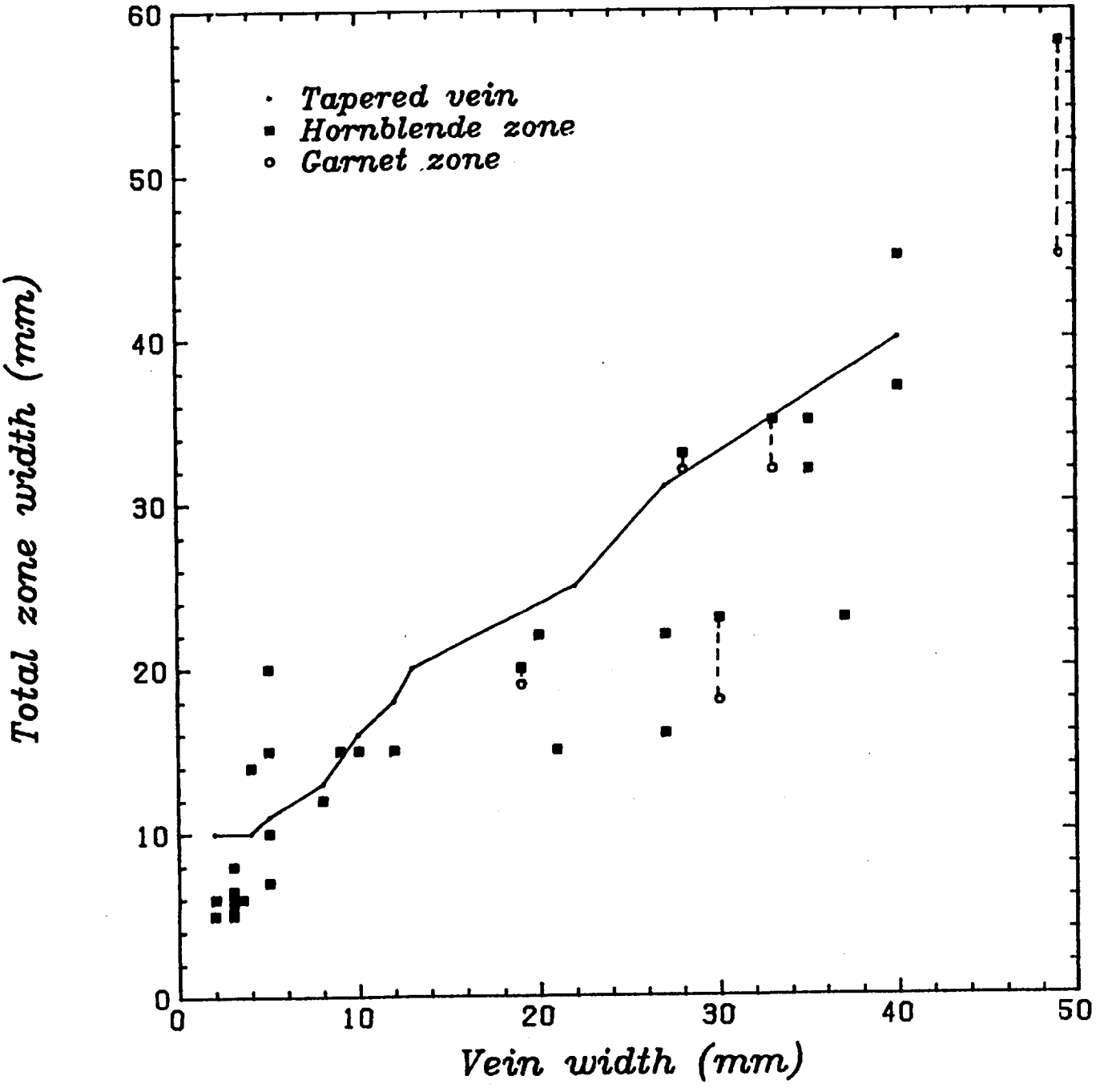


Fig 5.3 Aureole widths plotted against vein widths at Leenish

width, the hornblende zone becoming proportionally narrower relative to the vein.

Total aureole width and the presence or absence of a garnet zone are therefore broadly functions of vein size.

The width relationships between the hornblende and garnet zones suggest that the two zones overlap in some way, and may not be contemporaneous.

5.2.2 PETROGRAPHY

a. THE SCOURIE METADOLERITE

Where unaffected by acid veins, and except near the amphibolite margins, the host metadolerite dyke displays an intermediate granular texture with no apparent tectonic fabric. Pyroxene, plagioclase and usually garnet are apparent in hand-speciments.

In thin section, the assemblage hypersthene-augite-plagioclase-garnet is found, in an apparently equilibrium texture (Figure 5.5). There is no sign of the subophitic texture often found in Scourie metadolerites.

b. THE ACID VEINS

The sigmoidal growth of quartz already mentioned shows that crystallisation occurred from the vein margins during dilation or transverse movement of the fissures.

Feldspars may be 2-5mm long, while quartz may grow across the whole vein width. In thin section, the large feldspar (?)phenocrysts are subhedral and Carlsbad-twinned, and display coarse perthitic exsolution (alkali feldspar:plagioclase = 1:1) (Figure 5.4). The perthite plagioclase lamellae are albite-twinned. These twins presumably formed after exsolution, while the Carlsbad twins, which control the orientation of perthite lamellae, are clearly earlier, developing in an original homogeneous feldspar.

Between the large feldspars and quartz crystals is a fine interlocking matrix dominated by quartz and plagioclase, with minor alkali feldspar. Rare flakes of biotite are distributed irregularly. Accessory minerals are epidote, magnetite and monazite, while sericite often occurs along planes of alteration in the large perthites. In one section, small kyanite crystals were found, surrounded by fine alteration products (sericite, quartz, plagioclase). The kyanite is corroded and presumably represents a xenocryst phase.

c. THE AUREOLE ZONES (Figure 5.5)

The diffuse appearance of the outer margin of the hornblende zone is confirmed in thin section (Figure 5.5a). Augite (first) and then hypersthene are gradually replaced towards the vein margin by hornblende and magnetite, modal plagioclase also decreasing. Hypersthene continues as a

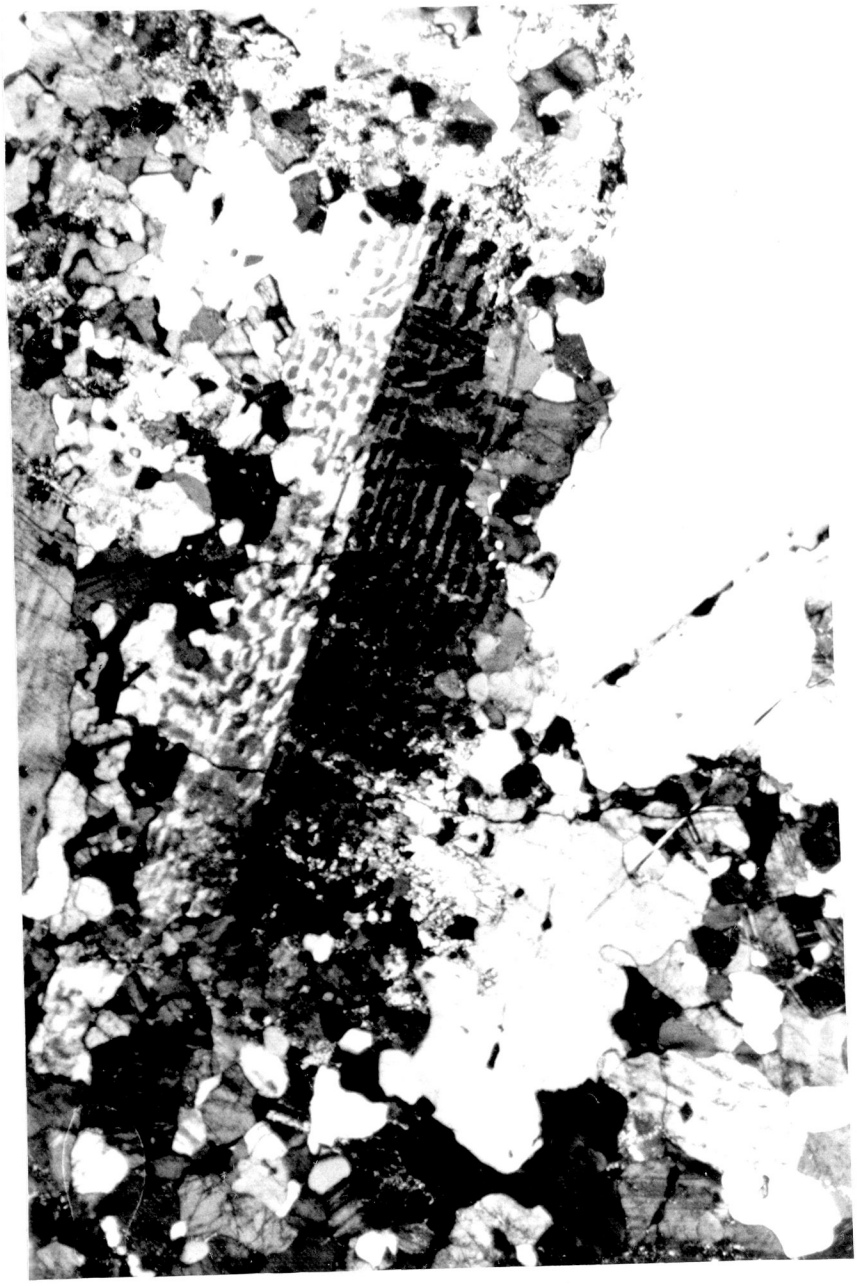
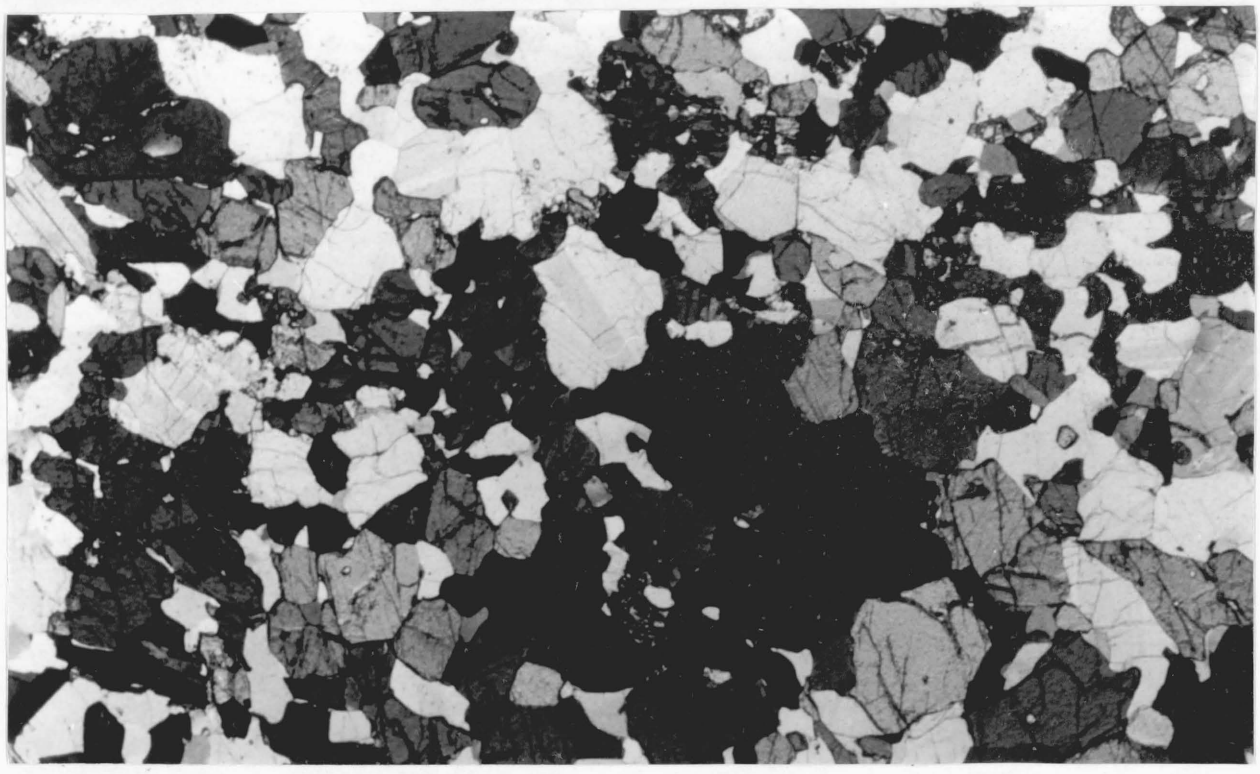


Fig 5.4 Coarse perthite from an acid vein, Leenish

a



b

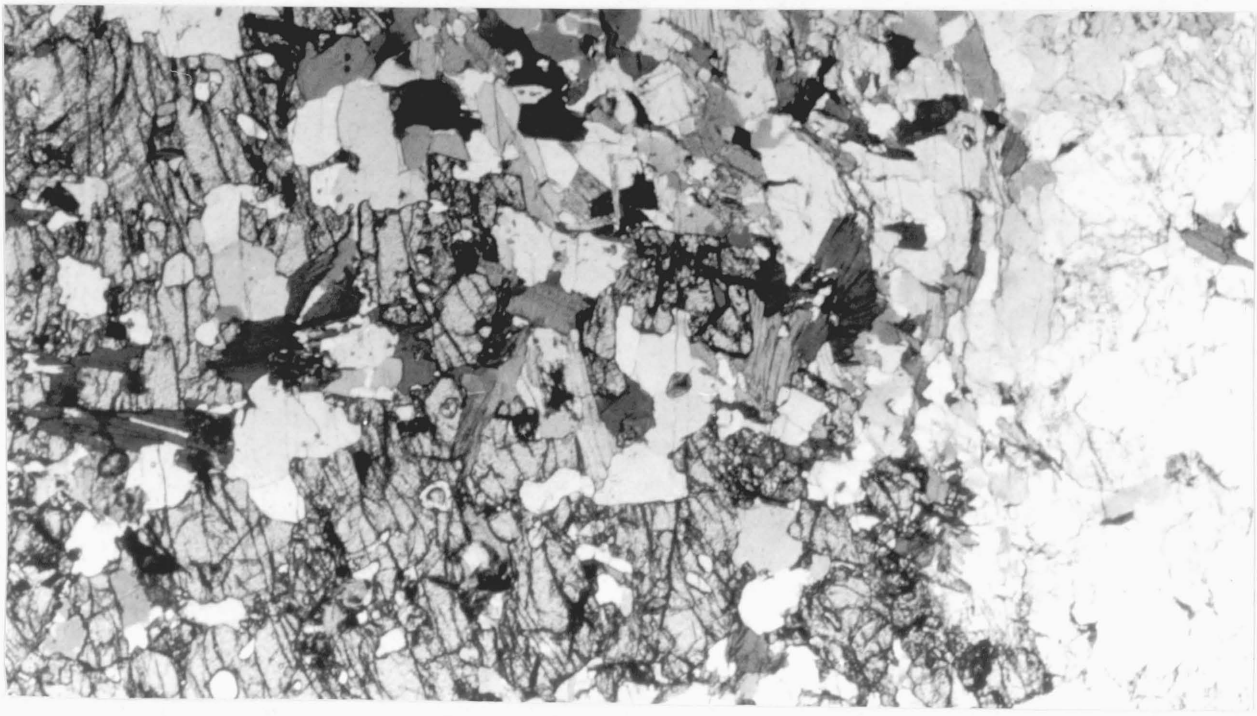


Fig 5.5 Microscopic features of a zoned aureole, Leenish

a. Hornblende zone.

b Garnet zone.

relict phase through the hornblende zone. The coarse texture apparent in the field is caused by the growth of hornblende-magnetite aggregates up to 2 mm in diameter (Figure 5.5b).

At the hornblende garnet zone boundary, hypersthene suddenly increases in modal amount, but just as quickly (within, say, 10% of the total garnet zone width) diminishes. Hornblende and the large magnetites typical of the hornblende zone disappear sharply at the interzonal boundary. Garnet forms large (5 mm) ragged crystals, some of which contain hypersthene and microcline inclusions. The matrix is biotite, quartz and plagioclase, the latter in very much smaller modal proportion than in the hornblende zone (Figure 5.5c).

Biotite and quartz surround the garnets, to the exclusion of plagioclase, suggesting they are retrogression products from garnet breakdown. In places the separation of hypersthene and garnet by quartz and biotite suggests a corona-like reaction. Vermicular biotite-quartz intergrowths, characteristic of corona biotites, are common. Towards the vein margin, garnet gives way almost completely to biotite, and the vein margin is slightly diffuse and may be schistose.

It is apparent that the garnet zone has undergone retrogression, with an earlier garnet-hypersthene-(?) alkali feldspar mineralogy replaced by biotite, quartz and magnetite. The concentration of hypersthene near to the hornblende-garnet interzonal boundary on the one hand, and the schistose, biotite-rich vein contact on the other,

suggests that retrogression was heterogeneously developed in the garnet zone, while the progressive reduction in clinopyroxene and hypersthene in the hornblende zone suggests a similar variation. It is concluded that growth of the garnet zone occurred first, the retrogressive textures of the garnet zone and formation of the hornblende zone following as a later, hydrating event.

5.2.3 MINERAL COMPOSITION AND ESTIMATION OF PHYSICAL CONDITIONS

A. MINERAL COMPOSITIONS

Analyses of the phases present in the metadolerite, acid vein and aureole assemblages are given in Table 5.1.

Plagioclases are in the range AN_{40-42} except at the edges of perthite lamellae, where optically-visible extinction variation suggests an albite-rich rim.

Garnets are unzoned in the metadolerite, and contain a higher proportion of grossular component than do the reaction zone garnets. The latter are markedly-zoned, with grossular increasing at the rims at the expense of almandine, pyrope and spessartine. Core and rim Mg:Fe ratios are about the same, despite the presence of zoning. This lack of Mg:Fe zoning suggests there has been no exchange with biotite during cooling.

Table 5.1 Mineral compositions from metadolerite, acid veins, and aureoles at Leenish

	AUGITE	HYPERSTHENES		HORNBLENDE	GARNETS		
	1	2	3	4	5	6	7
SIO2	51.51	51.21	50.86	41.97	38.15	38.79	38.45
TIO2	.22	0	0	2.09	0	0	0
A2O3	2.44	1.53	1.34	12.07	21.38	20.92	20.44
FEO	11.28	24.00	23.99	17.48	27.49	28.18	27.77
MNO	.20	.57	.74	.08	1.80	1.64	1.25
MGO	11.76	18.35	17.60	8.42	4.37	4.95	4.80
CAO	22.23	.36	.50	11.30	7.06	5.58	8.27
NA2O	.41	0	0	1.42	0	0	0
K2O	0	0	0	2.34	0	0	0
SUM	100.05	100.02	100.03	96.77	100.25	100.06	99.53
SI	7.775	7.840	7.838	6.381	5.996 5.996	6.069 6.069	6.054 6.064
AL	.225 8.000	.160 8.000	.162 8.000	1.619 8.000	3.960 3.960	3.870 3.870	3.901 3.901
AL	.209	.116	.082	.564			
FE	1.424	3.585	3.736	2.244	3.613	3.700	3.563
MN	.026	.074	.077	.010	.240	.218	.167
MG	2.646	4.187	4.043	1.926	1.024	1.158	1.128
CA	3.595 3.595	.059 .059	.083 .083	.241 4.286	1.189	.939	1.060
TI	.025 4.328	0 7.963	0 7.497	1.859 1.859	0 0.066	0 6.014	0 0.018
NA	.120	0	0	.423	0	0	0
K	0 .120	0 0	0 0	.458 .881	0 0	0 0	0 0
O	24.000	24.000	24.000	23.000	24.000	24.000	24.000
	MG 35.39	FS 46.63	46.67	FE-H 53.92	ALM 59.57	61.91	60.67
	DI 64.61	ENST 53.37	51.33	MG-H 46.08	SPE 3.95	3.63	2.77
					PYR 16.88	19.26	18.72
					GRO 19.60	15.60	17.61
	F/M .548	F/M .874	.958	F/M 1.170	F/M 3.764	3.382	3.399
	F/FM .354	F/FM .466	.467	F/FM .539	F/FM .790	.772	.772

	BIOTITES		FELDSPARS			
	8	9	10	11	12	13
SIO2	36.58	36.71	65.31	58.55	58.32	57.56
TIO2	5.33	5.01	18.55	26.63	26.52	26.55
A2O3	14.09	14.43	0	8.43	8.70	8.80
FEO	16.92	16.80	.78	6.51	6.55	6.33
MNO	0	0	15.48	.13	.20	0
MGO	12.00	11.82	100.12	100.25	100.29	99.30
CAO	0	0				
NA2O	.41	.32				
K2O	9.98	10.05				
SUM	95.31	95.14				
SI	5.554	5.575	12.007 12.007	10.431 10.431	10.407 10.407	10.366 10.366
AL	2.446 8.000	2.425 8.000	4.019 4.019	5.591 5.591	5.576 5.576	5.634 5.634
AL	.079	.157	0	1.609	1.663	1.710
FE	2.148	2.134	.278	2.249	2.266	2.210
MN	0	0	3.630 3.908	.030 3.887	.356 3.975	0 3.920
MG	2.716	2.676	32.000	32.000	32.000	32.000
TI	.609 5.548	.572 5.539	AN 0	41.39	41.85	43.61
CA	0	0	AB 7.11	57.85	57.01	56.39
NA	0 2.053	0 2.041	OR 92.89	.76	1.15	0
K	1.933 2.053	1.947 2.041				
O	22.000	22.000				
	ANN 44.17	44.37				
	PHLO 55.83	55.63				
	F/M .791	.797				
	F/FM .442	.444				

1 AUGITE, SCOURIE METADOLERITE, LEENISH
2 HYPERSTHENE, SCOURIE METADOLERITE
3 HYPERSTHENE, GARNET REACTION ZONE
4 HORNBLENDE, LEENISH HORNBLENDE ZONE
5 UNZONED GARNET, SCOURIE METADOLERITE
6 GARNET ZONE, GARNET CORE
7 GARNET ZONE GARNET RIM
8 BIOTITE, ACID VEIN
9 BIOTITE, GARNET ZONE
10 ALKALI FELDSPAR LAMELLAE, PERTHITE
11 PLAGIOCLASE LAMELLAE, PERTHITE
12 PLAGIOCLASE, GARNET ZONE
13 PLAGIOCLASE, SCOURIE METADOLERITE

Hypersthenes from the metadolerite and reaction zone have lower and higher Mg:Fe ratios respectively. The reaction zone hypersthenes are also poorer in alumina than those in the metadolerite.

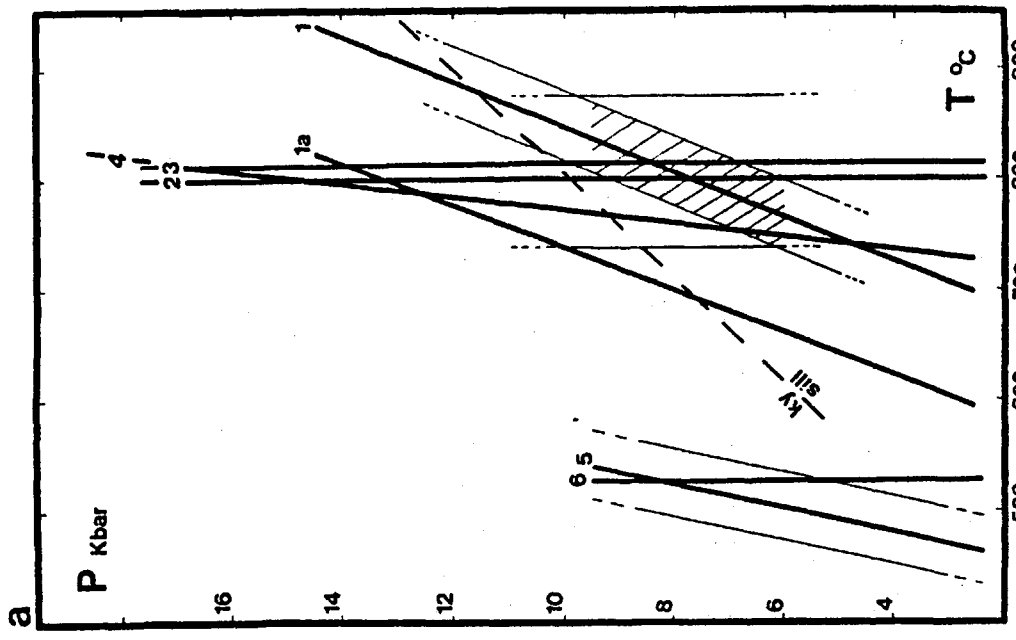
Biotites, hornblendes and magnetites show no compositional variations.

B. ESTIMATES OF PHYSICAL CONDITIONS

Metadolerite, acid vein and reaction zone assemblages can be used to provide some estimate of temperatures and pressures prevailing at several stages in the development of the Leenish reaction zones. The significance of such estimates depends upon the comparability of different mineral geothermometers and geobarometers, and also upon the geological interpretation of the relative times at which the various mineral pairs may have equilibrated. The aim here is to place some constraint on the discussion of chemical mass transfer in Section 5.2.4.

Textural and chemical (the absence of zoned minerals) evidence indicates that hypersthene, augite and garnet have equilibrated in the metadolerite. The sub-assemblages garnet-augite, garnet-hypersthene and augite-hypersthene have been used to calculate several equilibrium curves in pressure-temperature space, which are presented in Figure 5.6a.

Curves 1(a) and 1(b) have been drawn with the $\pm 70^{o}C$ error quoted by Wood and Banno (1973) and Wells (1977)



a. Estimated P,T conditions of equilibration of various mineral pairs in the metadolerite, acid vein and reaction zones at Leenish

Shaded area - probable limits for equilibration of the metadolerite.

Curves: 1. Garnet-hypersthene (Wood,1974)
1a. Scourie metadolerite
1b. Garnet reaction zone.

2. Hypersthene-augite (Wood and Banno, 1973)

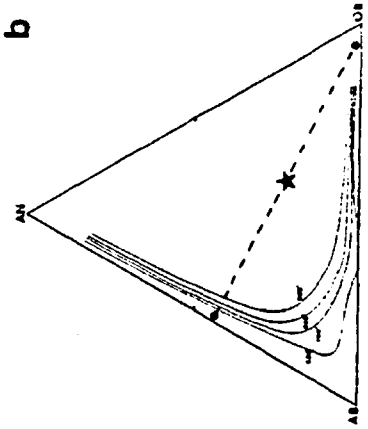
3. Hypersthene-augite (Wells, 1977)

4. Garnet-augite (Saxena, 1979)

5. Plagioclase-alkali feldspar (Powell and Powell, 1978)

6. Garnet-biotite (Thompson, 1976)

Kyanite/sillimanite phase boundary from Holdaway, 1971.



b. Ternary feldspar solvi determined by Seck (1971), compared with the estimated bulk composition of perthites from the acid veins (star) and compositions of perthite lamellae used to calculate curve (5) in Fig 5.6a.

Fig 5.6 Estimates of temperature and pressure in Leenish metadolerite, reaction zone and acid vein mineral assemblages.

respectively in their calibrations of the two-pyroxene geothermometer.

Wood (1974) gave a calibration for the equilibration of orthopyroxene and garnet, in which the alumina-content of the orthopyroxene is a sensitive function of pressure. The calculated curve (2) in Figure 5.6 intersects the two-pyroxene curves in the range 7-8 Kbar. Wood's (1974) model has been applied to rocks of similar composition to the Scourie dykes at similar temperatures and slightly higher pressures. Errors are not easy to assess, partly because the model used by Wood for natural mineral pairs involves empirical corrections for minor elements, and partly because of the uncertainty inherent in assigning the small proportion of aluminium present in the pyroxenes to tetrahedral and M1 sites respectively. An assumed error of 1 Kbar is probably not unduly pessimistic, and is used in curve 2. The intersection with the two-pyroxene temperatures thus lies in the pressure-range 6-9 Kbar, corresponding to crustal depths of emplacement in the region of 18-30 Km.

An empirical model for garnet-clinopyroxene equilibration derived by Saxena (1979) has been used to calculate curve (3). The indicated temperatures are some 30°-50°C below the two-pyroxene values, and the discrepancy is not considered to be significant.

It is concluded that the Scourie metadolerite mineral assemblage equilibrated at about 750°-850°C and 6-9 Kbar.

Coexisting plagioclase and alkali feldspar (both in the matrix and as perthite lamellae) have been used to calculate curves 4(a) and 4(b), using the models of Stormer (1974) and Powell and Powell (1977) respectively. The zoned edges of the plagioclase lamellae indicate that exchange continued with cooling below the temperatures estimated in curves (4), which may give a good estimate of the temperature of perthite exsolution, particularly as the An-content of the alkali feldspar member is low (see comments in Chapter 4 on feldspar thermometry). The temperature of crystallisation of the original homogeneous ternary feldspar (?)phenocrysts was presumably much higher than those estimated by curves 4. Ternary feldspar solvi determined by Seck (1971) at $P(H_2O)$ = 1Kbar are shown in Figure 5.6b, and demonstrate clearly the instability of ternary feldspars at low temperatures. The Leenish ternary feldspar composition lies well above the 900°C projection of the solvus into the composition plane, and Seck's conclusion that the effect of higher pressure is to lower the solvus would make 900°C an even lower minimum estimate at the likely pressures at which the vein crystallised.

Within the garnet zone, garnet may successively have equilibrated with hypersthene and then biotite. Curves (5) and (6) have been calculated using analysed minerals from the garnet zone, using the Wood (1974) model for garnet-hypersthene and Thompson's (1976) empirical calibration based on independent temperature estimates

in natural metapelites for the garnet-biotite pair. Assuming the same pressure-range for reaction zone formation as for the equilibration of the metadolerite assemblage, curve (5) indicates temperatures in the range 650°-700°C, some 100°C lower than the temperatures of dyke equilibration. Curve (6) suggests even lower temperatures for the retrogression of the reaction zone.

Finally, the superimposed kyanite - sillimanite phase boundary (Holdaway, 1971) shown in Figure 5.6 suggests that the kyanite found in the acid vein does not owe its existence to the sequence of events for which pressures and temperatures have been estimated here. By analogy with the corroded kyanite found in a late Scourian pegmatite in Sutherland (Chapter 2), it may have been derived from an unexposed kyanite-bearing metasediment.

C. SIGNIFICANCE OF THE ESTIMATED CONDITIONS

Some consideration of the geological meaning of the pressures and temperatures estimated is necessary to define the conditions under which metasomatism took place.

The Scourie metadolerite apparently equilibrated at some pressure significantly below those estimated for granulite-facies metamorphism in South Harris by Wood (1975), in agreement with earlier estimates from the Scottish mainland (Tarney, 1963, 1973; O'Hara (1961)) and the Outer Hebrides (Dearnley, 1973; Dickinson and Watson, 1976).

O'Hara (1961) considered the metamorphic assemblage found in the Scourie Dyke in Sutherland was the result of intrusion into hot, deeply-buried country rocks. It follows that P-T estimates reflect ambient country-rock conditions. However, the dykes themselves may have acted as local sources of heat which in hot host rocks could have taken a significant time to equilibrate thermally. Thus estimated temperatures may reflect the closure, under anhydrous conditions, of the mineral geothermometers as diffusive exchange between minerals ceased. While these temperatures may not therefore be of regional significance at the time of Scourie dyke emplacement, they may well provide a reasonable estimate of the conditions under which the garnet zones were formed, and this conclusion is supported by the fairly similar temperatures estimated for the equilibration of garnet and hypersthene in the reaction zones.

A second metamorphic event can be distinguished in the reaction zones, and this may be reflected in the lower temperature estimates provided by perthite lamellae and biotite-garnet pairs. The petrographical evidence of section 5.2.2 would suggest that the hornblende zone was formed during this second event.

The localisation of the acid veins within the anhydrous centre of the metadolerite suggests a relatively local origin, and the presence of (?) relict or restitic kyanite may indicate local fusion of the Lewisian gneisses, the heat source presumably being the metadolerite itself.

The overall process may thus have been a deep-seated equivalent of pyrometamorphic back-veining, and would indicate a rapid sequence of events from dyke intrusion through acid vein emplacement to garnet zone formation. This high-temperature, anhydrous sequence was then followed, after some cooling, by the development of the hornblende zones. In the next section, the extent of chemical mass transfer associated with each of these stages of zone formation is considered.

5.2.4 CHEMICAL MASS TRANSFER

A. GENERAL FEATURES

Mineralogical variations in the aureole zones surrounding the acid veins provide a clear indication that the bulk compositions of these zones have been modified by chemical masstransfer. The aim of this section is to examine the degree and extent of these changes in relation to the two metamorphic and metasomatic events identified.

Description of mass transfer requires some convention for the choice of components whose transport is described. Dissolved species in a hydrous fluid may be ionic or (more likely at the high temperatures obtaining in the present instance (Eugster, 1977)) molecular, and complexes may contain more than one measurable element. Since we are able only to examine the final products of metasomatism,

consideration of the nature of the dissolved species may not be useful, and indeed little may be deduced about the composition of the fluid itself. Transfer of chemical components will be described here in terms of fluxes of elements, without any suggestion that neutral atoms are realistic solute species.

16 modal estimates were obtained from a single thin section by traversing the section parallel to and at varying distances from an acid vein - metadolerite contact, across the garnet and hornblende zones and into the metadolerite. By combining the modal percentages obtained with analysed mineral compositions from Table 5.1, and using molar volume data from Robie et al. (1967) and Robie and Waldbaum (1968) corrected for solid solutions by assuming approximately linear molar volume variation with composition, bulk compositions were estimated. The thin section used is shown in Figure 5.7, and the modal estimates, molar volumes and bulk compositions listed in table 5.2.

The molar oxide variations across the reaction zones are shown in Figure 5.8, together with the average composition of the acid vein calculated in the same way. Clearly, both modal and bulk chemical variations are less-striking across the contact between the metadolerite and the hornblende zone than across that between the hornblende zone and garnet zone. Chemical contrasts at the former boundary are limited mainly to Si and hydroxyl, although Ca, K and possibly Al may be higher in the

1. Modes

Traverses	Modal percentage of mineral (Volume percentage)								
	OPX	CPX	HB	MT	PL	GT	BI	KF	QZ
1 (mdol)	9	5	15	5	50				6
2 (mdol)	11	6	33	2	53				4
3 (trans)	5	3	51	2	40				3
4 (h)	6		50	1	49				5
5 (h)	4		61	6	34				2
6 (h)	2		49	3	52				2
7 (h)			59	6	37				2
8 (h)	2		46	3	51				
9 (h)	1		55	5	40				
10 (h)	1		55	3	41				2
11 (h)	5		54	3	40				
12 (h)	4		58	2	37	1			2
13 (trans)	12		3	1	57	12	17		10
14 (g)	9			1	27	16	30		15
15 (g)					15	24	34		30
16 (g)					15	26	34		27
a.v.					35		3	19	43

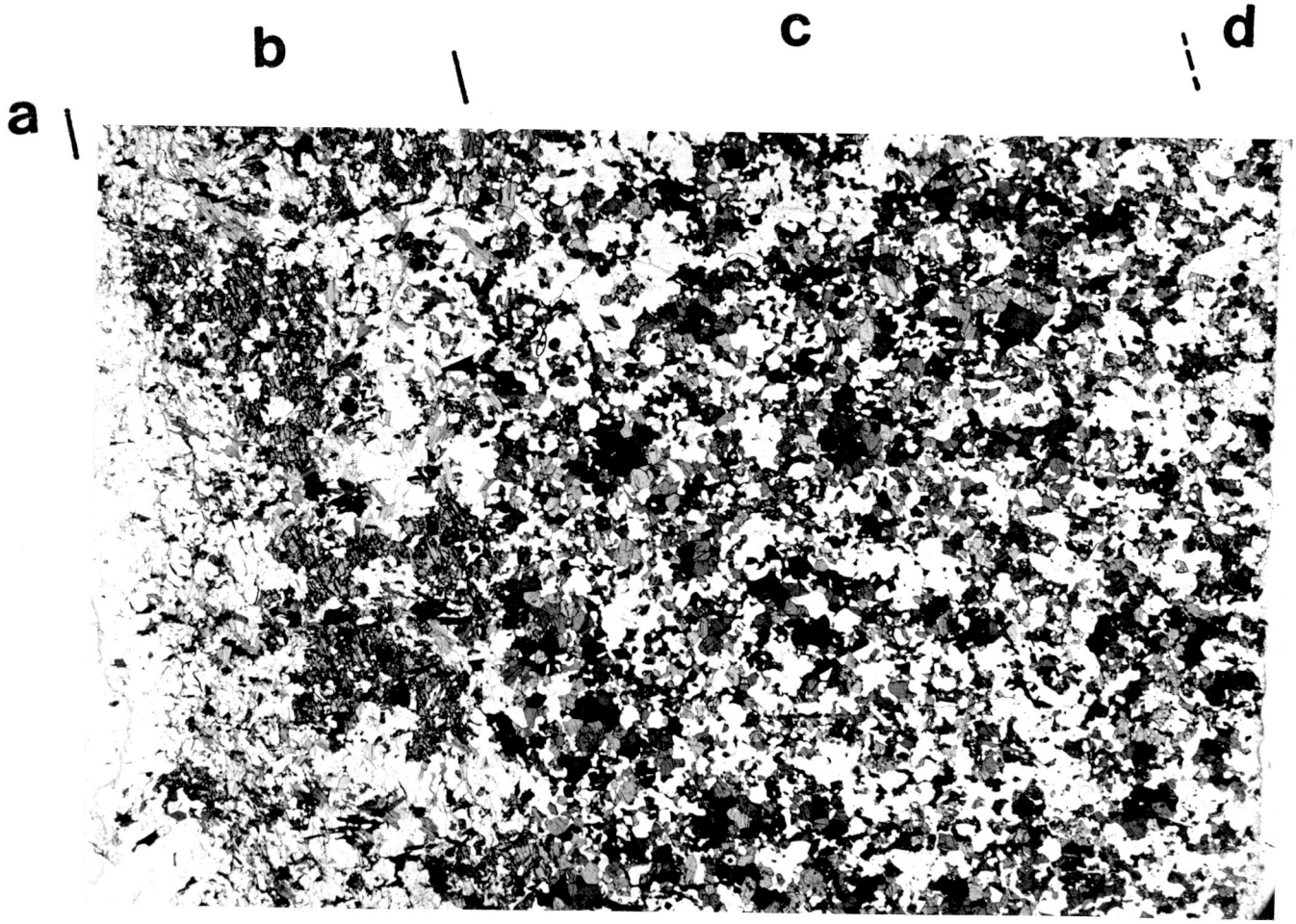
2. Molar volumes used (Robie et. al., 1967)

	OPX	CPX	HB	MT	PL	GT	BI	KF	QZ
(cm^3)	32.3	66.86	272	44.5	100.37	116.71	303.24	108.11	22.69

3. Moles of oxide constituents per 100cm^3 zone

Traverse	Oxides									
	SiO_2	TiO_2	Al_2O_3	FeO^T	MnO	MgO	CaO	Na_2O	K_2O	H_2O
1	2.9299	.0133	.3636	.6025	.0088	.5092	.4368	.3450	.0319	.1340
2	2.8979	.0217	.9677	.6206	.0098	.6004	.4922	.3232	.0528	.2220
3	2.5513	.0346	.9683	.6091	.0075	.5459	.5445	.2914	.0857	.3600
4	2.7113	.0317	1.0130	.5568	.0078	.5083	.5028	.3170	.0790	.3320
5	2.3915	.0384	.9161	.6926	.0070	.5256	.5185	.2609	.0957	.4020
6	2.4867	.0319	1.0648	.4955	.0049	.3966	.5188	.3402	.0795	.3340
7	2.3097	.0399	.9817	.6036	.0046	.4220	.5470	.2857	.0995	.4180
8	2.4506	.0317	1.0192	.5001	.0050	.3976	.5248	.3307	.0790	.3320
9	2.3328	.0382	1.0195	.5932	.0050	.4350	.5468	.3050	.0952	.4000
10	2.4219	.0378	1.0231	.5436	.0050	.4310	.5454	.3076	.0942	.3960
11	2.5362	.0372	1.0097	.6536	.0076	.5507	.5381	.3007	.0928	.3900
12	2.5428	.0392	.9926	.6358	.0080	.5367	.5451	.2830	.0976	.4100
13	2.9804	.0324	1.0562	.6257	.0171	.5489	.2791	.2930	.1017	.2200
14	2.9251	.0616	.9215	.7526	.0209	.6446	.1873	.1568	.1958	.4040
15	2.8441	.0665	.8517	.5772	.0120	.4061	.1572	.0827	.2113	.4360
16	2.7923	.0671	.8921	.6116	.0120	.4192	.1672	.0838	.2132	.4400
a.v.	3.3895	.0052	.6916	.0185	.0000	.0234	.1419	.2118	.1910	.0344

Table 5.2 Modal compositions of reaction zone and metadolerite traverses and estimation of bulk compositions.



zones:

a - acid vein

b - garnet

c - hornblende

d - metadolerite

Fig 5.7 Section across a zoned aureole from Leenish

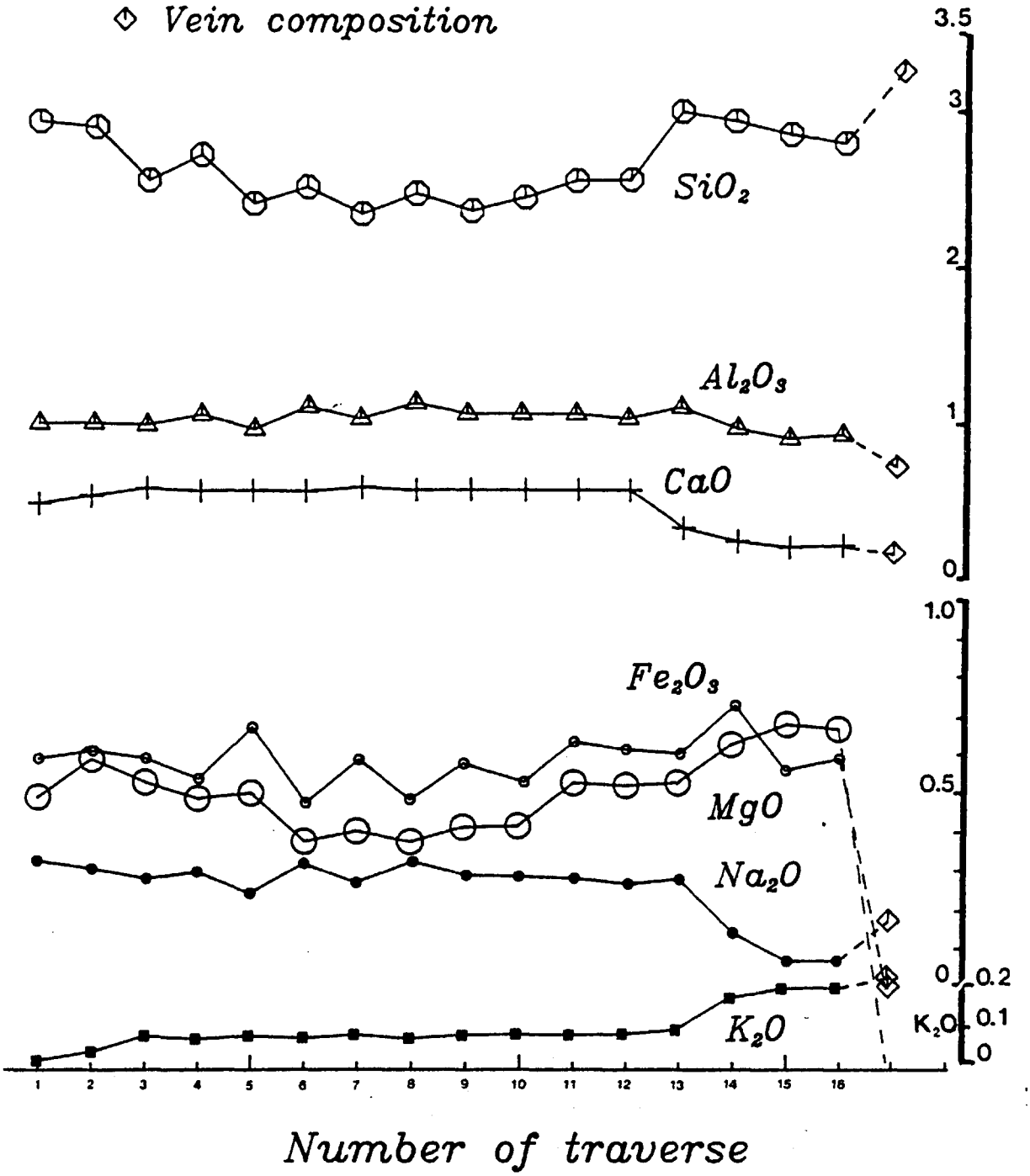


Fig 5.8 Estimated molar compositions of traverses across a zoned aureole

hornblende zone. Si appears to be the only element which varies internally within the hornblende zone.

Large differences are observed between the hornblende and garnet zones, chiefly in Si, Al, Ca (especially), K and Na, and in general these components occur in concentrations intermediate between those of the metadolerite and the acid vein. By contrast, the hornblende zone appears to be anomalously poor in Si and rich in Al and Ca, interrupting the smooth transition from metadolerite to acid vein compositions.

In Figure 5.9, oxide concentrations have been normalised to the average of the two metadolerite compositions to show the relative variations of individual components. The largest relative variations between the metadolerite and garnet zone are found to be for Ca, Na and K, and it is clear that during the high-temperature formation of the garnet zone the dominant fluxes were those of K away from and Ca + Na towards the acid vein. These relative fluxes would be consistent with the expected initial chemical potential gradients established by the juxtaposition of an alkali feldspar bearing vein and a basic rock in which the feldspar phase would be a relatively basic plagioclase. A decrease in Al in the garnet zone is consistent with a flux of Ca into the acid vein if local charge balance was maintained during reactions involving feldspars. That any coupling analogous to the simple $NaSi \gtrless CaAl$ plagioclase substitution was imperfect is shown by the clear departure of the garnet zone

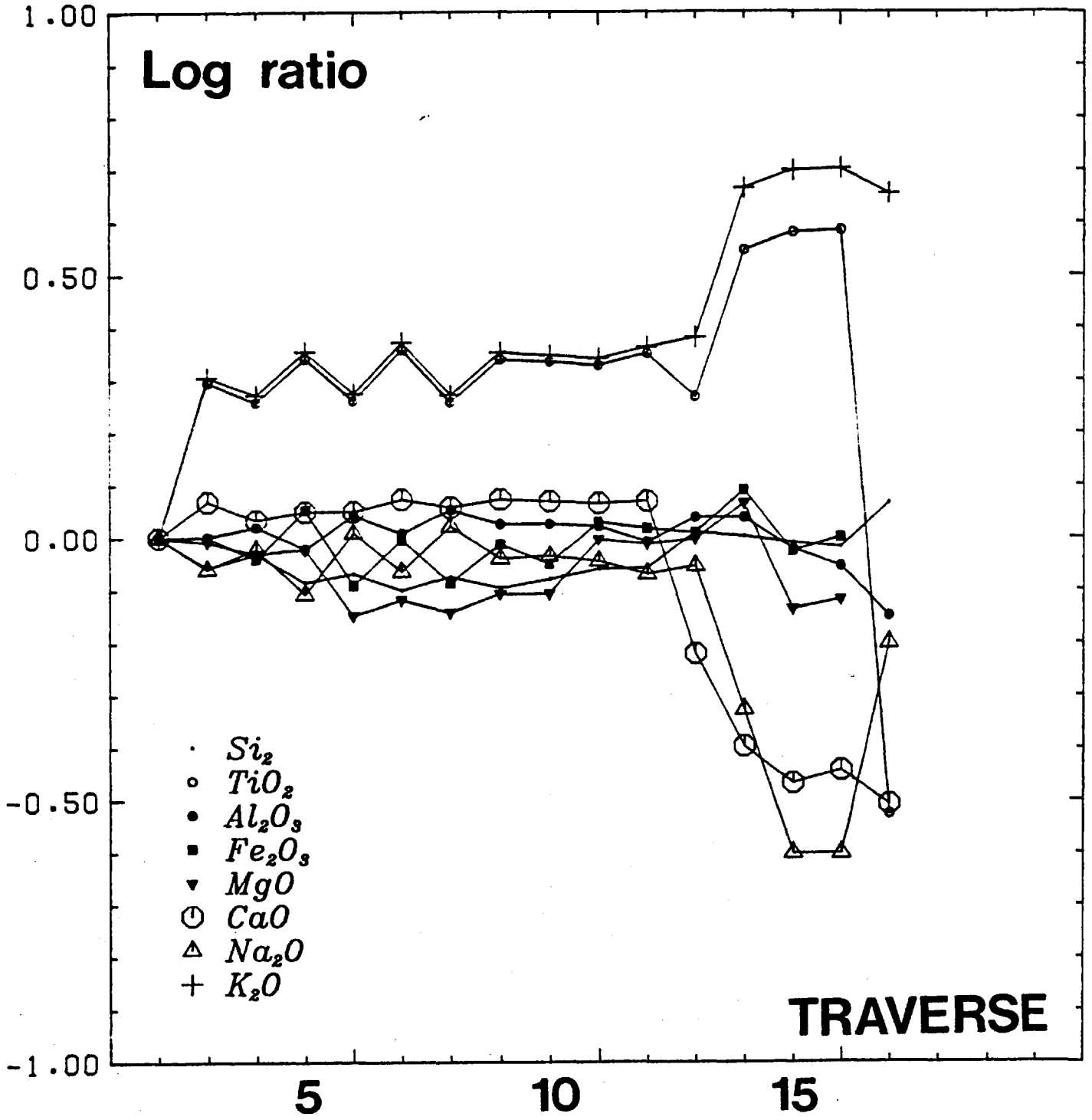


Fig 5.9 Variations of oxides across a zoned aureole normalised to the metadolerite composition

composition from an (alkalis + lime):(alumina) ratio dominated by feldspar stoichiometry and the development of an aluminous mineral, garnet. The dominant factor is clearly the much larger relative flux of Ca as compared with Al, and this is reflected as much by the Ca-poorer composition of the garnets relative to those occurring in places in the metadolerite as by the bulk zone composition.

The CIPW norms of the zones (Table 5.) show strong departures from compositions which might be thought to be 'intermediate' between the tholeiitic basalt norm of the metadolerite and the corundum-normative granite composition of the acid vein. The hornblende zone has a normative composition similar to that of an alkali basalt, while the garnet zone, which has a silica-content near to that of an andesite, has a low lime-content and very high normative corundum, so that comparison with typical igneous compositions is misleading, and in fact the composition and mineralogy of the garnet zone is very close to that of a semipelitic metasediment, lying almost completely within the system K(FM)ASH used by Thompson (1976) for the description of metamorphic phase relations in pelitic rocks.

B. EXTENT OF MASS TRANSFER

The variations in the reaction zones already identified suggest that the acid vein could have been extensively modified in composition during metasomatism. The object of

Oxide	Metadolerite	Hb zone	Gt zone	Acid vein
SiO_2	54.06	48.47	57.44	76.94
Al_2O_3	15.08	17.83	15.07	13.32
FeO^T	12.29	13.26	14.49	0.50
MgO	6.30	5.61	5.64	.36
CaO	7.52	10.09	3.09	3.01
Na_2O	3.28	3.34	0.88	2.48
K_2O	0.46	1.40	3.39	3.40
CIPW norms				
Qz			12.20	42.10
Co			4.34	.09
Or	2.72	8.27	20.03	20.09
Ab	27.75	16.38	7.45	20.99
An	25.07	29.52	15.33	14.93
Lc				
Ne		6.44		
Di	10.26	17.31		
(Wo)	5.11	8.57		
(En)	2.02	3.19		
(Fs)	3.16	5.55		
Hy	31.98		40.65	1.61
(En)	12.51		14.05	.90
(Fs)	19.46		26.61	.91
Ol	2.19	22.08		
(Fo)	.81	7.56		
(Fa)	1.39	14.52		

Table 5.3 Averaged molar oxide compositions and CIPW norms for Leenish zones.

mass-balance calculations will be to recover information about the original composition of the acid vein, since the small relative volume of the veins suggests one of the limiting factors controlling the extent of mass transfer was the finite volume of one member of the reacting pair of rocks. The ubiquity of an intermediate andesine in the whole range of rock compositions (Table 5.1) tends to support this, and leads to the conclusion that the process was essentially one involving the reduction of chemical potential gradients in the major alkali and alkaline-earth feldspar components.

It would be wrong, however, to ignore the polyphase nature of zone development, and mass balance calculations will be used in an exploratory way, in the hope of at least partially isolating the effects of the later hornblende zone formation. An additional complicating factor is the need to select a suitable reference frame on the basis of which to carry out the calculations. Assumptions about relative rock volumes involved in mass transfer necessary for a mass balance are subject to uncertainties; on the one hand the possibility of dilation of the acid veins during the metasomatic process and on the other the effect on the preservation of the high-temperature zone volumes during the second phase, when hydration may have been associated with volume changes within the zones and at the vein margin where a schistosity is developed.

Brady (1975) has discussed the choice of reference frames for the description of mass transfer processes.

Those most widely-used in geological problems are the constant-volume reference frame and mean-velocity reference frames. In the former the assumption is made that there is no overall gain or loss of volume during the development of reaction zones, while the latter involves the assumption that one or more component is fixed or diffusing with a constant mean velocity to which all other components can be referred. Fixed-Al reference frames have been used successfully by Fisher (1970, 1973) and Carmichael (1969) in studies relating local equilibrium to chemical transport.

Figure 5.10 shows the effect of fixing volume concentrations of Al_2O_3 and SiO_2 respectively in the Leenish reaction zones, by normalising all components to each in turn. The Al-fixed reference frame tends to exaggerate the variations in Si, and in particular the internal variations within the hornblende zone. The other components show no internal variation and a much less-pronounced change between the hornblende zone and the metadolerite. It could therefore be inferred that the hornblende zone composition is almost entirely the result of loss of Si associated with the hydration of the metadolerite assemblage; this is supported by the alkali-basalt norm of the hornblende zone (table 5.3). The apparent increase in Al, Ca, Na and K would then be a closure effect, these components being relatively immobile during the second metasomatic event.

The Si-fixed diagram tends to support these conclusions, since an apparent variation in all components other than Si

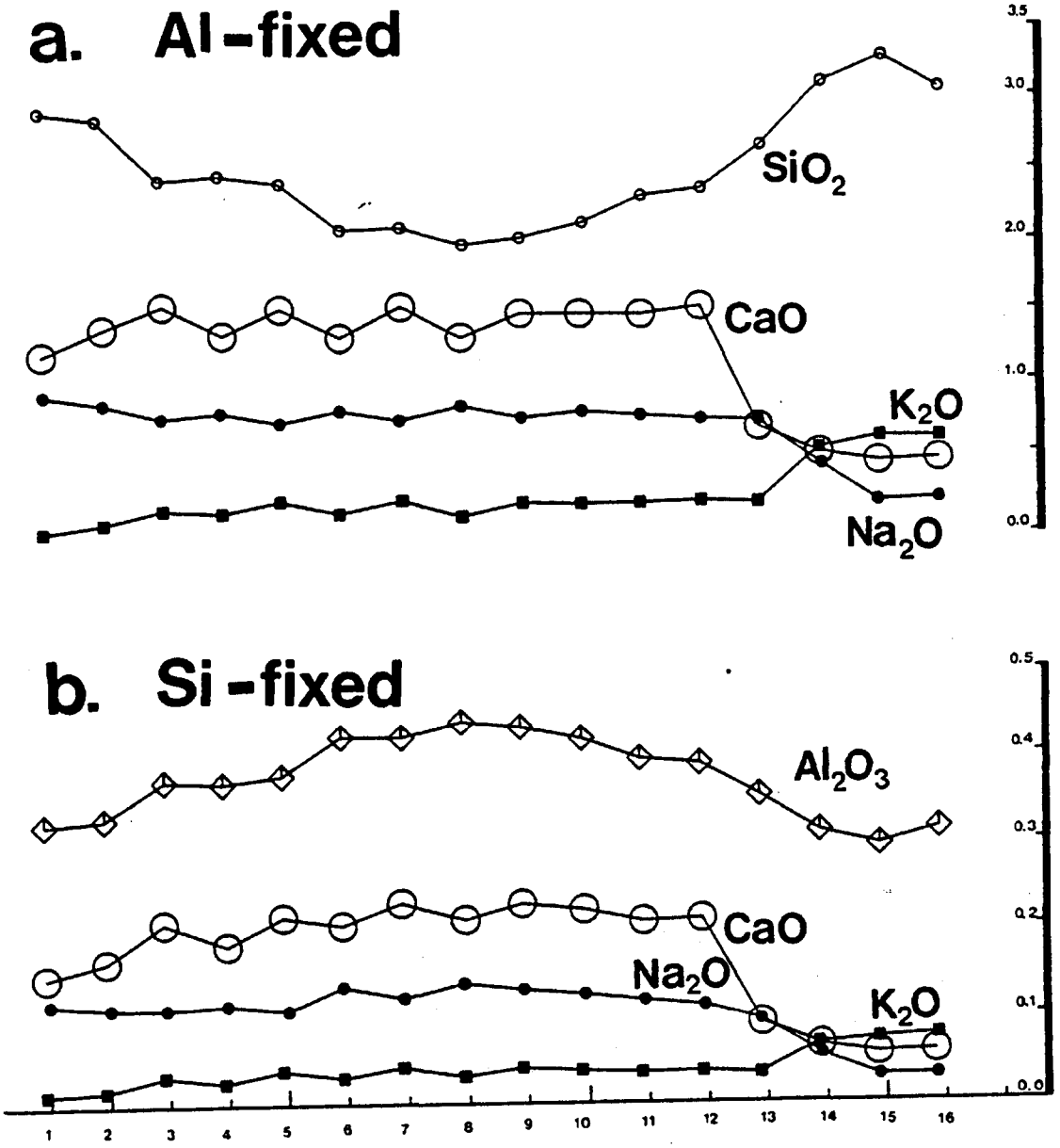


Fig 5.10 Al-fixed and Si-fixed oxide variation across a zoned aureole

is seen: clearly an unlikely event, reflecting the consequences of attempting to fix what was probably the most mobile component.

The relative success of the Al-fixed reference frame in isolating the effects of the second phase also suggests that volume may (at least approximately) have been conserved during the formation of the hornblende zone, since only Si and K (other than hydroxyl) show any variation relative to Al across the hornblende zone boundary with the metadolerite. The situation is less clear at the contact between the hornblende zone and the garnet zone, but it will be assumed that most mass transfer at this boundary occurred during the first metasomatic event, without any subsequent volume change.

A calculated mass-balance is given in Table 5.4a with the assumptions: (a) volume was conserved in the acid vein and reaction zones during metasomatism, (b) both the garnet and hornblende zones replaced metadolerite (i.e. the initial acid vein boundary was conserved), (c) the system was effectively closed, so that no material was lost or gained by the metadolerite + acid vein + reaction zones assemblage. These assumptions can be tested by examining the estimated initial vein composition.

Clearly, the derived vein composition is unsatisfactory. The initial vein composition is too poor in Si (less than the final concentration, and implying an unlikely flux of Si into the vein during megasomatism. K is unrealistically high, and Fe and Mg are represented by negative values. The indicated net transfer of Ca into the vein is less

Mass balance for reaction zones, Leenish

Zone compositions (moles/1000cm^3):

	Metadolerite	Hb zone	Gt zone	acid vein
SiO_2	2.9299	2.3950	2.8182	3.3895
Al_2O_3	.9636	1.0388	.8719	.6916
FeO^T	.6025	.5481	.5944	.0185
MgO	.5092	.4128	.4127	.0234
CaO	.4368	.5344	.1622	.1419
Na_2O	.3450	.3204	.0833	.2118
K_2O	.0319	.0883	.2123	.1910
H_2O	.1340	.3710	.4380	.0344

Zone widths(relative):

	23	15	22.5*

A. Assuming all zones formed simultaneously:

Mass balance:	M - H	M - G	M - V**	
			Total	÷ 22.5
SiO_2	12.3027	1.6755	13.9783	.6213
Al_2O_3	1.7296	1.3755	0.3541	.0157
FeO^T	1.2512	0.1215	1.3727	.0610
MgO	2.2172	1.4475	3.6647	.1629
CaO	2.2448	4.1190	1.8742	.0833
Na_2O	0.5658	3.9255	4.4913	.1996
K_2O	1.2972	2.7060	4.0032	.1779
H_2O	5.4510	4.5600	10.0110	.4449

*1/2-width of acid vein

**M - V = M - H + M - G

Table 5.4 Calculated mass-balance for reaction zones at Leenish.

B. Assuming formation of garnet zone from metadolerite only:

Mass balance:	H - G	H - G/22.5
	6.3480	.2821
	2.5035	.1113
	0.6945	.0309
	0.0015	.0001
	5.5830	.2481
	3.5565	.1581
	1.8600	.0827
	1.0050	.0447

*Mass-balance A **Mass-balance B

Original acid vein compositions (V^o) compared with present composition(V^1):

	V^1	V^o *	V^o **
SiO_2	3.3895	2.7682	3.6716
Al_2O_3	.6916	.7073	.5803
FeO^T	.0185	.0425	.0494
MgO	.0234	.1395	.0233
CaO	.1419	.0576	.1062
Na_2O	.2118	.4114	.0537
K_2O	.1910	.3689	.2737
H_2O	.0344	.4105	.0791

than that of Na, implying an initial Ca:Na ratio higher in the vein than in the metadolerite.

Dilation of the fissure occupied by the acid vein would not explain these discrepancies, since a continuing supply of acid magma would tend to maintain chemical potential differences in K, Na, Ca and Si which would be the reverse of those implied by the calculated apparent fluxes. Clearly the problem lies with the voluminous hornblende zone, with its anomalously-low Si content. If the hornblende zone is replaced in the mass-balance calculations by an equal volume of metadolerite (and it is assumed that later retrogression in the garnet zone was approximately isochemical) a second mass-balance is obtained (Table 5.4b'. The estimated initial vein composition is plausible as a granitic liquid composition, and satisfies all likely chemical fluxes in that the vein, in reaching its final composition, has lost Si and K, and gained Na, Al and large amounts of Ca.

The second metasomatic event took place at lower temperatures, yet the reaction zone developed extended further into the metadolerite than did that associated with the first, high-temperature event - a fact which suggests the relatively greater importance of infiltration metasomatism during the second phase. The anhydrous assemblages associated with the first phase may indicate that this was a diffusion-dominated event, the garnet zone widths thus giving an estimate of the characteristic

range of diffusion (of the order of 1cm) at those temperatures over the time available, although it seems more probable to the writer that the main factor limiting zone growth was the achievement of vanishingly small chemical potential gradients as the acid vein composition changed.

The source of water for the second event seems to have been outside the local vein + metadolerite system, so that the veins may have operated as fissures along which hydrous fluids could migrate. If this is so, it is not clear why there should be a simple width-relationship between the acid veins and hornblende zones (Figure 5.3) unless the volume of fluid in the veins was the main factor maintaining the local metasomatic process. Certainly a greater volume of fluid would act to maintain chemical potential gradients, although there is no reason why it should have any bearing on fluid pressure gradients. The width relationships may reflect the local influence of diffusion metasomatism at this stage. The low-temperature metasomatic event could be associated with a lower amphibolite-facies metamorphic event, perhaps during the Laxfordian cycle.

In addition to water, the local system may well have been open to K and Si during formation of the hornblende zone. This would reduce the initial potash-content required by mass balance (Table 5.4) in the acid veins, bringing their composition closer to the centre of the granite quartz - albite - orthoclase triangle, where

minimum melting compositions occur for a large range of pressures (Tuttle and Bowen, 1958).

It is concluded that two metasomatic events took place at Leenish. The first of these was a high-temperature (over 600°C) event dominated by diffusion mass transfer of components in response to chemical potential gradients, transport probably being through a small volume of intergranular fluid, while the second may have involved quite long-range infiltration of a K-rich fluid, and local combined infiltration-diffusion metasomatism involving transfer of K into the garnet and hornblende zones, and solution of Si in the fluid as amphibole replaced pyroxene and plagioclase in the hornblende zone. The chemical effects of these two events are clearly additive, and the largest uncertainties in calculating mass balances for the earlier event are in the two components, Si and K, which were mobile during the second. The contrasting natures of the two events resulted in completely different patterns of mass transfer.

5.3 GARRY-A-SIAR, BENBECULA: METASOMATIC ZONES ASSOCIATED WITH A LARGE ACID PEGMATITE

5.3.1 GEOLOGICAL RELATIONSHIPS AND MINERALOGY

A. GEOLOGICAL RELATIONSHIPS

The largest Laxfordian (Dearnley and Dunning, 1968) pegmatite at Garry-a-Siar occurs in an area of grey gneiss

which has undergone relatively low finite Laxfordian strain (Coward, 1969); the body cuts a discordant and almost undeformed Scourie metadolerite dyke. This pegmatite was described in Chapter 2.

Near the point where the pegmatite disappears under machair at the top of the beach, a block of metabasic gneiss composed mainly of amphibole and plagioclase is partly engulfed by the pegmatite on its northern side. The metabasic rock is apparently concordant with the gneisses, and is assumed to be older than the Scourie dykes.

At the contact between the two rock-types, striking evidence of reaction can be seen (Figure 5.11). A zone between 6cm and 10cm wide is composed of biotite, plagioclase and quartz, terminating fairly sharply against the relatively unaffected basic gneiss. Within the biotite-bearing zone, numerous magnetite porpyroblasts occur, each surrounded by a plagioclase-quartz halo.

Figure 5.12a shows the size-relationships between the magnetite porphyroblasts and their haloes relative to distance across the reaction zone shown in Figure 5.11a. Most of the spherical structures show a steady increase in magnetite radius towards the pegmatite, although the halo widths, defined as the difference between the halo radius and porphyroblast radius, remain fairly constant. Exceptionally large porphyroblasts are associated with much wider haloes, and may violate the apparently-simple size-distance relationship, in which case they occur close

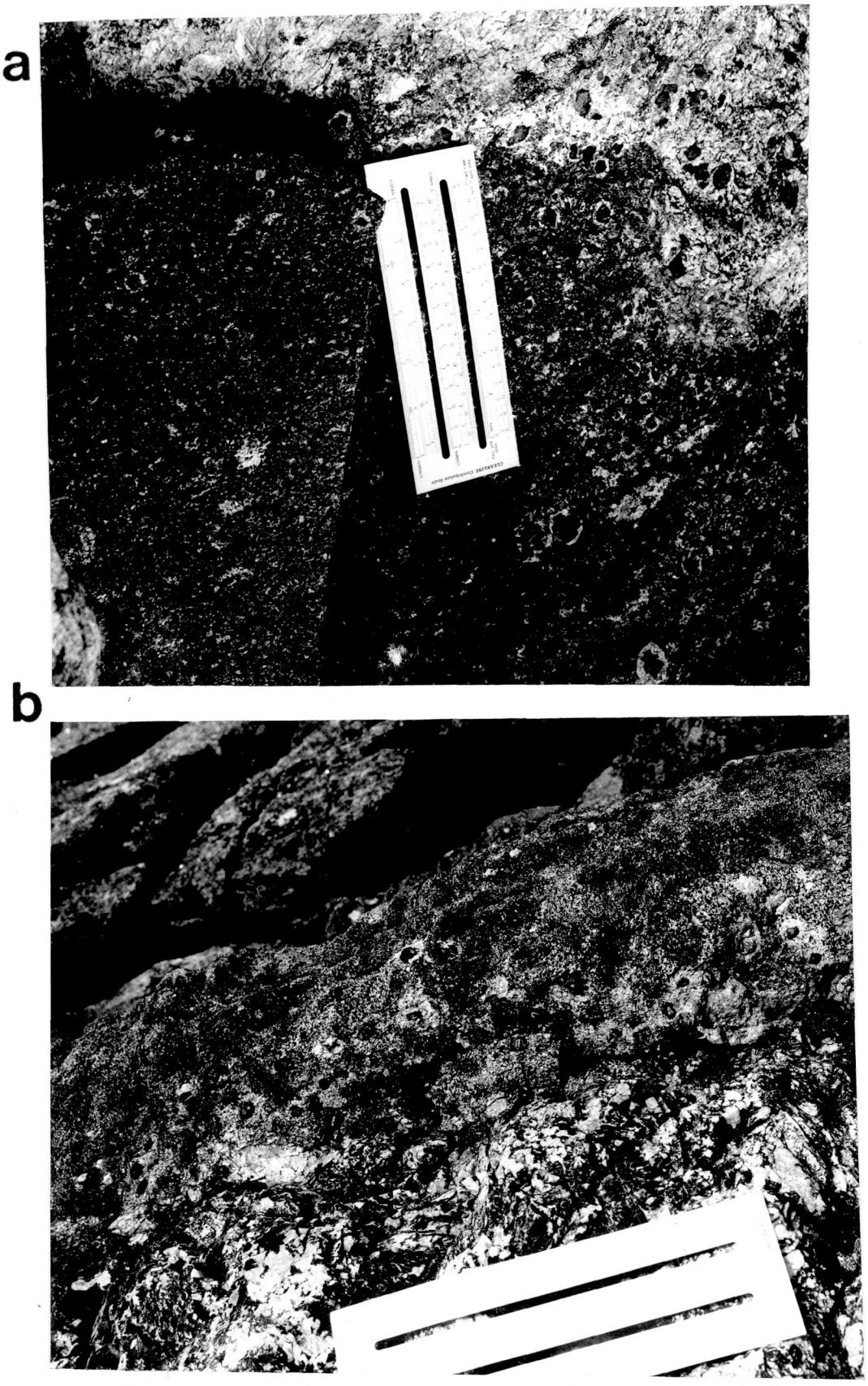


Fig 5.11 Metasomatic reaction zones at Garry-a-Siar, Benbecula

a. Apparently-unsheared metabasic host rock.
b. Sheared host rock. Relict shear fabric appears as dark streaks within the reaction zone.

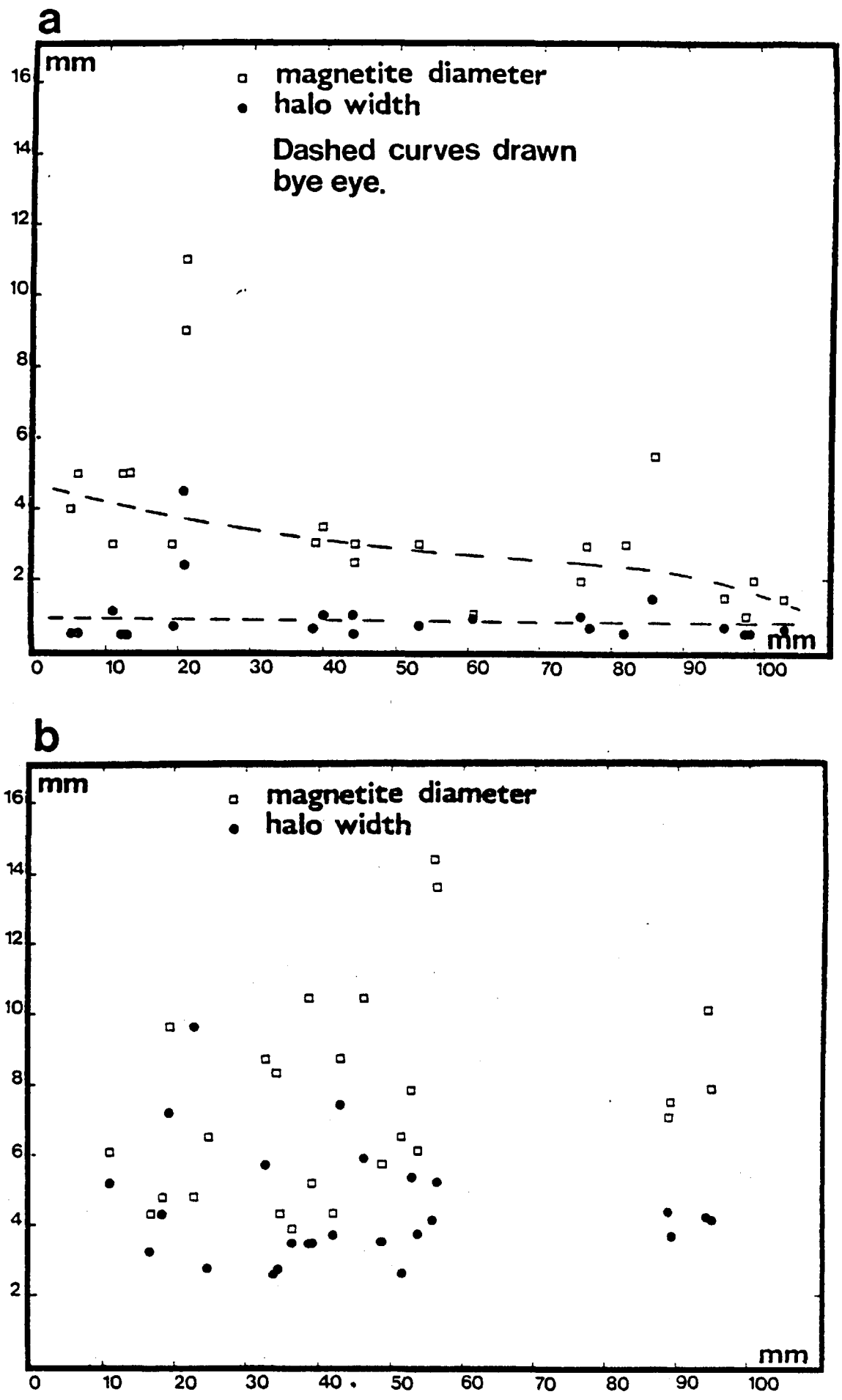


Fig 5.12 Relationships between size of spherical diffusion structures and distance from pegmatite contact.

to fractures within the reaction zone.

Figure 5.12b is a similar diagram, drawn for that part of the reaction zone shown in Figure 5.11b. Here, the metabasic rock was clearly sheared, although the preservation of the shear foliation as a relict fabric within and slightly oblique to the reaction zone shows that shearing took place before reaction zone formation. It seems likely that the shear fabric was formed in a ductile shear zone in the grey gneisses into which the pegmatite was subsequently emplaced. Near the margin of the pegmatite in this part of the reaction zone, the quartz-plagioclase haloes have interfered to such an extent that biotite is almost absent. In Figure 5.12b the gradual increase in porphyroblast size of Figure 5.12a is not apparent, although some relationship between the larger porphyroblasts and fractures (here represented by the relict shear fabric) may be discernible. A conclusion might be that in the absence of fractures, porphyroblast growth is a function either of time - that is, the spherical structures monitor the growth of the planar reaction zone as a whole - or of distance from the reaction zone contact with the metabasic rock, if the planar zone developed before the spherical structures nucleated.

Textures in the biotite-quartz-plagioclase matrix of the reaction zone are decussate, with some tendency to coarsening towards the pegmatite, and in Figure 5.11a towards some of the irregularly-developed fractures. Other features apparent in Figure 5.11 include: the

structure of the pegmatite, in which plagioclase, quartz and biotite are orientated perpendicularly to the margin: the similar mineralogy of the pegmatite marginal zones and the reaction zones: and the presence, in Figure 5.11a, of some magnetite (?)porphyroblasts within the pegmatite, some of them retaining traces of haloes in the form of a raised edge. The last observation may indicate that the pegmatite has encroached upon the reaction zone, so that the initial margin is not retained.

B. MINERALOGY

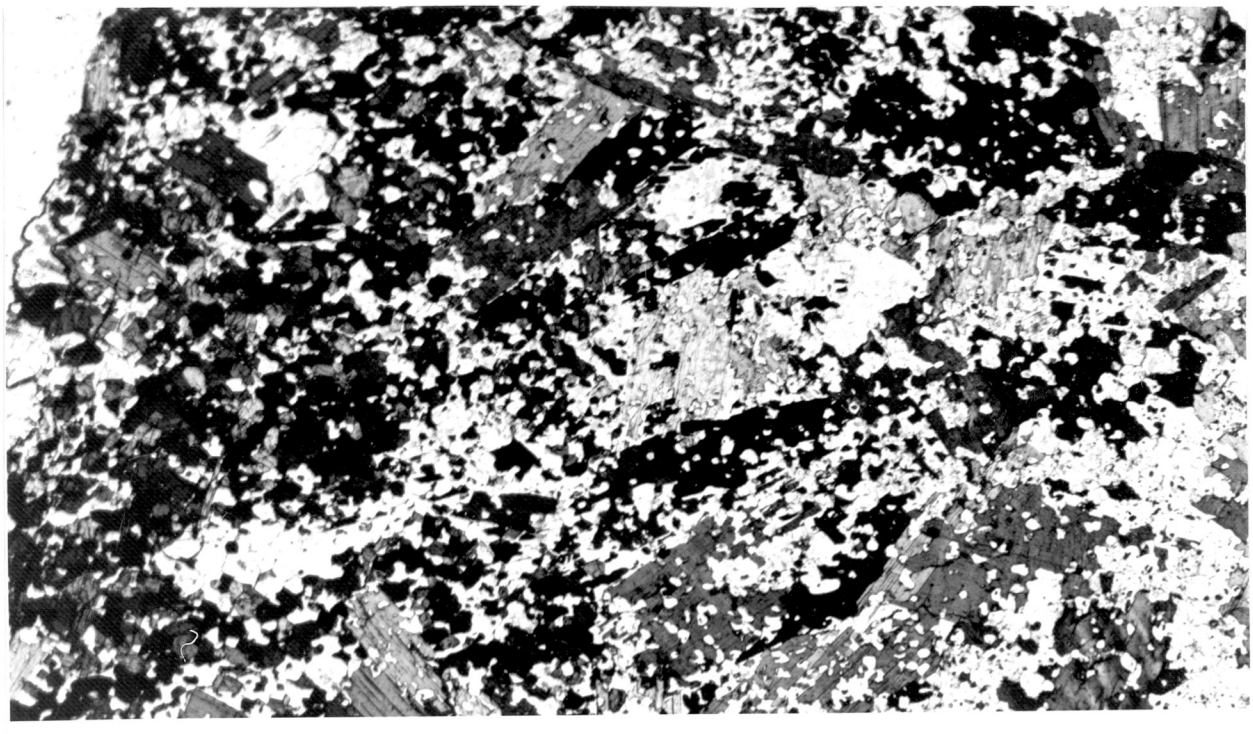
Figure 5.13 shows the microscopic textures developed at the contact between the reaction zone and the metabasic rock, and at various locations within the reaction zone.

Growth of the reaction zone proceeded along a planar front, which is sharp relative to the limitations set by grain size. Within the metabasic rock, large plates of biotite have grown as porphyroblasts at the expense of hornblende, and these plates are crudely surrounded by plagioclase-quartz haloes, the overall structure having the symmetry of the biotite plates and being the result of a reaction:

$$\text{hornblende} \rightarrow \text{biotite} + \text{quartz} + \text{plagioclase}$$

which implies the bulk exchange of Ca for K within the porphyroblast structures.

[illegible], The process by which the reaction zone fabric gradually replaces the metabasic hornblende-



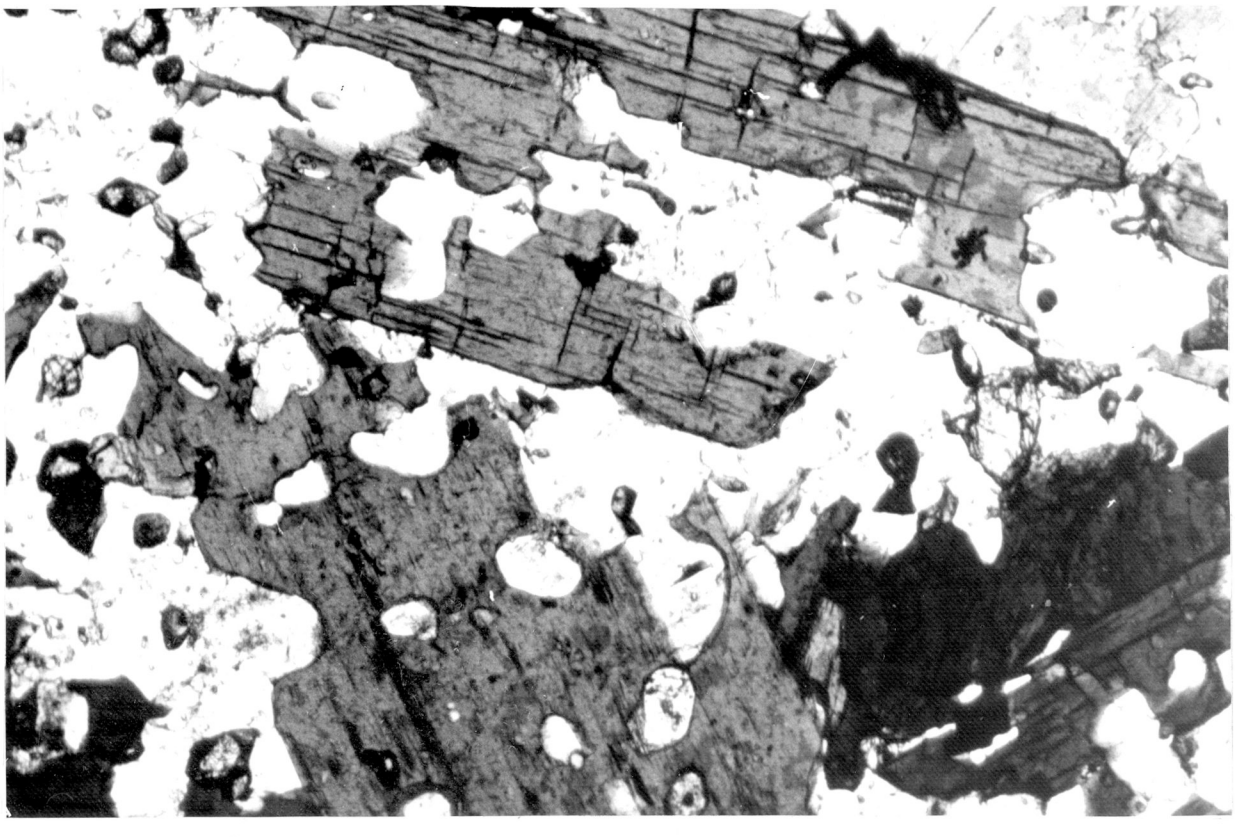
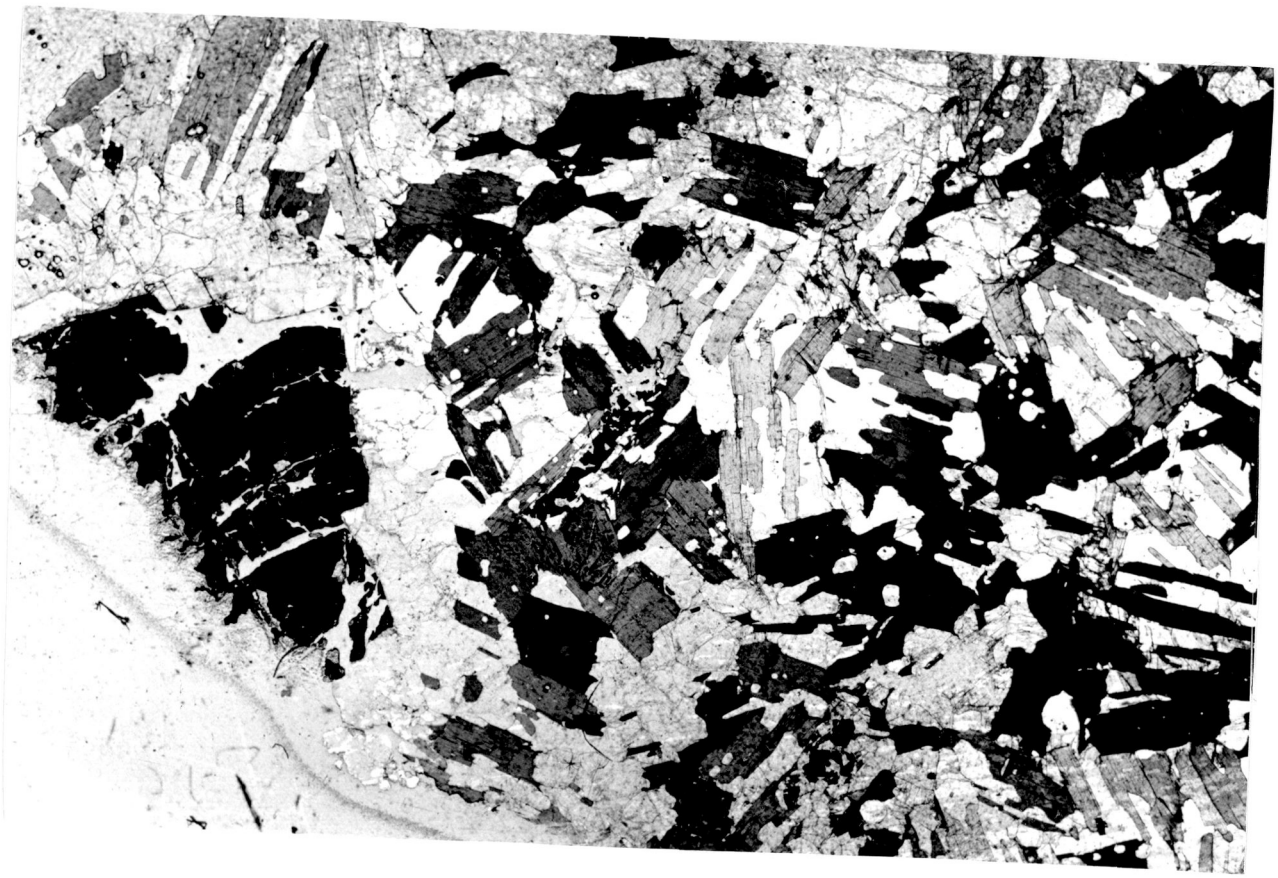


Fig 5.13 Microscopic features of the Garry-a-Siar reaction zones:

a. Boundary between reaction zone (left) and metabasic rock.

b. Detail of (a), showing relict amphibole armoured by quartz in poikiloblastic biotites.

c. Matrix and a porphyroblast-halo structure close to the pegmatite boundary.



plagioclase assemblage can be seen as triangular areas are formed between the decussate biotites, leaving relict hornblende-rich patches. Near to the boundary, biotites are strongly poikiloblastic, sieved with quartz-armoured relics of hornblende and plagioclase. The armouring of these relics and the occurrence of haloes around biotite porphyroblasts in the metabasic rock indicate that biotite and hornblende are nowhere in equilibrium, and are always spatially related by diffusion-controlled growth or dissolution halo structures (in fact biotite and hornblende are sometimes seen in contact in the metabasic rock).

In Figure 5.13e, which shows a part of the reaction zone close to the pegmatite, it can be seen that the biotites are no longer poikiloblastic. The transition from poikiloblastic to clear biotites takes place over a fairly short distance (Figure 5.14), and seems to be related to the imposition of a weak fabric at about this point. This transition appears to indicate that a small amount of deformation was sufficient to clear the biotites of relict phases.

At this stage it will be useful to consider phase compositions and their relation to the mineralogical variations already described. Typical analyses from various parts of the structures described are presented in Table 5.5.

The composition of plagioclase shows a large variation; typically near to An_{30} in the metabasic rock

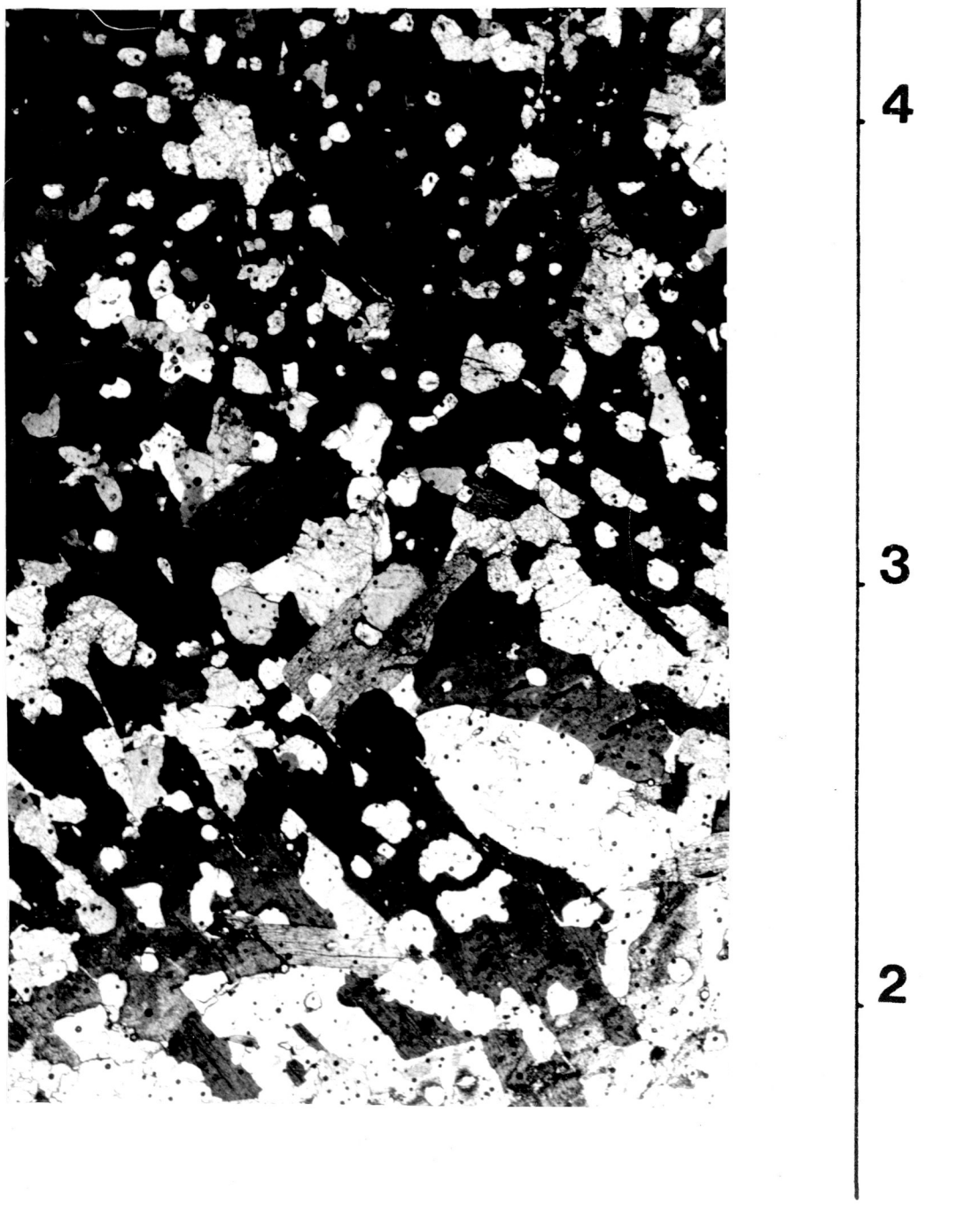


Fig 5.14 Transition from poikiloblastic to clear biotites

BIOTITES

	1		2		3	
SIO2	36.22		36.37		36.40	
TIO2	3.15		3.08		2.94	
AL2O3	16.09		15.87		15.74	
FEO	21.86		21.13		21.21	
MNO	.50		.52		.40	
MGO	8.58		9.15		9.66	
CAO	0		0		.05	
NA2O	.36		.32		.30	
K2O	9.44		9.94		9.86	
SUM	96.77		96.38		96.23	
SI	5.538		5.563		5.556	
AL	2.462	8.000	2.437	8.000	2.444	8.000
AL	.437		.423		.387	
TI	.363		.354		.337	
FE	2.795		2.703		2.707	
MN	.073		.067		.052	
MG	1.955	5.624	2.085	5.634	2.202	5.685
CA	0	2.045	0	2.034	0	2.008
NA	1.939	2.045	1.939	2.034	1.919	2.008
K	22.000		22.000		22.000	
A#N		58.24		56.44		55.14
PHL		41.16		43.56		44.86
F/M		1.467		1.328		1.253
F/FM		.595		.570		.556

AMPHIBOLES

	4		5	
SIO2	41.96		40.33	
TIO2	.83		.75	
AL2O3	12.00		12.45	
FEO	21.20		20.10	
MNO	.63		.34	
MGO	7.35		6.79	
CAO	11.37		11.11	
NA2O	1.55		1.76	
K2O	1.20		1.24	
SUM	98.20		95.58	
SI	6.427		6.360	
AL	1.573	8.000	1.640	8.000
AL	.593		.731	
FE	2.715		2.612	
MN	.082		.124	
MG	1.680		1.972	
TI	.096	5.166	.089	5.127
CA	1.866		1.880	
NA	.134	2.000	.120	2.000
NA	.356		.360	
K	.234	.590	.246	.625
O	23.000		23.000	
FE+M		62.47		63.50
MG+M		37.53		36.50
F/M		1.665		1.740
F/FM		.625		.635

PLAGIOCLASES

	6	7	8	9
SIO2	60.43	60.16	63.31	64.64
TIO2	.05	.04	.04	.10
AL2O3	25.01	25.20	22.84	23.20
FEO	.12	.10	.17	.10
MNO	.10	.10	0	0
MGO	0	0	0	0
CAO	6.47	6.75	4.28	4.27
NA2O	7.84	7.78	9.10	9.43
K2O	.04	.13	.16	.19
SUM	99.34	100.32	99.45	101.73
AN	31.16	32.17	20.34	19.80
AB	68.32	67.09	78.76	79.15
OR	.52	.74	.91	1.05

1. Biotite, reaction zone matrix near pegmatite
2. Biotite, reaction zone next to metabasic rock
3. Biotite porphyroblast in metabasic rock
4. Amphibole, metabasic rock
5. Amphibole, relict crystal in reaction zone
6. Plagioclase, reaction zone near metabasic rock
7. Plagioclase, metabasic rock matrix
8. Plagioclase, reaction zone matrix near pegmatite
9. Plagioclase, reaction zone magnetite halo

Table 5.5 Mineral compositions in Garry-a-Siar reaction zones and metabasic rock

and the outer edge of the reaction zone, it falls to An_{20} or less near to the pegmatite and in the diffusion haloes around magnetite porphyroblasts. Figure 5.15 shows the variation of plagioclase composition across the reaction zone. This distribution is interpreted as a relatively smooth fall in An-content towards the pegmatite, superimposed upon which is an area of considerable scatter between 2-3cm from the metabasic contact. This area of scatter coincides with the 'clearing' of biotites noted above, and is probably the result of a mixed population of armoured, An-richer crystals and the matrix compositions of the continuously-varying population. Supporting this view is the continuing fall in An-content of plagioclases closer to the pegmatite and the absence of An-poor compositions next to the metabasic rock. The plagioclase crystallising as a result of the reaction at the contact between the metabasic rock and the reaction zone is An-rich, and cannot represent relict material from the metabasic rock, but belongs to the continuously-varying population.

Of the other analysed minerals, only biotite can be said to show any variation, becoming slightly more annite-rich towards the pegmatite. Hornblende is constant in composition, and has a higher Fe/(Fe + Mg) ratio than all biotites. Magnetite has pure end-member composition. Sphene is a common accessory mineral in the metabasic rock, and appears to occur in unusual concentration along the contact between the metabasic

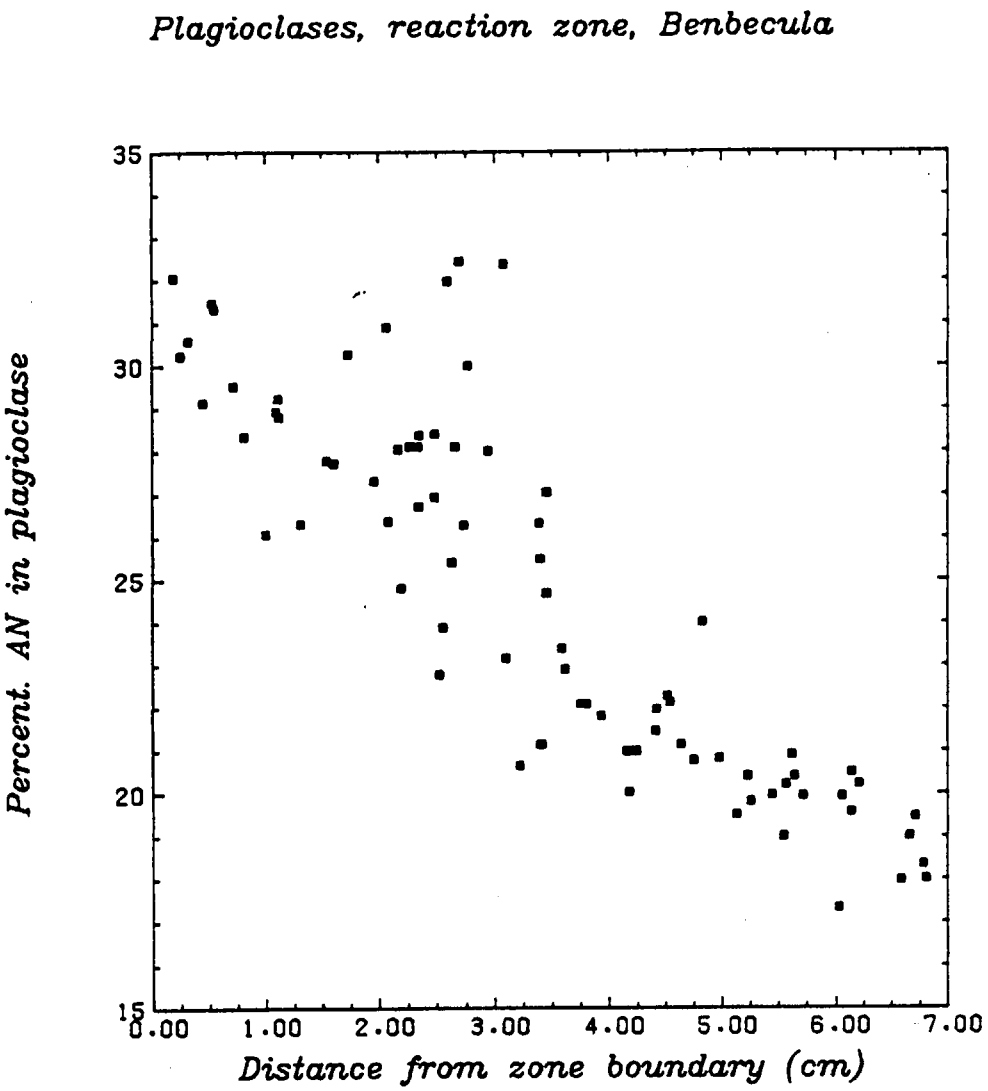


Fig 5.15 Variation of plagioclase composition across the reaction zone

rock and the reaction zone. Apatite and zircon are the relatively uncommon accessories in the reaction zone.

Textural and mineralogical features of the reaction zone and associated rocks suggest the complex interaction of several factors. The mass transfer of K and Ca is obviously a major feature of the overall process, a Ca-poor mineral assemblage replacing the original metabasic assemblage with the supply of K for biotite growth presumably coming from a pegmatite-derived fluid phase. The relative efficiency of the overall process was dependent to some extent on the presence of relict (Figure 5.11b) or imposed (Figures 5.11a, 5.14) fabrics, which may have provided strain energy (in the latter case) as well as possible easy transport paths for fluids. The association of the ferromagnesian phases and magnetite with diffusion-controlled halo structures at various locations not only suggests that nowhere do any two of these minerals form part of the *same equilibrium* assemblage, but also shows that the diffusion process alone is inadequate to account for the width of the reaction zone, operating on a relatively local scale. This, combined with the likelihood that the fluid phase present was derived from the pegmatite, suggests the dominant role of infiltration metasomatism, under conditions of variable porosity and tortuosity.

5.3.2 CHEMICAL MASS TRANSFER

A major problem in the assessment of the nature of mass transfer in the Garry-a-Siar zones is their complex

geometry. The presence of spherically-symmetrical structures not only results in a rock which is difficult to characterise compositionally, but from the point of view of any interpretation of the factors governing mass transfer implies great complexity in the transport paths of some components.

The approach adopted has been to carry out chemical analysis for a range of elements across part of the reaction zone - a single slab being sawn up into short sections - and separately to use mineral data to estimate the compositions of the metabasic rock and reaction zone matrices at different locations. The former method is obviously vulnerable to modal variations in small samples, although this can in some respects be turned to advantage when examining the behaviour of trace elements. Estimation of matrix compositions from mineral analyses involves a lack of information about trace elements, but will be useful when attempting to describe the various reactions taking place.

In Figure 5.16, the chemical variation across a 9cm section - of which the first centimetre (sample GS1) lies within the metabasic rock, while the second straddles the reaction zone boundary - is shown for a range of major and trace elements (concentrations are listed in Table 5.6).

Chemical variation can be seen across the section, and is divisible into two types: (a) large differences between the metabasic rock and the reaction zone, and (b) more or less steady variations within the reaction zone as the pegmatite margin is approached. The large

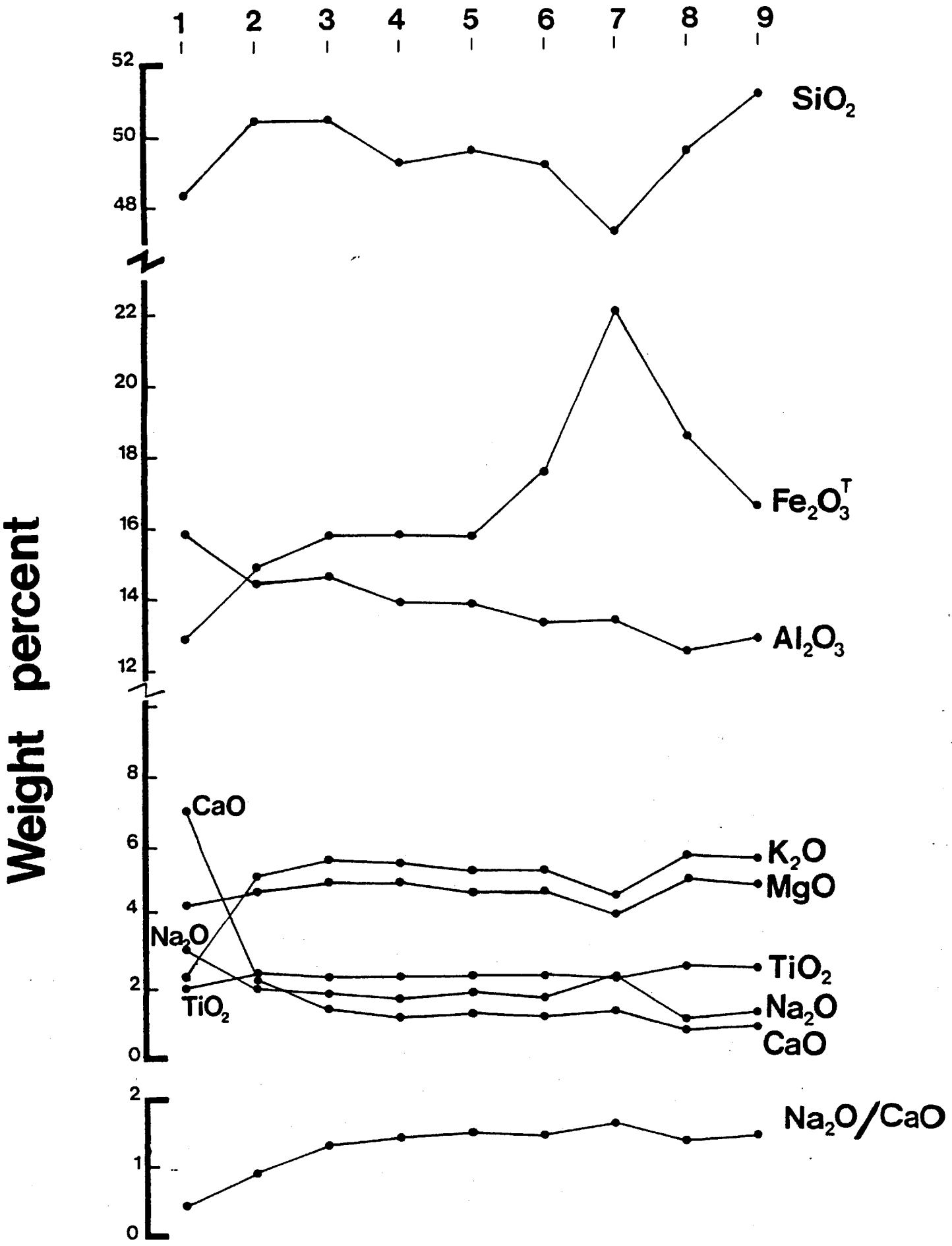


Fig 5.16 Major element variation across the reaction zone

Table 5.6 - Compositions of samples taken across a reaction zone, Garry-a-Siar, benbecula.

Oxides (wt. percent)

	GS1	GS2	GS3	GS4	GS5	GS6	GS7	GS8	GS9
SiO_2	48.32	50.44	50.45	49.22	49.52	49.18	47.25	49.54	51.18
TiO_2	2.07	2.45	2.33	2.33	2.37	2 38	2.26	2.61	2.57
Al_2O_3	15.87	14.43	14.61	13.91	13.84	13.29	13.37	12.49	12.84
$Fe_2O_3^T$	12.91	14.94	15.77	15.84	15.73	17.55	22.04	18.56	16.52
MnO	0.37	0.30	0.33	0.34	0.35	0.36	0.37	0.41	0.41
MgO	4.38	4.82	5.06	5.08	4.75	4.79	4.08	5.05	4.88
CaO	8.98	2.20	1.48	1.25	1.32	1.21	1.38	0.86	0.92
Na_2O	3.24	2.01	1.92	1.74	1.97	1.74	2.23	1.16	1.30
K_2O	2.38	5.23	5.65	5.54	5.34	4.66	4.62	5.79	5.61
P_2O_5	0.26	0.32	0.25	0.26	0.26	0.28	0.27	0.28	0.29
Sum	96.69	97.14	97.85	95.32	95.44	96.16	97.77	96.75	98.04

Trace elements (ppm)

Zn	138	192	203	225	208	214	260	242	228
Sr	147	106	71	59	60	60	60	33	35
Ba	189	250	205	158	130	115	89	108	101
Ni	70	98	73	85	86	72	74	72	70
V	255	264	242	224	205	188	228	177	166
Be	2	1	1	1	1	1	1	1	1
Zr	128	117	96	110	144	128	162	140	139
Cr	89	208	105	114	123	115	139	122	129
Rb	247	712	782	790	751	751	655	825	827
K/Rb	.97	73.5	72.3	70.1	71	71.5	71.7	70.2	67.8
Ba/Sr	1.3	2.36	2.9	2.7	2.2	1.9	1.6	3.3	2.9
Na/Ca	0 46	0.91	1.3	1.4	1.49	1.44	1.62	1.35	1.41

Table 5.6 - Compositions of samples taken across a reaction zone, Garry-a-Siar, benbecula.

differences at the interzonal contact are clearly the result of the reaction involving hornblende dissolution associated with reaction zone growth. Those within the reaction zone are sometimes irregular, but their existence is supported by the variations in plagioclase and perhaps biotite composition noted previously. Additionally, and probably more importantly, modal variations occur within the reaction zone, both in the relative increase in biotite-poor porphyroblast-halo structures and in the biotite-quartz-plagioclase matrix (see modal estimates in Table 5.7).

MAJOR ELEMENT VARIATIONS.

Given the nature of the reaction zone growth reaction, the large changes in K and Ca across the interzone boundary relative to all other elements are only to be expected. To some extent this sharp change is 'damped' in Figure 5.16, by the slightly hybrid composition of sample GS2 and by the fact that sample GS1 does not truly represent the initial metabasic composition since it contains biotite porphyroblasts. Real contrasts between the K and Ca contents of the two rocks would be sharper and more pronounced.

Na also falls markedly in the reaction zone, and both Na and Ca occur in very low concentrations near to the pegmatite contact (GS8/9). This is mainly due to low modal plagioclase relative to biotite in this

Table 5.7 Modes, molar volumes and estimates of matrix compositions for reaction zones, Garry-a-Siar, Benbecula.

Modes:

	HB	AN30	AN20	BI	QZ	SPH	MT
1.	72.9	21.5			2.9	2.7	
2.	.2	17.7		62.8	18.5	.8	.3
3.			17.7	57.0	24.7		.4

(1: matrix, metabasic rock, 2: reaction zone next to metabasic rock, 3: reaction zone next to pegmatite)

Molar volumes (Robie et. al., 1967):

(cm^3)	272	100.21	100.29	305	22.69	35.65	44.5

Bulk compositions(anhydrous basis):

	1	2	3
SiO_2	2.4572	2.4503	2.6197
TiO_2	0.0724	0.0882	0.0672
Al_2O_3	0.8869	0.8308	0.7912
FeO^T	0.7483	0.5957	0 5437
MgO	0.4157	0.4075	0.3682
CaO	0.6247	0.0677	0.0354
Na_2O	0.2436	0.1420	0.1583
K_2O	0.0697	0.4006	0.3624

(moles/1000cm^3)

Table 5.7 Modes, molar volumes and estimates of matrix compositions for reaction zones, Garry-a-Siar, Benbecula.

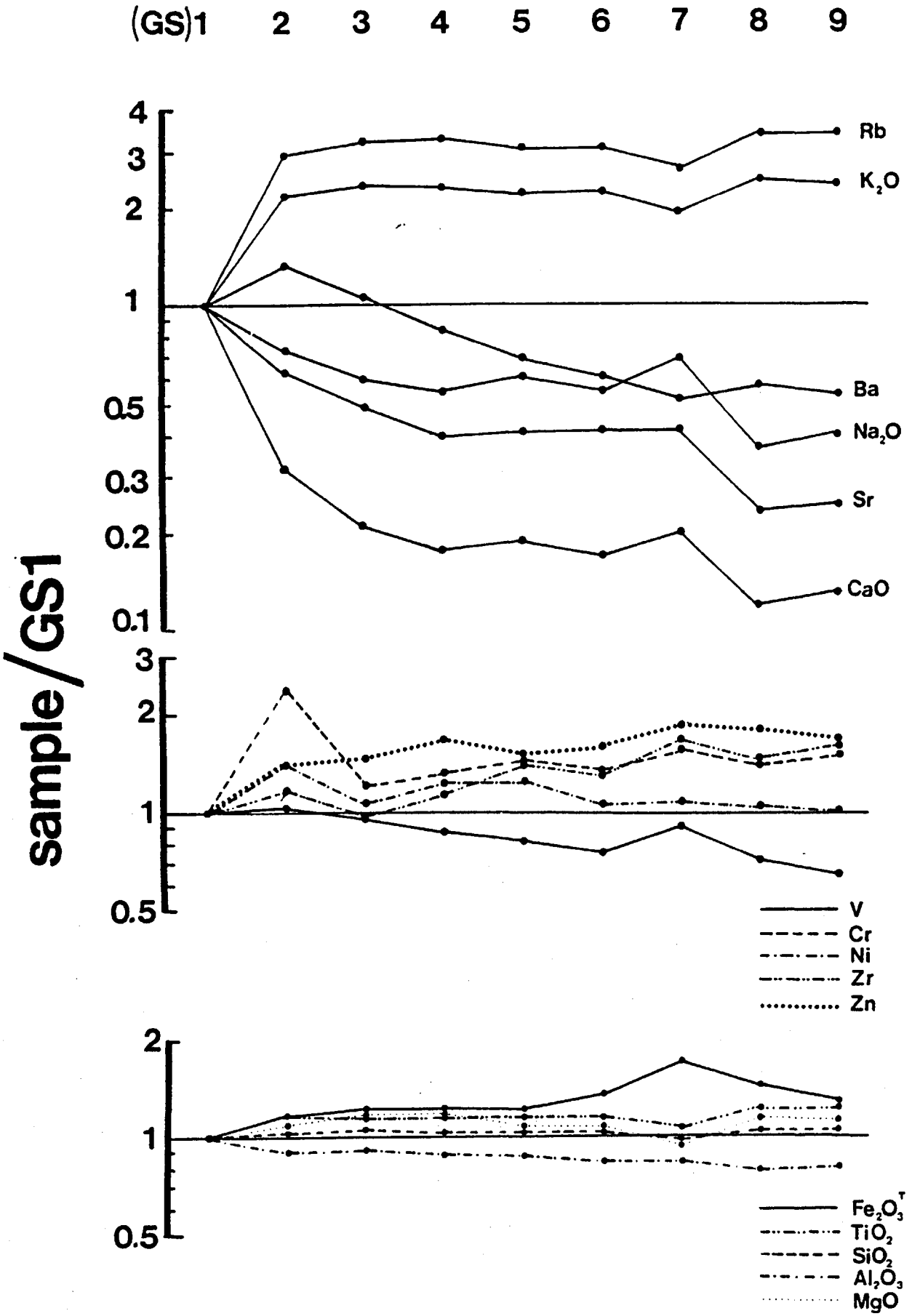
part of the section, and otherwise Na does not show the gradual decrease through the reaction zone which appears to apply to Ca. There is a steady increase in the ratio Na_2O:CaO through the reaction zone, consistent with the variation of plagioclase composition from An_{30} to An_{20}.

Al shows a small decrease into the reaction zone, continuing to fall through the zone. Fe, Mg and Ti all increase into the reaction zone, and Fe increases strikingly in concentration through the zone, presumably with an increasing modal content of magnetite. Sample GS7 clearly includes a large porphyroblast-halo structure, not only demonstrating the high Fe-content of these structures, but also the relatively high Ca and Na which is the result of the absence of biotite. The matrix composition estimates given in Table 5.7 must underestimate bulk Fe, Ca and Na.

TRACE ELEMENT VARIATIONS.

The variation of Rb, Sr and Ba can be expected to show significant relationships with those of K, Ca and Na. In Figure 5.17 the distribution of these elements is shown normalised to the (at least approximately initial metabasic) composition of GS1, showing the relative changes in each element in a comparable way.

Rb correlates strongly with K, and is presumably partitioned into biotite. Its source must be the



5.17 Variation of trace elements across the reaction zone

infiltrating pegmatite fluid. Ba and Sr both decrease in the reaction zone, suggesting that the pegmatite fluid was poor in these elements, a conclusion consistent with evidence from Laxfordian pegmatite geochemistry (Chapter 3) and alkali feldspar chemistry (Chapter 4). Both elements provide some evidence about relative partitioning amongst mineral phases and fluid in the reaction zone. Sr shows relative concentrations lower than those of Na and higher than those of Ca, suggesting intermediate partitioning into the fluid relative to plagioclase. Figure 5.17 shows that the ratio Sr:Na falls through the reaction zone, while Sr:Ca may be approximately constant. This might indicate not only that the relative flux of Sr was much more like that of Ca than that of Na, but also that the partitioning of Sr between plagioclase and fluid is a function of plagioclase composition, the partition coefficient being lowest (other things being equal) at high plagioclase albite contents.

The distribution of Ba is unusual in showing an initial increase relative to the metabasic concentration followed by a clearly-marked decline through the reaction zone. Its concentration in sample GS7 suggests that Ba partitions into biotite relative to plagioclase. Partition coefficients between minerals and igneous liquids quoted by Hanson (1978) show that for Ba the minerals present in the metabasic rock and reaction zone show the relative preference hornblende plagioclase biotite. If this pattern extends qualitatively to

mineral-fluid partitioning it can be applied to the behaviour of Ba in the reaction zone. The higher concentration of Ba in the metabasic rock must largely have been present in plagioclase rather than hornblende. In the reaction zone it has already been suggested that Ba partitions into biotite relative to plagioclase, while in the metasomatic structure as a whole Ba was transferred via the fluid phase into the pegmatite. The continuous fall in Ba through the reaction zone suggests, as with Sr, that partitioning of Ba between solid and fluid phases was not constant throughout the zone, Ba being lowest in concentration in GS8/9, where modal biotite is highest. The most problematical feature of Ba distribution remains the apparent increase in its concentration at the reaction zone contact with the metabasic rock.

Figure 5.17 shows that Zn, Zr, Cr, Ni and V partition into the porphyroblast-halo structures. Although most of these are presumably mainly present in magnetite, Zr would be most influenced by the presence of zircon inclusions in the porphyroblasts. While Zn, Zr and Cr generally increase in relative concentration through the reaction zone, in a similar manner to Fe, the trend of V is downwards.

In summary, the distribution of elements in the reaction zone indicates <u>net</u> fluxes towards the growing reaction zone front in K and Rb, and fluxes away from that front in Ca, Na, Sr and Ba. Variations are

observed in most other elements, and some of these variations seem to contradict what might be thought to be the expected fluxes. Fe and Mg display higher concentrations in the reaction zone than those in the metabasic rock, as do elements such as Cr, Ti and Ni. These elements are unlikely to have been present in higher initial concentrations in the pegmatite than in the metabasic rock. The contradictions revealed by these chemical variations are discussed in relation to possible mechanisms controlling the development of the reaction zones in the next section.

5.3.3 PROCESSES GOVERNING MASS TRANSFER

It has already been suggested that the reaction zones at Garry-a-Siar were formed by an infiltration-dominated metasomatism, in which the relative efficiency if the overall process was strongly dependent on the tortuosity of the transport path. Locally, reactions were diffusion-controlled, giving rise to characteristic structures which in the case of the magnetite porphyroblasts were of spherical symmetry. Thus the overall process involved at least statistically one-dimensional mass transfer, as would be expected for an infiltration process driven by a fluid pressure gradient perpendicular to the direction of reaction zone growth, while local diffusion processes giving rise to some redistribution of elements within the reaction zone were characterised by three-dimensional mass transfer. The interplay between these contrasting processes is discussed below.

A. ASSUMPTIONS.

It will be assumed in the following discussion that the geometrical and chemical features observed in the reaction zones were frozen in their present state when metasomatism ceased, and all the observed structures developed in a regular and mutually-dependent way from the onset of zone growth. This assumption is supported by the simple size-distance relations seen in Figure 5.12a and by the regular variation in plagioclase composition seen in the reaction zone, but not by the disequilibrium compositions of relict plagioclase at 2-3cm from the reaction zone margin. However, to separate in time the growth of the reaction zone from the development of the porphyroblast-halo structures would create serious difficulties over the distribution of Fe prior to magnetite growth, and would contradict the apparent engulfment of magnetites by the pegmatite margin noted in section 5.3.1. On balance, a steady-state model seems the best available.

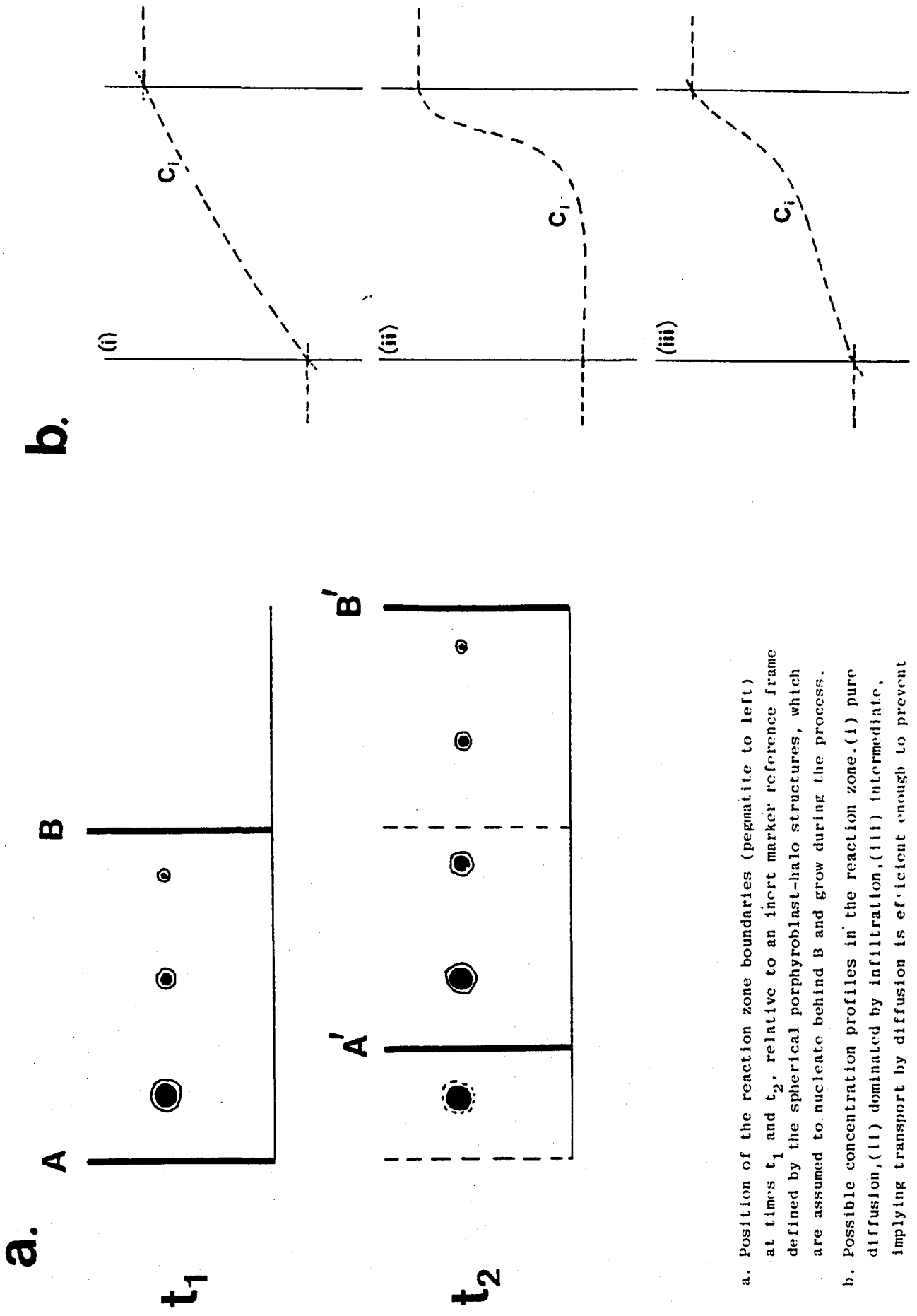
It is suggested that the similar apparent relative distributions of Fe, Cr, Zn and Zr in Figure 5.17b may be the result of the relative immobility of those components, and in particular that of Fe, which is likely to have controlled those of the others. This assumption is consistent with the large fluxes of 'plagioclase' components towards the pegmatite, leaving enhanced concentrations of most other elements and

resulting in apparent net fluxes of such components as Fe, Mg, Cr and Ti into the reaction zone because of the closure effect. Variation of Fe within the reaction zone may be the result of the cumulative nature of the net chemical compositions of GS2-9. Fe is clearly not 'immobile' relative to most other components on a local scale, since this would make the growth of large magnetite porphyroblasts impossible.

B. A SIMPLE MODEL OF REACTION ZONE GROWTH.

Figure 5.18 is used to illustrate the possible geometrical development of the reaction zones given the stated assumptions. In Figure 5.18a, a section across the reaction zone is shown as it would appear at two separate times after the initiation of growth. For a reaction zone to grow, boundary A must advance at a slower rate than B. Mobility of Fe on a local scale only requires constant nucleation of magnetite porphyroblasts behind boundary B, since the reaction zone matrix composition has a lower Fe/(Fe + Mg) ratio than that of the metabasic rock to the right of the boundary. Further growth of the porphyroblasts is the result of internal reaction between the two boundaries to preserve local equilibrium.

Fluid compositions in different parts of the developing structure are complex. Assuming solute concentrations to be fixed by equilibrium with large reservoirs to the left of A, A', etc. and to the right of B, B', etc., concentration gradients must occur in



a. Position of the reaction zone boundaries (pegmatite to left) at times t_1 and t_2, relative to an inert marker reference frame defined by the spherical porphyroblast-halo structures, which are assumed to nucleate behind B and grow during the process.

b. Possible concentration profiles in the reaction zone.(i) pure diffusion,(ii) dominated by infiltration,(iii) intermediate, implying transport by diffusion is efficient enough to prevent a concentration plateau developing.

Fig 5.18 Suggested growth of spherical porphyroblast-halo structures relative to reaction zone growth.

the reaction zone. The forms of diffusion-only (Weare et al., 1976) and mainly-infiltration (Fletcher and Hoffman, 1974) concentration profiles for an element with a net flux into the pegmatite are shown in Figure 5.18b. The convex-up curve in 5.18b(i) reflects internal solution of the element, while the flat profile over most of 5.18b(ii) represents a concentration plateau characteristic of infiltration metasomatism (Fletcher and Hoffman, 1974). Phase chemical variations described in section 5.3.1 and internal chemical variations described in section 5.3.2 indicate that such a plateau did not exist in the fluid concentration profile, and an intermediate profile is shown in 5.18b(iii). At all points in the reaction zone, the infiltrating fluid is in local equilibrium with the matrix mineral assemblage only, with local diffusion-dominated gradients between the inner and outer boundaries of each porphyroblast halo. The development of the spherical structures will be considered next.

Spherical segregations in metamorphic rocks have been described by several authors (Fisher, 1970, 1973; Weare et al., 1976; Atherton, 1976). Atherton applied considerations of local mass-balance to write simple reactions for the growth of porphyroblasts with depletion haloes, and Fisher also made the assumption that segregation-halo structures had integrated bulk compositions identical to those of the matrix in which they developed. In both cases these were reasonable assumptions, leading to the geometrical restrictions

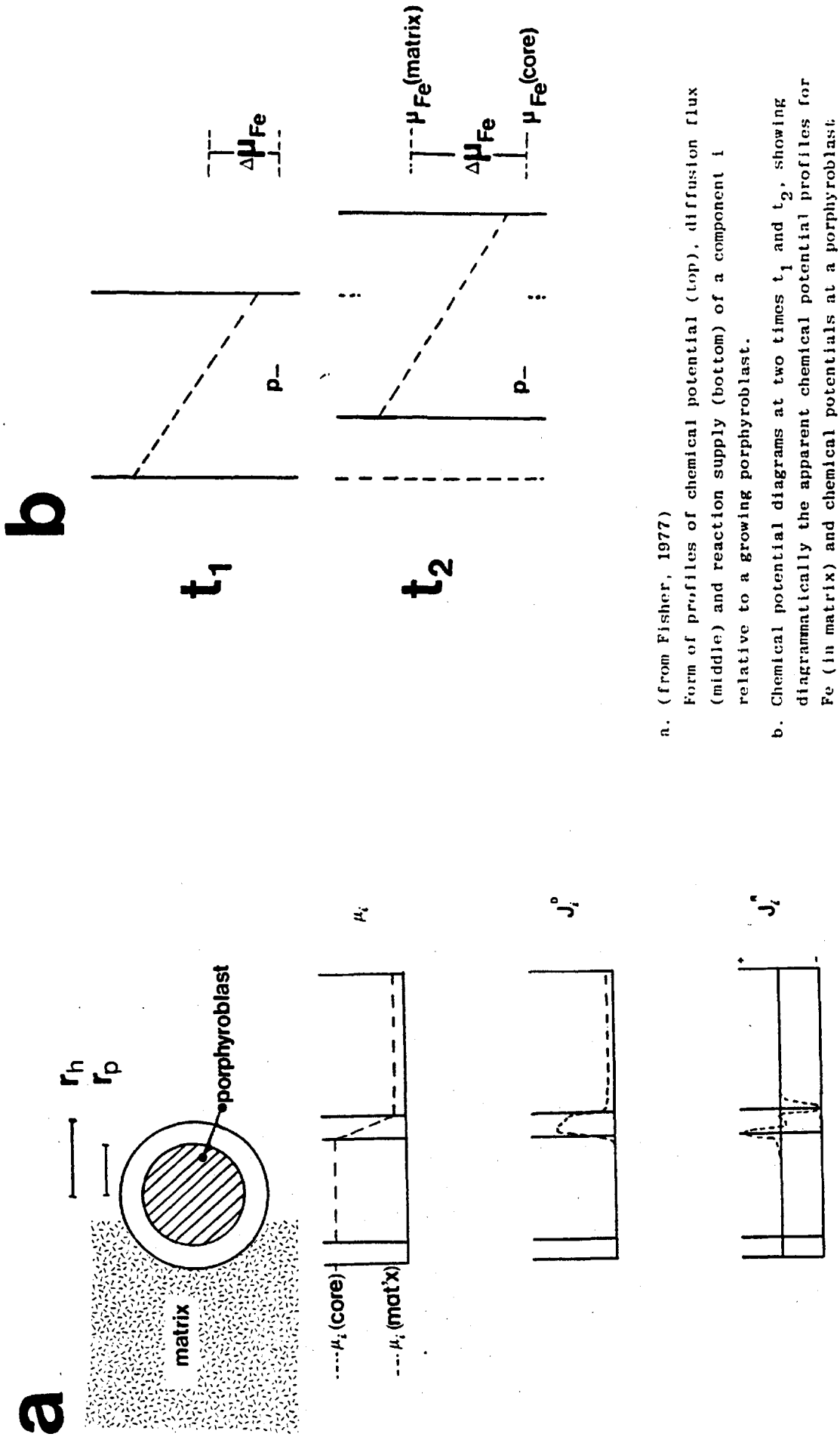
suggested by Atherton: (a) halo widths vary in a regular way (maintaining constant volume proportionality between the halo and porphyroblast) with porphyroblast size, and (b) haloes do not merge or interfere in any way. These restrictions, reasonable in many metamorphic rocks, are obviously violated in the Garry-a-Siar porphyroblasts in the following ways:

(i) Halo widths remain constant as the porphyroblasts grow, except in the case of very large porphyroblasts occurring near fractures.

(ii) In Figure 5.11b, haloes merge until the 'matrix' disappears or becomes restricted to small enclaves.

(iii) The spherical structures are not chemically equivalent to the matrix; they are almost entirely free of K, Mg and probably Ti. Nor do the haloes represent chemically-depleted zones, since the relative volumes of even the smallest magnetite porphyroblasts cannot be accounted for by diffusion of Fe within the spherical structures alone. Fe may be mobile on only a local scale, but this must involve diffusion over significantly greater distances than the size of the spherical structures would suggest.

Figure 5.19a shows diagrammatically the growth of a spherical porphyroblast-halo structure. Fe is transferred down a fluid concentration gradient (or chemical potential gradient) to the magnetite surface where it is precipitated. Assuming the chemical potentials of Fe in the matrix and at the magnetite surface to be fixed, the chemical potential



a. (from Fisher, 1977)
Form of profiles of chemical potential (top), diffusion flux (middle) and reaction supply (bottom) of a component i relative to a growing porphyroblast.

b. Chemical potential diagrams at two times t_1 and t_2, showing diagrammatically the apparent chemical potential profiles for Fe (in matrix) and chemical potentials at a porphyroblast surface(p). At time t_2 the chemical potential difference between core and matrix has increased as a result of the change in the matrix profile.

Fig 5.19 Relationships between chemical potentials, fluxes and growth of spherical porphyroblast-halo structures.

gradient is given by:

$$\nabla\mu = \frac{\mu^{e}_{Fe} - \mu^{i}_{Fe}}{r_p - r_h} \quad \ldots 5.6$$

approximately, where μ^e and μ^i refer to the matrix and porphyroblast chemical potentials, r_p is the porphyroblast radius and r_h is the radius of the complete spherical structure. Since the halo width remains the same (Figure 5.12a), the divisor in eq. 5.6 is a constant, as presumably must be the chemical potential of Fe at the magnetite surface. The chemical potential of Fe in the matrix may show some variation with time, and an attempt to represent this has been made in Figure 5.19b. If the small increase in the annite-content of biotite towards the pegmatite is the result of local equilibrium partitioning of Fe between biotite and the matrix fluid phase, it implies a fluid concentration gradient in the sense of that shown in Figure 5.19b. Thus during growth of the reaction zone the matrix chemical potential of Fe external to a porphyroblast-halo structure will tend to rise, and since this is the only variable in equation 5.6, the chemical potential gradient across the diffusion halo must rise, so that porphyroblasts can grow with time despite a constant halo width. Since Fe is here being treated as a relatively immobile component in the matrix, any apparent fluid concentration gradient such as that of Figure 5.19b must be interpreted as the result of

multicomponent mass transfer, in which other components are genuinely mobile over the reaction zone as a whole.

The key to Fe immobility is the nucleation and growth of the spherical structures, resulting in the largest chemical potential gradients of Fe being on a local scale, and not any intrinsic property of Fe relative to other components. The pegmatite-derived fluid was a source of oxygen for the growth of magnetite, a point which will be considered further when discussing the pegmatite fluid composition.

The simple model suggested for the linking of reaction zone growth with development of the spherical structures is consistent with the geometrical and chemical features observed. Ideally, local equilibrium was maintained throughout the reaction zone, although this was subject in practice to variations due to variable tortuosity and the local armouring of relict phases.

C. NATURE OF REACTIONS.

Given the steady-state assumptions above, reactions can be written to describe the production and consumption of components. The reactions are linked by fluxes of solute components between reaction sites, operating in the planar and spherical geometries described above.

Reactions are of both continuous and discontinuous type, the term 'continuous' being used here to denote solid-fluid exchange reactions in an unvarying assemblage in response to fluid concentration gradients, while

discontinuous reactions involve the disappearance or appearance of mineral phases. At Garry-a-Siar, the following reactions can be identified:

A. Continuous:

(i) Mg-Biotite + Fe (fluid) = Fe-Biotite + Mg (fluid) ... 5.7

(ii) Anorthite + NaSi (fluid) = Albite + CaAl (fluid) ... 5.8

... both reactions proceeding to the right as the pegmatite margin is approached, and representing exchange reactions between matrix phases and fluid.

B. Discontinuous:

(i) Hornblende + K,Rb (fluid) = Biotite + plagioclase + Quartz + Ca,Na,Sr,Ba (fluid) ... 5.9

(ii) Biotite + O (fluid) = Magnetite + plagioclase + K,Si,Mg,Ti (fluid) ... 5.10

... which describe the reaction at the contact between the reaction zone and metabasic rock, and the overall reaction for the growth of magnetite porphyroblasts, respectively.

The continuous reactions have already been used implicitly to suggest the possible form of fluid concentration gradients of solutes (Figure 5.18). Both discontinuous reactions could be broken down into local reactions describing small local systems. For example, reaction 5.9 would be a complete description of the interzone boundary if that boundary were perfectly sharp, but is used here to generalise the effects of biotite growth in the metabasic rock, and dissolution of hornblende and plagioclase in the reaction zone. Similarly, two reactions taking place at the inner and outer faces of the diffusion haloes are connected by component fluxes through the haloes, and 5.10 is only a description of the overall process.

D. COMPOSITION OF THE PEGMATITE FLUID.

The fluxes indicated in Figure 5.17 show that the fluid phase evolved by the pegmatite was poor in Ba, Sr, Ca and Na, and rich in K and Rb. In addition, the growth of magnetite suggests the relatively oxidising effect of the fluid.

Assuming the fluid phase to have equilibrated with the pegmatite minerals, the observed fluxes of these elements would result in:

(a) a fall in Rb/Sr in the pegmatite relative to its initial ratio,

and

(b) a change in the Sr-isotopic geochemistry of the pegmatite such that its $^{87}Sr:^{86}Sr$ ratio would lie on a

'mixing line' between its original value and that of the metabasic rock.

These effects are limited by the relatively narrow reaction zone developed; on the other hand, the selective nature of the metasomatism indicates that the extent of such trace element mixing is much greater than would be the case with simple assimilation of a volume of metabasic rock equivalent to the outward migration of the pegmatite margin. The overall process at Garry-a-Siar can best be described as selective assimilation in which some of the trace element characteristics of the pegmatite have been modified from possibly-extreme (high Rb, low Sr and Ba) 'igneous' values.

5.4 CONCLUSIONS

5.4.1 PROCESSES IN METASOMATISM

The two examples of reaction between acid pegmatites and basic country rocks found in the Outer Hebrides provide a basis on which to assess the relative effects of a number of factors on the final products and the extent of modification possible in the original rocks.

Extensive metasomatism at the relatively low (perhaps of the order of 500-550°C) temperatures prevailing at Garry-a-Siar and in the second metasomatic event at Leenish apparently depends on the availability of an

infiltrating fluid, which in the former case seems to have been evolved osmotically from the pegmatite itself, while in the latter case the acid vein may have acted largely as an easy fluid transport path. Diffusion metasomatism may have been the dominant mechanism in the early, high-temperature event at Leenish, and was important in determining the local spatial development of the reaction zone at Garry-a-Siar, where it was clearly an important rate-limiting factor at the growing reaction zone front. Slow rates of diffusion impeded the development of steady-state composition gradients in the mineral phases because of the persistence of relict plagioclase compositions, and may have caused the apparent disequilibrium distribution of Ba, which shows an initial bulk increase in the reaction zone followed by a steady fall.

Local equilibrium partitioning of elements between solids and fluids is indicated by the consistency between the senses of fluxes suggested by reaction zone chemistry on the one hand and on phase compositional variations on the other. It can be suggested that where they are preserved, phase compositional variations give more information than reaction zone chemistry, (a) because they represent instantaneous equilibrium between solids and fluids, whereas reaction zone bulk chemical variations are cumulative over the whole period of zone growth, and (b) because, as at Garry-a-Siar, they may allow some statement to be made about fluid concentration profiles

and the likely relative influence of infiltration and diffusion. At Garry-a-Siar, profiles characteristic of combined diffusion-infiltration metasomatism are thought to have been present (Figure 5.18b). Local equilibrium may more efficiently have been achieved near to the pegmatite, and it is essential to take account of the influence of variations in the fluid transport path here.

Coarser matrix grain size, characteristically larger spherical structures with wide diffusion haloes, and the relatively extreme structural heterogeneity seen in Figure 5.11b in the presence of a relict foliation in the reaction zone, and in Figure 5.11a near to irregular fractures, demonstrate the importance of transport path tortuosity in controlling the development of reaction zones. On the whole, in the reaction zones examined here, factors such as the rates of local diffusion, tortuosity and degree of infiltration appear to have a much greater influence on net mass transfer than any supposed intrinsic relative mobility of elements. Thus Fe appears to be immobile in the overall process at Garry-a-Siar only because it is locally fixed in magnetite porphyroblasts. This could be seen as a tendency for Fe to migrate down the steepest available chemical potential gradient, which in the reaction zone is always towards a growing porphyroblast. Aluminium, favoured as an 'immobile' element by Carmichael (1969) for example, probably has a

net flux into the acid rocks in both examples described here which is larger than that of any major element other than Ca or Na (Figure 5.17c), if Fe is assumed not to vary. This is required for the preservation of electrostatic neutrality during exchange reactions involving plagioclase such as reaction 5.8 above.

5.4.2 EXTENT OF CHEMICAL MODIFICATION

The degree to which acid intrusive rocks can be modified by reaction with country rocks in the site of crystallisation is a consideration important in this thesis as a whole. In addition to temperature (of which diffusivity is a function) and the availability of fluids and fluid pressure gradients to drive infiltration, two additional important factors may be relative reservoir sizes and compositional contrasts between acid rocks and host rocks.

It is quite possible that the acid veins at Leenish were extensively changed in composition because of their similarity in size to the metasomatic rocks (the garnet zones) with which they are associated. It has already been suggested that metasomatism was limited by the decline of all chemical potential gradients to insignificant sizes, on the grounds that a single plagioclase composition occurs in all the associated rock-types. Here it can be envisaged that the initial $^{87}Sr:^{86}Sr$ ratio of the acid vein magma, which might have been high if the magma

were derived from old crustal rocks, would completely have re-equilibrated with the (presumed) mantle initial ratio of the Scourie metadolerites.

At Garry-a-Siar, the pegmatite is very large compared with the reaction zones - even a continuous reaction zone (which is certainly not present) on both margins would have a volume less than 1% of that of the pegmatite. Nevertheless, the pegmatite margin near the reaction zones is apparently basified (that is, free of alkali feldspar); although it is not possible to determine if this is entirely because of metasomatism, some plagioclase growth at the margin is certainly associated with reaction zone growth. When trace elements are considered, much larger contrasts in initial concentrations may well have existed than those for major elements, so that Rb, Sr and Ba concentrations in the final pegmatite may bear little relation to their initial values. Ba values of less than 10ppm occur in some Laxfordian pegmatites, so the leaching of half the Ba in the reaction zone could have increased its concentration in the pegmatite by the order of 100%. Similar effects on Sr could drastically change the pegmatite initial Sr ratios, and would certainly mean that those ratios would be buffered by those of the host rocks. This is a crucial consideration in the interpretation of Sr initial ratios as an indication of granite genesis.

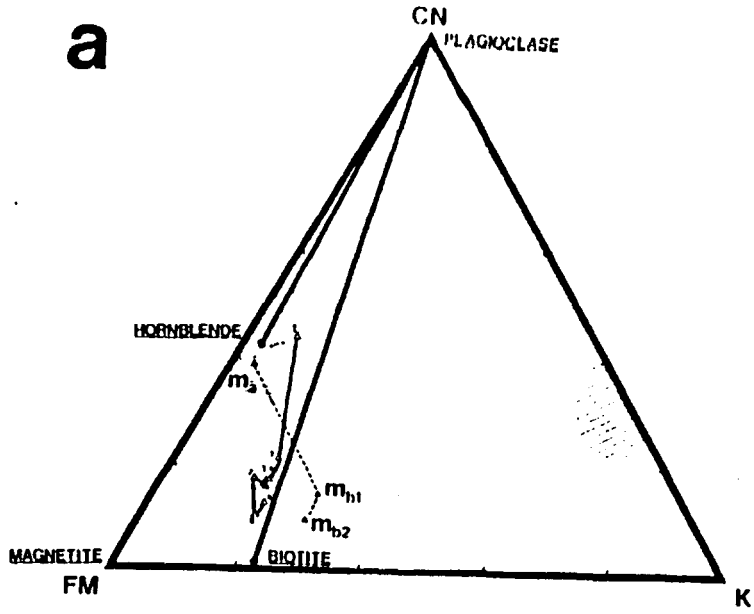
The contrast in composition between the acid and basic rocks described here is important to the preservation of

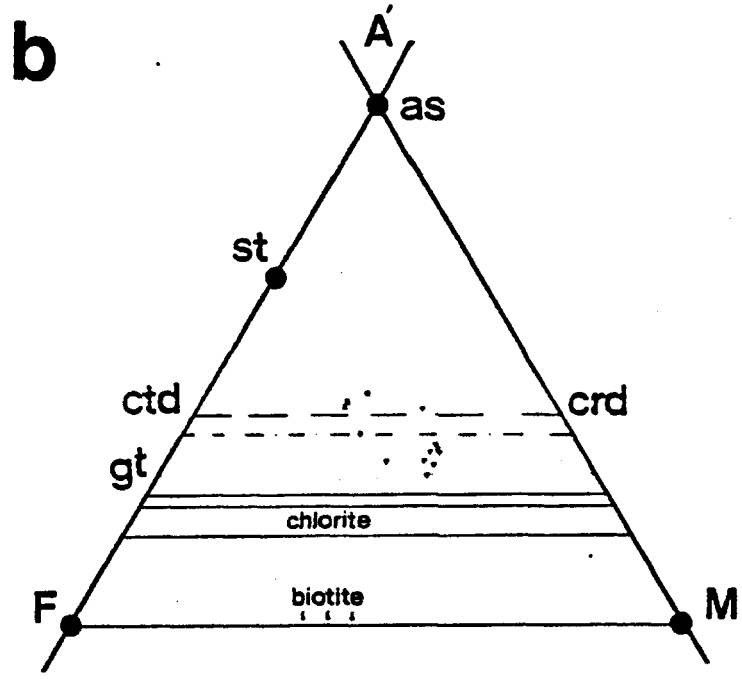
the geometrical features characteristic of metasomatism. At Garry-a-Siar, no evidence has been found for reaction between the pegmatite and the more common intermediate to acid country rocks it intrudes. Bowen (1928) showed that interaction between igneous and country rocks could involve melting (hardly in any case to be expected at Garry-a-Siar) only when the igneous rock was undersaturated with respect to the minerals of the host rock / xenoliths. Reaction was possible with rocks more basic than the igneous rock, and would lead to extensive crystallisation, not of minerals characteristic of the host rock, but of minerals with which the igneous rock was just saturated. Many granitic rocks may be just saturated with an acid plagioclase, large volumes of which might crystallise given a relatively modest addition of Ca to the magma. Not only is reaction of this type seen at Leenish and Garry-a-Siar, but a balancing loss of K is seen which could only enhance the formation of plagioclase. Basification is seen at Garry-a-Siar and, perhaps more extensively, at Leenish. Of course, these rocks are not granites, but they demonstrate the possible effects. It can be recalled that Laxfordian granites have a thin-sheeted geometry, occasionally show some evidence (in the Outer Hebrides) of xenolith assimilation, and have heterogeneous Sr initial ratios in Harris (Van Breemen et al., 1971). This question will be further considered in Chapter 6, in relation to other processes in granite evolution.

5.4.3 PRODUCTS OF METASOMATISM

It was pointed out in section 5.2 that the Leenish garnet zones are chemically not dissimilar to semipelitic metasediments. The same is clearly true of the reaction zones at Garry-a-Siar, and is in the same way caused by the large opposing fluxes of K on the one hand and Ca and Na on the other, with relatively smaller fluxes in Al.

In Figure 5.20, the reaction zone compositions from Garry-a-Siar have been projected into the compositional system $(CaO + Na_2O) - K_2O - (Fe_2O_3 + MgO)$. All phases coexist with quartz, and tie-lines can be drawn between plagioclase and each of the phases magnetite, biotite and hornblende, to give two- (with quartz, effectively three-) phase assemblages. All equilibrium assemblages observed lie on one or other of the tie-lines. The chemical compositions of GS1-9 lie, as expected, on or near to the tie-lines, errors being attributable to the hybrid nature of the samples. Also shown in Figure 5.20 are the approximate locations in this projection of a wide range of typical basaltic and granitic rocks. The reaction zone compositions fall well away from the area directly between the basalt and granite fields, the direction of apparent deflection indicating extensive loss of the components CaO and NaO. The conservation of mass requires the existence of a volume of material which would plot somewhere near the plagioclase-biotite tieline close to the CN apex. Plotted in the





a. Shaded areas represent compositions of common basic(left) and granitic(right) rocks. Filled triangles: matrix composition estimates for metabasic rock (M_a), reaction zone near metabasic boundary (M_{b1}) and near pegmatite (M_{b2}). Numbered open triangles refer to analyses in Table 5.6.

b. Squares - Leenish reaction zones; triangles - analyses in Table 5.6, Garry-a-Siar.
as - aluminium silicate, st - staurolite, ctd - chloritoid, crd - cordierite, gt - garnet.

5.20 Reaction zone compositions plotted in the systems CN-K-FM and AKFM

system AKFM (Thompson, 1957) the reaction zone compositions are clearly too poor in the A-component to contain an Al_2SiO_5 polymorph (Figure 5.20b).

The mineral assemblages found in the reaction zones merit some comment. They generally contain few phases, a feature of many metasomatic rocks (Thompson, 1959), except where polymetamorphism is evident. At Garry-a-Siar, only one ferromagnesian phase is ever present in any assemblage. However, the mineral phases typical of these zones formed between acid and basic rocks (garnet, plagioclase, biotite and hypersthene) are all solid solution phases. In calc-silicate rocks and in black-wall zones around ultramafic rocks, monomineralic zones often form, typically in complex series across which steady compositional variation is observed. In the examples seen here, only one zone is formed at any time, despite the internal complexity it shows at Garry-a-Siar. The solid-solution phases seen here are also characteristic of regional metabasic rocks (of which the host rocks are effectively examples), and perhaps in the same way that regional metabasic assemblages are characterised by continuous reactions in response to changing grade, without the sequences of mineral zones typical of pelitic and calcareous metamorphic rocks, these phases are able to accommodate variations of component fluxes without discontinuous reactions occurring other than at zone boundaries. It could however be argued that at Garry-a-Siar two zones are present, showing planar and spherical geometry respectively.

In relation to Lewisian geology, it may finally be noted that the association metabasite-metasediment has been found in many areas of the Lewisian basement (Coward et al., 1969). While occurrences such as the largest, in South Harris, seem clearly to be instances of the intrusion of basic igneous rocks into metasediments with subsequent deformation, the reaction zones described here show a similar compositional sequence. It is possible that some minor Lewisian 'brown schists' may be older and deformed equivalents of the reaction zones at Leenish and Garry-a-Siar.

CHAPTER 6

DISCUSSION AND CONCLUSIONS

6.1 THE PROBLEM OF THE GRANITE AND PEGMATITE SOURCE

6.1.1 GEOCHEMICAL AND MINERALOGICAL EVIDENCE

The conclusions reached (within the limitations of the type of evidence used) in Chapters 3-5, can be summarised:

a. GEOCHEMISTRY.

The origin of the Laxfordian granites can perhaps be defined reasonably clearly only in the case of the Laxford sheets, which may represent deep-crustal magmas formed by the melting of granulite-facies rocks. In contrast, the Outer Hebrides granites show abundant evidence that the possible influence upon their composition of crystal-liquid equilibria in a source region may have been extensively masked by some combination of restite material retention, crystal fractionation or reaction/assimilation. Ominously for the more general question of granite genesis, this latter group of rocks shows geochemical characteristics, particularly in trace-element concentrations, which are not dissimilar to many other occurrences of granites *sensu stricto*.

Certain groups of pegmatites clearly were evolved from the granites, presumably at a late stage under water-saturated conditions, and their geochemistry shows rational relationships with the compositions of the granites from which they were derived; contrasts between those associated with the Laxford granite sheets on the one hand, and the Outer Hebrides granites on the other can be explained in terms of the contrasts between the two groups of granites and the processes of late-stage crystallisation (see Chapter 3).

Many other Laxfordian pegmatites show no clear affinity with the granites, and many are spatially far removed from them. A recurring feature is very low concentrations of Ba and Sr, and often very high Rb, taking to an extreme the similar patterns of partitioning of these elements observed in the granite-derived pegmatites.

The Late Scourian pegmatites, on the other hand, show almost a reverse pattern, with spectacular levels of Ba and Sr and low Rb providing an analogy with aspects of the geochemistry of the much younger Laxford granites.

b. MINERALOGY.

The common mineral assemblage quartz-alkali feldspar-plagioclase-biotite-magnetite has been used to provide rough estimates of temperature and oxygen fugacity, and

even more approximate estimates of f_{H_2O} of crystallisation. The methods used and the uncertainty of equilibration were discussed in Chapter 4. However, relative indications of high T-f_{O_2} conditions preserved in the late Scourian pegmatites are consistent with textural evidence (perthites of ternary bulk composition), and suggest contrasting conditions for the pegmatites formed in Laxfordian times; in many of these later pegmatites, the mineral assemblage above is replaced or succeeded by quartz-albite-richer plagioclase-muscovite-garnet, suggesting their evolution to lower temperatures and a strong departure from the probable T-f_{O_2} conditions of the QFM buffer implied by the earlier assemblage. The evolution of fluids in these hydrous, low temperature bodies is further discussed in relation to the pegmatite environment in section 6.1.3.

6.1.2 STRUCTURAL EVIDENCE

The structural development of the Lewisian was outlined in Chapter 1, and the relationship between this structure and granite and pegmatite emplacement summarised in Chapter 2.

The location of all the Laxfordian granites in or near to major interfaces between gneiss terrains of contrasting metamorphic state might indicate the importance of deep-seated shear zones (a) in transporting granite magmas to a high crustal level and (b) possibly in the

melting process itself, for example by juxtaposing relatively hotter and cooler crustal segments, or even by bringing together crustal and mantle rocks.

If such a major shear zone is present in South Harris, its surface expression is unclear, perhaps providing the cause of the diffuse pattern of granite sheet emplacement in Harris and Lewis. An apparently less efficient transport path for these granites might be related to the evidence for their shallow-level evolution, as might their emplacement into amphibolite-facies rocks containing alkali feldspar.

A deep source seems unlikely for the pegmatites. Their concentration in zones of low Laxfordian strain is consistent with relatively local generation. The crucial questions about these pegmatites - their relative age in the Laxfordian cycle and the related question of the thermal state of the grey gneisses at that time - are at present unresolved, although mineralogical evidence indicates a relatively low temperature of crystallisation. Coward (1969) identified a late migmatite metamorphism (restricted mainly to E. South Uist) which postdated the main (F_3) Laxfordian folds, while Myers (1968) has also postulated a relatively late stage of mobilisation in N.W. Harris and northern South Harris. It must be said that the mineral assemblages characteristic of the Harris granites and their host rocks (with which they appear to have equilibrated during emplacement) indicate ambient conditions characteristic of the epidote-amphibolite facies,

apparently ruling out melting in the grey gneisses. Although the thermal response of the Lewisian gneisses to a metamorphic event would probably be heterogeneous (especially since the absence of potentially-convecting fluids would reduce heat transport in the granulites), the existence of a source zone of mobilised rocks at the same time as lower-amphibolite emplacement zones suggests temperature gradients which would be difficult to achieve.

Thus it is apparent that, while the influence of structural heterogeneity upon the distribution of the rocks discussed here is clear, detailed knowledge of the Laxfordian structural and intrusive sequence (i.e. the age of the pegmatites relative to the granites) is insufficient to define the thermal regime in which the pegmatites originated.

6.1.3 THE PEGMATITE ENVIRONMENT

The feature common to most models of pegmatite evolution is the presence of abundant water, probably involving a hydrous fluid phase. Experimental investigations into this unusual environment have not so far been successful (see comments of Burnham, 1967,p.49; Luth, 1976), so that discussion of vapour phase/liquid relations is bound to be essentially qualitative. The approach adopted in this discussion is (a) to examine

models of pegmatite formation both in the presence and absence of cogenetic granites, (b) to attempt to relate such features of the fluids associated with Lewisian pegmatites as can be deduced from the evidence of Chapters 3-5 with what is known of pegmatite behaviour.

(a) MODELS OF PEGMATITE EVOLUTION

The comprehensive model of Jahns and Burnham (1969) envisages the magmatic generation of a pegmatite liquid/fluid, either by late crystallisation leading to water-saturation and resurgent boiling in granitic magmas, or by the production of minor amounts of hydrous magmas by anatectic melting of crustal rocks. The possible range of pathways leading to a variety of pegmatitic and aplitic products is summarised in Figure 6a. In Figure 6b and 6c, paths are traced for contrasting Laxfordian acid rocks, based upon the interpretations given in Chapters 3-5. The Laxford granite/pegmatite association represents a sequence in which pegmatites evolve from a pre-existing and volumetrically dominant granitic magma, while the large Gary-a-Siar pegmatite may have originated as a hydrous pegmatitic melt. Given only the assumption that a silicate liquid was at some stage present in the Gary-a-Siar pegmatite, the very distinct products of the two examples chosen lead to quite different sequences of processes. Although consideration of Figure 6a might suggest alternative details, the essential difference

Fig 6.1 (from Jahns and Burnham, 1969)

a. A model for the generation of granite pegmatites.

b. Possible evolution of the Laxfordian granites and associated pegmatites.

c. Possible evolution of the large pegmatite at Garry-a-Siar

A Mechanical emplacement of magma or rest magma containing some water.

B Segregation of water-bearing rest magma within a crystallising igneous body.

C Partial melting of crustal material in situ and in the presence of some water.

D Crystallisation of anhydrous minerals, with or without reaction between solid phases and silicate melt, +process A or B.

E Crystallisation of anhydrous minerals, with or without reaction between solid phases and silicate melt.

F Reduction in total confining pressure on the system.

G "Osmotic" separaration of water from the silicate melt.

H Partial escape of aqueous fluid from the host body of silicate melt, with movement of materials by and through the free phase.

I Marked reduction in total confing pressure on the system, with attendant "quench" crystallisation.

J Crystallisation from silicate melt and aqueous fluid, with or without reaction between the solid and fluid phases, + process A.

K Partitioning of nonvolatile constituents between silicate melt and increasing amounts of aqueous fluid, with diffusion of materials along concentration gradients, especially in the aqueous phase; crystallisation from both fluid phases, segregation of solid products according to amount and degree of interconnection of the aqueous fluid, and reaction between solid phases and the fluid phases.

L Crystallisation from aqueous fluid or fluids (and possibly, in rare instances, from some residual melt), with reaction among solid and fluid phases, exsolution of solid phases with diffusive transfer of materials over a wide range of scales, and development of mineral assemblages stable at relatively low temperatures.

X Crystallisation from silicate melt, with or without reaction between the solid phases and liquid, followed in late or very late stages by K or K and L.

The final products, which are interrelated and commonly intergradational, can be identified as follows:

I - Pegmatite, hybrid rocks with pegmatitic material, mineral impregnations, and other products of metasomatism in country rocks.

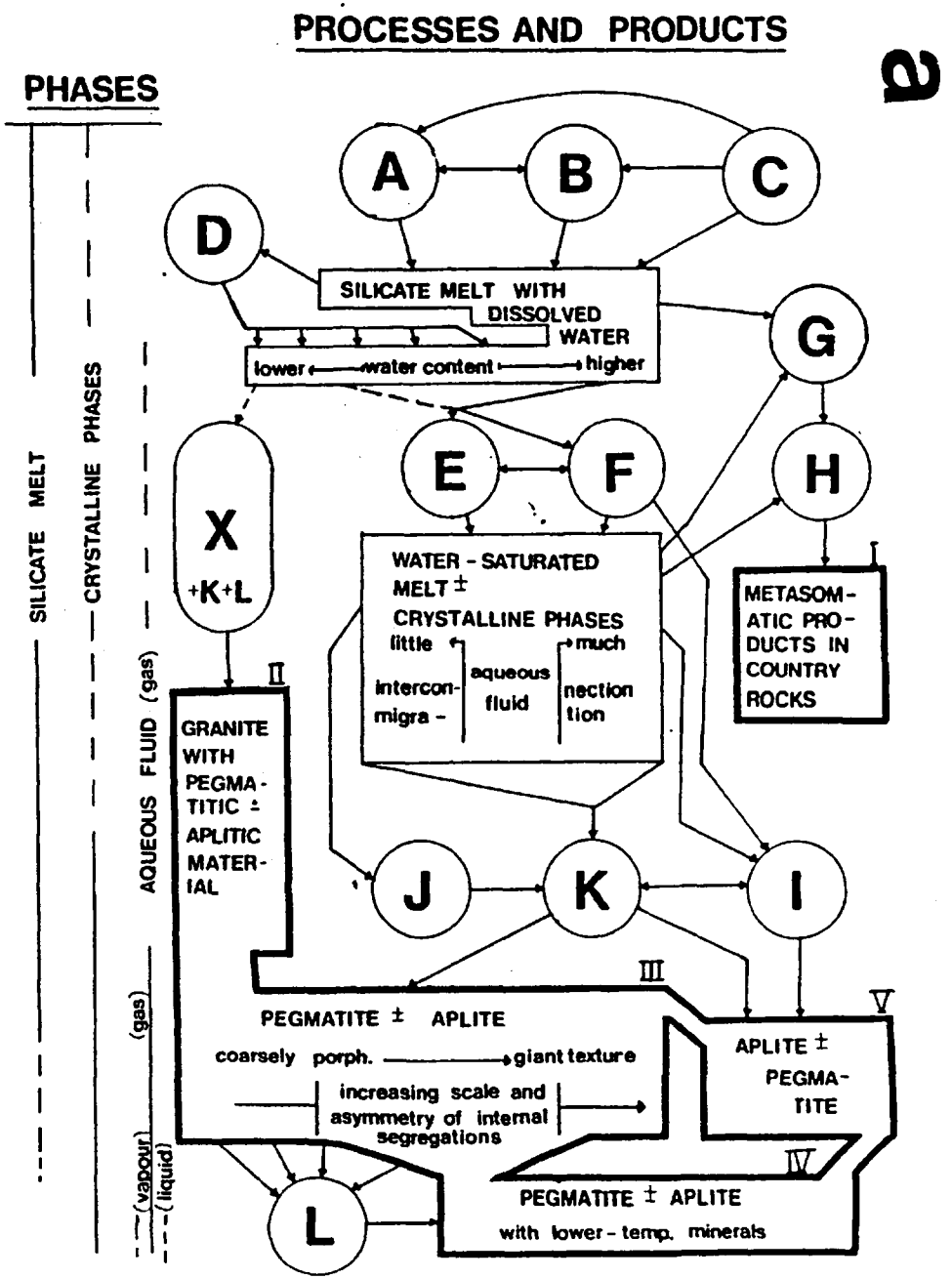
II- Granite with miaroles, small amounts of autoinjection pegmatite, interstitial aplitic material, or interstitial analogues of final reaction and replacement products of process L.

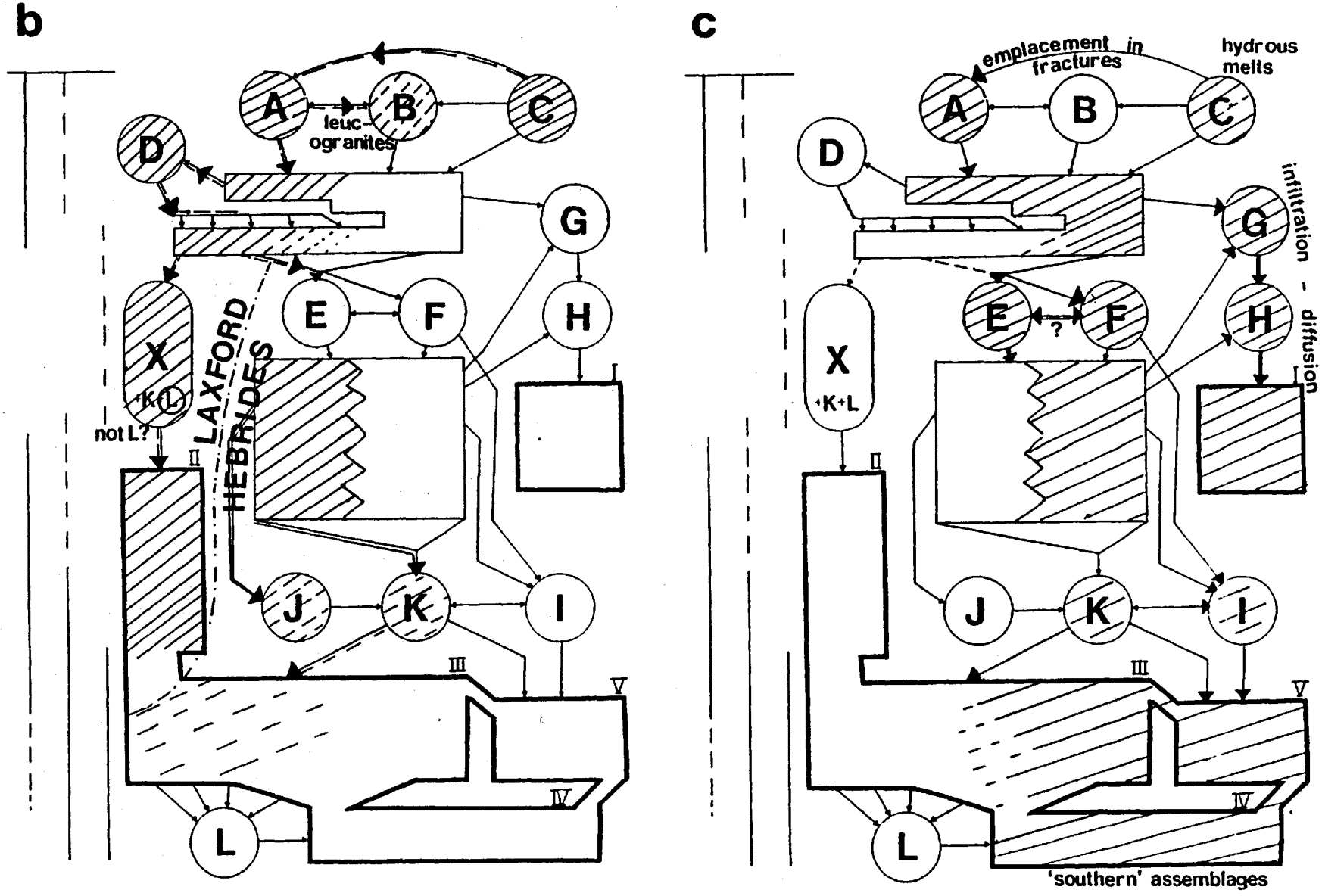
III - Pegmatite with or without aplite, the following spectrum of rock types in general representing a range from relatively small to relatively large amounts of aqueous fluid in the systems:

1. Very coarsely porphyritic pegmatite, granite or aplite or combinations thereof.
2. Pegmatite with clusters, pods and lenses of very coarse-grained to giant-textured mater
3. Pegmatite with marked distribution of minerals, generally with sodic, fine-grained to aplitic groundmass costituents.
4. Pegmatite with markedly asymmetric zonal distribution of minerals, commonly with well-defined masses of sodic aplite.

IV - Pegmatites and pegmatitic rocks as III above, but with more abundant and widespread features ascribable to corrosion and mineral replacement, together with hydrothermal minerals formed at relatively low temperatures.

V - Aplite, with or without masses of pegmatite.




b
A
B
C
leuc-
ogranites
D
G
E
F
H
X
+K+L
not L?
LAXFORD
HEBRIDES
I
J
K
L
II
III
IV
V
c
emplacement in
fractures
hydrous
melts
infiltration - diffusion
?
'southern' assemblages

between the two derived evolutionary models lies in the amount of water or hydrous vapour available at any time. On the whole 'more-hydrous' processes lie on the right-hand side of Figure 6a, and the relative 'right-handedness' of the Garry-a-Siar sequence at all stages is very clear. A number of points are suggested by the comparison:

(i) The consistent contrast in apparent water-content throughout the sequences may suggest that a more- (or less-) hydrous pattern is set at an early stage. In the case of the Laxford granites this less-hydrous trend may reflect the relatively anhydrous nature of the granulites from which these granites are proposed to have been derived, while the Garry-a-Siar body may have been derived from amphibolite-facies rocks containing both hydrous minerals and an intergranular fluid phase.

(ii) In neither case do processes such as B, involving segregation and concentration of water, need to play an important part. Figures 6b and c suggest that the evolution of a water-poor granitic magma or a hydrous magma would in both cases be quite rapid, in contrast to conceptually-"gradual" segregation favoured clearly by Jahns and Burnham (1969) and Burnham (1967) and perhaps more applicable to large granitic plutons rather than the thin sheets examined here. However, this is a question of

relative stress, and it should be noted that only very large pegmatite bodies in general show a variety of sequential phenomena, suggesting increasing "gradualism" with volume.

(iii) Comments (i) and (ii) may be combined by suggesting that in examining Lewisian acid rocks, the question of "available water" for magma saturation is of greater importance than models such as that of Burnham (1974) which concentrates upon water solubility in magmas in a predictive way. Such models predict only maximum water-contents, which may not be achievable in basement rocks.

(iv) Jahns and Burnham's model takes no account of the possible effect of metasomatic exchange between granitic rocks and country rocks, i.e. processes G and H are "one-way". At Garry-a-Siar at least, some influence on the evolution of the pegmatite can be seen in the apparent marginal growth of abundant plagioclase. However, the position of G and H on the far right of the diagram (as with the evolution of lower-temperature minerals, at bottom, Figure 6a) is consistent with observations in Chapters 3-5. The Outer Hebrides granites might follow an intermediate path involving a more-hydrous magma and larger amounts of aqueous fluid than those

available at Loch Laxford, allowing the crystallisation of cogenetic pegmatites from an aqueous-fluid-dominated environment.

Gresens (1967) has proposed a model for pegmatite generation without the participation of a magmatic phase, in which an alkali chloride solution acts as a fluid medium with which, alternatively, white mica and feldspars may be in equilibrium at high and low pressures respectively. Migration of such a fluid into low-pressure zones (tectonically generated by fissure-dilation) would result in alkali feldspar crystallisation in those zones, followed, with pressure equalisation, by late muscovite replacement of feldspars. These features are commonly observed in migmatitic segregations in metamorphic terrains (Bradbury, 1979; Ashworth, 1979) and provide a satisfactory working model for the production of some migmatites at temperatures below the water-saturated granite solidus (Bradbury, 1979). Muscovite-alkali feldspar relationships can be observed in the South Harris pegmatites, and muscovite clearly replaces alkali feldspar as a member of a succeeding paragenesis. Muscovite only replaces biotite by reaction. In addition, muscovite-bearing assemblages are precipitated as primary assemblages in dilating fissures, so that pressure increase or equalisation cannot be invoked to explain the presence of this mineral. Clearly, phengitic muscovite is a late, low-temperature pegmatite mineral,

and the successive parageneses in South Harris and elsewhere are related to fluid compositional evolution with falling temperature. The role of dilation-induced pressure gradients is limited to providing the driving force for emplacement.

Thus the writer considers that the involvement of a silicate liquid at some stage in the histories of all the Laxfordian acid rocks is probably inevitable; the generation of such liquids may have been simultaneous with the evolution of a silicate-rich aqueous phase in most of the pegmatites.

(b) AQUEOUS PHASE COMPOSITION AND LAXFORDIAN PEGMATITES

The composition of an aqueous phase in equilibrium with granite liquid and/or crystals has been experimentally investigated by Burnham (1967). Burnham's conclusions are:

"1. The total solute content ranges from 0.65 weight percent at 20Kbar and 500°C to 9.2 percent at 10Kbar and 650°C.

2. The proportion of normative quartz (Q) is highest at low pressures and high temperatures, and lowest at high pressures and high temperatures.

3. The concentration ratio of normative orthoclase (Or) to orthoclase plus albite (Ab) in the aqueous phase is nearly the same as in the

coexisting condensed phases (crystals and/or liquid), except at pressures near 10Kbar where the ratio decreases somewhat.

4. Normative albite (Ab) + orthoclase (Or) + quartz (Q) exceeds 96 percent of the total solute in every case, as compared with 94.2 percent for the starting material."

The first point establishes falling temperatures and pressures (for example with transport down a pressure gradient into a dilating fissure) as causing oversaturation of the aqueous phase with respect to silicate components. Reasonable physical conditions for granite and aqueous phase equilibration might lie somewhere halfway between the reported pressures and temperatures, suggesting silicate content in the aqueous phase to lie somewhere in the order of 4-5 weight percent. Condensation of this material alone to produce large pegmatites implies the evolution of very large volumes of aqueous fluid. This problem would be reduced if a vapour-rich silicate liquid coexisted with the aqueous phase, as Jahns and Burnham (1969) suggest.

Point 2 provides a mechanism for the origin of quartz-rich pegmatite cores, found commonly in otherwise granitic pegmatites. The remaining points suggest that, in terms of normative granite components (Or, Ab, Q), the aqueous phase differs little from the crystals and/or

liquid with which it equilibrates, except at pressures near 10 Kbar, which are probably not realistic in the Laxfordian at exposed levels. The observation in Chapter 3 that granites with a higher Ab/(Or + Ab) ratio are associated with pegmatites in which that ratio is even higher (the Laxford granites) while those (the Outer Hebrides granites) with a lower Ab/(Or + Ab) ratio show the reverse, i.e. extremely Or-rich pegmatites, apparently contradicts these observations unless, on its formation, the pegmatite-precipitating medium, be it liquid or fluid, equilibrated selectively with liquid rather than crystals.

Volatiles other than water may well be present in an evolving granite system, notably CO_2, F and Cl. F tends to partition selectively into crystals or liquids relative to a vapour phase (Burnham, 1967) but the influence of CO_2 and Cl may be considerable, CO_2 tending to lower the solubility of all granite components, but especially alkalis, whereas Cl tends to increase alkali solubilities. The apparently-opposite effects of these two volatiles makes their relative influence difficult to assess. Remaining fluids in granulite-facies rocks are known to be CO_2-rich, but this need not be the case for amphibolite-facies rocks.

It has already been suggested that the increasing influence of an aqueous vapour phase is reflected strongly in the concentrations of several trace elements in pegmatites. Ba, Sr and REE seem to partition very poorly

into the aqueous phase, so that products condensed from this medium are poor in these elements, while Rb, K and Nb appear to be concentrated in fluids. Not only the pegmatite compositions from South Harris (Chapter 3) but also the inferred composition of the fluid phase involved in the metasomatic reaction at Garry-a-Siar support this view. It is suggested that these elements can be used to monitor the relative importance of a silicate-rich aqueous phase as against that of a silicate liquid. Arguments that rare-earth elements are 'complexed' and transported easily by a vapour phase (e.g. Mineyev, 1960), and used to explain low REE concentrations in supposedly igneous end-stage pegmatites seem unnecessary, and probably underestimate the influence of the aqueous vapour as an important pegmatite-crystallising medium.

(c) THE SCOURIAN PEGMATITES

Generation of an acid magma by local partial melting of gneisses and intrusion into reactivated shear zones presents a much less serious thermal problem in the case of the late Scourian pegmatites, which evidently crystallised at temperatures above 650°C and perhaps as high as 800°C.

In relation to the preceding arguments about the Laxfordian igneous rocks, it can be seen that evidence for the dominant role of an aqueous vapour phase in the formation of these pegmatites is lacking, and their high concentrations of Ba, Sr and REE (Chapter 4) indicate

the important influence of a granite liquid. That this liquid was probably water rich is suggested both by the calculations of F_{H_2O} in Chapter 4, and by the presence of giant textures, a feature possibly highly reliant on rapid chemical transport in a hydrous or water-saturated medium.

Using the Jahns-Burnham model, the evolutionary path of the Late Scourian pegmatites differs little from that of the Laxford granites, although a stage of granite formation is absent, possibly reflecting a more hydrous magma resulting from an initially-small volume of melt.

The geochemical similarities between the Late Scourian pegmatites and the Laxford granites, specifically high Ba, Sr and REE, and relatively low Rb and K, are likely to reflect their common origin in the granulite facies gneisses, but these similarities do not extend to major-element feldspar compositions, nor probably to bulk compositions. The Late Scourian pegmatites contain a more basic oligoclase and a ternary alkali feldspar, and must contain higher normative anorthite (An) than the Laxford granites. Details of feldspar composition indicate relatively lower temperatures of equilibration in the Laxford granites (Chapter 4), in agreement with geological observation (Chapter 2). Bulk compositions, however, may reflect relatively lower-pressure melt compositions for the Late Scourian pegmatites. The evolution of these pegmatites of high temperatures and

low pressures soon after the end of Scourian granulite-facies metamorphism would tend to contradict the conclusions of O'Hara (1977) regarding the evolution of the Scourie granulites, which were suggested by O'Hara to have cooled more rapidly than they were uplifted. Rapid uplift from at least 30-40 km (Savage and Sills, 1980) to fairly moderate depths under relatively isothermal conditions might be more consistent with models of amphibolite facies/granulite facies relationships like those of Beach et al. (1974) and Graham (1980) which concentrate upon thrust tectonics, rather than the more gentle process of erosional uplift and cooling envisaged by O'Hara (1977).

6.2 CONCLUSIONS

The overall conclusions of this study will be presented in the form of a relatively simple model for Lewisian granite and pegmatite evolution in relation to which a series of complicating factors and their likely influence will be considered.

It is proposed that all or most Lewisian acid intrusions originated in a more ductile and probably hotter environment than that in which they subsequently froze or were precipitated. A water-bearing silicate magma or a silicate-rich aqueous phase, or most probably in many cases some combination of both, was generated in the former environment, and migrated into the latter,

driven by dilation-induced pressure gradients or by intrinsic buoyancy.

Such a general model can be applied on a range of scales, which, with examples, may be:

a. Deep-crustal melting to generate granitic to granodioritic liquids which were then transported up the major Laxford shear zone and emplaced at a high level as the Laxford granite sheets. Scale of the order of 10^4m.

b. Combined ductile and brittle response to Laxfordian (and late Scourian ?) metamorphism in the heterogeneous Lewisian gneisses. Generation of combined hydrous magmas and silicate-rich fluids in ductile, hot regions and their intrusion into reactivated early shear zones to form the widespread Laxfordian pegmatites. Scale order: 10^2m

c. Fracturing of largely-crystalline, ductilely-deforming granite sheets (in response to irregularly-varying strain rates during intrusion ?) and migration into the fractures of fluid-rich liquids or fluids only, precipitating small cogenetic pegmatites in the Laxfordian granites. Continued deformation of these pegmatites to form noded or ptygmatic intrusions. Scale order: 0-10m

This type of process, operating on all these scales, was associated with a chemically-varied range of products whose ultimate composition was a combined function of source rock geochemistry and the relative influence of aqueous or liquid phases upon their evolution, the latter influence itself probably being a function of source rock water availability (see previous section). Extremes of composition are represented by the Laxford granites and late Scourian pegmatites on the one hand, and the Southern-type Laxfordian pegmatites on the other, and these extremes relate to contrasted sources and evolutionary paths.

Two further types of process need to be brought into this discussion: (a) the influence of cumulus crystallisation and (b) metasomatism.

a. Cumulus crystallisation. Cumulus effects in the Laxfordian granites were discussed in Chapter 3, where it was suggested they provided the key to the geochemical differences between mela- and leuco-granites, and (in the case of the Laxford granite sheets) this influence was apparent within the melagranites, producing an increasing negative Eu anomaly with increasing silica, and an overall drop in REE total amounts as a result of accessory mineral crystallisation. Discussion of crystal/liquid/vapour phase equilibrium in order to define the geochemical evolution of pegmatites is affected if crystalline phases are relatively refractory with respect to some elements.

In the case of the Laxford granites, cumulus crystallisation of accessory minerals (REE) and plagioclase (Ba, Sr) may have made these elements unavailable for incorporation into pegmatites unless vapour/crystal equilibration was continuous.

In a similar way, the precipitation of crystals from a hydrous pegmatite-generating medium is a cumulus effect, and the evidence about the nature of the aqueous phase obtained by analysing the crystalline phases is indirect. Although qualitative statements can be made about geochemical partitioning, the relative role of cumulus crystallisation depends on quantitative knowledge of rates of diffusive transport in crystals (slowest), hydrous silicate liquids and silicate-rich aqueous phases (fastest), as well as an understanding of the much greater potential for rapid physical transport of the low-viscosity (7-14 orders of magnitude lower than that of acid silicate liquids (Franck, 1961)) aqueous vapour phase.

b. Metasomatism. Reaction between acid and basic rocks was shown (Chapter 5) to result in large fluxes of K and Ca over a large range of temperatures, resulting in the formation of marginal reaction zones of unusual composition. The example studied at Garry-a-Siar, Benbecula, evidently involved the imposition of a pegmatite-derived fluid phase, as an infiltration mechanism controlled partly by rock porosity and tortuosity, and driven by a pegmatite-country rock fluid pressure gradient,

with subsequent (mainly) diffusive exchange of chemical components, whose transport was controlled both by chemical potential gradients in the fluid, and also (especially in the case of trace components) by element partition coefficients of phases stable in the reaction zones.

Metasomatism as observed occurs on a larger scale than could reasonably be expected by diffusive mass transfer alone, and the assessment of its importance to large granite intrusions depends on the limits to this scale, and also to the relative sense of element transport. Clearly, at Garry-a-Siar, the effect of metasomatism is to transfer Ba and Sr into the pegmatite, reversing the expected evolutionary trend suggested in the previous section.

In relation to the Southern-type pegmatites, metasomatism could be responsible for the falling of the aqueous phase, but falling temperature (Chapter 4) would tend to produce the same sequence of mineral assemblages. The apparent preferential location of these pegmatites in the South Harris metasedimentary belts may provide some grounds for suspecting metasomatic reaction, although, again, tectonic arguments in favour of this form of localisation of these bodies could also be involved.

A similar dilemma occurs when the evolution of the Harris granites is considered. Metasomatic reaction and perhaps some assimilation of the most acid gneisses, if it

took place on a sufficient scale, could completely mask any evidence about the ultimate origin of these rocks. The isotopic evidence of Van Breemen et al. (1971) may suggest (by an apparently-variable initial $^{87}Sr:^{86}Sr$ ratio) a heterogeneous source in the crust or upper mantle, but it may also indicate selective contamination and/or melting of the heterogeneous grey gneisses now intruded by the granites.

Evidence for xenolith assimilation and reaction is observed in the Harris granites (though, as with metasomatic reaction zones in the pegmatites, not commonly), and the major imponderable is the extent of this process. Ultimately, the granites are the products of crystal/liquid and crystal/liquid/aqueous-phase equilibria, whatever the range of sources from which they are derived, and Bowen's (1928) conclusion about the influence of assimilation upon crystal/liquid evolution remains incontestable: "All of these actions are, however, an emphasizing of normal processes possible in the absence of foreign matter. It is doubtful whether the presence of foreign matter is ever essential to the production of any particular type of differentiate."

It could be added, given the advances made in geochemistry since 1928, that isotope geochemistry has not resolved problems of this nature, and the extent and mechanism of crustal involvement in granite petrogenesis remains contentious.

Abbey, S., 1973:
Studies in "standard samples" of silicate rocks and minerals. Geol. Surv. Canada Pap., 73-36, 25 pp.

Arth, J.G., and Hanson, G.H., 1975:
Geochemistry and origin of the early Precambrian crust of northeastern Minnesota. Geochim. et Cosmochim. Acta, 39, 325-362.

Ashworth, J.R., 1979:
Textural and mineralogical evolution of migmatites. In Harris, A.L., Holland, C.H. and Leake, B.E. (Eds.) The Caledonides of the British Isles - reviewed. Scottish Academic Press.

Atherton, M.P., 1976:
Crystal growth models in metamorphic tectonites. Phil. Trans. Roy. Soc. Lond., 283, 255-270.

Beach, A., 1974:
The measurement and significance of displacements on Laxfordian shear zones, north-west Scotland. Proc. Geol. Ass., 85, 13-21.

Beach, A., 1976:
The interrelations of fluid transport, deformation, geochemistry and heat flow in early Protozoic shear zones in the Lewisian complex. Phil. Trans. Roy. Soc., A 280, 569-604.

Beach, A., Coward, M.P., and Graham, R.H., 1974:
An interpretation of the structural evolution of the Laxford Front, North-West Scotland. Scott. J. Geol., 9, 297-308.

Bikerman, M., Bowes, D.R., and Breemen, O. van, 1975:
Rb-Sr whole rock isotope studies of Lewisian metasediments and gneisses in the Loch Maree region, Ross-shire. J. Geol. Soc. Lond., 131, 237-69.

Borley, G.D., and Frost, M.T., 1963:
Some observations on igneous ferrohastingsites. Min. Mag., 33, 646-662.

Bowen, N.L., 1928:
The evolution of the igneous rocks. Princeton University Press.

Bowes, D.R., 1969:
The Lewisian of north-west Highlands of Scotland. In M. Kay (Ed.) North Atlantic geology and continental drift, a symposium. Mem. Am. Ass. Petrol. Geol., 12, 575-94.

Bowes, D.R., and Khoury, S.G., 1965:
Successive periods of basic dyke emplacement in the Lewisian Complex, south of Scourie, Sutherland. Scott. J. Geol., 1, 295-99.

Bradbury, H.J., 1979:
Migmatisation, deformation and porphyroblast growth in the Dalradian of Tayside, Scotland. In Harris, A.L., Holland, C.H., and Leake, B.E. (Eds.). The Caledonides of the British Isles - reviewed. Scottish Academic Press.

Brady, J.B., 1975:
Reference frames and diffusion coefficients. Amer. J. Sci., 275, 954-983.

Brady, J.B., 1977:
Metasomatic zones in metamorphic rocks. Geochim. et Cosmochim. Acta, 41, 113-125.

Breemen, O. van, Margaret Aftalion, and Pidgeon, R.T., 1971:
The age of the granitic injection complex of Harris, Outer Hebrides. Scott. J. Geol., 7, 139-152.

Brock, K.J., 1972:
Genesis of Garnet Hill skarn, Calaveras County, California. Bull. Geol. Soc. Am., 83, 3391-3404.

Buddington, A.F., and Lindsley, D.H., 1964:
Fe-Ti Oxide minerals and synthetic equivalents. Jour. Petrol., 5, 310-357.

Buma, G., Frey, F.A., and Wones, D.R., 1971:
New England granites: trace element evidence regarding their origin and differentiation. Contrib. Miner. Petrol., 31, 300-320.

Burnham, C.W., 1967:
Hydrothermal fluids at the magmatic stage. In Barnes, H.L. (Ed.). Geochemistry of hydrothermal ore deposits. Holt, Rinehart and Winston.

Carmichael, D.M., 1969:
On the mechanism of prograde metamorphic reactions in quartz-bearing pelitic rocks. Contrib. Miner. Petrol., 20, 244-267.

Carmichael, I.S.E., 1967:
The iron-titanium oxides of salic volcanic rocks and their associated ferromagnesian silicates.
Contrib. Miner. Petrol., 14, 36-49.

Carmichael, I.S.E., and Nicholls, J., 1967:
Iron-titanium oxides and oxygen fugacites in volcanic rocks. J. Geophys. Res., 72, 4665-4687.

Carmichael, I.S.E., Turner, F.J., and Verhoogen, J., 1974:
Igneous Petrology. McGraw Hill.

Chapman, H.J., 1979:
2390 M.yr. Rb-Sr whole-rock isochron for the Scourie dykes of N.W. Scotland. Nature, 277, 642.

Chapman, H.J., and Moorbath, S., 1977:
Lead isotope measurements from the oldest recognised Lewisian gneisses of north-west Scotland.
Nature, 268, 41-42.

Chappell, B.W., and White, A.J.R., 1974:
Two contrasting granite types. Pac. Geol., 8, 173-174.

Compton, P., 1978:
Rare-earth evidence for the origin of the Nuk gneisses, Buksefjorden region, southern West Greenland.
Contrib. Miner. Petrol., 66, 283-293.

Coward, M.P., 1969:
The structural and metamorphic geology of South Uist, Outer Hebrides. Unpublished Ph.D. thesis, Univ. of London.

Coward, M.P., Francis, P.W., Graham, R.H., Myers, J.S., and Watson, J.V., 1969:
Remnants of an early metasedimentary assemblage in the Lewisian complex of the Outer Hebrides. Proc. Geol. Ass., 80, 387-408.

Coward, M.P., Francis, P.W., Graham R.H. and Watson, J.V., 1970:
Large-scale Laxfordian structures of the Outer Hebrides in relation to those of the Scottish Mainland.
Tectonophysics, 10, 425-435.

Curtis, C.D., and Brown, P.E., 1969:
The metasomatic development of zoned ultrabasic bodies in Unst, Shetland. Contrib. Miner. Petrol., 24, 275-292.

Davies, F.B., 1976:
Early Scourian structures in the Scourie-Laxford region and their bearing on the evolution of the Laxford Front. J. Geol. Soc. Lond., 132, 543-554.

Dearnley, R., 1962:
An outline of the Lewisian Complex of the Outer Hebrides in relation to that of the Scottish Mainland. J. Geol. Soc. Lond., 118, 143-166.

Dearnley, R., 1973:
Scourie dykes of the Outer Hebrides. In, Poole, R.G., and Tarney, J. (Eds.), The early Precambrian of Scotland and related rocks of Greenland. Univ. of Birmingham Press.

Dearnley, R., and Dunning, F.W., 1968:
Metamorphosed and deformed pegmatites and basic dykes in the Lewisian Complex of the Outer Hebrides and their geological significance. J. Geol. Soc. Lond., 123, 335-378.

Dickinson, B.B., and Watson, J.V., 1976:
Variations in crustal level and geothermal gradient during the evolution of the Lewisian complex of northwest Scotland. Precamb. Res., 3, 363-374.

Drake, M.J., and Weill, D.F., 1974:
Partition of Sr, Ba, Ca, Y, Eu^{2+}, Eu^{3+}, and other REE between plagioclase feldspar and magmatic liquid: an experimental study. Geochim. et Cosmochim. Acta, 39, 689-712.

Eugster, H.P., 1970:
Thermal and ionic equilibria among muscovite, K-feldspar and aluminosilicate assemblages. Fortschr. Miner., 47, 106-123.

Eugster, H.P., 1977:
Compositions and thermodynamics of metamorphic solutions. In Fraser, D.G. (Ed.), Thermodynamics in geology. Reidel.

Evans, C.R., and Tarney, J., 1964:
Isotopic ages of Assynt dykes. Nature, 204, 638-641.

Evans, C.R., and Lambert, R. St.J., 1973:
The Lewisian of Lochinver, Sutherland; the type area for the Inverian metamorphism. J. Geol. Soc. Lond., 130, 125-50.

Ferry, J.M., and Spear, F.S., 1978:
Experimental calibration of the partitioning of Fe and Mg between biotite and garnet. Contrib. Miner. Petrol., 66, 113-117.

Fettes, D.J., Graham, C.M., Sassi, F.P., and Scolari, A., 1976:
The basal spacing of potassic white mica and facies series variation across the Caledonides. Scott. J. Geol., 12, 227-236.

Fisher, G.W., 1970:
The application of ionic equilibria to metamorphic differentiation: an example. Contrib. Miner. Petrol., 29, 91-103.

Fisher, G.W., 1973:
Non-equilibrium thermodynamics as a model for diffusion-controlled metamorphic processes. Amer. J. Sci., 273, 897-924.

Fisher, G.W., 1977:
Nonequilibrium thermodynamics in metamorphism. In, Fraser, O.G. (Ed.), Thermodynamics in geology. Reidel.

Fitton, J.G., 1972:
The genetic significance of almandine-pyrope phenocrysts in the calc-alkaline Borrowdale volcanic group, N. England. CMP 36, 231-248.

Flanagan, F.J., 1973:
1972 values for international geochemical reference samples. Geochim. et Cosmochim. Acta, 37, 1189-1212.

Fletcher, R.C., and Hofmann, A.W., 1974:
Simple models of diffusion and combined diffusion-infiltration metasomatism. In Hofmann et al. (Eds.), Geochemical transport and kinetics. Carnegie Inst. Wash., Publication 634.

Foland, K.A., 1974:
Alkali diffusion in orthoclase. In, Hofmann et al., (Eds.), Geochemical transport and kinetics. Carnegie Inst. Wash. Publication 634.

Francis, P.W., 1969:
Some aspects of the Lewisian geology of the Isle of Barra and adjacent small islands. Unpublished Ph.D. thesis, Univ. of London.

Francis, P.W., Moorbath, S., and Welke, H.J., 1971:
Isotopic age data from Scourian intrusive rocks on the Isle of Barra, Outer Hebrides, north-west Scotland. Geol. Mag., 108, 13-22.

Frantz, J.D., and Mao, H.K., 1976:
Bimetasomatism resulting from intergranular diffusion: I. A theoretical model for minomineralic reaction zone columns. Amer. J. Sci., 276, 817-840.

Fyfe, W.S., 1970:
Some thoughts on granitic magmas. In, Newall, G., and Rast, N. (Eds.), Mechanisms of igneous intrusion. Geol. J. Spec. Issue 2, 201-216.

Gait, R.I., Ferguson, R.B., and Coish, H.R., 1970:
Electrostatic charge distributions in the structure of low albite, $NaAlSi_3O_8$. Acta Crystallogr., B26, 68-77.

Gay, P., and Roy, N.N., 1969:
The mineralogy of the potassium-barium feldspar series. III: subsolidus relationships. Min. Mag., 36, 914-932.

Giletti, B.J., Moorbath, S., and Lambert, R.St.J., 1961:
A geochronological study of the metamorphic complexes of the Scottish Highlands. J. Geol. Soc. Lond., 117, 233-273.

Graham, R.H., 1980:
The role of shear belts in the structural evolution of the South Harris igneous complex. Jour. Structural Geol., 2, 29-37.

Green, T.H., 1977:
Garnet in silicic liquids and its possible use as a P-T indicator. Contrib. Mineral. Petrol., 65, 59-67.

Green, T.H., and Ringwood, A.E., 1968:
Genesis of the calc-alkaline igneous rock suite. Contrib. Mineral. Petrol., 18, 105-162.

Green, T.H., and Ringwood, A.E., 1972:
Crystallisation of garnet-bearing rhyodacite under pressure hydrous conditions. J. Geol. Soc. Austr., 19, 203-212.

Gresens, R.L., 1967:
Tectonic-hydrothermal pegmatites. I. The model. Contrib. Miner. Petrol., 15, 345-355.

Guidotti, C.V., 1978:
Muscovite and K-feldspar from two-mica adamellite in northwestern Maine: composition and petrogenetic implications. Am. Miner., 63, 750-753.

Haggerty, S.E., 1976:
Opaque mineral oxides in terrestrial igneous rocks. In, D. Rumble III (Ed.), Oxide Minerals. Mineralogical Society of America.

Hamilton, P.J., Evensen, N.M., O'Nions, R.K., and Tarney, J., 1979
Sm-Nd systematics of Lewisian gneisses: implications for the origin of granulites. Nature, 277, 25-28.

Hanson, G.M., 1978:
The application of trace elements to the petrogenesis of igneous rocks of granitic composition. Earth. Planet. Sci. Letters, 38, 26-43.

Heier, K.S., 1973:
Geochemistry of granulite facies rocks and problems of their origin. Phil. Trans. Roy. Soc. Lond., A., 273, 429-442.

Helgeson, H.C., 1967:
Solution chemistry and metamorphism. In, Abelson, P.H. (Ed.), Researches in geochemistry, vol. 2. Wiley.

Holdaway, M.J., 1971:
Stability of andalusite and the aluminium silicate phase diagram. Am. J. Sci., 271, 97-131.

Holland, J.G., and Lambert, R. St.J., 1972:
Major element chemical composition of shields and continental crust. Geochim. et Cosmochim. Acta, 36, 673-683.

Holland, J.G., and Lambert, R. St.J., 1973:
Comparative major element geochemistry of the Lewisian of the mainland of Scotland. In, Park, R.G., and Tarney, J. (Eds.), The early Precambrian of Scotland and related rocks of Greenland. Univ. of Birmingham Press.

Holland, J.G., and Lambert, R. St.J., 1975:
The chemistry and origin of the Lewisian gneisses of the Scottish mainland: the Scourie and Inver assemblages and sub-crustal accretion. Precamb. Res., 2, 161-188.

Hollister, L.S., 1969:
Contact metamorphism in the Kwoiek area of British Columbia: an end member of the metamorphic process. Bull. Geol. Soc. Am., 80, 2465-2494.

Hurd, D.C., and Theyer, F., 1975:
Changes in the physical and chemical properties of biogenic silica from the Central Equatorial Pacific - I. Solubility, specific surface area, and solution rate constants of acid-cleaned samples. In, T.R.P. Gibb (Ed.), Analytical methods in oceanography. Adv. in Chem. Ser., 147, 211-230.

Jahns, R.H., and Burnham, C.W., 1969:
Experimental studies of pegmatite genesis: I. A Model for the derivation and crystallisation of granitic pegmatites. Econ. Geol., 64, 843-864.

Jensen, B.B., 1973:
Patterns of trace element partitioning.
Geochim. et Cosmochim. Acta, 37, 2227-2242.

Kennedy, W.Q., 1948:
On the significance of thermal structure in the Scottish Highlands. Geol. Mag. 85, 229-234.

von Knorring, O., and Dearnley, R., 1960:
The Lewisian pegmatites of South Harris, Outer Hebrides.
Min. Mag., 32, 366-378.

Korzhinskii, D.S., 1970:
Theory of metasomatic zoning (Trans. J. Agrell).
Oxford University Press.

Krauskopf, K.B., 1967:
Introduction to geochemistry. McGraw Hill.

Larsen, L.M., 1976:
Clinopyroxenes and coexisting mafic minerals from the alkaline Ilimaussaq intrusion, South Greenland.
J. Petrol., 17, 258-290.

Leake, B.E., 1978:
Nomenclature of amphiboles. Am. Miner., 63, 1023-1052.

Lerman, A., Mackenzie, F.T., and Bricker, O.P., 1975:
Rates of dissolution of aluminosilicates in seawater.
Earth. Planet. Sci. Letters, 25, 82-88.

Luth, W.C., 1976:
Granitic rocks. In, Bailey, D.K., and Macdonald, R., (Eds.), The evolution of the crystalline rocks. Academic Press.

Martin, R.F., 1974:
Controls of ordering and subsolidus phase relations in the alkali feldspars. In, Mackenzie, W.S., and Zussman, J., (Eds.), The feldspars. Manchester Univ. Press.

Mineyev, D.A., 1963:
Geochemical differentiation of the rare earths. Geochemistry 12, 1129-1149.

Mitchell, R.H., and Platt, R.G., 1978:
Mafic mineralogy of ferroaugite syenite from the Coldwell alkaline complex, Ontario, Canaca. J. Petrol., 19, 627-651.

Moorbath, S., and Park, R.G., 1972:
The Lewisian chronology of the southern region of the Scottish mainland. Scott. J. Geol., 8, 51-74.

Moorbath, S., Powell, J.L., and Taylor, P.T., 1975:
Isotopic evidence for the age and origin of the "grey gneiss" complex of the southern Outer Hebrides, Scotland. J. Geol. Soc. Lond., 131, 213-222.

Moorbath, S., Welke, H.J., and Gale, N.H., 1969:
The significance of lead isotope studies in ancient high-grade metamorphic basement complexes, as exemplified by the Lewisian rocks of north-west Scotland. Earth. Planet. Sci. Letters, 6, 245-56.

Myers, J.S., 1968:
The tectonic and metamorphic history of the Lewisian migmatite complex of western Harris, Outer Hebrides, Scotland. Unpublished Ph.D. thesis, Univ. of London.

Myers, J.S., 1970:
Gneiss types and their significance in the repeatedly deformed and metamorphosed Lewisian Complex of Western Harris, Outer Hebrides. Scott. J. Geol., 6, 186-199.

Myers, J.S., 1971:
The late Laxfordian granite-migmatite complex of western Harris, Outer Hebrides. Scott. J. Geol., 7, 254-284.

Nakamura, N., 1974:
Determination of REE, Ba, Fe, Mg, Na and K in carbonaceous and ordinary chondrites. Geochim. et Cosmochim. Acta, 38, 757-775.

Nash, W.P., and Wilkinson, J.F.G., 1971:
Shonkin Sag Laccolith, Montana: pt. II, Bulk rock geochemistry. Contrib. Mineral. Petrol., 33, 162-170.

Neiva, A.M., 1974:
Geochemistry of coexisting aplites and pegmatites and of their minerals from central northern Portugal. Chem. Geol., 16, 153-177.

O'Hara, M.J., 1961:
Petrology of the Scourie dyke, Sutherland. Min. Mag., 32, 848-865.

O'Hara, M.J., 1977:
Thermal history of excavation of Archaean gneisses from the base of the continental crust. J. Geol. Soc. Lond., 134, 185-200.

Park, R.G., 1970:
Observations on Lewisian chronology. Scott. J. Geol., 6, 379-399.

Park, R.G., 1973:
The Laxfordian belts of the Scottish mainland. In, R.G. Park and J. Tarney, (Eds.), The early Precambrian of Scotland and related rocks of Greenland. University of Birmingham Press.

Parker, R.J., 1977:
Factors affecting the quality of major element rock analysis by x-ray fluorescence combined with flux-fusion sample preparation. Tech. Rep. No. XRF-2B, Dept. of Geology, Imperial College, London.

Peach, B.N., Horne, J., Gunn, W., Clough, C.T., and Hinxman, L.W., 1907:
The geological structure of the NW Highlands of Scotland. Mem. Geol. Surv. U.K.

Pidgeon, R.T., and Aftalion, M., 1978:
Cogenetic and inherited zircon U-P6 systems in granites: Palaeozoic granites of Scotland and England. In, Bowes, D.R., and Leake, B.E., (Eds.), Crustal evolution in northwestern Britain and adjacent regions. Geol. J. Spec. Issue No. 10, 183-248.

Pitcher, W.S., 1978:
The anatomy of a batholith. President's anniversary address 1977. J. Geol. Soc. Lond., 135, 157-182.

Powell, M., and Powell, R., 1977a:
Plagioclase-alkali feldspar geothermometry revisited. Min. Mag., 41, 253-256.

Powell, R., and Powell, M., 1977b:
Geothermometry and oxygen barometry using coexisting iron-titanium oxides: a reappraisal. Min. Mag., 41, 257-264.

Pride, C., and Muecke, G.K., 1980:
Rare earth element geochemistry of the Scourian complex, N.W. Scotland - evidence for the granite-granulite link. Contrib. Mineral. Petrol., 73, 403-412.

Read, H.H., 1934:
On zoned associations of antigorite, talc, actinolite and biotite in Unst, Shetland Islands. Min. Mag., 23, 519-540.

Read, H.H., 1957:
The granite controversy. New York, Interscience publishers.

Robie, R.A., Bethke, P.M., and Beardsley, K.M., 1967:
Selected X-ray crystallographic data, molar volumes and densities of minerals and related substances. Bull. U.S. Geol. Surv., 1248.

Robie, R.A., and Waldbaum, D.R., 1968:
Thermodynamic properties of minerals and related substances at 298.15°K (25°C) and one atmosphere (1.013 bars) pressure and at higher temperatures. Bull. U.S. Geol. Surv., 1259.

Savage, D.S., 1979:
Geochemistry and petrology of layered basic intrusions in the Lewisian complex around Scourie. Unpublished Ph.D. thesis, Univ. of London.

Savage, D.S., and Sills, J.D., 1980:
High pressure metamorphism in the Scourian of N.W. Scotland: evidence from garnet granulites. Contrib. Miner. Petrol., 74, 153-164.

Saxena, S.K., 1979:
Garnet-clinopyroxene geothermometer. Contrib. Miner. Petrol., 70, 229-236.

Seck, H.A., 1971:
Koexistierende Alkalifeldspäte und Plagioklase im System $NaAlSi_3O_8$ - $KAlSi_3O_8$ - $CaAl_2Si_2O_8$ - H_2O bei Temperaturen von 650°C bis 900°C. N. Jb. Miner. Abh., 115, 315-345.

Shand, S.J., 1927:
Eruptive rocks: their genesis, composition, classification, and their relation to ore-deposits with a chapter on meteorites. Murby, London.

Sheraton, J.W., Skinner, A.C., and Tarney, J., 1973:
The geochemistry of the Scourian gneisses of the Assynt district. In, R. G. Park, J. Tarney, (Eds.), The early Precambrian of Scotland and related rocks of Greenland. Univ. of Birmingham press.

Statham, P.J., 1976:
A comparative study of techniques for quantitative analysis of the spectra obtained with a Si(Li) detector. X-ray Spectrom., 5, 16-28.

Smith, J.V., 1974:
Feldspar minerals (2 vols.) Springer-Verlag.

Stormer, J.C., 1975:
A practical two-feldspar geothermometer. Am. Miner., 60, 667-674.

Stormer, J.C., 1977:
The distribution of $NaAlSi_3O_8$ between coexisting microcline and plagioclase and its effect on geothermometric calculations. Am. Miner., 62, 687-691.

Sutton, J., and Watson, J.V., 1951:
The Pre-Torridonian metamorphic history of the Loch Torridon and Scourie areas in the NW Highlands and its bearing on the chronological classification of the Lewisian. J. Geol. Soc. Lond., 106, 241-308.

Tarney, J., 1963:
Assynt dykes and their metamorphism. Nature, 199, 672-674.

Tarney, J., 1973:
The Scourie dyke suite and the nature of the Inverian event in Assynt. In, Park, R.G., and Tarney, J., (Eds.), The early Precambrian of Scotland and related rocks of Greenland. Univ. of Birmingham Press.

Tarney, J., and Windley, B.F., 1977:
Chemistry, thermal gradients and evolution of the lower continental crust. J. Geol. Soc. Lond., 134, 153-172.

Tarney, J., and Windley, B.F., 1979:
Chemistry, thermal gradients and evolution of the lower continental crust - a reply to S.R. Taylor and S.M. McLennan. J. Geol. Soc. Lond., 136, 501-504.

Taylor, S.R., and McLennan, S.M., 1979:
Discussion on "Chemistry, thermal gradients and evolution of the lower continental crust", by J. Tarney and B.F. Windley. J. Geol. Soc. Lond., 136, 497-500.

Thompson, A.B., 1976:
Mineral reactions in pelitic rocks: I. Prediction of P-T-X (Fe-Mg) phase relations. Amer. J. Sci., 276, 401-424.

Thompson, A.B., 1976:
Mineral reactions in pelitic rocks: II. Calculation of some P-T-X (Fe-Mg) phase relations. Amer. J. Sci., 276, 425-454.

Thompson, A.B., 1975:
Calc-silicate diffusion zones between marble and pelitic schist. J. Petrol., 16, 314-346.

Thompson, J.B. Jnr., 1957:
The graphical analysis of mineral assemblages in pelitic schists. Am. Miner. 42, 842-858.

Thompson, J.B., Jnr., 1959:
Local equilibrium in metasomatic processes. In, Abelson, P.M. (Ed.), Researches in geochemistry (Vol. I). Wiley, New York.

Tuttle, O.F., and Bowen, N.L., 1958:
Origin of granite in the light of experimental studies in the system $NaAlSi_3O_8$-$KAlSi_3O_8$-SiO_2-H_2O.
Geol. Soc. Am. Mem., 74, 153 pp.

Velde, B., 1966:
Phengite micas: synthesis, stability, and natural occurrence. Amer. J. Sci., 263, 886-913.

Vennum, W.R., and Meyer, C.E., 1979:
Plutonic garnets from the Werner batholith, Lassiter coast, Antarctic peninsula. Am. Miner., 64, 268-273.

Vidale, R., 1969:
Metasomatism in a chemical gradient and the formation of calc-silicate bands. Amer. J. Sci., 267, 857-874.

Vidale, R., and Hewitt, D., 1973:
"Mobile" components in the formation of calc-silicate bands. Am. Miner., 58, 991-997.

Warren, R.C., 1970:
Electron microprobe investigations of almandine garnets from a quartz diorite stock and adjacent metamorphic rocks, British Columbia. (Abstract.)
Am. Geophys. Union Trans., 51, 444.

Watson, J.V., 1949:
The geology of the Lewisian of the Scourie area.
Unpublished Ph.D. thesis, Univ. of London.

Watson, J.V., 1975:
The Lewisian Complex. In A. L. Harris and others (Eds.), A Correlation of the Precambrian rocks in the British Isles. Geol. Soc. Lond. Spec. Report, No. 6, 15-29.

Weare, J.H., Stephens, J.R., and Eugster, H.P., 1976:
Diffusion metasomatism and mineral reaction zones: general principles and application to feldspar alteration. Amer. J. Sci., 276, 767-816.

Wells, P.R.A., 1977:
Pyroxene thermometry in simple and complex systems.
Contrib. Miner. Petrol., 62, 129-139.

Whittaker, E.J.W., and Muntus, R., 1970:
Ionic radii for use in geochemistry.
Geochim. et Cosmochim. Acta, 34, 945-956.

Winkler, H.G.F., 1976:
Petrogenesis of metamorphic rocks. (4th edn.).
Springer-Verlag.

Wones, D.R., and Eugster, H.P., 1965:
Stability of biotite: experiment, theory and application.
Am. Miner., 50, 1228-1272.

Wood, B.J., 1974:
The solubility of alumina in orthopyroxene coexisting with garnet. Contrib. Mineral. Petrol., 46, 1-15.

Wood, B.J., 1975:
The influence of pressure, temperature and composition on the appearance of garnet in orthogneisses - an example from S. Harris, Scotland. Earth Planet. Sci. Letters, 26, 299-311.

Wood, B.J., and Banno, S., 1973:
Garnet-orthopyroxene and orthopyroxene-clinopyroxene relationships in simple and complex systems.
Contrib. Mineral. Petrol., 42, 109-24.

Wyllie, P.J., 1978:
Crustal anatexis: an experimental review.
Tectonophysics, 43, 41-71.

APPENDIX 1

TABLES OF ROCK ANALYSES

Key

LXG	Laxford granites
LXP	Laxford pegmatites
HRG	Harris granites
HRP	" related pegmatites
LWG	Lewis granites
LWP	Lewis pegmatites
N	Northern-type pegmatites
S	Southern-type pegmatites

	81	68	66	78	64	84	63	74
SIO2	67.71	68.75	68.99	68.99	69.36	69.64	70.04	70.46
TIO2	.39	.37	.36	.35	.32	.31	.38	.29
AL2O3	16.11	16.14	15.77	16.07	15.50	15.39	15.60	15.07
FE2O3	.29	.28	.28	.25	.26	.26	.27	.23
FEO	1.61	1.56	1.54	1.39	1.42	1.44	1.48	1.28
MNO	.03	.03	.03	.02	.03	.02	.02	.02
MGO	.91	.80	.73	.80	.74	1.14	.60	.73
CAO	1.24	.90	1.22	1.12	1.07	.54	1.45	.90
NA2O	4.86	4.16	4.23	4.32	4.29	4.65	4.20	5.14
K2O	5.69	5.99	5.46	5.40	5.39	5.49	4.98	4.56
P2O5	.18	.15	.16	.17	.11	.12	.11	.12
H2O-	.20	.22	.14	.08	.20	.10	.14	.04
LOI	.59	.67	.69	.58	.64	.63	.51	.50
TOTAL	99.83	100.02	99.60	99.54	99.32	99.73	99.78	99.34
F3/F2	.18	.18	.18	.18	.18	.18	.18	.18
K2O/NA2O	1.17	1.44	1.29	1.25	1.26	1.18	1.19	.89
MGO/K2O	.16	.13	.13	.15	.14	.21	.12	.16
F3+F2/CA	1.86	2.48	1.81	1.78	1.90	3.83	1.46	2.04
K2O/CAO	4.59	6.66	4.48	4.82	5.04	10.17	3.43	5.07
CAO/MGO	1.36	1.12	1.67	1.40	1.45	.47	2.42	1.23

F3/F2 = FE2O3/FEO
F3+F2/CA = (FE3+ + FE2+)/CA2+

V	30	30	23	30	23	23	25	25
CR	8	8	6	17	10	8	9	9
NI	8	7	6	8	7	7	5	8
TH	26	28	41	25	18	21	26	23
RB	118	175	146	153	128	135	143	105
SR	1980	1334	1554	1559	1182	1403	1377	1430
Y	15	16	13	14	10	12	15	13
ZR	408	354	357	329	299	320	303	253
NB	8	5	10	9	12	11	3	10
BA	5131	3856	3526	4205	3423	4106	3319	3210
K/RB	400.	284.	310.	293.	350.	338.	289.	361.
RB/SR	.060	.131	.094	.098	.108	.096	.104	.073
TH/K	.0006	.0006	.0009	.0006	.0004	.0005	.0006	.0006
DI	87.56	88.06	86.83	87.14	87.50	89.41	86.48	89.66
QZ	12.61	17.40	18.73	18.63	19.31	17.57	21.46	19.18
CO	0	1.08	.62	.99	.53	.63	.51	0
ZR	.08	.07	.07	.07	.06	.06	.06	.05
OR	33.66	35.45	32.31	31.96	31.89	32.49	29.47	26.98
PL	46.52	39.89	42.01	42.35	41.96	42.52	43.12	48.06
(AB)	41.29	35.20	35.79	36.55	36.30	39.35	35.54	43.49
(AN)	5.23	4.69	6.21	5.79	5.66	3.17	7.58	4.56
DI	1.17	0	0	0	0	0	0	.18
(WO)	.59	0	0	0	0	0	0	.09
(EN)	.30	0	0	0	0	0	0	.05
(FS)	.28	0	0	0	0	0	0	.04
HY	3.82	4.07	3.88	3.80	3.76	4.79	3.40	3.45
(EN)	1.97	1.99	1.82	1.99	1.84	2.84	1.49	1.77
(FS)	1.85	2.08	2.06	1.80	1.92	1.96	1.90	1.68
MT	.42	.41	.41	.36	.38	.38	.39	.33
IL	.74	.70	.68	.66	.61	.59	.72	.55
AP	.43	.36	.38	.40	.26	.28	.26	.28

LXG ⟶

	70	62	61	71	79	67	75	65
SIO2	73.57	73.84	74.44	74.45	74.50	74.86	75.13	75.64
TIO2	.05	.10	.09	.06	.03	.02	.05	.03
AL2O3	14.90	14.02	13.96	14.51	14.57	14.06	14.95	14.17
FE2O3	.12	.12	.13	.04	.10	.07	.08	.06
FEO	.64	.67	.72	.22	.57	.39	.46	.31
MNO	.02	.02	0	0	.01	.01	.01	.02
MGO	.34	.32	.33	.20	.26	.21	.26	.27
CAO	1.02	1.12	1.02	.64	1.44	.86	.90	.69
NA2O	4.70	4.40	4.09	4.61	5.50	4.62	5.62	4.40
K2O	4.68	4.89	4.86	5.03	2.72	4.88	3.18	4.68
P2O5	.03	.08	.05	.02	.01	.12	.01	.02
H2O-	.13	.10	0	.05	.11	.08	.06	.01
LOI	.35	.25	.11	.31	.32	.56	.26	.31
TOTAL	100.55	99.93	99.80	100.14	100.15	100.75	100.98	100.61
F3/F2	.18	.18	.18	.18	.18	.18	.18	.18
K2O/NA2O	1.00	1.11	1.19	1.09	.49	1.06	.57	1.06
MGO/K2O	.07	.07	.07	.04	.10	.04	.08	.06
F3+F2/CA	.90	.85	1.01	.50	.57	.66	.74	.64
K2O/CAO	4.59	4.37	4.76	7.86	1.89	5.67	3.53	6.78
CAO/MGO	3.00	3.50	3.09	3.20	5.54	4.10	3.46	2.56

F3/F2 = FE2O3/FEO
F3+F2/CA = (FE3+ + FE2+)/CA2+

V	11	22	10	3	10	4	7	9
CR	7	10	5	7	10	10	12	8
NI	5	6	5	4	4	6	5	4
TH	38	20	16	23	13	40	4	4
RB	154	155	146	191	79	186	74	119
SR	267	1015	288	154	324	379	1170	666
Y	21	14	10	13	7	2	2	2
ZR	115	315	98	61	122	35	129	71
NB	0	3	4	13	6	1	8	0
BA	723	2856	881	254	401	842	1484	1995
K/RB	252.	262.	276.	219.	286.	218.	357.	326.
RB/SR	.577	.153	.507	1.240	.244	.491	.063	.179
TH/K	.0010	.0005	.0004	.0006	.0006	.0010	.0002	.0001
DI	92.58	92.57	92.25	95.36	90.82	95.15	93.71	94.71
QZ	25.10	26.39	28.88	26.56	28.18	27.16	27.34	29.79
CO	.23	0	.13	.32	0	0	.40	.43
ZR	.02	.06	.02	.01	.02	.01	.03	.01
OR	27.71	28.95	28.77	29.79	16.10	28.90	18.82	27.69
PL	44.87	41.27	39.61	42.15	53.56	42.28	52.63	41.14
(AB)	39.77	37.23	34.61	39.01	46.54	39.09	47.55	37.23
(AN)	5.10	4.04	5.00	3.14	7.02	3.18	5.07	3.91
DI	0	1.58	0	0	.20	.49	0	0
(WO)	0	.79	0	0	.10	.25	0	0
(EN)	0	.35	0	0	.04	.11	0	0
(FS)	0	.44	0	0	.06	.14	0	0
HY	1.88	1.01	1.89	.77	1.48	.92	1.36	1.18
(EN)	.85	.45	.82	.50	.61	.41	.65	.67
(FS)	1.03	.56	1.07	.27	.87	.51	.71	.51
MT	.17	.17	.19	.06	.14	.10	.12	.09
IL	.09	.19	.17	.11	.06	.04	.09	.06
AP	.07	.19	.12	.05	.02	.28	.02	.05

LXG ——| LXP ——————|

	604	614	602	610	613	621	606	601
SIO2	72.73	72.94	74.13	74.27	74.67	76.03	69.37	70.00
TIO2	.05	.13	.02	.05	.03	.07	.43	.35
AL2O3	14.91	13.90	13.98	14.09	13.79	13.11	14.57	14.85
FE2O3	.20	.15	.00	.06	.03	.08	.45	.39
FEO	1.12	.86	.02	.36	.15	.46	2.48	2.18
MNO	0	.03	0	.01	0	.01	.03	.01
MGO	.13	.39	.01	.22	.08	.41	.72	.70
CAO	1.38	.81	.15	.58	.27	1.16	1.47	1.54
NA2O	3.62	2.35	2.17	3.41	1.99	2.69	2.93	4.71
K2O	5.69	7.34	9.39	7.00	8.75	5.59	6.30	5.54
P2O5	.01	.07	.02	.02	.02	.03	.12	.10
H2O-	.02	.03	.02	.08	.02	.03	.02	.04
LOI	.19	.23	.04	.33	.12	.27	.51	.32
TOTAL	100.05	99.23	99.95	100.48	99.92	99.95	99.39	100.73
F3/F2	.18	.18	.18	.18	.18	.18	.18	.18
K2O/NA2O	1.57	3.12	4.33	2.05	4.40	2.08	2.15	1.18
MGO/K2O	.02	.05	.00	.03	.01	.07	.11	.13
F3+F2/CA	1.16	1.52	.15	.88	.82	.57	2.42	2.03
K2O/CAO	4.12	9.06	62.60	12.07	32.41	4.82	4.29	3.60
CAO/MGO	10.62	2.08	15.00	2.64	3.37	2.83	2.04	2.20

F3/F2 = FE2O3/FEO
F3+F2/CA = (FE3+ + FE2+)/CA2+

V	18	15	3	4	8	5	33	31
CR	6	10	4	10	8	6	5	15
NI	4	8	4	6	4	5	6	7
TH	3	52	0	3	2	8	53	47
RB	174	234	294	294	256	187	177	171
SR	262	271	273	295	252	236	259	239
Y	2	21	0	2	21	4	30	26
ZR	11	151	16	18	20	34	427	300
NB	0	2	0	0	0	0	3	5
BA	821	1351	1566	938	1870	946	1952	1351
K/RB	271.	260.	265.	198.	284.	248.	295.	269.
RB/SR	.664	.863	1.077	.997	1.016	.792	.683	.715
TH/K	.0001	.0009	0	.0001	.0000	.0002	.0010	.0010
DI	90.12	91.59	99.08	96.14	97.25	91.37	84.53	89.30
QZ	25.81	28.26	25.14	25.83	28.62	35.51	22.45	16.65
CO	.21	.64	0	0	.42	.49	.36	0
ZR	0	.03	0	0	0	.01	.09	.06
OR	33.68	43.45	55.58	41.46	51.79	33.09	37.29	32.79
PL	37.66	23.81	18.99	31.27	18.51	28.59	31.78	42.84
(AB)	30.63	19.89	18.36	28.85	16.84	22.76	24.79	39.85
(AN)	7.03	3.92	.63	2.42	1.67	5.83	6.99	2.99
WO	0	0	.13	0	0	0	0	0
DI	0	0	.06	.51	0	0	0	3.67
(WO)	0	0	.03	.26	0	0	0	1.82
(EN)	0	0	.02	.13	0	0	0	.66
(FS)	0	0	0	.13	0	0	0	1.19
HY	2.13	2.27	0	.84	.40	1.70	5.32	3.01
(EN)	.32	.97	0	.42	.20	1.02	1.79	1.08
(FS)	1.81	1.30	0	.42	.20	.68	3.53	1.93
MT	.29	.22	0	.09	.04	.12	.65	.57
IL	.09	.25	.04	.09	.06	.13	.82	.66
AP	.02	.17	.05	.05	.05	.07	.28	.24

HRP ——————————— HRG →

	626	611	609	615	618	607	605	612
SIO2	70.04	71.00	71.13	71.27	71.42	71.51	71.65	71.70
TIO2	.28	.28	.31	.33	.36	.32	.27	.28
AL2O3	14.80	14.91	14.33	14.67	14.40	14.39	14.32	14.35
FE2O3	.28	.28	.35	.35	.39	.35	.31	.33
FEO	1.56	1.57	1.96	1.95	2.17	1.94	1.74	1.86
MNO	.05	.01	.01	.03	.03	.02	.01	.01
MGO	.89	.80	.56	.57	.51	.57	.42	.41
CAO	1.52	1.40	1.60	1.47	1.41	1.48	1.46	1.42
NA2O	3.44	3.15	3.40	3.24	3.31	3.41	3.19	3.27
K2O	6.02	5.87	5.15	5.61	5.72	5.09	5.77	5.47
P2O5	.14	.12	.07	.10	.10	.08	.08	.08
H2O-	.04	.05	.07	.04	.05	.09	.03	.04
LOI	.38	.47	.30	.15	.20	.31	.29	.27
TOTAL	99.45	99.91	99.24	99.78	100.07	99.56	99.55	99.49
F3/F2	.18	.18	.18	.18	.18	.18	.18	.18
K2O/NA2O	1.75	1.86	1.51	1.73	1.73	1.49	1.81	1.67
MGO/K2O	.15	.14	.11	.10	.09	.11	.07	.07
F3+F2/CA	1.48	1.61	1.76	1.91	2.21	1.88	1.71	1.88
K2O/CAO	3.96	4.19	3.22	3.82	4.06	3.44	3.95	3.85
CAO/MGO	1.71	1.75	2.86	2.58	2.76	2.60	3.48	3.46
V	22	30	23	30	26	29	18	21
CR	10	17	7	15	11	7	11	9
NI	7	13	6	6	8	6	5	6
TH	56	50	35	29	35	32	47	48
RB	193	212	199	220	193	195	169	255
SR	326	304	187	222	217	209	248	157
Y	32	57	20	17	197	18	27	27
ZR	471	500	250	296	304	233	245	236
NB	1	2	12	2	3	9	0	8
BA	1516	1227	1044	1295	1132	1012	1111	1050
K/RB	259.	230.	215.	212.	246.	217.	283.	178.
RB/SR	.592	.697	1.064	.991	.889	.933	.681	1.624
TH/K	.0011	.0010	.0008	.0006	.0007	.0008	.0010	.0011
DI	86.27	86.54	85.39	86.39	87.04	85.96	87.30	86.98
QZ	21.52	25.13	26.12	25.75	25.17	26.96	26.16	26.91
CO	.03	.98	.31	.70	.32	.66	.24	.55
ZR	.09	.10	.05	.06	.06	.05	.05	.05
OR	35.64	34.76	30.50	33.22	33.86	30.14	34.15	32.41
PL	36.14	33.16	36.52	34.39	34.65	35.95	34.02	34.45
(AB)	29.11	26.65	28.77	27.42	28.01	28.85	26.99	27.67
(AN)	7.04	6.51	7.75	6.97	6.64	7.09	7.02	6.78
HY	4.48	4.20	4.21	4.22	4.39	4.20	3.56	3.72
(EN)	2.22	1.99	1.39	1.42	1.27	1.42	1.05	1.02
(FS)	2.26	2.21	2.82	2.80	3.12	2.78	2.51	2.70
MT	.41	.41	.51	.51	.57	.51	.45	.48
IL	.53	.53	.59	.63	.68	.61	.51	.53
AP	.33	.28	.17	.24	.24	.19	.19	.19

F3/F2 = FE2O3/FEO
F3+F2/CA = (FE3+ + FE2+)/CA2+

HRG ⟶

	616	619	617	1012	622	620	108	112
SIO2	71.90	72.27	73.03	73.36	74.09	74.37	71.24	71.91
TIO2	.30	.28	.20	.22	.15	.11	.36	.30
AL203	14.37	14.33	14.72	14.12	14.14	13.36	14.46	14.58
FE203	.35	.33	.15	.28	.13	.16	.35	.32
FEO	1.92	1.84	.83	1.56	.73	.91	1.94	1.80
MNO	.03	0	0	.03	0	0	.01	.03
MGO	.47	.67	.18	.32	.34	.32	.69	.48
CAO	1.27	1.41	1.45	1.26	1.54	.86	1.44	1.59
NA20	3.13	3.35	4.71	3.00	3.61	2.47	3.54	4.02
K20	5.80	5.33	4.97	5.50	4.76	6.74	5.06	4.46
P205	.09	.10	.04	.07	.04	.02	.10	.05
H20-	.04	.05	.05	.03	.04	.01	.04	.01
LOI	.33	.27	.20	.25	.29	.15	.46	.21
TOTAL	100.00	100.23	100.53	100.01	99.86	99.49	99.69	99.76
F3/F2	.18	.18	.18	.18	.18	.18	.18	.18
K20/NA20	1.85	1.59	1.06	1.83	1.32	2.73	1.43	1.11
MGO/K2O	.08	.13	.04	.06	.07	.05	.14	.11
F3+F2/CA	2.17	1.88	.82	1.78	.68	1.52	1.94	1.62
K20/CAO	4.57	3.78	3.43	4.37	3.09	7.84	3.51	2.81
CAO/MGO	2.70	2.10	8.06	3.94	4.53	2.69	2.09	3.31

F3/F2 = FE203/FEO
F3+F2/CA = (FE3+ + FE2+)/CA2+

V	25	25	14	19	13	11	32	25
CR	11	8	7	9	10	8	8	10
NI	5	7	5	6	6	4	7	6
TH	55	39	47	30	32	22	32	28
RB	244	240	205	279	137	208	235	339
SR	187	474	157	146	240	136	187	167
Y	31	22	26	7	10	12	18	16
ZR	248	221	114	193	121	76	316	247
NB	5	7	0	9	0	2	15	24
BA	1119	1006	662	828	1319	753	1092	856
K/RB	197.	184.	201.	164.	288.	269.	179.	109.
RB/SR	1.305	.506	1.306	1.911	.571	1.529	1.257	2.030
TH/K	.0011	.0009	.0011	.0007	.0008	.0004	.0008	.0008
DI	87.70	87.15	92.63	88.64	89.27	91.99	85.96	86.59
QZ	26.86	27.23	23.34	30.66	30.55	31.19	26.03	26.11
CO	.73	.58	0	1.01	.21	.40	.66	.27
ZR	.05	.04	.02	.04	.02	.02	.06	.05
OR	34.35	31.57	29.44	32.59	28.17	39.90	29.98	26.47
PL	32.48	35.04	44.17	31.39	38.27	25.23	36.73	41.80
(AB)	26.49	28.35	39.85	25.39	30.55	20.90	29.95	34.02
(AN)	6.00	6.70	4.31	6.01	7.72	4.33	6.77	7.79
DI	0	0	2.39	0	0	0	0	0
(WO)	0	0	1.17	0	0	0	0	0
(EN)	0	0	.36	0	0	0	0	0
(FS)	0	0	.86	0	0	0	0	0
HY	3.97	4.31	.30	3.12	1.83	2.15	4.42	3.80
(EN)	1.17	1.67	.09	.80	.85	.80	1.72	1.20
(FS)	2.80	2.64	.21	2.33	.99	1.36	2.70	2.60
MT	.51	.48	.22	.41	.19	.23	.51	.46
IL	.57	.53	.38	.42	.28	.21	.68	.57
AP	.21	.24	.09	.17	.09	.05	.24	.12

HRG ⟵ LWG →

	105	106	110	104	111	100	1009	603
SIO2	72.01	74.89	76.05	74.15	75.11	75.72	71.79	72.39
TIO2	.25	.07	.07	.02	.05	.04	.12	.21
AL2O3	14.54	13.72	13.63	14.45	14.15	13.86	15.65	14.94
FE2O3	.29	.13	.11	.07	.13	.09	.16	.23
FEO	1.59	.71	.59	.38	.70	.53	.90	1.30
MNO	0	.01	.01	.01	.01	0	0	0
MGO	.56	.18	.15	.11	.18	.22	.75	.65
CAO	1.13	1.15	1.05	.28	1.17	1.07	2.93	2.81
NA2O	3.53	3.76	4.00	2.79	4.27	3.50	4.70	4.35
K2O	5.82	5.36	4.83	7.67	4.76	5.68	1.90	2.36
P2O5	.07	.02	.01	.02	.02	.01	.03	.14
H2O-	.04	.04	0	.03	0	0	.07	.03
LOI	.46	.22	.21	.15	.23	.16	.27	.28
TOTAL	100.28	100.26	100.70	100.13	100.77	100.88	99.27	99.70
F3/F2	.18	.18	.18	.18	.18	.18	.18	.18
K2O/NA2O	1.65	1.43	1.21	2.75	1.11	1.62	.40	.54
MGO/K2O	.10	.03	.03	.01	.04	-.04	.39	.28
F3+F2/CA	2.02	.89	.80	1.94	.85	.71	.44	.66
K2O/CAO	5.15	4.66	4.60	27.39	4.07	5.31	.65	.84
CAO/MGO	2.02	6.39	7.00	2.55	6.50	4.86	3.91	4.32

F3/F2 = FE2O3/FEO
F3+F2/CA = (FE3+ + FE2+)/CA2+

V	21	14	4	7	9	7	12	21
CR	10	10	10	10	6	6	41	13
NI	6	9	5	6	5	6	20	8
TH	52	20	14	12	24	20	16	44
RB	260	394	324	889	346	244	75	92
SR	166	85	44	16	42	68	357	287
Y	29	11	8	7	13	11	5	25
ZR	211	122	67	39	59	51	114	897
NB	6	18	2	42	26	78	1	1
BA	1130	168	61	18	85	261	357	425
K/RB	186.	113.	124.	72.	114.	193.	210.	213.
RB/SR	1.566	4.635	7.364	55.563	8.238	3.588	.210	.321
TH/K	.0011	.0004	.0003	.0002	.0006	.0004	.0010	.0022
DI	89.27	93.04	93.91	96.60	93.19	93.83	80.19	81.25
QZ	24.92	29.42	31.42	27.38	28.82	30.57	29.16	30.46
CO	.43	0	0	1.04	0	0	.53	.39
ZR	.04	.02	.01	.01	.01	.01	.02	.18
OR	34.48	31.80	28.65	45.61	28.24	33.64	11.25	13.98
PL	35.30	36.48	38.77	24.88	41.46	34.91	54.30	50.01
(AB)	29.87	31.82	33.85	23.61	36.13	29.62	39.77	36.81
(AN)	5.43	4.66	4.92	1.27	5.33	5.29	14.53	13.20
DI	0	.83	.21	0	.32	.02	0	0
(WO)	0	.41	.11	0	.16	.01	0	0
(EN)	0	.12	.03	0	.05	0	0	0
(FS)	0	.30	.08	0	.12	.01	0	0
HY	3.66	1.13	1.16	.90	1.40	1.37	3.19	3.47
(EN)	1.39	.33	.34	.27	.40	.54	1.87	1.62
(FS)	2.27	.80	.82	.63	1.00	.83	1.32	1.85
MT	.42	.19	.16	.10	.19	.13	.23	.33
CM	0	0	0	0	0	0	.01	0
IL	.47	.13	.13	.04	.09	.08	.23	.40
AP	.17	.05	.02	.05	.05	.02	.07	.33
	LWG			LWP			N	N

	1006	608	624	623	200	250	625	1010
SIO2	72.81	76.89	75.03	75.50	75.79	75.94	76.54	78.84
TIO2	.03	.13	.02	.05	.17	.02	.02	.02
AL2O3	15.62	13.42	14.44	13.20	13.44	14.62	13.95	12.82
FE2O3	.11	.14	.06	.18	.18	.03	.09	.03
FEO	.61	.77	.31	1.02	.98	.18	.51	.15
MNO	.30	0	.17	.53	.02	.06	.32	.08
MGO	.23	.39	.22	.25	.51	.18	.27	.12
CAO	.49	2.67	.85	.98	2.54	.81	.80	1.64
NA2O	4.37	4.48	5.78	4.27	3.99	5.72	5.24	5.21
K2O	5.16	.90	2.66	3.32	1.82	2.77	2.61	.53
P2O5	.02	.07	0	.01	.17	.01	.01	.01
H2O-	.04	.02	0	.03	.03	.02	.02	.06
LOI	.25	.25	.19	.29	.35	.23	.19	.25
TOTAL	100.04	100.13	99.73	99.64	99.99	100.59	100.57	99.75
F3/F2	.18	.18	.18	.18	.18	.18	.18	.18
K2O/NA2O	1.18	.20	.46	.78	.46	.48	.50	.10
MGO/K2O	.04	.43	.08	.08	.28	.06	.10	.23
F3+F2/CA	1.79	.42	.52	1.50	.56	.32	.92	.13
K2O/CAO	10.53	.34	3.13	3.39	.72	3.42	3.26	.32
CAO/MGO	2.13	6.85	3.86	3.92	4.98	4.50	2.96	13.67
V	5	15	4	9	17	3	2	5
CR	6	9	7	6	9	7	10	9
NI	5	11	4	4	12	6	6	4
TH	12	9	15	42	38	20	12	64
RB	771	48	355	209	76	384	346	12
SR	28	266	23	44	268	23	22	42
Y	7	5	8	24	22	11	7	22
ZR	76	93	20	125	108	28	42	67
NB	55	0	68	114	0	90	93	68
BA	64	163	7	93	349	18	14	6
K/RB	56.	156.	62.	132.	199.	60.	63.	367.
RB/SR	27.536	.180	15.435	4.750	.284	16.696	15.727	.286
TH/K	.0003	.0012	.0007	.0015	.0025	.0009	.0006	.0145
DI	93.15	83.96	93.38	90.07	83.70	94.72	93.13	89.88
QZ	25.43	40.72	28.64	34.25	39.16	29.83	33.26	42.66
CO	1.95	.34	.48	.80	.63	.74	1.05	.71
ZR	.02	.02	0	.03	.02	.01	.01	.01
OR	30.74	5.33	15.83	19.69	10.78	16.49	15.54	3.14
PL	39.30	50.81	53.13	40.96	45.41	52.37	48.25	52.17
(AB)	36.98	37.91	48.91	36.13	33.76	48.40	44.34	44.09
(AN)	2.32	12.91	4.23	4.83	11.65	3.96	3.91	8.09
HY	2.11	2.06	1.35	3.25	2.68	.83	2.10	.67
(EN)	.57	.97	.55	.62	1.27	.45	.67	.30
(FS)	1.54	1.08	.80	2.63	1.41	.38	1.42	.37
MT	.16	.20	.09	.26	.26	.04	.13	.04
IL	.06	.25	.04	.09	.32	.04	.04	.04
AP	.05	.17	0	.02	.40	.02	.02	.02
	N	N	S	S	N	S	S	S

F3/F2 = FE2O3/FEO
F3+F2/CA = (FE3+ + FE2+)/CA2+

RARE EARTH ELEMENT CONCENTRATIONS

A. Nine Laxford melagranites

	62	63	64	66	68	74	78	81	84
La	54.3	120	80.6	124	91.8	76.0	156	202	128
Ce	201	258	211	297	311	184	326	432	320
Nd	38.9	90.2	53.8	93.9	77.2	58.8	136	167	117
Sm	6.3	11.7	7.6	12.2	10.4	8.8	16.7	21.3	14.7
Eu	1.4	1.4	1.3	2.4	2.2	1.8	3.7	4.9	3.5
Tb	1.1	1.2	1.0	1.4	1.4	1.2	1.4	1.7	1.4
Yb	.2	.2	.2	.2	.2	.5	.5	.7	.7

B. Two Laxford Leucogranites

	61	70
La	10.9	4.2
Ce	46.3	23.9
Nd	7.4	4.9
Sm	1.1	5.7
Eu	0.08	0.35
Tb	0.56	1.59
Yb	0.17	0.47

C. Six Outer Hebrides granites

	601	609	616	105	108	112
La	180	54.2	31.6	113	108	85.0
Ce	290	163	147	233	185	186
Nd	105	46.5	17.2	35.0	83.1	56.1
Sm	9.1	5.1	2.8	12.3	11.8	9.5
Eu	1.2	0.86	0.43	0.07	1.15	0.83
Tb	0.87	0.63	0.39	0.73	0.54	0.57
Yb	0.76	1.13	0.72	1.12	0.40	1.84

U concentrations in Laxfordian granites and related pegmatites

Sample	U concentration*	
61	1.08	lg
62	1.57	lg
63	1.53	lg
64	3.02	g
65	0.60	p
66	3.26	g
67	1.47	p
68	3.49	g
70	2.39	lg
71	2.33	p
74	3.38	g
75	1.83	p
78	3.04	g
79	8.50	p
81	3.34	g
84	4.04	g
601	3.67	g
609	4.32	g
616	5.51	g
105	3.01	g
108	5.30	g
112	3.23	g

*method: Instrumental Neutron Activation Analysis

APPENDIX 2

ANALYTICAL METHODS

A. ROCK ANALYSIS

Rock samples were jaw-crushed and then ground in a 'Tema' tungsten carbide mill to about 200 mesh.

Na_2O was determined by flame photometry, a technique which was also used to determine K_2O in samples GS1-GS9 from the metasomatic locality at Garry-a-Siar, Benbecula.

Except in the case of GS1-GS9, all major elements (SiO_2, TiO_2, total Fe_2O_3, MnO, MgO, CaO, K_2O and P_2O_5) were analysed on a Philips PW 1212 automatic X-ray fluorescence spectrometer, using a flexible calibration line based on recommended data for international rock standards. A range of trace elements (Cr, Ni, Zr, Rb, Sr, Th, Y, Ba, V and Nb) was analysed in the same way. Full details of the XRF methods used at Imperial College are described by Parker (1977).

Data reduction was carried out using programs written by R.J. Parker and J.P. Willis. CIPW norms were calculated using the program AGNORM (University of California at Berkeley).

Rare-earth elements were analysed by Instrumental Neutron Activation Analysis. 0.1 gm of rock powder was heat-sealed in a polythene capsule. Batches of samples

and solution standards were sealed into a polythene tube, which was then irradiated at the University of London Reactor Centre, Silwood Park, for approximately 32 hours at a neutron flux of 10^{12}n cm^{-2} sec^{-1}. A Ge(Li) detector (La) and an intrinsic Ge detector (Ce, Nd, Sm, Eu, Tb, Yb and Lu) were used to analyse the irradiated samples, using an automatic sample changer and a Link Systems 4000 channel analyser and Nova mini-computer. The resulting energy-dispersive spectra were treated in the following way: backgrounds were fitted to the peaks of interest, either by hand or using polynomial background-fitting routines (e.g. CFIT (ULRC, modified by the writer)); interference corrections were then made (Table A1) and the absolute concentrations calculated by program RIALTO (ULRC), which corrects for flux variations across the sample tubes and the radioactive decay during counting.

Samples GS1-GS9 were analysed for a range of major and trace elements using a combination of atomic absorption, colorimetry and spark-source plasma spectrometry (using an ARL plasma spectrometer).

B. MINERAL ANALYSIS

All major elements were analysed using a Cambridge Instruments Microscan 5 electron microprobe fitted with a lithium-drifted silicon detector, the resulting energy-dispersive spectra being analysed by a Link Systems Nova

mini-computer. The methods used for data reduction are similar to those described by Statham (1976).

Operating conditions on the microprobe were 15Kv accelerating voltage with a takeoff angle of 75°, and a specimen current of 3.5, 4.0, or 5.0 na, and sample count times of 80-100 live seconds. Olivine and jadeite standard minerals were used to assess the quality of the results.

Except in the case of the Fe-Ti oxides, no attempt has been made to estimate the Fe^{3+} content of minerals, and all Fe is assumed to be Fe^{2+}. Since the ratio $Fe^{2+}/(Fe^{2+} + Fe^{3+})$ is likely to be close to 1.0 in the micas, garnets and amphiboles in the rocks studied here, quite small errors in the calculated stoichiometry of ferromagnesian minerals, resulting from variations in the accuracy of the calibration of individual oxide standards on the microprobe, are bound to introduce large relative errors in the estimation of Fe^{3+}.

Mineral formulae were calculated by program SUPER RECAL (J.C. Rucklidge). Fe-Ti oxides were recalculated using the method recommended by Carmichael (1967), using the program ILMAG (J.C. Rucklidge).

Mineral samples analysed for trace elements were prepared by hand-picking (or, if possible, by using single crystal samples) and grinding in an agate mortar.

Analysis of these samples was by XRF, using the methods described above.

TABLE A1

PEAKS USED AND CORRECTIONS APPLIED TO
RARE EARTH ELEMENT GAMMA-RAY SPECTRA

1.	2.	3.	4.
La^{140}	1596	-	91.7
Ce^{144}	145	9.25% of 113.8(Yb)	179
Nd^{147}		-	61.2
Sm^{153}	103.2	82% 106.1(Np^{239}) 8.4% 94.8 (Pa^{233})	7.3
Eu^{152}	121.1	-	1.44
Tb^{160}	86.6	25.8% 94.8(Pa^{233})	0.42
Yb^{175}	113.8	259% 208.4(Lu^{177})	1.07

1. Isotope used in gamma-ray spectrometry.
2. Energy of peak (keV).
3. Percentage correction applied to counts on peak.
4. Average concentration of USGS G-2 standard granite.